Characterising the Immune Response to Liposomal Adjuvant Formulations: A Systems Biology Approach

Melanie R. Neeland

Bachelor of Science (Honours)

A thesis submitted for the degree of Doctor of Philosophy at the Department of Physiology, Monash University

October 2014

*Many times a day I realize how much my own outer and inner life is built
upon the labors of my fellow peers, both living and dead, and how earnestly I must exert
myself in order to give in return as much as I have received.*
- Albert Einstein, 1931

Copyright Notices

Notice 1

Notice 2

Table of Contents

Summary

Despite the remarkable success of vaccination, there are a range of human and veterinary diseases that are in need of new vaccines. The rational design of vaccines against these diseases relies on increased understanding of the immunological mechanisms that contribute to vaccine immunity, the development of novel vaccine delivery systems and the characterisation of immune stimulants that are able to increase vaccine efficacy. Vaccine formulations incorporating stimulants that target innate immune receptors have been shown to significantly increase vaccine induced immunity. When incorporated into liposome-based delivery systems, the TLR ligands CpG and poly(I:C) are able to induce protective, long lasting cellular and humoral immune responses in mice. However, the cellular targets of these liposomal adjuvant formulations and the *in vivo* mechanisms of immune induction remain to be elucidated.

The early immune response to vaccination is characterised by activation of cells present at the injection site and their subsequent migration to the local lymph node via the afferent lymphatics. The immunological signals received by innate cells at the peripheral injection site are conveyed to lymphocytes in the local lymph node, leading to the generation of an adaptive immune response where antigen specific lymphocytes emigrate via the efferent lymphatics to perform their tailored effector function. Examination of the afferent and efferent lymphatic compartments during the innate and adaptive phases of an immune response permits the quantification and characterisation of the *in vivo* biological mechanisms triggered following vaccination.

By directly cannulating the ovine lymphatic vessels, the results of this thesis demonstrate that the addition of poly(I:C) or CpG to a liposomal vaccine formulation enhances the immediate inflammatory response at the site of injection, improves antigen uptake by innate cell populations and induces genetic signatures associated with interferon-mediated antiviral immune responses in afferent lymph. The liposomal adjuvant formulations also increased the production of antigen-specific antibodies in the circulation following vaccine challenge. The results additionally show that CpG and poly(I:C) target distinct pathways in afferent lymph to induce their immunological effects, where CpG uniquely increased dendritic-cell associated antigen transport and induced the maturation of monocytes and dendritic cells 72h after

injection. CpG also induced the persistence of gene programs involved in cell migration, intracellular DNA sensing and cytotoxic immunity in afferent lymph at this time point. These immunological effects were not observed with liposomal poly(I:C) or liposomes alone. This further translated into an extended period of lymph node cell shut down, the induction of IFNγ positive T cells in efferent lymph and enhanced production of antigen-specific antibodies after injection of liposomal CpG when compared to liposomal poly(I:C) and liposomes alone. The development of a preliminary mathematical model of DC trafficking and T cell activation in the local lymph node showed that all liposomal formulations induce a sufficient number of antigen positive DCs to scan the T cell receptor repertoire and that the adjuvanted formulations induce at least a four-fold excess of antigen positive DCs than required. This model was further utilised to simulate the effect of reducing antigen dose, revealing the optimal number of antigen positive DCs entering the lymph node for an effective immune response and the contribution of DC migration kinetics on vaccine efficacy.

The work presented within this thesis provides a comprehensive analysis of the real time *in vivo* kinetics of cell migration, antigen uptake and gene expression induced by the innate adjuvants poly(I:C) and CpG when incorporated into a liposome-based delivery system. The results demonstrate that liposomal vaccine formulations require the addition of adjuvants to enhance their immunogenicity and that poly(I:C) and CpG target distinct pathways in the lymphatic system to induce their immunological effects. This work quantifies the immunological signals that connect the peripheral injection site with the local draining lymph node, revealing that the cellular and transcriptional immune response induced by adjuvants at the site of injection influences adaptive and memory immune outcomes. Collectively, this body of research enhances our understanding of the complex immune response to vaccination and quantifies the *in vivo* immune mechanisms induced following injection with liposomal adjuvant formulations in a vaccination setting comparable to that administered to humans.

General Declaration

In accordance with Monash University Doctorate Regulation 17.2 Doctor of Philosophy regulations the following declarations are made:

I hereby declare that this thesis contains no material which has been accepted for the award of any other degree or diploma at any university or equivalent institution and that, to the best of my knowledge and belief, this thesis contains no material previously published or written by another person, except where due reference is made in the text of the thesis.

This thesis includes two original papers published in peer reviewed journals, one original paper accepted for publication in a peer reviewed journal and one unpublished chapter. The core theme of the thesis is vaccine immunology. The ideas, development and writing up of all the papers in the thesis were the principal responsibility of myself, the candidate, working within the Department of Physiology under the supervision of Dr. Michael de Veer and Professor Els Meeusen.

The inclusion of co-authors reflects the fact that the work came from active collaboration between researchers and acknowledges input into team-based research.

Contribution by others to this thesis:

Professor Els Meeusen and Dr. Michael de Veer supervised the candidate, contributed to experimental design, interpretation of results and manuscript editing. Dr. Martin Elhay provided reagents, contributed to experimental design and manuscript editing. Jackie Nathanielsz also provided reagents. Dr. Michael de Veer and Gary Nguyen assisted in surgical procedures. Dr. David Powell and Dr. Fernando Rossello performed the bioinformatics analysis of RNA sequencing samples. Professor Kate Smith-Miles contributed to the design of the mathematical model and was involved in setting up appropriate collaborations. Dr. Mark Flegg designed the mathematical model (with assistance from Qianqian Wu) and contributed to manuscript editing.

In the case of Chapters 3-6, my contribution to the work involved the following:

Thesis chapter	Publication title	Publication status	Nature and extent of candidate's contribution
3	Vaccination with liposomal poly(I:C) induces discordant maturation of migratory dendritic cell subsets and anti-viral gene signatures in afferent lymph cells	Published	I was responsible for the design of the majority of the experiments, I conducted the experimental work and analysed the data. Assistance was required for surgical procedures. I interpreted the results and wrote the manuscript with assistance from co-authors. **Contribution: 80%**
4	Incorporation of CpG into a liposomal vaccine formulation increases the maturation of antigen loaded dendritic cells and monocytes to improve local and systemic immunity	Published	I was responsible for the design of the majority of the experiments, I conducted the experimental work and analysed the data. Assistance was required for surgical procedures. I interpreted the results and wrote the manuscript with assistance from co-authors. **Contribution: 80%**
5	Transcriptional profile in afferent lymph cells following vaccination with liposomes incorporating CpG	Accepted	I was responsible for the design of the majority of the experiments. Bioinformatic analysis of RNA sequencing data was performed by co-authors on the manuscript. I performed further gene expression analysis of RNA sequencing data. I conducted the experiments and analysis for the real time PCR data. I interpreted the results and wrote the manuscript with assistance from co-authors. **Contribution: 70%**
6	Mathematical modelling of DC trafficking and T cell activation in the local lymph node	In preparation	I was responsible for setting up the collaboration for the work included in this manuscript. The mathematical model was developed by co-authors on the manuscript with my assistance. I generated the figures, interpreted the results and wrote the manuscript with assistance from co-authors. **Contribution: 60%**

I have renumbered sections of submitted or published papers in order to generate a consistent presentation within the thesis.

Signed:

Date: ………23.02.15………………………

Acknowledgements

First and foremost I would like to express my sincere gratitude to my supervisors Professor Els Meeusen and Dr. Michael de Veer for their constant support during my PhD. Els, thank you for inviting me into your lab as an undergraduate student and for believing in me ever since. I am thankful for your advice, encouragement and your expert knowledge of scientific research. Mike, I find it difficult to express in words how grateful I am to have completed my PhD under your supervision. Thank you for your unwavering support every day of the past four years. Thank you for the countless opportunities and for encouraging me to chase down ideas. Thank you for providing me with an invaluable foundation for a career in scientific research.

Dr Mark Flegg, thank you for your patience, immense help and willingness to learn immunology. Dr Martin Elhay, thank you for your collaboration and advice. I am grateful also to Associate Professor David Piedrafita, Dr Rob Bischof, Associate Professor Ramesh Rajan and Dr David Reser for their support and mentorship.

Thank you to all past and present members of the Biotechnology Research Laboratories with whom I am honoured to have worked with. I would like to thank Jenna for her heart of gold, and Gary for his assistance in surgery and love of dance. To Yugeesh, Sarah and Vanessa, thank you for your warm friendship.

To Chris, my partner in the lab and also in life, thank you for being you. I learn so much from you every day and I am so grateful to have found you on this journey. Thank you for your constant belief in me, I could not have done this without you.

Finally, a huge thank you to my amazing family. Mum, Tash and Hayden, thank you for being my source of inspiration and for supporting me always. The best parts of me are because of you.

Publications

Publications arising from PhD thesis

Published:

MR Neeland, E Meeusen and MJ de Veer. Afferent Lymphatic Cannulation as a Model System to Study Innate Immune Responses to Infection and Vaccination. *Vet Immunol Immunopathol* 2014; 158 (1-2): 86-97

MR Neeland, MJ Elhay, J Nathanielsz, E Meeusen and MJ de Veer. Incorporation of CpG into a Liposomal Vaccine Formulation Increases the Maturation of Antigen-Loaded Dendritic Cells and Monocytes to Improve Local and Systemic Immunity. *Journal of Immunology* 2014; 192 (8): 3666-3675

MR Neeland, MJ Elhay, E Meeusen and MJ de Veer. Vaccination with liposomal poly(I:C) induces discordant maturation of migratory dendritic cell subsets and anti-viral gene signatures in afferent lymph cells. *Vaccine* 2014;http://dx.doi.org/10.1016/j.vaccine.2014.09.036

Accepted:

MR Neeland, MJ Elhay, DR Powell, FJ Rossetto, E Meeusen and MJ de Veer. Transcriptional profile in afferent lymph cells following vaccination with liposomes incorporating CpG. *Accepted in **Immunology** October 2014*

Other publications

MJ de Veer, **MR Neeland**, M Burke, J Pleasance, J Nathanielsz, MJ Elhay and E Meeusen. Cell Recruitment and Antigen Trafficking in Afferent Lymph after Injection of Antigen and poly(I:C) Containing Liposomes, in Aqueous or Oil-based Formulations. *Vaccine* 2013; 31: 1012-1018

M Burke, MJ de Veer, J Pleasance, **MR Neeland**, MJ Elhay, P Harrison and E Meeusen. Innate Immune Pathways in Afferent Lymph Following Vaccination with poly(I:C)-containing Liposomes. *Innate Immunity* 2014; 20: 501-510

List of Abbreviations

A1HV-1	Alcelaphine herpesvirus-1
Ag	Antigen
AL	Afferent lymph
ANOVA	Analysis of variance
APC	Antigen presenting cell
BCG	Bacillus Calmette–Guérin
CAB	Centre for Animal Biotechnology, University of Melbourne
CCL	C-C motif ligand
CD	Cluster of differentiation
cDNA	Complimentary DNA
CFP	Culture filtrate protein
CLEC	C-type lectin domain family
CpG ODN	Cytosine phosphate guanine oligonucleotides
CTL	Cytotoxic T lymphocyte
CXCL	C-X-C motif ligand
DC	Dendritic cell
DNA	Deoxyribonucleic acid
dsRNA	Double-stranded RNA
DT	Diphtheria toxoid
ELISA	Enzyme linked immunosorbent assay
FDR	False discovery rate
FMDV	Foot and mouth disease virus
FSC	Forward scatter
GAPDH	Glyceraldehyde 3-phosphate dehydrogenase
GZMA	Granzyme-A
HBSAg	Hepatitis B virus surface antigen
HIV	Human immunodeficiency virus
HPV	Human papilloma virus
HRP	Horseradish peroxidase
IFI	Interferon-induced protein
IFIT	Interferon-induced protein with tetratricopeptide repeats
IFN	Interferon
Ig	Immunoglobulin
IL	Interleukin

ILC	Innate lymphoid cell
iNKT	Invariant natural killer cell
ISCOM	Immune stimulating compound
ISG	Interferon-stimulated gene
LPS	Lipopolysaccharide
MDA5	Melanoma differentiation associated protein 5
MHC	Major histocompatibility complex
MPL	Monophosphoryl lipid-A
mRNA	Messenger RNA
NK	Natural killer
NOD	Nucleotide-binding oligomerization domain receptors
OAS	2'-5' oligoadenylate synthetase
OD	Optical density
OVA	Ovalbumin
PAMP	Pathogen associated molecular pattern
PBMC	Peripheral blood mononuclear cell
Poly(I:C)	Polyinosinic:polycytidylic acid
PPD	Purified protein derivative
PRF1	Perforin
PRR	Pattern recognition receptor
PSMA2	Proteasome subunit alpha type-2
RhuADV5	Recombinant human adenovirus 5
RIG-I	Retinoic acid-inducible gene 1
RNA	Ribonucleic acid
SEM	Standard error of the mean
SSC	Side scatter
TB	Tuberculosis
TCR	T cell receptor
Th	T helper
TLR	Toll-like receptor
TRIM	Tripartite motif family
Treg	T regulatory
VLP	Virus-like-particle
vNKT	Variant natural killer cell

CHAPTER ONE

General Introduction

1.1 Vaccination: the global picture

Vaccination is the most successful and cost-effective medical intervention for the control of infectious disease in human and veterinary medicine (1, 2). The remarkable success of vaccination in recent years is due to increased access to current vaccines and the development of novel research strategies to create new vaccines for major diseases. Global access to immunisation has increased considerably since the establishment of the Global Alliance for Vaccines and Immunisation (the GAVI Alliance) in 2000. The GAVI alliance contributed to preventing 4.8 million future deaths in 2010 and has currently immunised 370 million children that would have otherwise been left unvaccinated. The Bill & Melinda Gates Foundation is a significant player in vaccine research and development. Working closely with their global partners, the foundation provides significant funding for the creation of new vaccines for the worlds three biggest killers; human immunodeficiency virus (HIV), malaria and tuberculosis (TB), which together kill more than 5 million people each year. In addition to these three global threats, there are a range of other human bacterial, viral and parasitic diseases that are in need of vaccines, including meningococcus group B, dengue fever and leishmaniasis (Table 1). Recently, there has also been significant interest in the development of therapeutic vaccines against a range of cancers, allergies and addictions (3).

Table 1. Prophylactic and therapeutic vaccines under investigation or development.

Bacterial diseases/organisms	Viral diseases/organisms	Parasitic diseases/organisms	Therapeutic treatments
Clostridium difficile	Cytomegalovirus	Fascioliasis	Allergic rhinitis
Chlamydia	Dengue fever	Hookworm	Alzheimer's
Escherichia coli	Ebola	Leishmaniasis	Breast cancer
Helicobacter pylori	Epstein-Barr	Lymphatic filariasis	Cocaine addiction
Leprosy	Hepatitis C	Malaria	Colorectal cancer
Meningococcus B	Hepatitis E	Schistosomiasis	Lung cancer
Pseudomonas	HIV		Melanoma
Staphylococcus	Influenza		Multiple sclerosis
Streptococcus	SARS		Nicotine addiction
Tuberculosis	West Nile		Pediatric tumours

Table adapted from (3).

New vaccines against a number of animal diseases are also required, not only to improve the health of companion animals and increase production of livestock, but also to prevent the animal-to-human transmission of infectious diseases (2). A major case of animal-to-human transmission is the H5N1 avian influenza pandemic which began in China in 1996 and has a human mortality rate of 60% (4). It is believed that the development of veterinary vaccines against zoonotic infections can reduce human transmission by as much as 80% (5). However, veterinary vaccines are only available for a fraction of the diseases affecting animals (4). The One Health initiative aims to improve health at the animal-human-ecosystem interface through the integration of human medicine, veterinary medicine and environmental sciences. A major goal of One Health is to increase control of animal disease through the production of new vaccines against a range of emerging animal infections, including bovine spongiform encephalopathy, West Nile virus and foot-and-mouth disease (4).

Until recently, vaccines have been developed empirically, such that they are able to induce protective immunity but the mechanisms by which they do this are currently not well understood (6). In both human and veterinary medicine, the rational design of new vaccines and improved efficacy of current vaccines relies on increased understanding of the immunological mechanisms that contribute to vaccine-induced immunity.

1.2   Vaccine immunity

The concept of vaccination was first promoted by Edward Jenner in 1796 following his observation that people exposed to the cowpox virus were naturally resistant to the human smallpox disease. Based on this observation, he inoculated humans with a less pathogenic form of the cowpox virus and challenged the same patients with fresh smallpox virus (7). When no smallpox disease developed in these patients, Jenner concluded that his vaccination was successful and protection was complete. This was shortly afterwards followed by the "germ theory of disease" established by Louis Pasteur, who observed that weakened or attenuated germs could protect against virulent organisms, and went on to develop preliminary vaccines against cholera, anthrax and rabies (8, 9). Due to the notable success of these discoveries, it was established that the theory of vaccination can be applied to a variety of infection settings, where pathogen resistance can be achieved through injection of a non-pathogenic form of the pathogen itself (9). From these empirical beginnings in the 18th century, vaccination has made extremely significant progress in combating infectious disease, with the introduction of successful vaccines against a range of diseases including tetanus, polio, measles mumps and rubella, hepatitis and human papillomavirus (HPV) (8, 10, 11).

1.2.1   Innate immunity

The innate immune system plays an important role in the defence against pathogens as it is the first system to recognise the molecular patterns of infectious, non-self molecules. The structural motifs that the innate system distinguishes as foreign include components of microbial membranes, cell walls, proteins, RNA and DNA (12). These are collectively termed pathogen-associated molecular patterns (PAMPs) and are generally included in successful vaccine formulations. PAMPs are recognised by cells of the innate system via a variety of pattern recognition receptors (PRRs) (13). PRRs are expressed on the cell surface and in intracellular compartments of a variety of innate cell types, including dendritic cells (DCs), monocytes and neutrophils (13). Some PRRs are also expressed on non-immune cells, such as epithelial cells which often encounter the first contact with a pathogen (14). An important family of PRRs are the toll-like receptors (TLRs), which have broad specificity for

a range of molecular patterns. More recently discovered families of PRRs include the NOD proteins which recognise intracellular bacteria and the RIG-I receptors which recognise double stranded RNA (15, 16). Activation of these PRRs upon recognition of PAMPs leads to the upregulation of genes that are responsible for distinct events in the immune response, such as the production of inflammatory cytokines and chemokines that recruit appropriate cells to the site of infection (17). Antigen presenting cells (APCs), such as DCs, ingest the antigen and migrate to the local lymph node where the antigen is presented via the major histocompatibility complex (MHC) to T cells in the T cell area of the lymph node. T cells that are specific for the antigens being presented differentiate and proliferate into effector cells that are able to specifically combat the pathogen (18). The activation of these specific T cells in the lymph node represents the first step in the generation of an adaptive immune response.

1.2.2 Adaptive immunity

T cell subsets are classified based on surface marker expression and cytokine production. Defining surface markers include CD4 or CD8 expression, and the production of cytokines that characterise their effector function. CD4 T cells are also known as T helper (Th) cells as they are able to assist B cell differentiation into antigen specific antibody-secreting plasma cells (18). CD8 T cells are known as cytotoxic T cells as they are able to kill pathogen infected cells (19). There are multiple subsets of effector CD4 T cells, including Th1, Th2, Th17 and Treg cells, each with distinct functions and cytokine secretion profiles. Th1 cells eliminate intracellular pathogens by producing IFNγ and IL2 (20). IFNγ is an essential cytokine that induces phagocytosis, while IL2 promotes the proliferation of effector CD8 T cells (21). In mice, cytokines of the Th1 pathway are also responsible for the production of IgG2a and IgG2b antibodies, such that effective immune responses against intracellular pathogens often require increased Th1 cellular activation and IgG2 antibody production (22). In humans, Th1 cytokines induce IgG1 and IgG3 antibodies, functional counterparts of the murine IgG2a and IgG2b (23). Th2 cells play a role in immune responses against extracellular parasites and are also involved in the induction of allergic disease (20, 24). IL4, IL5, IL10 and IL13 are the key effector cytokines produced by a Th2 immune response, leading to enhanced eosinophil activation, increased IgE antibody production and the inhibition of Th1-mediated immune responses (20, 25). The cytokine IL4 also favours the

production of IgG1 antibodies in mice, and IgG4 antibodies in humans (22, 26). The function of Th17 cells in adaptive immunity remains to be fully elucidated; however recent evidence suggests they are involved in pro-inflammatory immune responses through the production of the cytokines IL17, IL21 and IL22 (27). Th17 cells have also been associated with the generation of autoimmune disease, where neutralisation of IL17 results in the rapid reversal of an autoimmune phenotype in patients with psoriatic lesions (28). Treg cells, or regulatory CD4 T cells, play an essential role in the maintenance of an immune response by preventing immunopathology (20). TGFβ and IL10 are the major cytokines involved in this response, where mice with a deletion in the TGFβ gene show uncontrolled proliferation of pro-inflammatory T cells resulting in severe immunopathology (29). Effector CD8 T cells, also known as cytotoxic T lymphocytes (CTLs), play an essential role in immunity against intracellular viruses and bacteria. CTLs produce cytokines such as IFNγ and the cytolytic molecules perforin and granzymes that are able to kill pathogen infected cells, thereby preventing the spread of infection (30). CD8 T cells can also include minor subsets that produce IL4 or IL17; however the functions of these subsets are incompletely understood (19).

1.2.3   Bridging innate and adaptive immunity

The development of a fully functional immune response requires the interaction of multiple components of innate and adaptive immunity. Whilst most cell types can be functionally categorised within the innate or adaptive arms of the immune response, the distinction is less clear for several cell populations, including innate lymphoid cells (ILCs), natural killer (NK) T cells and γδ T cells, which share biological characteristics of both systems. ILCs are cytokine-secreting cells that lack an antigen specific receptor yet function similarly to T helper lymphocytes. ILCs play important roles in the innate response to infection in the tissue and can be classified into three groups based on their cytokine-secretion profile (31). Group 1 ILCs produce the Th1-associated cytokine IFNγ and include cytotoxic NKp46-expressing NK cells and non-cytotoxic ILC1 cells; Group 2 ILCs produce the Th2-associated cytokines IL5 and IL13; Group 3 ILCs produce Th17-associated cytokines and include LTi cells that produce both IL17A and IL22, NKp46+ ILC3s that produce only IL22 and NKp46- ILC3s that produce IL17A, IL22 and IFNγ (31). Mucosal-associated invariant T (MAIT) cells are

another population of ILCs that are abundant at mucosal sites and have been shown to play an important role in anti-bacterial immunity (32). The diversity of these ILC subsets assists in the generation of a sophisticated, early immune response against a range of pathogens. Evidence also suggests that ILCs are significant players in the recruitment of other innate and adaptive effector cells to the site of infection (33).

Whilst NKT cells and γδ T cells express antigen-specific receptors, the repertoire of these receptors is limited, bearing similarities to PRRs of the innate immune system (34). NKT cells respond to lipid or glycolipid antigens presented by the MHC class I-related glycoprotein CD1d, present on a variety of innate cell populations (34). There are two types of NKT cells, invariant NKT (iNKT) and variant NKT (vNKT) cells, which often play opposing roles to one another. Stimulation of NKT cells through their TCR leads to robust secretion of cytokines and the acquisition of cytotoxic activity. Depending on the type of infection, NKT cells are able to express a range of cytokine secretion profiles, including a Th1-profile, secreting IFNγ and TNFα, or a Th2-profile, secreting IL4 and IL13 (35). NKT cells appear to play important roles in autoimmune disease, tumour surveillance and infectious diseases (35). γδ T cells are of particular interest in immunity as they are abundant in peripheral tissues and are ideally located to play a role in innate immune defence. Unlike the conventional αβ-TCR expressing CD4 and CD8 T cells, these γδ-TCR expressing T cells do not require MHC-restricted presentation to recognise their antigens (36). Human γδ T cells have been shown to recognise non-protein phosphoantigens and lipoproteins whilst murine γδ T cells recognise mycobacterial heat shock proteins (37). Activated γδ T cells that produce IFNγ have been identified as early as two days after listerial infection (38). In fact, depletion of IFNγ+ γδ T cells resulted in impaired bacterial clearance from 3 days after infection (39). IL17-producing γδ T cells have also been identified following infection with *M. bovis*, *E.coli* and *C.albicans* (40-42). In the above infection models, the γδ T cells were responsible for enhanced neutrophil recruitment to the site of infection, suggesting they play important roles in the local inflammatory immune response.

1.2.4 *Immunological memory*

In addition to cellular and antibody mediated immune responses, the adaptive system is responsible for the induction of immunological memory, where a subset of antigen-specific effector lymphocytes remain in the circulation as long lived memory cells that are able to respond faster and with greater power upon subsequent infection with the same pathogen (43). Successful vaccination strategies require the induction of immunological memory, and therefore, appropriate activation of the adaptive immune response. The smallpox and yellow fever vaccines are highly successful vaccines. Both of these vaccines induce potent Th1 and CD8 T cell effector and memory immunity capable of lifelong protection against their respective viruses (44). It was recently revealed that the induction of strong adaptive and memory immunity is entirely dependent on appropriate activation of the innate immune system (13, 45). As the ultimate goal of vaccination is to elicit long lived antigen-specific immune responses and induce immunological memory, new vaccines that target both innate and adaptive immune responses are required.

1.3   Innate immune stimulators as vaccine adjuvants

Current vaccine formulations can be divided into two categories; live attenuated vaccines and non-living vaccines. Live attenuated vaccines comprise weakened versions of pathogens that often provide immunity for several decades with a single immunisation (6). As the live pathogens are able to infect cells, these vaccines can replicate and induce strong antibody and cellular immune responses (2). It is due to these strong immune responses that live attenuated vaccines are the most powerful vaccines for disease control and eradication (10). Live attenuated vaccines that have been developed for human use include smallpox, yellow fever, rabies, measles, mumps and rubella (6). Despite their success, live attenuated vaccines pose the risk of residual virulence and reversion to their pathogenic wild type (10). Such effects may cause mild to severe adverse reactions in some patients (46). The second group of vaccines, non-living vaccines, do not pose such a risk as they contain safer, inactivated subunits of pathogens that are unable to infect cells (6). Although more stable than live attenuated vaccines, non-living vaccines are generally less effective and require multiple administrations to boost the immune response over time (2). Consequently, non-living vaccines often require the addition of immune stimulants known as adjuvants, which enhance adaptive and memory immune responses generated to the vaccine (46). Adjuvants can also influence the type of immune response generated, enhancing the selectivity and specificity of the vaccine (47). The success of an adjuvant is traditionally quantified via adaptive outcomes such as antigen-specific antibody titre and protection from infection after antigenic challenge (48). The ability of adjuvants to enhance vaccine immune outcomes has several benefits in a clinical setting, such as reducing antigen dosage and decreasing the number of administrations required to successfully immunise a patient (49, 50).

The effect of adjuvants was first observed in 1930, when the addition of aluminium hydroxide to a tetanus vaccine induced a 1000 fold increase in antibody production (51). Until recently, aluminium-based formulations were the only adjuvants licenced for human use, due to their impeccable safety profile and ability to elicit strong antibody mediated immune responses. Despite this, the exact mechanisms by which aluminium adjuvants induce their immunostimulatory effects are currently unknown and are a topic of debate within the field (52-54). Additionally, aluminium adjuvants enhance Th2 immune responses, and are not protective against pathogens that require Th1 immune responses, such as intracellular

8

pathogens (55). This highlights the need to understand the immunological mechanisms of adjuvants and develop new stimulators that are effective against Th1 immune pathogens.

1.3.1   TLR ligands

The recent recognition for the role of the innate immune system in underpinning the adaptive immune outcomes of vaccines has led to great interest in adjuvants that target innate immune pathways. Several well defined innate immune stimulators, such as TLR ligands, are selectively developed to be included as adjuvants within vaccine formulations (8, 56). In fact, a TLR 4 agonist known as monophosphoryl lipid A (MPL) was recently included in the human cervical cancer vaccine, which has proven effective against several strains of the human papilloma virus (HPV) (57). TLR 4 recognises the bacterial endotoxin lipopolysaccharide (LPS), present on the outer membrane of Gram-negative bacteria (58). Activation of the TLR 4 complex induces increased expression of co-stimulatory molecules and the production of the pro-inflammatory cytokines TNFα and IL-6 by innate cell populations, ultimately leading to the development of Th1 adaptive immunity (58). The MPL adjuvant is a chemically modified derivative of LPS formulated to reduce toxicity whilst maintaining the immunostimulatory properties of LPS (59). The HPV vaccine Cervarix™ containing MPL has been shown to increase the number of antigen carrying dendritic cells and monocytes in the local lymph node and enhance the production of pro-inflammatory cytokines at the site of injection (60). Another study demonstrated that MPL promotes IFNγ production by antigen specific T cells, skewing the immune response to a Th1 profile that is able to combat viral pathogens (61). The incorporation of MPL in human vaccine formulations represents a proof of principle that TLR ligands can be both safe and effective when used as adjuvants within vaccines.

Several other TLR ligands are under investigation for development as adjuvants, the most characterised of these are TLR 3 and TLR 9 ligands. Both TLR 3 and TLR 9 are endosomal receptors that recognise microbial nucleic acids. TLR 3 is adept at recognising the double stranded RNA found in viral genomes, whilst TLR 9 is activated by DNA motifs found in both viral and bacterial genomes (62-64). Activation of TLR 3 and TLR 9 trigger defensive innate immune responses such as pro-inflammatory chemokine production and maturation of innate cell populations that lead to increased capacity to eliminate the pathogen (Figure 1)

(64-67). When employed as adjuvants within vaccines, TLR 3 and TLR 9 ligands generate immune responses that are tailored to combat intracellular pathogens, skewing the immune response towards a Th1 inflammatory phenotype (68, 69).
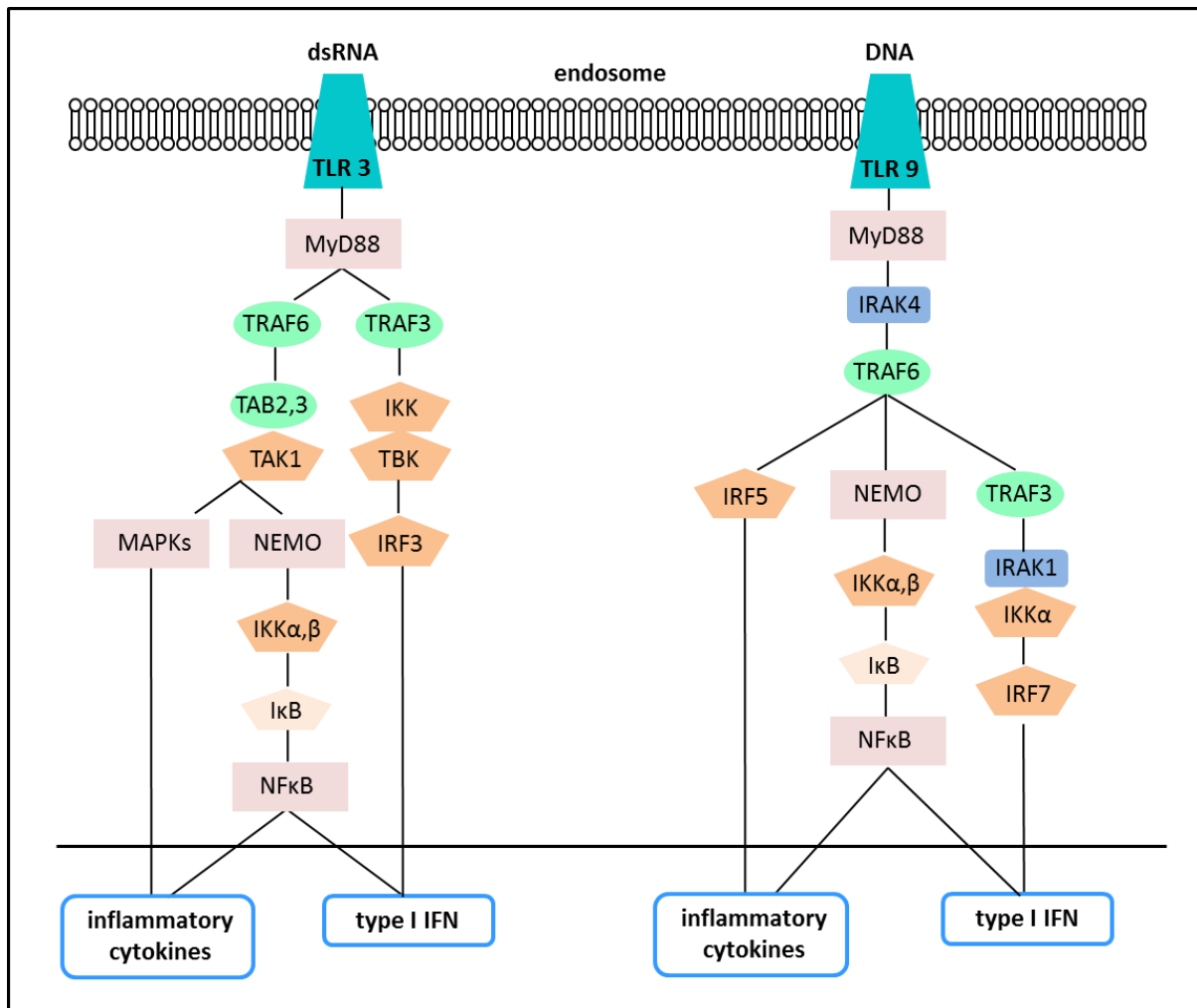
Figure 1. Intracellular TLR 3 and TLR 9 signalling pathways. TLR 3 recognises double stranded RNA (dsRNA) and TLR 9 recognises foreign DNA. Activation of TLR 3 and TLR 9 triggers the induction of signalling cascades that lead to the production of pro-inflammatory cytokines, including type I interferon (IFN), and the generation of the innate immune response. Figure adapted from (70).

Polyinosinic:polycytidylic acid, referred to as poly(I:C), is a synthetic dsRNA complex that activates TLR 3. Several studies conducted in mice have investigated the immunostimulatory effects of poly(I:C) when incorporated into vaccine formulations. Poly(I:C) was shown to induce strong type I IFN production by DCs and monocytes when added to a HIV gag protein vaccine. This study also found that the IFN-AR receptor is required for DCs to directly respond to poly(I:C), as activation of DCs was not observed (measured by CD80 and CD86 expression), when this receptor was removed (71). Similarly, addition of poly(I:C) to this

vaccine induced protective CD4 T cell responses against the HIV antigen (72). Administration of poly(I:C) was also shown to promote rapid induction of inflammatory cytokines in the serum, including IL-6, TNFα, and IFNγ (73). Poly(I:C) added to a foot-and-mouth disease vaccine induced high levels of neutralising antibodies (74). The immunostimulatory effects of poly(I:C) have also been demonstrated in rhesus macaques, where injection of poly(I:C) promoted Th1 cellular and antibody mediated immune responses to both HPV and SIV antigens (75, 76).

CpG-containing oligodeoxynucleotides (CpG-ODN) are a family of un-methylated, synthetic oligonucleotides that signals through TLR 9 and mimic the immunostimulatory activity of microbial DNA. CpG has been studied extensively as an adjuvant and, like poly(I:C), has been shown to strongly polarise the immune response towards a Th1 immune phenotype (48, 69). Several studies have demonstrated that the addition of CpG to DNA vaccine formulations significantly increases antibody mediated antigen specific immune responses (77, 78). Similarly, incorporating CpG into the licenced human Anthrax vaccine induced antigen specific antibody titres in mice that were significantly higher and persisted for longer than those induced by the vaccine alone (79). Enhanced antibody titres generated by CpG have also been observed in non-human primates (80) and in human clinical trials (81-83). Several early studies report the cellular immune responses induced by CpG, with increases in production of cytokines including IL-6, IL-12 and IFNγ by T cells following stimulation with CpG motifs (84-86). Human B cells were also shown to differentiate into both antibody secreting cells and memory B cells after stimulation with CpG (87). In a recent study, the number and survival of CD8 T cells was dramatically enhanced when CpG was co-administered with a peptide vaccine, doubling the number of CD8 T cells present in the circulation when compared to the vaccine alone (88).

There are several reports that dsRNA and microbial DNA can signal through TLR-independent pathways. The cytoplasmic receptor RIG-I was shown to bind and mediate immune activation of shorter dsRNAs, while MDA5 preferentially recognises longer dsRNAs, including the adjuvant poly(I:C) (89, 90). Deletion of TLR 3 and MDA5 leads to a failure to elicit any detectable immune response to poly(I:C), suggesting that both pathways are required for an effective immune response to poly(I:C) (91). The receptor DEC-205, present on a variety of cells, was recently identified as an alternative signalling molecule for CpG DNA. Mice deficient in the DEC-205 receptor produced sub-optimal immune responses

following stimulation with CpG, suggesting that DEC-205 is an important receptor required for CpG-induced adjuvanticity (92).

1.3.2   Safety vs. efficacy

Growing evidence from experimental models therefore supports the hypothesis that the innate stimulators poly(I:C) and CpG have the required immunostimulatory properties to be used as adjuvants within vaccine formulations. However, of equal importance in vaccine development is the safety profile of these stimulators when administered in humans. Several studies have evaluated the safety and immunogenicity of a stabilised analogue of poly(I:C), poly ICLC, in patients following intramuscular or subcutaneous injection. Two phase I/II clinical trials found that intramuscular injection of poly ICLC can be well tolerated in patients with malignant brain tumours, with severe adverse toxicities rarely recorded. These studies also reported significantly improved immune responses, suggesting that poly ICLC can be used in novel vaccine formulations or as an adjunct therapy to chemoradiation in these patients (93, 94).   Subcutaneous injection of poly ICLC in healthy volunteers, however, resulted in local adverse events including erythema and induration at the site of injection. Systemic reactogenicity events were also recorded, including mild flu-like symptoms (95). These events were not reported following intramuscular injection, suggesting that the administration route can alter the frequency of adverse side effects and should be considered in future studies using this stimulant.

The safety and immunogenicity of CpG as an adjuvant for vaccines has also been investigated in clinical trials. When added to a pneumococcal vaccine, CpG was shown to improve antigen specific IgG responses for approximately one year in adults infected with HIV (96). However, this trial also reported higher incidences of influenza-like symptoms following injection with the CpG-coupled vaccine when compared to the vaccine alone (96). Conversely, in a separate study where CpG was added to a commercial influenza vaccine, adverse reactions occurred at similar frequencies to control groups (97).   Interestingly, the addition of CpG to $1/10^{th}$ the dose of the influenza antigen resulted in significantly higher levels of IFNγ secretion, restoring immunity to that observed with the full-dose vaccine (97). This suggests that addition of CpG to vaccines may permit the use of reduced antigen dosage without sacrificing immunogenicity. CpG has also been trialled as an adjuvant for an

experimental malaria vaccine in malaria-exposed adults where antibody responses were over 2 fold higher in the CpG group at all time points after secondary vaccination, with no vaccine related systemic adverse events recorded (98).

Poly ICLC and CpG have both demonstrated efficacy as adjuvants within experimental and commercial human vaccines. These stimulators are generally well tolerated, however several studies report mild to severe local and/or systemic side effects. Injection of soluble poly(I:C) in mice, for example, was associated with adverse effects due to the release of pro-inflammatory cytokines into the circulation (99). To increase the safety of these innate stimulators, substantial research is focused on the development of novel delivery systems that are able to encapsulate antigen and adjuvant within one compartment, thereby enhancing the immunostimulatory capacity of the formulation whilst reducing the potential harmful side effects of soluble adjuvants following systemic release of pro-inflammatory cytokines.

1.4   Vaccine delivery systems

The ultimate goal of a vaccine formulation is to deliver antigens to the immune system in the most appropriate manner. The characterisation of new vaccine delivery systems that induce appropriate antigen-specific cell-mediated and humoral immune responses are therefore required for the development of safe and effective vaccines. The stability, reproducibility, dosage and cost of the formulation are also important factors in rational vaccine design. Nanoparticles represent promising candidates to be included in vaccine formulations as they can operate as both a delivery system and an adjuvant to enhance immunity (100). The major advantage of nanoparticles is their small size, ranging from 1-1000 nanometres. This is comparable to the size of pathogens, permitting nanoparticle uptake by APCs and the subsequent generation of effective cell-mediated immune responses (101). There are several types of nanoparticles under investigation for vaccine delivery, including virus-like particles (VLPs), immune stimulating complexes (ISCOMs), emulsions and liposomes (Figure 2).
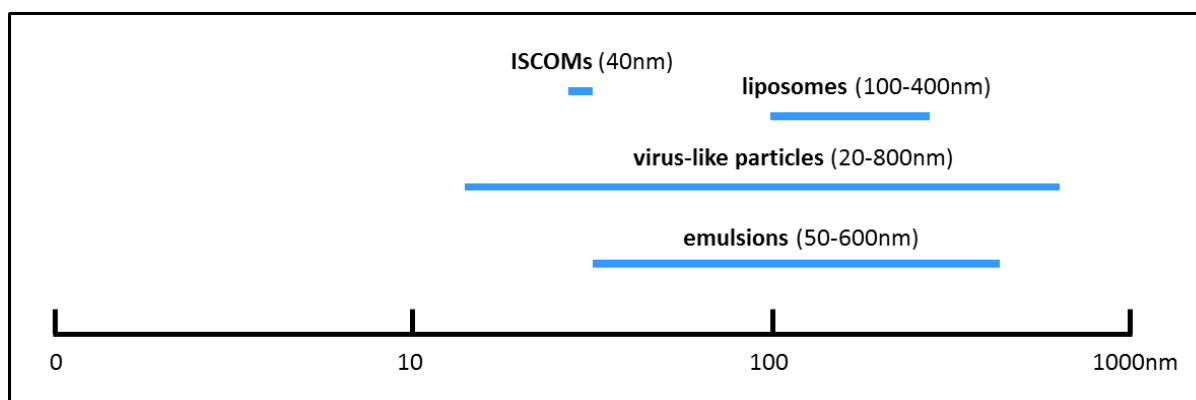
Figure 2. The relative sizes and groups of nanoparticles under investigation for vaccine delivery systems. Figure adapted from (100).

A number of VLP-based vaccines have been approved for human use or are currently in clinical trials (102, 103). However, there is limited knowledge of the safety and efficacy of non-VLP nanoparticle vaccine formulations. Increased understanding of the *in vivo* behaviour of nanoparticles, including their fate and interaction with immune cells following vaccine administration, is required to accelerate the design of these novel vaccines. This review will

focus on liposomes, their use as antigen delivery vehicles and their ability to increase antigen-specific immune responses when complexed with innate immune stimulants.

1.4.1   *Liposomes for antigen delivery*

Liposomes are phospholipid bilayer vesicles with an aqueous core. They have been extensively investigated as delivery vehicles as they are able to encapsulate molecules in their core and facilitate delivery of these molecules to specific cells (104). Liposomes can also protect vaccine antigens from degradation and enhance or modulate the immunogenicity of the vaccine. As they are composed of lipids that occur naturally in cell membranes, liposomes are also biodegradable. One major advantage of liposomes is their versatility, which allows antigens of many sizes and charges to be incorporated into the formulation (105). Variation of liposome composition can create anionic, neutral or cationic liposomes that are able to associate with antigens via electrostatic interactions (106). The surface charge of liposomes can also alter their immunogenicity, where cationic liposomes have been shown to induce stronger immunity compared with neutral or anionic liposomes (107). The mechanisms behind these effects are unclear, however as most antigens are negatively charged, cationic liposomes may enhance encapsulation and protection of antigen (104). Liposomes have also shown to be safe and well tolerated in humans. Virosomes, which are liposomes composed of virus membranes, are components of licenced influenza and hepatitis A vaccines (108, 109). Several other liposome based vaccines are currently in clinical trials; however they have not yet reached the market.

In mice, liposome antigen formulations administered intranasally were shown to be effective at inducing protective cellular and humoral immune responses against the influenza virus (110). The liposome formulation induced strong local and systemic immune responses due to long local retention in the upper respiratory tract. Antigen specific antibodies against several sub-types of the viral strains included in the vaccine were also induced, suggesting that this vaccine may offer protection against antigenic drifts during influenza infection. The vaccine formulation is needle free and has the potential to be self-administered, which should increase patient compliance, cost effectiveness and rapid distribution to large populations in the case of an influenza pandemic (110). Interestingly, this formulation was recently investigated in

ferrets, an established model of influenza infection, and was shown to significantly increase antibody titres, reduce the severity of infection following viral challenge and be well tolerated (111).

Similarly, mice subcutaneously injected with liposomes incorporating the Hepatitis B virus surface antigen (HBsAg) showed stronger Th1/Th2 immune responses and produced more antigen specific IgG1 and IgG2a antibodies than mice injected with HBsAg combined with aluminium adjuvant (112). The liposome formulation was also more effective at increasing immunity to HBsAg in non-responder recipients, inducing a 100% sero-conversion rate after two injections. The authors suggested that the capacity to overcome unresponsiveness was due to the balanced Th1/Th2 profile induced by the liposomal formulation when compared to aluminium adjuvant, which only induced a Th2 response. The physical characteristics of the liposome may have also enhanced the uptake of antigen by APCs, thereby promoting Th1 immunity (112). If future toxicological studies demonstrate these liposomes are safe for use in humans, the results of this study suggest that liposomal vaccine formulations may be used to enhance immunity in low-responder populations, such as the elderly.

Whilst enhanced vaccine immunity has been observed with the addition of liposomes, the above studies utilised antigens that inherently induce strong immune responses. There are several reports that suggest liposomes have little to weak immunostimulatory capacity with other antigens. Incorporation of ovalbumin (OVA) antigen into liposomes was shown to enhance the ability of murine bone marrow derived DCs to internalise OVA *in vitro* (113). The liposomes also mediated MHC II restricted antigen presentation to OVA specific CD4 T cells. However, despite efficient T cell activation, no increase in the maturation of DCs was observed. These results suggest that liposomes function primarily as a delivery vehicle to facilitate antigen uptake, and may not induce efficient innate cell maturation. Similar results were obtained in a separate study, where liposomal antigen formulations induced weak innate immune responses when compared to liposome formulations that incorporated an immunomodulator, such as a TLR ligand (114).

The safety and efficacy of a liposome formulation incorporating a HIV antigen was investigated in a phase I clinical trial. As the major transmission route for HIV is the genital and mucosal areas, a vaccine that effectively induces mucosal immunity and protection is required. Immunisation with recombinant HIV envelope protein subunit, gp160, was shown to be safe in healthy volunteers, however only weak HIV specific antibody and CTL

responses were induced after vaccination (115). This study investigated the ability of a liposomal formulation to improve the immunogenicity of gp160 in HIV seronegative female volunteers (116). Following vaccine administration either intranasally or by the vaginal route, no anti-gp160 antibodies were detected in serum, saliva, cervicovaginal or nasal secretions, even after three immunisations. However, the liposome formulation was shown to be safe and well tolerated in these subjects (116).

It is difficult to compare the studies investigating liposomal efficacy, as there are many factors that influence the findings, including route of administration, composition of liposome, antigen dosage and choice of experimental model. Modern vaccines are now being developed to deliver both antigen and adjuvant to a single APC to induce the most appropriate immune response. Liposomes (antigen delivery) complexed with TLR ligands (adjuvant) have been shown to enhance adaptive and memory immunity.

1.4.2   Liposomes incorporating TLR ligands

Liposomes incorporating MPL were investigated in a mouse model of TB utilising the antigen ESAT-6 (117). This study showed that the formulation induced potent antigen specific T cell responses and elicited protective immunity that was comparable to the licensed *Mycobacterium bovis* BCG vaccine. The liposome antigen formulation without MPL did not induce antigen specific immune responses. Likewise, MPL and antigen formulations without liposomes also demonstrated low efficacy (117). This suggests that combinations of liposomes and TLR ligands demonstrate higher efficacy than when either is administered alone.

Immunity induced by liposomal MPL formulations was also investigated in humans against the hepatitis B surface antigen (118). This study found that 80% of the subjects acquired seroprotective antibody levels after a single dose. The formulation also induced strong and persistent Th1 cell mediated immunity after a second administration. These results are consistent with previous findings that investigated the same formulation incorporating a malaria antigen in rhesus macaques (119). The safety of the formulation was also investigated, with tolerable local symptoms occurring in most subjects and no serious adverse events reported. Interestingly, a third administration of the formulation did not significantly enhance immunity and was often linked to higher reactogenicity (118). This suggests that a two dose

immunisation procedure would be appropriate to provide the critical balance between immunogenicity and safety.

Liposomes incorporating poly(I:C) and OVA antigen induced strong CD8 T cell responses in mice that were maintained for more than two months (120). Interestingly, the liposomal formulation prevented the rapid and non-specific production of the pro-inflammatory cytokines TNFα and IL6 in the serum that occurred after injection of free poly(I:C). This study highlights the importance of appropriate formulation design when investigating the safety of innate stimulators as adjuvants. Liposomes containing poly(I:C) can also limit the dose of antigen and number of immunisations required to induce immunity. Antigen-specific IgG and IgA responses were induced by immunisation of mice with liposomal poly(I:C) incorporating lower quantities of a human para-influenza virus antigen. No antigen specific immune responses were observed in mice immunised with liposome and antigen alone (121). A study in mice also found that liposomes formulated with poly(I:C) or CpG induce effective CD8 T cell responses *in vivo*, protecting against *M. tuberculosis* aerosol challenge and generating effective anti-tumour immunity (122). Similar anti-tumour activity of liposomal poly(I:C) has been reported in several studies, where this formulation was more potent than poly(I:C) alone or liposomes alone at inducing tumour-specific immune responses and suppressing tumour growth in mice (123, 124). Liposomal poly(I:C) uniquely enhanced DC maturation and production of type I IFN, suggesting that this may promote the superior anti-tumour immunity observed by this formulation. Taken together, these results suggest that liposomal poly(I:C) may act as an effective adjuvant to increase the therapeutic efficacy of cancer vaccines.

The immune response generated in mice immunised with the *Leishmania* antigen rgp63 co-administered with liposomes containing CpG has also been investigated (125). The protection induced by liposomal CpG was significantly greater than that induced by CpG alone for up to 14 weeks after parasitic challenge. This formulation also increased the concentration of IFNγ, reduced the level of IL4 and induced greater IgG2a antibody production when compared to CpG alone, suggesting that liposomal CpG preferentially induces a more potent Th1 immune response (125). In a mouse model of influenza, CpG loaded liposomes were more efficient at enhancing hemagglutinin specific IgG2a humoral immune responses when compared to liposomes alone (126). Similar effects were also demonstrated when CpG encapsulated liposomes were utilised as a vaccine for both influenza and hepatitis B in mice. A low dose of liposomal CpG co-administered with a low dose of viral antigen was up to 30 fold more

potent than a high dose of soluble CpG (127). In this study, CpG was equally effective as an adjuvant when entrapped in the same liposomes with the antigen or in separate liposomes. Interestingly, the type of immunity elicited by the formulation was influenced by the nature of the antigen and the route of administration. Intramuscular injection induced a strong Th1 response against influenza whilst intranasal administration induced a mixed Th1/Th2 response against hepatitis B (127).

It is therefore clear that liposomal formulations incorporating both antigen and adjuvant are able to significantly enhance the immunogenicity of each component alone. The enhanced innate activation observed with liposomal poly(I:C) and CpG may be due to the ability of liposomes to promote entry of the adjuvant to the endosome, where the TLR 3 and TLR 9 receptors are expressed. Additionally, it has previously been shown that when CpG is administered in liposomal form, the proximity of the antigen and adjuvant is maintained and the *in vivo* degradation of CpG is reduced (128). These factors may account for the enhanced immunogenicity of these liposomal formulations; however the precise mechanisms that control these effects are unclear, including the cellular and molecular targets of these formulations at the site of injection. Whether poly(I:C) and CpG target similar or distinct biological pathways to induce their immunostimulatory effects *in vivo* also remains to be elucidated. The safety and efficacy of liposomal CpG and poly(I:C) are also largely unknown, and this needs to be evaluated in the target species. Further studies are also required to define the optimal liposomal formulations and the routes of administration, which may have to be tailored to each antigen.

1.5   Large animal models for vaccine research

Experimental mouse models continue to dominate the field of immunology, yielding tremendous insight into the cellular and molecular components of the immune system. There are a number of advantages for the use of these models, including the ability to breed a range of genetically identical and easily manipulated strains of mice (26, 129, 130). Many studies that have defined the biological pathways of adjuvant activity have been performed in genetically engineered mice. The information obtained from these studies has been and will continue to be vital for the theoretical understanding of the immune system in health and disease. However, the experimental conditions often do not reflect the practice of human vaccination, and it is common for these studies to be performed *in vitro* (48).

To some extent, these limitations can be addressed by the use of large animal models, representing outbred populations with physiologies that are similar to humans (8). They are particularly useful for the investigation of vaccine delivery, as it is possible to follow immune responses in real time within a single animal (129). In addition, such studies can be directly relevant to vaccination in veterinary practice for both companion animals and commercial livestock. However, there are also disadvantages to large animal models, including a lack of inbred and genetically manipulated animals. Their large size also makes housing both difficult and expensive. Although there is lower availability of appropriate reagents for large animals than those available for mice, reagents have been developed for key parameters of immunity and will continue to be produced as both the bovine and ovine genomes have recently become available.

Vaccine formulations incorporating innate stimulators as adjuvants have been shown to induce disease protection in several large animal species. Poly(I:C) combined with a novel foot-and-mouth viral vaccine completely protected pigs against virulent viral challenge after a single injection. This study also found that addition of poly(I:C) to the vaccine reduced the animal to animal variation observed with the vaccine alone (131). CpG added to a formalin-inactivated bovine respiratory syncytial virus vaccine increased cellular immunity against the virus, inducing IFNγ secretion and a reduction in viral load of the lungs in calves (132). Similar results were also observed in newborn piglets, where CpG increased cellular and antibody mediated immune responses to a pseudo-rabies attenuated virus vaccine (133). The

results from these studies suggest that innate stimulators have an immunostimulatory function that is conserved across multiple species. Large animal models can therefore provide valuable information on the safety and efficacy of novel vaccine formulations and adjuvants in an outbred population similar to humans. Of particular interest for vaccine development is the immune response initiated in the lymphatic network draining the site of injection. This compartment cannot be investigated in mouse models as the lymphatic vessels are technically too difficult to access. Several large animal lymphatic cannulation models have been developed to investigate the cellular and soluble factors required for the generation of an effective immune response in the local lymph node following vaccine administration.

1.6   Lymphatic cannulation models

The early immune response to vaccination at the site of injection is characterised by a rapid and significant increase in cells and inflammatory factors present in the afferent lymph. These activated cells are transported to the local draining lymph node via the afferent lymphatic vessels, where they convey the immunological signals received in the periphery to functionally specialised areas within the lymph node. Antigen-bearing DCs present their antigens to specific T and B cells, which differentiate into effector cells and migrate out of the lymph node via the efferent lymphatics which eventually drains back into the circulation (Figure 3). After the pathogen has been eliminated, a subset of these effector lymphocytes remains in the lymphatic system and circulation as memory cells.
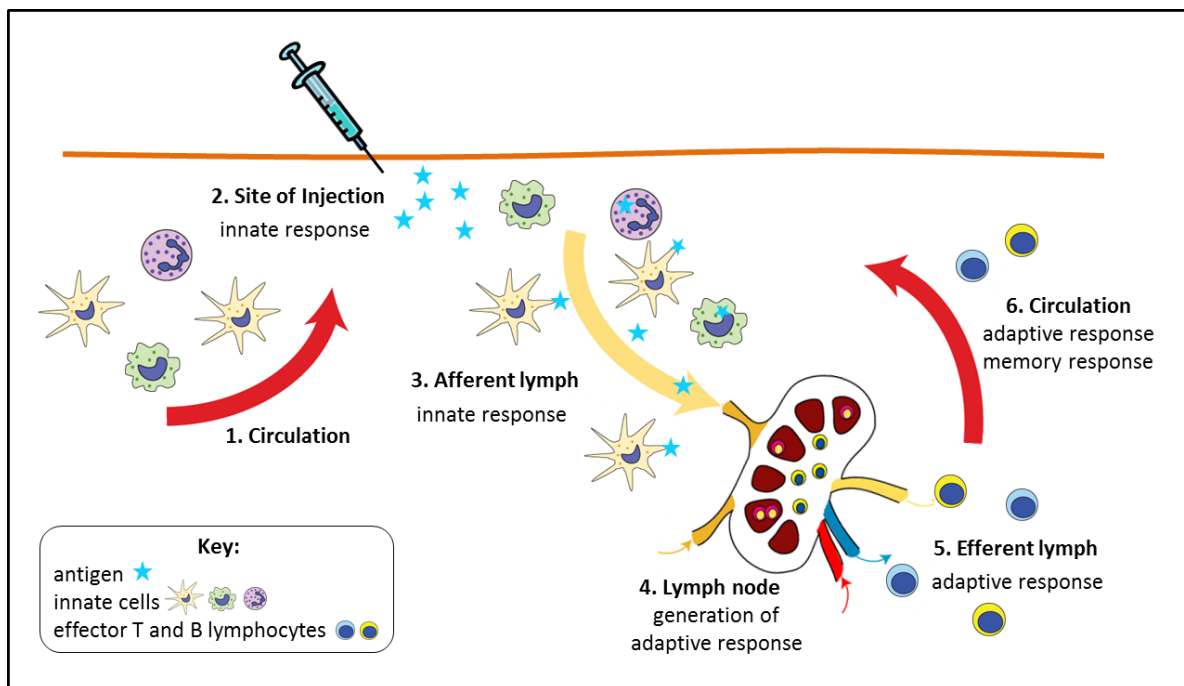
Figure 3. Schematic of the immune response to vaccination. The innate response occurs at the site of injection and within the afferent lymph. This is followed by the generation of an adaptive immune response in the local lymph node. The antigen-specific effector lymphocytes leave the lymph node via the efferent lymphatic, which eventually drains back into the blood, where they perform their effector and memory functions.

1.6.1   Afferent lymphatic cannulation

The afferent lymphatics are crucial in the development of primary immune responses as they carry both antigen and immune cells to lymph nodes. In fact, the components of afferent lymph in both homeostatic and stimulated conditions have been extensively studied, yielding valuable information regarding the processes involved in innate immune responses to infection and vaccination. Due to their small size, the afferent lymphatic vessels are difficult to surgically access, even in large animals. Consequently, a two-step surgical procedure must be performed in order to cannulate these vessels for long term studies (Figure 4). The first step involves surgically removing the local lymph node. Over a period of 2-3 months, the small afferent lymphatic vessels re-anastomose with the remaining efferent vessel forming a much larger vessel, termed the pseudo-afferent lymphatic vessel. Cannulation of this newly formed vessel allows the direct collection, in real time, of the components in afferent lymph that would normally traffic from the tissue into the local lymph node. There are several established afferent lymph cannulation procedures in various large animal models. The most characterised of these is the ovine model, which comprises cannulation of the intestine (134), head tissues (135, 136), and the hind leg, including prefemoral (137) and popliteal (138) cannulation. Most bovine afferent lymph studies have used the prescapular cannulation model (139). There are also two procedures established in pigs, the lumbar (140) and intestinal cannulations (141). In addition to large animal models, the rat cannulation models have been thoroughly characterised, most of which have been performed by accessing the thoracic lymphatic duct to sample lymph from the intestine (142) and the liver (143). As it does not originate from a single lymph node, this type of lymphatic cannulation often results in the collection of a mixture of afferent and efferent lymph. Following removal of the regional lymph nodes, innate phagocytic cells, including dendritic cells, have been observed in lymph collected from the thoracic duct (141,142).

Under homeostatic conditions, there is a continual migration of cells circulating through the tissue and the blood via the afferent lymphatics. These cells monitor the tissue for the presence of invading organisms and are ready to respond upon antigenic challenge. The afferent lymphatic cannulation models therefore provide a unique opportunity to investigate the phenotype and function of the innate cells that are emigrants from peripheral tissue and

carry the instructions required for the initiation of a primary immune response in the lymph node.
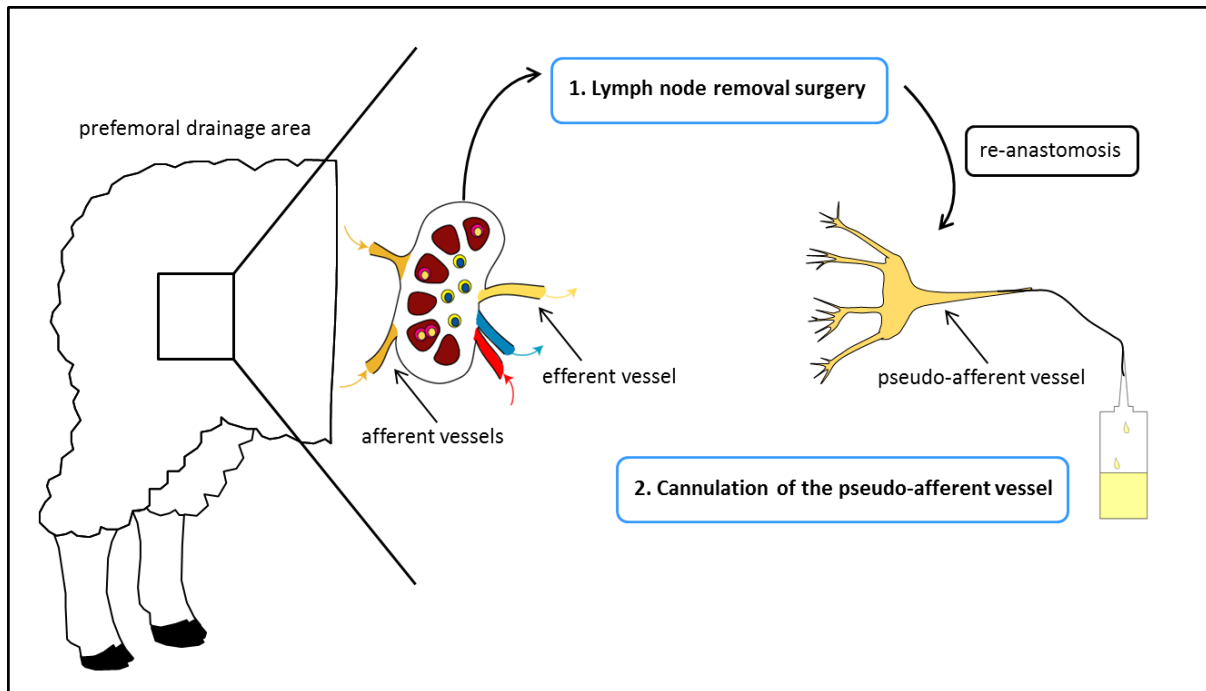
Figure 4. Schematic of the prefemoral ovine pseudo-afferent lymphatic cannulation model. A two-step surgical procedure must be performed to collect afferent lymph. The first surgery involves removal of the prefemoral lymph node. Following this, a recovery period is given, allowing the afferent vessels to re-anastomose with the remaining efferent vessel forming the pseudo-afferent vessel. This vessel is large enough to cannulate. Many peripheral lymphatic vesssels can be cannulated in this manner, the figure above shows ovine prefemoral lymphatic cannulation.

Two major populations of conventional DCs have been identified in the afferent lymph of various tissues (Table 2). These populations are remarkably consistent in both phenotype and function across the different species. In the ovine models, the two DC subsets can be identified as CD26$^-$ SIRPα^{high} DCs and CD26$^+$ SIRPα^{low} DCs (144, 145). In the bovine models, they are CD11a$^-$ SIRPα^{high} DCs and CD11a$^+$ SIRPα^{low} DCs (146-148). In the swine models, the two major DC subsets are CD163$^{\pm}$ SIRPα^{high} DCs and CD163$^-$ SIRPα^{low} DCs (149, 150). Finally, in the rat models, they are identified as CD4$^+$ SIRPα^{high} DCs and CD4$^-$ SIRPα^{low} DCs (151, 152). In all defined animal models, the SIRPα^{high} DCs are more efficient at antigen uptake, presentation and activation of CD4+ T cells than the SIRPα^{low} DCs. The SIRPα^{high} DCs have also been shown to produce inflammatory cytokines IL-1 and IL-6 after TLR stimulation (147, 151-156). In contrast, the SIRPα^{low} DCs are less efficient at antigen uptake and stimulation of CD4+ T cells, and appear to be specialised in the transport of apoptotic

bodies and are more efficient at cross-presenting antigen to CD8+ T cells (144, 145, 147, 156). In the ovine model, this cross presentation was shown to be mediated by the unique expression of XCR1 on this DC subset (157). Recently, a comparative genomics study revealed that the function and phenotype of these two DC subsets was uniform across multiple species. The ovine SIRPα^{high} DCs were shown to genetically and functionally represent the mouse CD11b+ DC and the human BDCA1+ DC (144). Similar to the SIRPα^{high} DCs found in afferent lymph, mouse lymphoid tissue CD11b+ DCs are specialised to activate and present antigen to CD4+ T cells (158, 159). The comparative study also revealed that the ovine SIRPα^{low} DCs represent the mouse CD8α+ DC and the human BDCA3+ DC (144). The mouse CD8α+ DC appear to be more efficient at cross priming and tolerance and play a similar role to the SIRPα^{low} DCs found in afferent lymph (158). This unified function between sheep, cow, rat, mouse and human migratory DCs provides compelling evidence that DC function and phenotype is conserved across multiple species. It also highlights that significant information can be gained from using comparative genomics as a tool to study immunological processes (160). As more information is gained about the function of afferent lymph DCs during the early stages of infection, the potential exists to target these cell types for the induction of antigen specific immune responses in future vaccine or therapeutic settings.

Although DCs are the most characterised cell type in afferent lymph, other innate cell populations, such as monocytes and granulocytes, also carry antigen and immunostimulatory signals to the lymph node (Table 2). Monocytes have been defined as CD14^{high} CD11b^{high} cells that express low to intermediate levels of MHC class II. They are responsible for antigen uptake within the first 48h after administration of antigen (161-163). Granulocytes can be distinguished from monocytes based on their size (forward scatter; FSC) and granularity (side scatter; SSC) characteristics in flow cytometry and low expression of CD14 (163). Granulocytes, particularly neutrophils, have been shown to rapidly recruit to sites of inflammation within the first 24h, and the severity of inflammation positively correlates with the presence of neutrophils in the afferent lymph (164). This rapid increase in neutrophil number is associated with increased antigen uptake between 6h and 24h post injection (161, 162). Overall, these data suggest that DCs are not the only cell type able to carry antigen and other immunostimulatory signals *in vivo* and immunity to pathogens is likely to result from a combination of innate cells transmitting signals from the periphery to the lymph node.

There are also several studies that investigate T cell subset phenotypes within the afferent lymph. The majority of T cells circulating in afferent lymph are of the memory phenotype (CD4+ CD45R-) and are able to respond to previously encountered antigen (165). CD4 T cells, CD8 T cells and γδ T cells have all been identified in afferent lymph. During inflammation, there is an increase in γδ T cells and CD4 T cells in the afferent lymph (164). Activated CD8 T cells derived from lymph have been shown to possess cytolytic function *in vitro* (166). T cell populations in the swine intestinal lymph have been identified, including a unique CD4+ CD8+ double positive subset, however their function during a primary immune response has not been established (167). In homeostatic conditions, there is a sustained migration of a large number of γδ T cells in afferent lymph (165, 168). These cells do not express the costimulation factors CD40 and CD86, the IL-2 receptor or MHC class II (168). In addition, afferent lymph γδ T cells do not express the chemokine receptor CCR7, which is required for entry into the lymph node via interaction with its ligand CCL7 present on high endothelial venules (169). The migration pattern of this unique T cell subset and their function in inflammatory or infectious conditions in several animal models is largely unknown and future work is required to elucidate this.

There are several studies investigating the phenotype of B cells in afferent lymph. CD21+ B cells have been identified in the skin draining afferent lymph of calves (168), MHC II+ CD45R+ Ig+ B cells have been found in the mesenteric afferent lymph of rats, and CD45R+ B cells have been identified in the skin draining afferent lymph of sheep (164). A recent study revealed that these sheep skin draining B cells also express MHC II, pan-B cell marker 2-104, CD11b, CD21, L-selectin, B7.1/B7.2 and IgM (170). In both homeostatic conditions and during skin inflammation, these afferent lymph B cells displayed higher expression of CD11b, B7.1/B7.2 and IgM when compared to B cells from skin lymph nodes. Additionally, during inflammation, there was an increase in the number of afferent lymph B cells as well as an increase in total antibody levels in the afferent lymph supernatant (170). These results suggest a novel role for skin-derived B cells during chronic inflammation of the skin.

Taken together, the innate cell populations within the afferent lymph are well defined and appear to be consistent between species. The afferent cannulation model allows the direct collection of lymph without further processing or cellular manipulation, generating results that closely resemble the immunological processes occurring *in vivo*. Additionally, a major advantage of the afferent cannulation model is the ability to follow immune responses as they occur in real time.

Table 2. The phenotype and function of cellular populations identified in afferent lymph.

Cell Subset	Phenotype	Function
OVINE		
SIRPα^{high} DC	Sirpα+ CD26- MHCII+ CD45RA+ CD86+ DEC-205+ CD206+ CD207+ CD14+	equivalent to mouse CD11b+ DC, human BDCA1+ DC, mRNA expression: IL-10, IL-1β
SIRPα^{low} DC	Sirpα- CD26+ CADM1+CLEC9A+ CD205+ XCR1+ MHC II+ CD45RA- CD86+ DEC-205+	equivalent to mouse CD8α+ DC and human BDCA3+ DC, activate CD8+ T cells via cross presentation and transport apoptotic bodies, mRNA expression: IL-12p40
Plasmacytoid DC	CD11c-DEC-205- CD14- CD45RB+	production of type1 IFN
Monocytes	CD14+ CD11b+	antigen uptake
Granulocytes	CD14int CD11b+	antigen uptake, early recruitment to site of inflammation
CD4+ T cells	CD4+ IL-2Rα+ FSC/SSC low	increased migration during inflammation
CD8+ T cells	CD8+ FSC/SSC low	cytotoxic function *in vitro*
γδ T cells	γδ TCR+ IL-2Rα+	increased migration during inflammation
Memory T cells	β1+ CD2+ CD45R- L-selectin- β7+	
B cells	CD45R+ MHC II+ CD11b+ CD21+ L-selectin+ B7.1/B7.2+ IgM+	
BOVINE		
SIRPα^{high} DC	Sirpα+ CD11a- CD5-WC10- CD11c+ DEC205+ CD8- CC81Ag-	*in vivo* antigen uptake, activate CD4+ and CD8+ T cells *in vitro,* produce IL-1, mRNA expression: IL-6, IL-10, no type 1 IFN
SIRPα^{low} DC	Sirpα- CD11a+ CD5+ WC10+ CD11c+ DEC205+ CD8- CC81Ag+	transport apoptotic bodies *in vivo,* unable to present antigen to T cells *in vitro,* produce IL-12, no type 1 IFN
Monocytes	CD14+ CD11b+	
Granulocytes	CD11b+ CD14low	
CD4+ T cells	CD4+ CD26L+ CCR7+ β1+ β2+ mRNA: CCR4+ CCR10+	
γδ T cells	γδ-TCR+ CCR7- CD26L+ WC1+ β1+ β2+ CD40- CD86- MHC II- CD4- CD8- CD25- CD1b- CD2- CD3+	migrate in large numbers, no evidence for IFN-γ, TNF-α or IL-1 production after stimulation, mRNA expression: CCR4+ CCR10+
NK cells	CD335+	production of IFN-γ after stimulation
B cells	CD21+	
SWINE		
SIRPα^{high} DC	Sirpα+ CD163± CD11b+	activate resting CD4+ T cells,migrate in semi mature state and matured upon PAMP stimulation, intestinal DCs do not stimulate proliferation in PBMC suggesting tolerogenic function
SIRPα^{low} DC	Sirpα- CD163- CD11b+	
Plasmacytoid DC	CD4+SIRP+	production of type1 IFN
CD4+ T cells	CD4+ CD2+	
CD8+ T cells	CD8+ CD2+	majority of T cells in afferent lymph are CD8 positive
CD4+ CD8+ T cells	CD4+ CD8+ CD2+	
RAT		
SIRPα^{high} DC	Sirpα+ MHC II+ CD11b/c^{low} CD32^{low} CD4+	IL-6 and IL-12p40 secretion after activation by TLR ligands, present antigen and stimulate proliferation in CD4+ T cells 20 fold more potently than Sirpα- DC , mRNA expression: TLR 7- TLR8+
Sirpα^{int} DC	Sirpα^{int} MHC II+ CD11b/c^{high} CD32^{high}	activate naïve T cells to produce Th1 cytokines, mRNA expression: TLR7- TLR8+
SIRPα^{low} DC	Sirpα- MHC II+ CD11b/c^{int} CD32^{int} CD4-	activate naïve T cells to produce Th1 cytokines but to a lesser extent than the other subsets, poor stimulators, transport apoptotic enterocytes and cytoplasmic apoptotic DNA, tolerogenic/specialised to acquire self antigen, mRNA expression:TLR7- TLR8-
Plasmacytoid DC		Not identified in hepatic and intestinal lymph
B cells	MHCII+ CD45R+ TCRαβ-CD45RA- Ig+ CD5- CD90-CD200- Siglec-H-	

Data from the literature, white spaces refer to information not available

1.6.2   *Efferent lymphatic cannulation*

Once activated by immunological signals received within the lymph node, antigen specific lymphocytes migrate out of the lymph node via the efferent lymphatic vessel, which eventually drains into the circulation (171). The efferent lymph is therefore ideal to study the phenotype and activation status of lymphocytes during the adaptive phase of the immune response. This surgical procedure is less technically difficult than afferent lymphatic cannulation, with the efferent lymphatic vessel large enough to be directly cannulated (Figure 5).
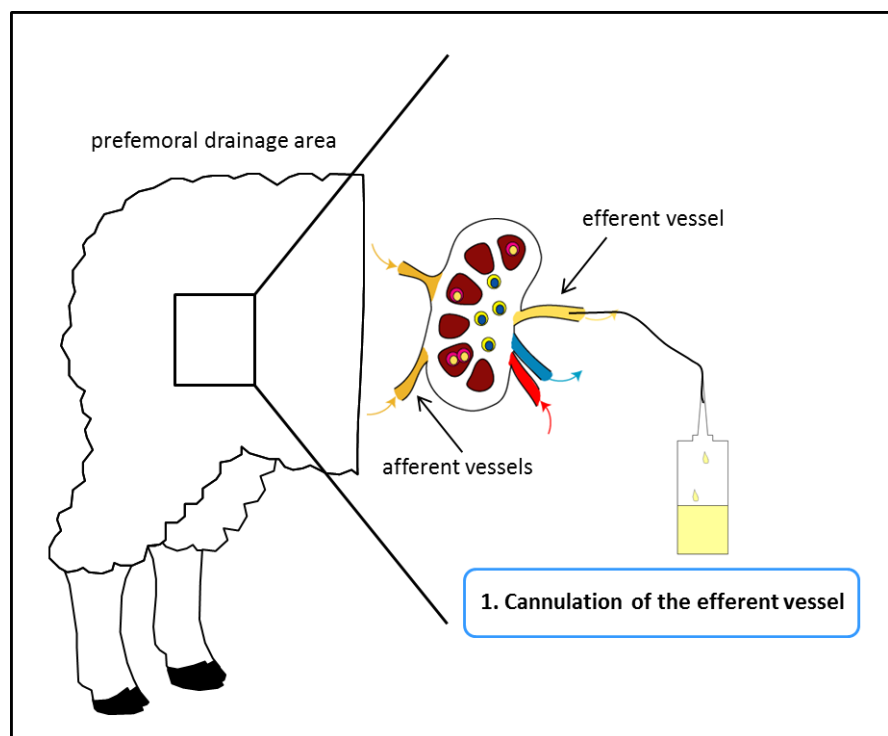
Figure 5. Schematic of the prefemoral ovine efferent lymphatic cannulation model. The efferent lymphatic vessel is large enough to directly cannulate, and therefore only one surgery is required for this lymphatic cannulation model. Many efferent lymphatic vesssels can be cannulated in this manner, the figure above shows ovine prefemoral lymphatic cannulation.

Efferent lymph cell populations are less diverse than afferent lymph cells. Efferent lymph is composed of 99% lymphocytes, including CD4 T cells, CD8 T cells, γδ T cells and B cells (Figure 6). Unlike lymphocytes in afferent lymph, the lymphocytes circulating in efferent lymph display a naïve phenotype (171). Large blast cell populations have also been identified in efferent lymph 3 days after local challenge with the parasite *T. circumcincta* (172). Innate cell populations, such as dendritic cells and monocytes, have not been identified in efferent

lymph under homeostatic conditions, suggesting they are recycled after reaching the lymph node. There are profound differences between afferent and efferent total cell output and lymph flow rate. In a resting state, total cell numbers are approximately 10 fold greater and lymph flow rate per hour is approximately 2 fold higher in efferent lymph (173, 174).
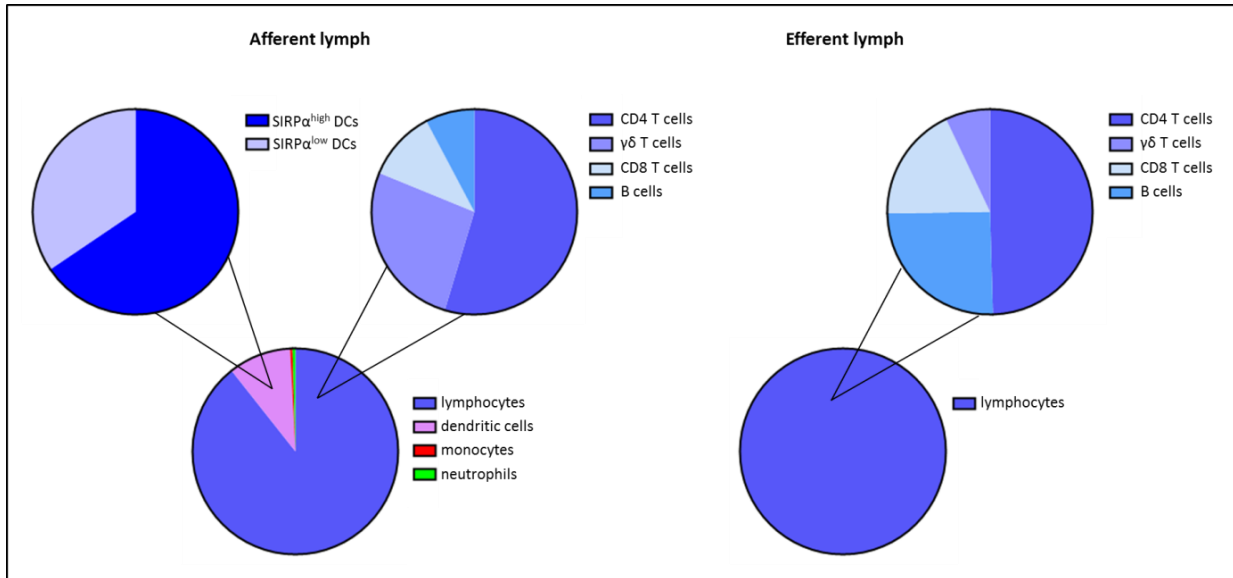
Figure 6. The cellular composition of afferent and efferent lymph. Afferent lymph is composed of lymphocytes, dendritic cells, monocytes and neutrophils. Efferent lymph is composed of 99% lymphocytes. Populations and relative percentages obtained from the authors laboratory.

Under inflammatory conditions, a dramatic bi-modal change in cell output and flow rate is observed in efferent lymph. The initial phase, known as 'lymph node shutdown', is characterised by a severe reduction in cell output, generally lasting between 4h and 24h after stimulation (175). This is followed by a recruitment phase, where the cell output increases to greater than baseline numbers for several days (176). This effect has been observed in ovine efferent lymph after injection of the pro-inflammatory cytokines TNFα and IL6, with the shutdown period lasting between 10h and 48h in different animals (174). Injection of mycobacterial purified protein derivative (PPD) also induced lymph node cell shut down, and increased concentration of the cytokines IFNγ and IL6 were observed during this process (177). It has been hypothesised that this cell shut down occurs to increase the time for antigen carrying APCs and antigen specific lymphocytes to interact in the lymph node, promoting the generation of an adaptive immune response. However, the immunological role and mechanism of lymph node cell shut down remains unclear.

Efferent lymphatic cannulation allows the direct collection of lymphocytes and soluble factors involved in the immune response following innate activation in the local lymph node. These immune responses can be followed within a single animal for several weeks following primary or secondary injection of antigen or immunomodulatory agents. Further characterisation of the cellular populations in efferent lymph will yield valuable information regarding the *in vivo* adaptive immune response induced by vaccination.

1.7 Vaccine immunity in the lymphatic network

1.7.1 Innate immune responses in afferent lymph following vaccination

Several studies have utilised the afferent lymphatic cannulation model to study immune responses to vaccine adjuvants and delivery systems. Our laboratory investigated the real time *in vivo* release of soluble antigen and the cellular uptake of particulate antigen following injection with aluminium adjuvant (161). We found that aluminium adjuvant significantly reduced the amount of soluble antigen entering the afferent lymph in the first 24h by 60% when compared to antigen injected with saline. Aluminium adjuvant also increased the number of DCs carrying particulate antigen 24h-72h following injection. These results suggest that the ability of aluminium adjuvant to both retain antigen at the site of injection and increase the phagocytic function of DCs may account for its enhanced adjuvanticity (161). We also showed that antigen co-injected with the adjuvant MPL induced a rapid and significant increase in neutrophil and monocyte recruitment into the afferent lymph 0-12h post injection when compared to antigen injected with saline (162). MPL also induced a greater and more sustained uptake of particulate antigen (antigen-coated fluorescent beads) over a 24h period by DCs, neutrophils and monocytes, with the majority of particulate antigen carried by the neutrophil population. Although neutrophils carried the majority of single particulate antigen, DCs were the most effective scavengers of multiple beads with over 30% of antigen positive DCs carrying four or more beads in both saline and MPL treated groups (162). Afferent lymphatic cannulation has also been used to study nanoparticle-based adjuvants (178). This study showed that afferent lymph DCs are able to ingest the 40-50nm nanoparticles 3 hours after immunisation

Oral administration of resiquimod (R-848), a synthetic agonist of TLR 7 and 8, has been shown to induce potent innate immune stimulatory activity, including stimulating DCs to up-regulate costimulatory factors and produce large amounts of pro-inflammatory cytokines. R-848 has also been shown to skew the immune response towards a Th1 antibody response and inhibit the production of a Th2 response (179). Intestinal afferent lymphatic cannulation allowed the *in vivo* analysis of the immune response to R-848 in an anatomically relevant tissue after oral administration. Yrlid and colleagues analysed the effects of oral R-848 on

DCs derived from the intestinal lymph of rats (180). They found that R-848 induced an approximate 30 fold increase in intestinal lymph DCs; however it did not stimulate the up-regulation of the costimulatory molecule CD86 but CD25 was up-regulated. In a follow up study, the same group characterised the DC subsets that were migrating from the intestine in response to R-848 (151). They found that intestinal lymph DCs consist of three subsets: $SIRP\alpha^{high}$, $SIRP\alpha^{int}$ and $SIRP\alpha^{low}$. These subsets do not express TLR 7 mRNA and only the SIRPα positive subsets express TLR 8. All three subsets increase their migration after R-848 administration, suggesting that even though the TLR 7^- TLR 8^- $SIRP\alpha^{low}$ DC subset cannot respond to R-848 directly, it is being induced to migrate by other factors of the immune system. In addition, only TLR 8^+ $SIRP\alpha^+$ DCs express CD25 and of these subsets, only the $SIRP\alpha^{high}$ subset secretes IL-12p40 and IL-6 without further *in vitro* stimulation. Taken together, these results provide new information about the role of TLR ligand expression on afferent lymph DCs and their consequent function in response to oral adjuvants. This study also provides evidence for intestinal afferent lymph DC subsets as suitable targets for orally administered vaccines.

Due to their superior ability to infect and manipulate host cells to express viral proteins, viruses are ideal candidates for vaccine delivery vehicles that induce antigen specific immune responses. A viral vector vaccine is designed to express the desired antigen and the resulting recombinant virus can infect host cells, leading to the expression of the antigen on the cell surface and subsequent presentation to the immune system (181). Cattle inoculated with recombinant human adenovirus 5 (rhuAdV5) GFP vector with the addition of oil adjuvant showed a significant rise in migrating GFP-expressing DCs during the first 15h (182). To investigate the antigen specific function of these vectors *in vivo*, rhuAdV5 expressing foot and mouth disease virus (FMDV) was injected with or without oil adjuvant. While both injections resulted in FMDV-specific IgG antibody responses, the addition of adjuvant caused an increase in the frequency of CD4+ IFN-γ+ and CD4+TNF-α+ T cells and also increased CD4+ T cell IFN-γ release. These results suggest that the immune response to antigen delivered *in vivo* by viral vectors can be enhanced by the addition of oil adjuvant (182).

1.7.2 Adaptive immune responses in efferent lymph following vaccination

Few studies have investigated the adaptive immune response in efferent lymph induced by vaccination. Immunisation of cattle with mononuclear cells infected with the protozoan *Theileria annulata* induced the activation of CD4 T cells that proliferated in an antigen-specific manner after *in vitro* stimulation (183). Activated CD8 T cells were observed following this response, suggesting that antigen-specific CD4 T cells may play a role in the activation of CD8 T cells. Both CD4 and CD8 T cell responses in efferent lymph appeared earlier and were stronger than in peripheral blood, indicating that the antigen-specific immune response was generated in the local lymph node (183). A recent study investigated the primary immune responses generated by vaccination with 70 kDa heat-shock protein (Hsp70), which has previously been shown to be protective against paratuberculosis in cattle (184). The results demonstrate that vaccination with Hsp70 induced proliferation of CD4 T cells and B cells in efferent lymph between 3 and 5 days following vaccination. Hsp-70 specific antibodies were detected from day 7 (184). Injection of a circular plasmid containing the adjuvant CpG induced a rapid increase in the number of cells present in efferent lymph 24h after injection (185). This effect was shown to be dose dependent, such that excessive amounts of CpG had no effect on cell trafficking. Interestingly in this study, CpG did not increase the activation status of lymphocytes in efferent lymph at any time after injection (185).

A separate study found that local injection of Flu antigen combined with the adjuvant ISCOMATRIX resulted in an extended lymph node cell shut down period and increased blast cell production when compared to Flu antigen alone (186). The subsequent recruitment phase persisted for up to 11 days, 2.5 fold longer than antigen alone. Significant increases in antigen-specific antibodies were also observed, with the antigen and adjuvant combination inducing a substantial IgA antibody response (186). Increased antigen-specific antibody responses have also been observed following vaccination with a variety of adjuvants, where increased IgG1 and IgG2 titres were observed following vaccination with incomplete Freund's adjuvant when compared to aluminium adjuvant (187). The cytokines IFNγ and IL8 were only detected in efferent lymph following injection of Quil A (187, 188).

Collection of afferent and efferent lymph following vaccination can assist in revealing the mechanisms involved in the generation of protective cellular and humoral immune responses. In this thesis, the ovine prefemoral afferent and efferent lymphatic cannulation models have been utilised in combination to investigate the immunogenicity of vaccine adjuvant formulations in the local draining lymphatic network of vaccinated sheep. The results obtained from these models can be directly applied to and assist in the design of novel veterinary and human vaccine formulations.

1.8   Investigating vaccine immunity: a systems biology approach

The immune response to vaccination requires the synergistic interaction of multiple biological pathways. The complexity of this immune response highlights the need for a systems biology approach to vaccine development (189). The tools of systems biology include high-throughput technologies such as microarrays, deep sequencing and mass spectrometry. These are used in combination with immunological assays, such flow cytometry and cytokine profiling, to assess the whole immune response at multiple biological levels (190) (Figure 7).
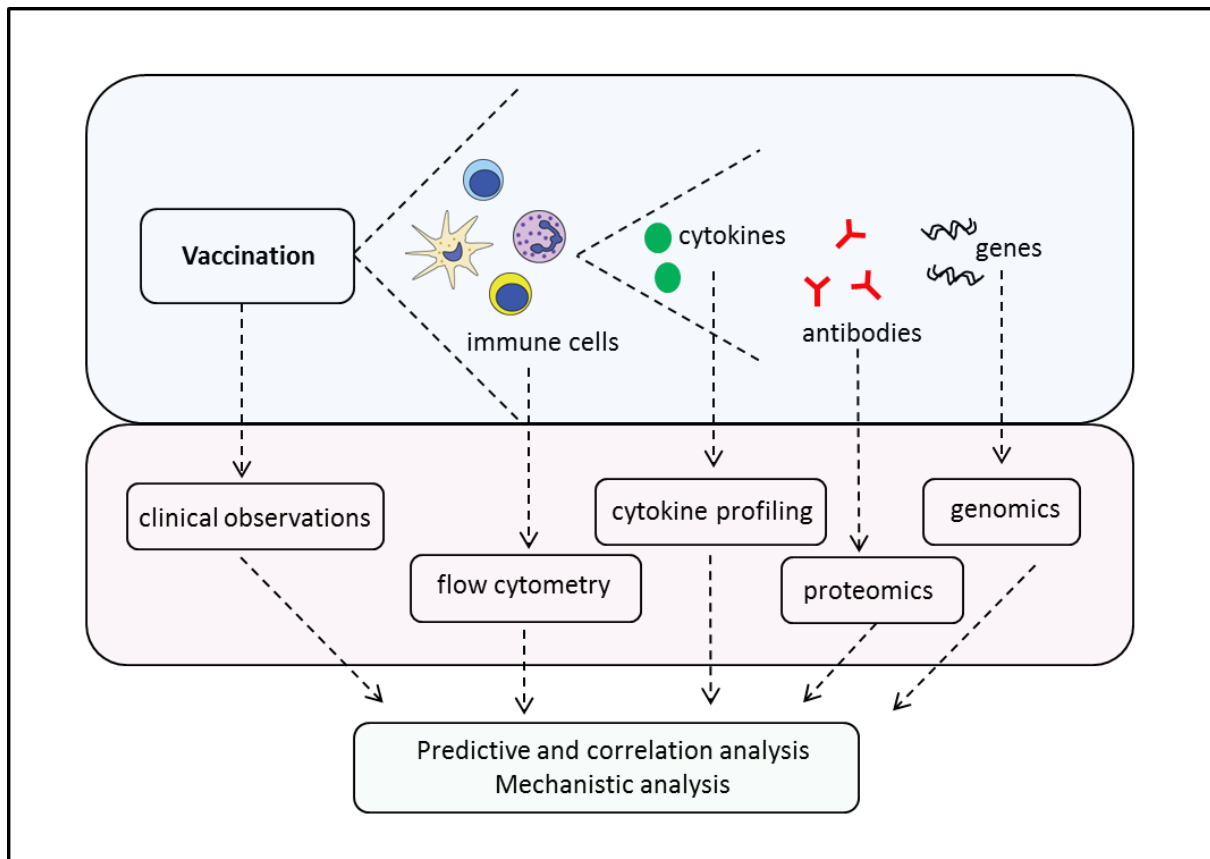
Figure 7. Investigating vaccine immunity with systems biology. This involves analysing the whole immune response at multiple levels, including cellular, protein and transcriptomic responses, to reveal the mechanisms of vaccine efficacy and predict immune outcomes. Figure adapted from (190).

Systems biology approaches have been successful in revealing the genetic signatures predictive of the immune response to vaccination in humans. TLR 7, RIG-I, STAT1 and IRF7 were identified as the genes responsible for innate sensing and signalling immediately following vaccination with the yellow fever vaccine (YF17D). Similarly, the antiviral type I interferon, complement and inflammasome pathways were revealed as genetic signatures during the development of the adaptive immune response 3-7 days after vaccination (191, 192). Computational modelling was also used to predict adaptive immune outcomes from early gene expression signatures, yielding at least 80% accuracy in predicting the magnitude of the immune response (191). Predictive modelling was also applied to an inactivated influenza vaccine, where the gene expression signatures of individuals on day 3 or 7 post vaccination could accurately predict the antibody responses that occurred in these individuals 30 days after vaccination (193). A systems biology approach to vaccinology therefore has the potential to elucidate the mechanisms involved in the generation of an immune response and identify the biomarkers responsible for vaccine protection.

RNA sequencing can be used to analyse the whole transcriptome response to vaccination. This technology is able to identify novel transcripts and its sensitivity allows transcriptional responses to be detected within a minor cell population in a mixed sample. Our laboratory recently applied RNA sequencing, in combination with flow cytometry, to investigate the phenotype and transcriptomic profile of afferent lymph cells following injection of a liposomal vaccine formulation incorporating the antigen diphtheria toxoid (DT) and the adjuvant poly(I:C) (194). We showed that over a 72h period, the signals derived from the injection site evolve from a pro-inflammatory phenotype, characterised by the up-regulation of genes including IL1β, CXCL2, RIGI and IRF7, to a specific immune response, including the induction of anti-viral pathways and the development of Th17 immunity (194). These genetic signatures were consistent with observed cellular migration patterns in afferent lymph, where a rapid and significant increase in neutrophil numbers was observed immediately after vaccination (195). Peak monocyte and DC migration into afferent lymph also coincided with peak gene expression of monocytic chemokines and DC-associated signalling (194, 195). This study details the cellular and molecular mechanisms that link the injection site with the draining lymph node and also highlights afferent lymphatic cannulation as an ideal model to apply systems biology approaches for the investigation of vaccine immunity in an outbred population following administration of novel vaccine and adjuvant formulations.

1.8.1   Scope of the thesis

The current thesis aims to significantly extend the findings from our previous reports and provide a comparison of the immune responses induced in the local draining lymphatic network by liposomal antigen formulations that incorporate the innate stimulators poly(I:C) or CpG. The ability of these innate adjuvants to enhance or modulate the immunogenicity of liposomes will be investigated by comparison to a control formulation that does not contain the stimulatory component. A systems biology approach will be used to identify the cellular, soluble and transcriptional factors that are induced following vaccination with a liposomal-nucleic acid adjuvant formulation. Mathematical modelling will be applied to determine the optimal number of antigen carrying cells required in afferent lymph to induce T cell activation in the lymph node after vaccination. Both ovine afferent and efferent lymphatic cannulation models will be used to investigate the innate and adaptive cellular and humoral immune responses induced by primary and secondary vaccination with the respective liposomal formulations. Systemic humoral memory immunity will also be assessed following primary, secondary and tertiary vaccination.

The global hypothesis of this thesis is that the addition of poly(I:C) or CpG to the liposome antigen formulation will enhance innate and adaptive immune responses in the local draining lymphatic network and improve the systemic memory response of vaccinated sheep.

The specific aims of the experimental chapters are -

1. To investigate the cellular and transcriptional innate immune response in afferent lymph following vaccination with liposomal adjuvant formulations.

2. To analyse the cellular and humoral adaptive immune response in efferent lymph following vaccination with liposomal adjuvant formulations.

3. To examine the systemic antigen-specific antibody response following vaccination with liposomal adjuvant formulations.

4. To develop a mathematical model of lymphatic cellular trafficking and T cell activation in the local lymph node after primary vaccination with liposomal adjuvant formulations.

CHAPTER TWO

General Methods

2.1 Surgical procedures

2.1.1 Animal housing

Adult merino sheep were housed at Prince Henry's Animal Facility, Werribee. The sheep were maintained at pasture, and received food and water *ad libitum*. For cannulation surgery, sheep were transported to the Large Animal Facility at the Department of Physiology, Monash University. Sheep were housed in metabolic cages, fed twice daily and had access to water *ad libitum.* The sheep were given at least one week to acclimatise to the housing facility, following which the prefemoral lymphatic cannulation surgeries were performed at the Department of Physiology animal surgery. Handling of animals and experimental procedures were approved by the Monash University Animal Ethics Committee in accordance with the relevant licencing agreement.

2.1.2 Pre-operative preparation and anaesthesia

The sheep were deprived of food 24 hours prior to surgery to prevent ruminal tympany and reduce the risk of regurgitation. The surgery site of each sheep was closely clipped with small animal clippers. Immediately prior to surgery, the surgery site was washed with antiseptic detergent and a 70% ethanol solution. Prior to anaesthesia, sheep were injected with the antibiotic Oxytetracycline intramuscularly at 20mg/kg and the analgesic Carprofen subcutaneously at 4mg/kg. Anaesthesia was performed by intravenous injection of Thiobarbiturate (Sodium Thiopentone 20mg/kg) followed by tracheal intubation. Anaesthesia was maintained by inhalational anaesthesia (Isoflurane 1.5-2.5% in 70/30 O_2/N_2O).

2.1.3 Prefemoral lymph node removal surgery

After preparation for surgery, the sheep was placed on the operating table and covered with sterile surgical drapes, leaving only a minimal area of the skin exposed approximately 10cm below the protruding bone of the hip. All procedures were performed under strict aseptic techniques. Following location of the prefemoral lymph node, a small 5cm incision was made. The node was then dissected from the subcutaneous fat and excised using surgical scissors. The incision site was closed with 2/0 surgical silk. The site was then sprayed with antiseptic

solution and 70% ethanol. Following completion of the surgery, the inhalation anaesthesia was switched off.

2.1.4   Prefemoral pseudo-afferent lymphatic cannulation surgery

After preparation for surgery, the sheep was placed on the operating table and covered with sterile surgical drapes, leaving only a minimal area of the skin exposed. All procedures were performed under strict aseptic techniques. An incision was made above the lymph node removal surgical site, approximately 3-5cm below the top of the pelvic bone. The fatty layer and thigh muscle were gently lifted to reveal the draining lymphatic duct. The connecting tissue layer covering the vessel was carefully removed and the duct clipped with small surgical scissors. The sterile cannula (30cm of 0.45mm heparinised plastic tubing individually packaged and sterilised with ethylene oxide) was flushed with sterile saline and carefully inserted into the pseudo-afferent lymphatic vessel. The heparinised cannula was obtained from Walker Scientific, WA, AUS. The cannula was then anchored using a 3/0 surgical silk suture and re-enforced with at least two sutures above and below the incision site. The cannula was exteriorised through a small hole in the skin above the incision site and secured using a purse suture with 2/0 silk (162, 196, 197). Several sutures were tied to attach the cannula onto the skin and minimise the risk of the cannula being pulled from the surgical site. The incision site was closed with 2/0 surgical silk. The site was then sprayed with antiseptic solution and 70% ethanol. Following completion of the surgery, two layers of tubular net bandage were placed around the torso between the front and hind legs. Sterile flasks containing heparin were placed beside the surgery site and secured between the two layers of tubular net bandage (Figure 1). The cannulae were then inserted into the sterile flasks. The inhalation anaesthesia was switched off.

2.1.5   Prefemoral efferent lymphatic cannulation surgery

Unlike the pseudo-afferent lymphatic cannulation procedure, the prefemoral efferent lymphatic cannulation surgery does not require removal of the prefemoral lymph node prior to cannulation. The efferent lymphatic vessel was directly cannulated as described in section 2.1.4

2.1.6   Post-operative care

The endotracheal tube was removed when laryngeal reflexes had returned. The sheep was then monitored until awake and able to hold the head upright. The sheep was transferred to the housing facility and monitored until complete recovery from anaesthetic was observed. In the case of the prefemoral lymph node removal surgery, the sheep was then returned to the paddock where food and water were freely available. In the case of the prefemoral pseudo-afferent and efferent lymphatic cannulation surgeries, the sheep was placed in a single metabolic cage where food and water was supplied. The sheep was closely monitored during the experimental period for signs of discomfort or stress. The flask containing lymph was replaced twice daily and the cannula cleaned with 70% ethanol.

Figure 1. A sheep following the prefemoral pseudo-afferent lymphatic cannulation surgery. The cannula is placed in the sterile collection tube for 1h as afferent lymph is collected for analysis following vaccination.

2.1.7   Surgical outcomes

The lymphatic cannulation surgeries are technically challenging, with previous studies reporting an average success rate of 50% (144). The success rate observed in this thesis was consistent with this, where success was defined as the lymphatic vessel successfully cannulated and the cannula flowing for the complete time course within a single animal. Therefore, to achieve the two cohorts of 15 sheep used in this thesis (n=30 total), each with reliable lymphatic flow for the entire time course, with a 50% success rate, approximately 60 sheep were investigated throughout the course of the presented studies. Due to housing constraints, a maximum of 10 sheep were investigated at a single time. All afferent lymph sheep and all efferent lymph sheep were from the same age cohort and livestock supplier.

2.2 Study design

2.2.1 Immunisations

Ovalbumin (OVA) was labelled with A647 by resuspending 5mg of OVA at 1mg/ml in PBS and adding a 15M excess of A647 succinimidyl ester (Invitrogen) resuspended in DMSO at 5mg/ml and incubating at room temperature for 1h. Unconjugated fluorophore was removed from solution using an Amicon Ultracel 3K centrifugal filter (Millipore) by centrifuging at 2000 x g for 30min and washed with PBS five times. All injections consisted of 500µl sterile PBS mixtures of liposomes (12% soy bean lecithin:cholesterol (9:1) obtained from Lipoid GmBH, Ludwigshafen, Germany) containing 375µg of OVA and 25 µg of OVA-A647 with or without the addition of 50µg of CpG or poly(I:C), kindly provided by Pfizer Animal Health, Parkville, Victoria (now Zoetis Research and Manufacturing). Liposomes and antigen solution +/- adjuvant were homogenised at 13,000 RPM for 10 minutes and extruded through a 0.2µm sterile filter. The CpG included in the formulations was the P class CpG 23877: 5' JU*C-G*T*C*G*A*C*G*A*T*C*G*G*C*G*G*C*C*G*C*C*G*T 3' (Patent # US 2013/0084306 Al), kindly provided by Pfizer Animal Health (now Zoetis Research and Manufacturing). For lymph collection, the liposome preparations were injected subcutaneously in the area drained by the prefemoral lymph node at 500µl per injection using a 25 gauge needle. For sera collection, the liposome preparations were injected subcutaneously in the prescapular area at 500µl per injection using a 25 gauge needle.

2.2.2 Lymph and blood collection

Afferent and efferent lymph was collected in sterile 50ml tubes containing 0.05IU of heparin and 20µl of 100X cell culture penicillin-streptomycin for a period of 1h at the time point required. Immediately after collection, lymph was placed on ice and processed fresh for analysis unless otherwise stated. Whole blood was collected by venepuncture using an 18 gauge needle and placed into a sterile 15ml tube and left to clot at room temperature for at least 1h. The clot was removed by centrifugation at 1000 x g for 10 minutes. The supernatant (serum) was collected and stored at -20°C until required for antibody analysis.

2.2.3   Animal cohorts

Each sheep within the afferent lymph study received the prefemoral lymph node removal surgery and the pseudo-afferent lymphatic cannulation surgery. Fifteen sheep with reliable lymphatic flow were randomly allocated to receive one of the three vaccine formulations detailed in section 2.2.1. Formulations were injected in the prefemoral drainage area. Afferent lymph was collected prior to injection and 4h, 24h, 48h and 72h following primary injection for flow cytometry, FACS and gene expression analysis at each time point within each animal (Figure 2).
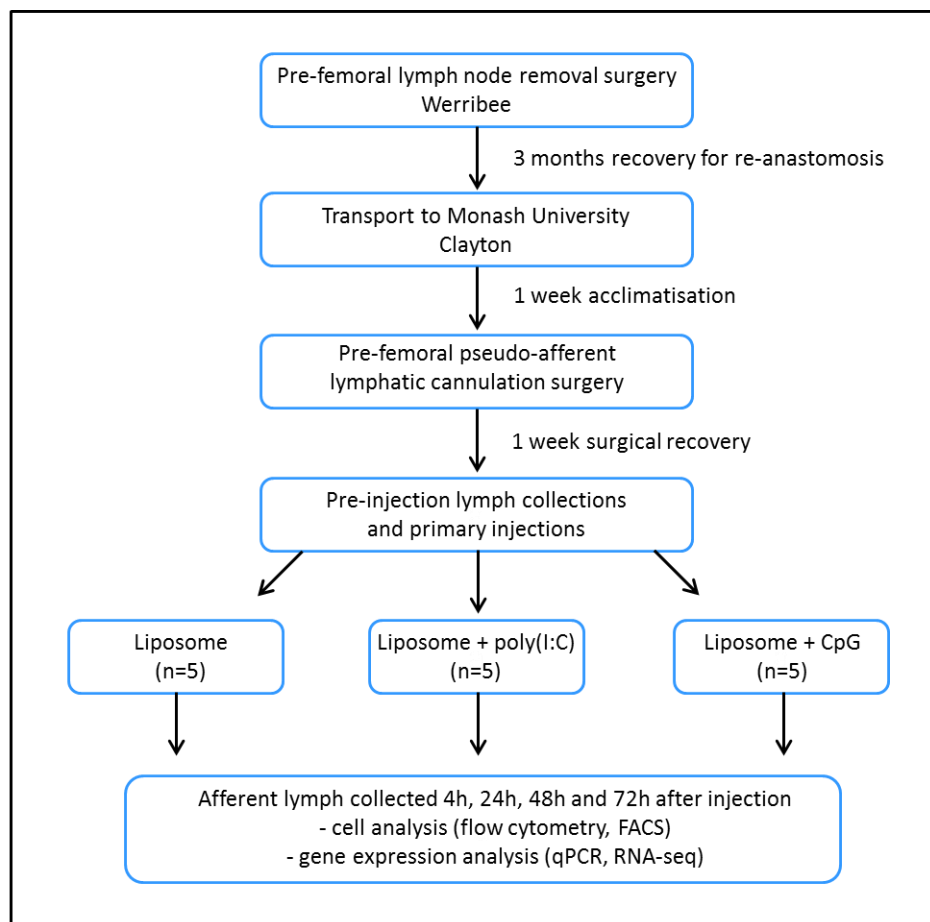
Figure 2. Experimental design and timeline for the afferent lymph study.

Each sheep within the efferent lymph allocation received the efferent lymphatic cannulation surgery. Fifteen sheep with reliable efferent lymphatic flow were randomly selected to receive three injections of their allocated vaccine formulation. Injections were performed in the prefemoral and prescapular drainage areas. Secondary injections were performed 4 weeks following primary injections, and tertiary injections were performed 3 months following secondary injections. Efferent lymph was collected prior to secondary injection, 4h, 1d, 2d, 3d, 6d, 8d, 10d and 13d following secondary injection for flow cytometry and antibody analysis at each time point within each animal (Figure3). Blood was collected prior to each injection, 7 and 10 days after secondary vaccination and 3, 5, 7, 10 and 30 days after tertiary vaccination for antibody analysis at each time point within each animal (Figure 3).
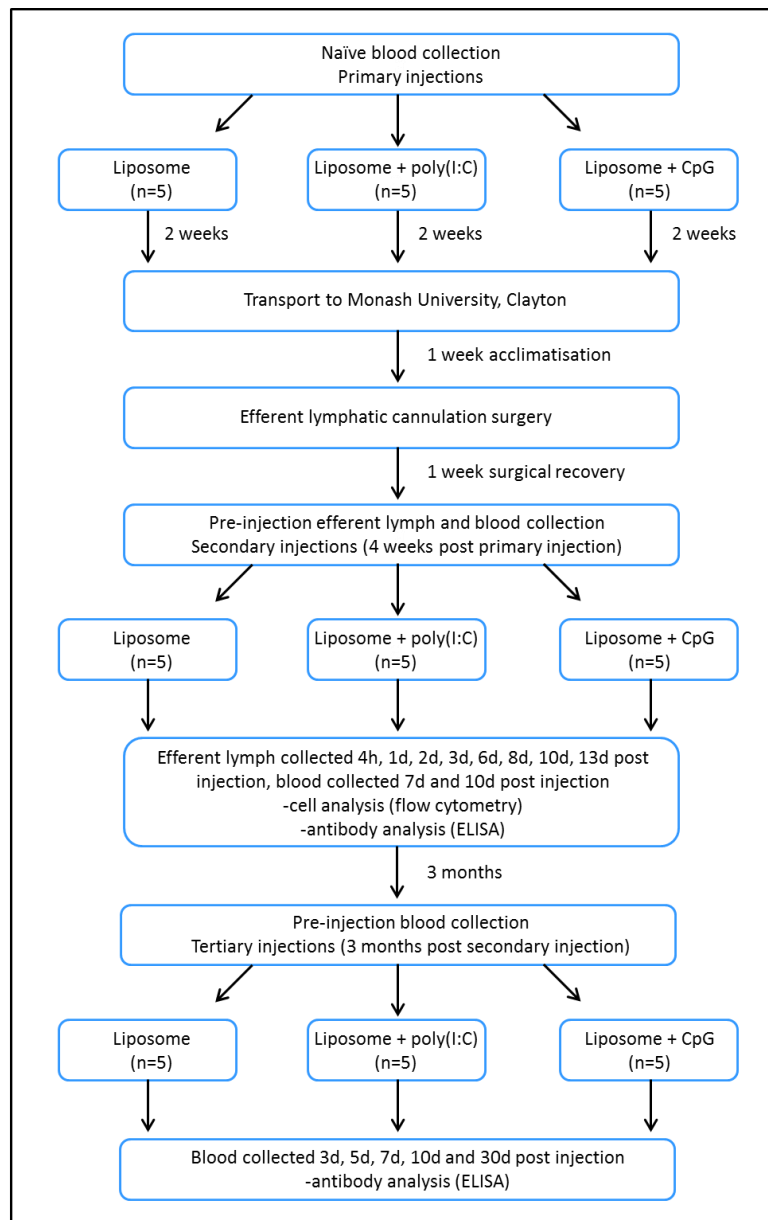
Figure 3. Experimental design and timeline for the efferent lymph and blood study.

2.3   Cell biology

2.3.1   Flow cytometry

For flow cytometry, cells from afferent and efferent lymph were prepared in the same manner. Immediately after collection, fresh lymph cells and supernatant were separated by centrifugation at 400 x g at 4°C. The cell pellet was washed with 10ml of ice cold PBS + 2mM EDTA and resuspended in 1ml of 0.093mM ammonium chloride with 0.4M Tris (pH 7.2) to lyse red blood cells. After 3 minutes on ice, 9ml of cold FACS buffer (5% horse serum, 2mM EDTA in PBS) was added and the cells centrifuged, washed with FACS buffer and used for flow cytometry analysis. All samples for flow cytometry were prepared by resuspending 3×10^6 cells in 25µl Fc-block (2% BSA, 2mM EDTA, 0.05% azide, 5% sheep serum in PBS) and then adding 25µl of 2X surface marker antibody mixes and incubating on ice for 20 minutes (Table 1) (196). All samples were run on a Becton Dickinson LSR2 machine and analysed using the FlowJo software. Figure 4 details the gating strategies utilised to identify cell populations and antigen positive cells in afferent lymph. Figure 5 provides a phenotypic analysis of afferent lymph DCs. Figure 6 details the gating strategies utilised to identify lymphocyte populations in efferent lymph.

Table 1. Antibodies used for identification of cell populations by flow cytometry

Primary Ab	Isotype	Source	Dilution	Secondary Ab	Source	Dilution
Anti-MHCII-PB	IgG2a	CAB	1:2000	NA	NA	NA
Anti-CD14-A700	IgG2a	AbD Serotec	1:400	NA	NA	NA
Anti-CD172a (SIRPα)	IgG1	VMRD Inc	1:250	Anti-IgG1 PE	Caltag	1:1000
Anti-CD80	IgG1	AbD Serotec	1:2000	Anti-IgG1 PE	Caltag	1:1000
Anti-CD86	IgG1	AbD Serotec	1:200	Anti-IgG1 PE	Caltag	1:1000
Anti-CD11a FITC	IgG2a	CAB	1:100	NA	NA	NA
Anti-CD11b	IgG2b	CAB	1:10	Anti-IgG2b FITC	BD Pharma	1:500
Anti-CD11c	IgM	VMRD Inc	1:400	Anti-IgM FITC	Caltag	1:600
Anti-CD1a FITC	IgG1	CAB	1:5	NA	NA	NA
Anti-CD1b	IgG2a	VMRD Inc	1:250	Anti-IgG2a FITC	Caltag	1:500
Anti-CD1w2	IgG1	In house	1:50	Anti-IgG1 PE	Caltag	1:1000
Anti-CD40	IgG1	In house	1:10	Anti-IgG1 PE	Caltag	1:1000
Anti-CD4 FITC	IgG2a	AbD Serotec	1:500	NA	NA	NA
Anti-CD8 PE	IgG2a	AbD Serotec	1:200	NA	NA	NA
Anti-γδ TCR-A647	IgG1	CAB	1:5000	NA	NA	NA
Anti- γδ TCR-FITC	IgG1	CAB	1:1000	NA	NA	NA
Anti-CD45R	IgG1	CAB	1:10	Anti-IgG1 PE	Caltag	1:1000

*CAB: Centre for Animal Biotechnology, University of Melbourne, Australia (161, 162).
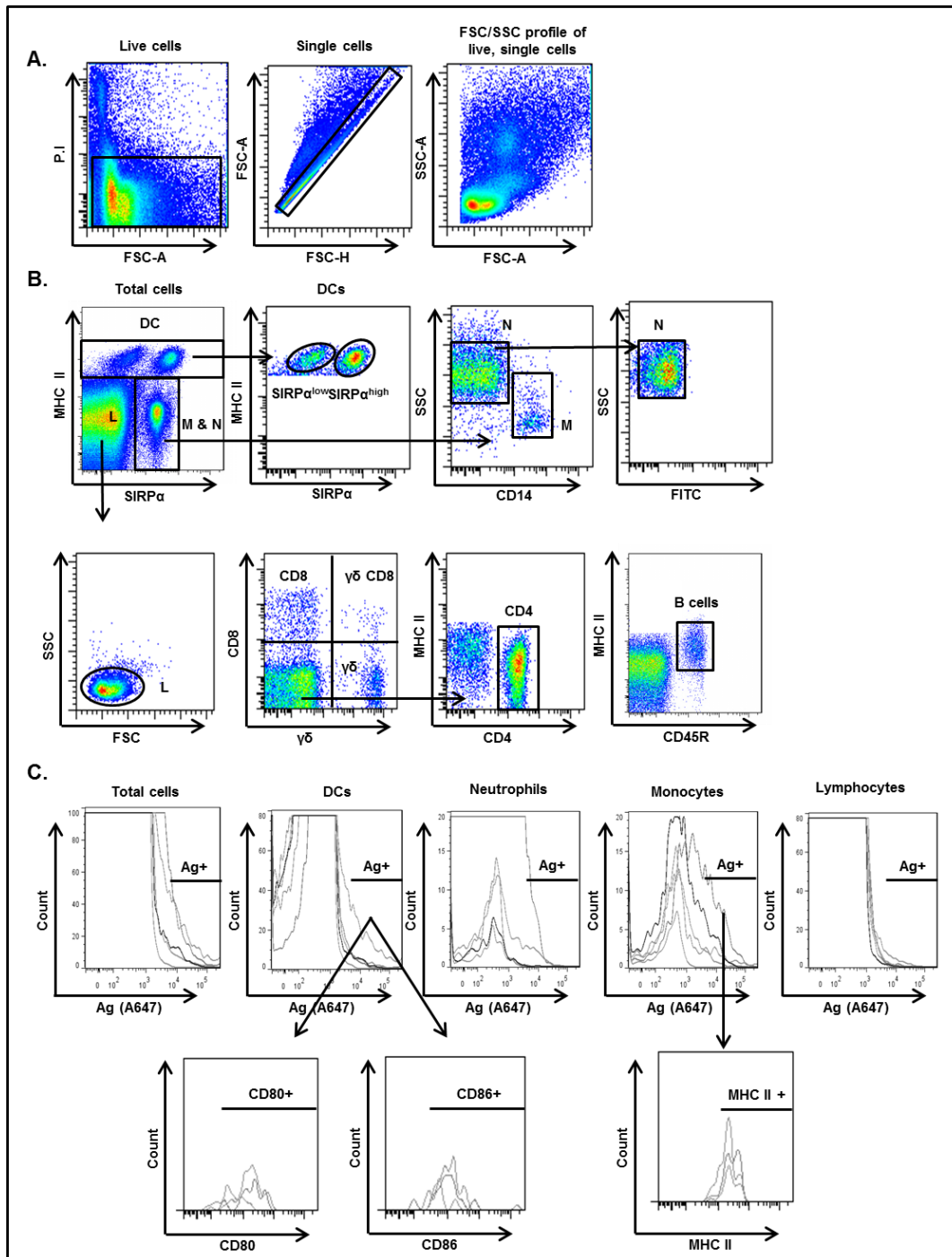
Figure 4. Flow cytometry gating strategies of cell populations and antigen positive cells in afferent lymph. (A) Preliminary gating for live cells using propidium iodide (PI), single cell identification and the size (FSC) and granularity (SSC) profile of live, single cells in afferent lymph. (B) DCs were gated based on SIRPα and MHC II expression, monocytes (M) and neutrophils (N) were firstly gated on SIRPα expression and further distinguished based on CD14 expression for monocytes and high SSC profile and no auto-fluorescence (empty FITC channel) for neutrophils. Lymphocytes (L) were defined based on low FSC/SSC profile and divided into T cells based on CD4, CD8 and γδ expression and divided into B cells based on CD45R and MHC II expression. (C) Antigen positivity was determined based on A647 fluorescence that is greater than pre vaccination levels. The mean fluorescence intensity (MFI) of CD80 and CD86 expression was investigated on A647 positive DCs and the MFI of MHC II investigated on A647 positive monocytes. Flow cytometry plots are of one representative animal.

Figure 5. Phenotypic analysis of afferent lymph DCs gated on high MHC II expression. CD11a, CD11b, CD11c, CD1a, CD1b, CD1w2, CD86, CD80, CD40 and CD45R expression was analysed under homeostatic conditions on the cells present within the MHC II high gate used in Figure 4B to confirm the presence of DCs. Black lines represent DC expression and grey lines are the matched isotype control. Flow cytometry plots are of one representative animal.
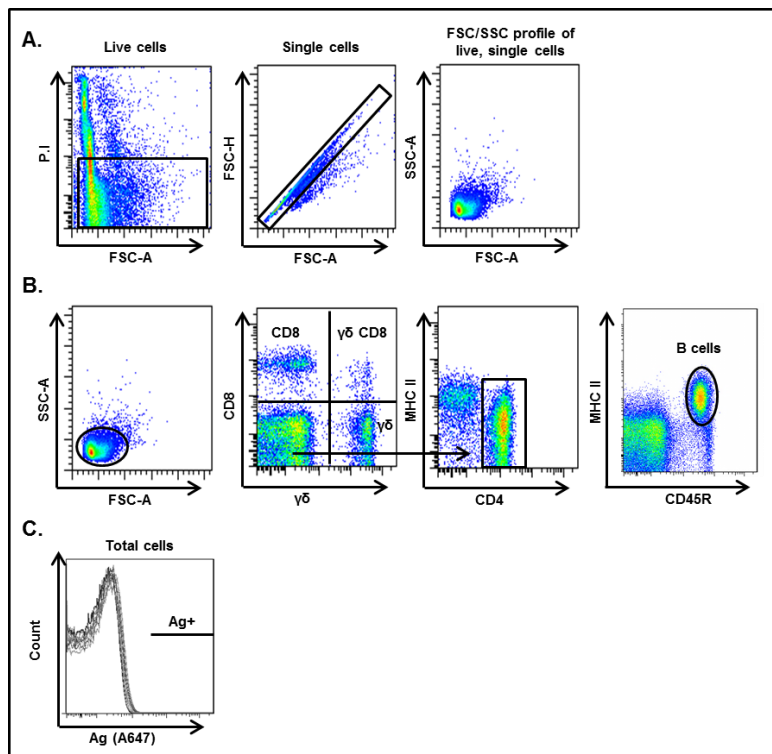
Figure 6. Flow cytometry gating strategies of cell populations in efferent lymph. (A) Preliminary gating for live cells using propidium iodide (PI), single cell identification and the size (FSC) and granularity (SSC) profile of live, single cells in efferent lymph. (B) Lymphocytes are gated on low FSC/SSC profile and divided into T cells based on CD4, CD8 and γδ expression and divided into B cells based on CD45R and MHC II expression. Flow cytometry plots are of one representative animal. (C) Antigen positivity is determined based on A647-OVA+ fluorescence that is greater than pre vaccination levels (no antigen positive cells observed in efferent lymph). Flow cytometry plots are of one representative animal.

2.3.2   Fluorescence activated cell sorting (FACS)

Samples for FACS were prepared in the same manner as for flow cytometry (2.3.1). The gating strategies in Figure 4 were applied to sort DC subsets, monocytes, neutrophils and lymphocytes from total afferent lymph cells. Afferent lymph cell populations were sorted using an Influx cell sorter (Becton Dickinson). Following cell sorting, a 100µl aliquot of sorted cells was used for cytospot analysis (spun at 1000RPM for 5 minutes at 4°C) to confirm sorted cell populations via microscopy, based on morphology and staining pattern (Figure 7). The remaining sorted cells were centrifuged immediately and resuspended in 350µl buffer RLT (Qiagen) and stored at -80°C until required for gene expression analysis.
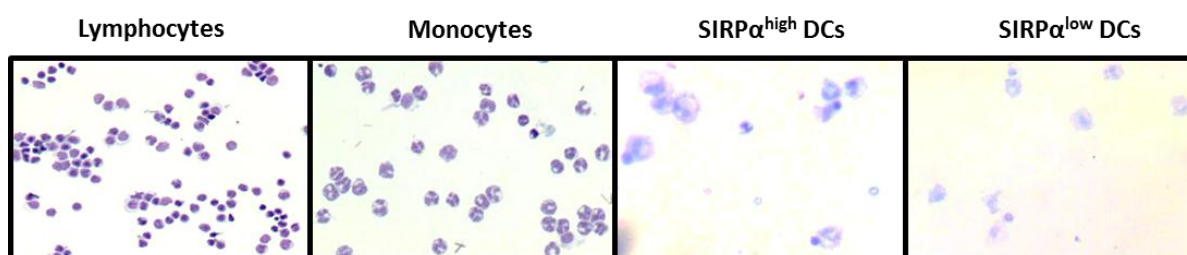
Figure 7. Microscopy images of FACS sorted lymphocytes, monocytes, SIRPα^{high} DCs and SIRPα^{low} DCs from afferent lymph stained in DiffQuik. Sorting experiments revealed >90% purity for all cell populations.

2.3.3 Flow cytometry analysis

The FlowJo software was used to analyse all flow cytometry data using the gating strategies detailed in Figures 4-6. Cell trafficking data in afferent lymph is expressed as a percentage of total cells or as a percentage of the cell subset; for example, DC subsets are expressed as a percentage of total DCs.

Antigen uptake data is expressed as the number of antigen positive cells per 10,000 cells in afferent lymph:

$$no.\ of\ antigen+\ cells\ per\ 10,000\ cells = \frac{percentage\ of\ antigen\ positive\ cells\ x\ no.\ of\ cell\ type\ per\ 10,000\ cells}{100}$$

Antigen uptake data is also expressed as the average amount of antigen per cell:

$$amount\ of\ antigen\ per\ cell = \frac{sum\ of\ the\ fluorescence\ intensity\ of\ each\ cell}{no.\ of\ cells}$$

To determine the relative expression of surface markers MHC II, CD80 and CD86 on antigen positive cells over time, the MFI was calculated and expressed as a fold change from baseline expression.

Cell trafficking data in efferent lymph is expressed as cell number per hour:

$$cells\ per\ hour = \frac{percentage\ of\ cell\ type}{100}\ x\ no.\ of\ total\ cells\ per\ hour$$

This was chosen as, unlike afferent lymph, there is a significant change in the total volume and cell number of efferent lymph over time.

For intracellular cytokine staining, IFNγ or IL4 positive cells are expressed as a percentage of total lymphocytes or as a percentage of the cell subset; for example, IFNγ+ CD8 T cells as a percentage of total CD8 T cells in efferent lymph.

2.4   Gene expression

2.4.1   RNA extraction

Gene expression analysis was performed on total afferent lymph cells and sorted afferent lymph cell populations using real-time quantitative PCR. Total afferent lymph cells were separated from lymph by centrifugation at 400 x g at 4°C. The cell pellet was washed with 10ml ice cold PBS + 2mM EDTA and resuspended in 1ml of 0.093mM ammonium chloride with 0.4M Tris (pH 7.2) to lyse red blood cells. After 3 minutes on ice, the cells were washed with PBS + 2mM EDTA and resuspended at $1x \ 10^7$/ml in Qiazol (Qiagen). Qiazol preparations were stored at -80°C until required. Cellular RNA was extracted from total afferent lymph cells using the Qiazol RNA extraction protocol and RNeasy Micro Kit (with on-column DNase digestion) according to manufacturer's instructions (Qiagen). RNA quantity was measured using a Nanodrop (Nanodrop Technologies) by absorbance at 260nm (194).

Sorted afferent lymph cell populations were centrifuged immediately after sorting (section 2.3.2), resuspended in 350μl buffer RLT (Qiagen) and stored at -80°C until required. Cellular RNA was extracted from sorted afferent lymph cells using an RNeasy Micro Kit with on-column DNase digestion (Qiagen) according to manufacturer's instructions. RNA quantity was measured using a Nanodrop (Nanodrop Technologies) by absorbance at 260nm.

2.4.2   cDNA synthesis and real time PCR

cDNA was synthesised from RNA of total afferent lymph cells and sorted afferent lymph cells using a Quantitect Reverse Transcription kit (Qiagen) according to manufacturer's instructions. Primers were designed to span an intron where possible using Primer 3 software on annotated mRNA sequences (Table 2). If the ovine mRNA sequences were not available, sequences were identified by alignment of bovine orthologues to the ovine genome. Real-time quantitative PCR was performed on individual samples in triplicate using SYBR green master mix on an Eppendorf Realplex 4 (Eppendorf). A standard curve using defined dilutions of pooled cDNA was run with each primer pair to obtain the PCR efficiency and relative copy number.

2.4.3   Real time PCR analysis

The Eppendorf Realplex software was used to calculate all real time PCR data. All results were normalised to the housekeeping gene GAPDH which showed the least variation relative to input cell number and treatment. β-actin was also investigated for use as a housekeeping gene, however expression of this gene was variable and therefore was excluded as a housekeeping gene. The PCR efficiency of each primer pair was calculated using the Eppendorf Realplex software (Table 2).

Real time PCR results from total afferent lymph cells in Chapter Three and sorted afferent lymph cells in Chapter Five are expressed as the mRNA levels relative to GAPDH. Real time PCR results from sorted afferent lymph cells in Chapter Three are expressed as the relative contribution of each cell type to gene expression, described in the equation:

$$contribution\,of\,cell\,type = \frac{normalised\,gene\,expression}{no.\,of\,cells\,sorted\,in\,that\,sample} \; x \; no.\,of\,cell\,type\,in\,afferent\,lymph$$

This measurement was chosen to determine the relative contribution of each sorted cell population to gene expression within afferent lymph for the genes of interest.

2.4.4   Next generation RNA-sequencing

Total cell RNA samples from three animals in the liposome alone and liposome + CpG groups (pre (-2h) and 72h) were also sent for next generation sequencing (RNA-seq) at the Medical Genomics Facility at the Monash Institute of Medical Research (Clayton, Australia). For these samples, RNA was extracted as described in section 2.4.1 and quality was assessed using an Agilent Bioanalyzer (Agilent Technologies). All samples had RNA Integrity Number (RIN) scores of greater than 8.5. mRNA library preparation, cluster generation and RNA-sequencing was performed with 100ng of RNA per sample using the Illumina sequencing platform as described within the relevant experimental chapter. Bioinformatics analysis was performed by the Victorian Bioinformatics Consortium at Monash University (Clayton, Australia). Reads were aligned to the ovine genome which became publicly available in 2014. Differential gene expression in afferent lymph cells within treatment groups (pre vs 72h for both formulations) and between treatment groups (72h liposome alone vs 72h liposome + CpG) was calculated based on the following parameters: $p < 0.05$, false

discovery rate (FDR) <0.01, ±1.5 mean fold change and a total of 50 reads across all replicates. Fulfilment of all four parameters was required to reach significance. Detailed information on the bioinformatics analysis can be found in the relevant experimental chapter. The Metacore knowledge database and software suite (Thomson Reuters) was used to identify biological processes and networks that were over-represented in the data set. Real-time quantitative PCR was also performed on these samples as described to validate the RNA sequencing results.

Table 2. List of genes and primers for real time quantitative PCR

Gene	Primer Sequence	Efficiency
CCL2	F: GCTGTGATTTTCAAG R: GGCGTCCTGGACCCATT	1.06
CLEC4F	F: ATTCAACCGTGCGTTTTGGG R: TCATTCCACTTCCGCTGCAT	0.89
CXCL10	F: GCTCATCACCCTGAGCTGTT R: AGCTGTCAGTAGCAAGGCTG	0.94
GAPDH	F: GTCCCCACCCCCAACGT R: TCTCATCATACTTGGCAGGTTTCTC	0.98
IFIT3	F: GTTGTCGAGGCTCTGGGAAA R: TCCAGTGCCCTTAGCAACAG	0.94
IL17A	F: AGGAGCTACCATGGCGTCTA R: CCTCACATGCTGTGGGAAGT	1.10
IL1β	F: CGAACATGTCTTCCGTGATG R: TCTCTGTCCTGGAGTTTGCAT	1.04
IL6	F: CCTCCAGGAACCCAGCTATG R: GGAGACAGCGAGTGGACTGAA	1.02
PSMA2	F: TGGTGTATAGTGGCATGGGC R: TGAGCTGTGGGAATGGGTTC	0.91
RIGI	F: GCCTCAGTTGGTGTTGGAGA R: GACGTGTCGAGAGAAGCACA	0.86
TLR3	F: ACAATCAGCCACACGACCTT R: AGATGTGGAAGCCAGGCAAA	1.00
TLR7	F: TCTCCAAGGTGCTTT R: CCACCAGACAAACCA	1.01
TLR9	F: CCCTGGAGAAGCTGG R: GACAGGTCCACGAAG	0.97
βactin	F: GGAGTCCTGCGGCATTCA R: GATGTCCACGTCACACTTCATGA	0.92

2.5   Antibodies

2.5.1   ELISA

Antigen-specific antibodies were measured in each efferent lymph and serum sample of vaccinated sheep using Enzyme-Linked Immunosorbent Assay (ELISA). 100µl per well of OVA (4µg/ml in PBS) was added to a flat bottom 96 well plate (Immunosorb, NUNC) and left to bind overnight at 4°C. The plate was washed twice with 0.05% PBS tween (PBST) and blocked with 1% horse serum in PBS at 200µl per well for 1h at room temperature. Following five washes with PBST, serum (diluted 1/500) or efferent lymph (diluted 1/2000) samples were added at 100µl per well for 1h at room temperature. The wells were then washed five times with PBST. 100µl of rabbit anti-sheep immunoglobulins/HRP antibody (DAKO, diluted 1/1000 in PBS) was added to each well for 1h at room temperature. The wells were then washed five times with PBST. The ELISA was developed using Tetramethylbenzidine (TMB) substrate (Invitrogen) at 100µl/well and stopped by the addition of 50µl/well of 2M H_2SO_4. The absorbance of each well was read at 450nm on a spectrophotometer (Molecular Devices, Spectramax Plus).

2.5.2   ELISA analysis

The concentration of antibody is expressed as optical density (OD) at 450nm and also as mean end-point antibody titre. Antibody titres were determined by serially diluting the efferent lymph and serum samples until the OD was within 2 standard deviations of the control wells. The last dilution factor where antibody was detected was selected as the end-point antibody titre for that sample.

2.6   Statistical analysis

All data were analysed using the statistical computer software GraphPad Prism version 6.0. Unless otherwise stated, results are presented as mean ± standard error of the mean (SEM) with five animals in each treatment group. For cellular data and real time PCR data, differences between groups and within a group were calculated with a two-way repeated measures analysis of variance (ANOVA) using a Sidak post-test to correct for multiple comparisons. For real time PCR data on sorted cells where gene expression was detected only within a single cell population, a one-way ANOVA was used to determine statistical significance over time. For all data, significance was determined as the confidence interval being greater than 95% ($p<0.05$). The specific statistical analysis conducted for each experiment is described in the relevant sections of each experimental chapter.

Vaccination with liposomal poly(I:C) induces discordant maturation of migratory dendritic cell subsets and anti-viral gene signatures in afferent lymph cells

Melanie R. Neeland[a], Martin J. Elhay[b], Els N.T. Meeusen[a], Michael J. de Veer[a]

[a]Biotechnology Research Laboratories, Department of Physiology, Monash University, VIC 3800, Australia

[b]Zoetis Research and Manufacturing Australia P/L, 45 Poplar Road, Parkville VIC 3052, Australia

This manuscript was published in **Vaccine** in October 2014

The current status of this manuscript is 'published'

Note: Supplemental figures are supplied at the end of this chapter

Declaration for Chapter Three

In the case of Chapter Three, the nature and extent of my contribution to the work was the following:

Nature of contribution	Extent of contribution
I was responsible for the design of the majority of the experiments, I conducted the experimental work and analysed the data. Assistance was required for surgical procedures. I interpreted the results and wrote the manuscript with assistance from co-authors.	80%

The following co-authors contributed to the work:

Name	Nature of contribution	Extent of contribution for student co-authors only
Martin Elhay	Provided reagents, assisted with experimental design and manuscript editing	N/A
Els Meeusen	Assisted with experimental design, interpretation of results and manuscript editing	N/A
Michael de Veer	Assisted with experimental design, surgical procedures, interpretation of results and manuscript editing	N/A

The undersigned hereby certify that the above declaration correctly reflects the nature and extent of the candidate's and co-authors' contributions to this work

Candidate's Signature	██████████	Date 23.02.15

Main Supervisor's Signature	██████████	Date 23.02.15

CHAPTER THREE

Vaccination with liposomal poly(I:C) induces discordant maturation of migratory dendritic cell subsets and anti-viral gene signatures in afferent lymph cells.

3.1   Chapter Summary

The results presented within this chapter provide a comparison of the immune response induced by a control liposomal antigen formulation and a liposomal antigen formulation with the addition of the innate stimulator poly(I:C). Due to requirements established during the publication process, the results for the liposomal poly(I:C) and liposomal CpG formulations are presented in two separate chapters (manuscripts) within this thesis. The aims of this chapter were to investigate the innate, adaptive and memory immune responses induced by liposomal poly(I:C) in the afferent lymph, efferent lymph and circulation of vaccinated sheep, respectively. Due to technical difficulties of the surgical procedures outlined in section 2.1.7, the efferent lymphatic cannulations of the animals allocated to the poly(I:C) group were not successful, with only 1 out of 10 animals flowing for the complete 13 day time course. Despite significant time and effort, due to the reorganisation of the company and staff that provided the vaccine formulations for these studies (Pfizer Animal Health restructured to Zoetis Research and Manufacturing), we were unable to obtain additional vaccine formulations to repeat the poly(I:C) efferent lymphatic cannulations. This chapter therefore investigates the innate cellular immune response in afferent lymph and the systemic memory humoral immune response following vaccination with liposomal poly(I:C). The results show that poly(I:C) enhances the inflammatory cellular and transcriptional immune response in afferent lymph, increase cellular associated antigen uptake and induces a unique pattern of DC maturation. The addition of poly(I:C) to the formulation also increases the systemic antigen-specific humoral immune response. The results of this study provide a comprehensive analysis of the real time *in vivo* innate immune response induced at the site of injection that is translated to the local lymph node following vaccination.

3.2   Abstract

Vaccine formulations administered in the periphery must activate naive immune cells within the lymph node. In this study, we have directly cannulated the ovine lymphatic vessels to investigate the cellular and molecular mechanisms that transfer information from the periphery into the local draining lymph node via the afferent lymph. Inclusion of poly(I:C) into a liposomal vaccine formulation enhances the neutrophil-associated inflammatory immune response in afferent lymph and increases antigen uptake by migratory dendritic cells (DCs). Interestingly, antigen positive migratory DCs undergo discordant maturation, with peak expression of CD86 at 4h and CD80 at 48-72h post vaccination. Afferent lymph monocytes up-regulate expression of genes related to inflammatory and anti-viral immune phenotypes following vaccination however show no differentiation into APCs prior to their migration to the local lymph node as measured by surface MHC II expression. Finally, this study reveals the addition of poly(I:C) increases systemic antigen-specific humoral immunity. These findings provide a detailed understanding of the real time *in vivo* immune response induced by liposomes incorporating the innate immune agonist poly(I:C) utilising a vaccination setting comparable to that administered in humans.

3.3   Introduction

The recent discovery that stimulation of the innate immune system leads to the induction of an adaptive immune response has led to the development of innate receptor ligands serving as adjuvants within vaccine formulations. A major class of innate immune stimulants are the TLR ligands. Poly(I:C) is a synthetic dsRNA complex that activates anti-viral recognition pathways, including TLR 3 and melanoma differentiation associated protein 5 (MDA5). Poly(I:C) has been shown to influence the maturation of innate cell populations, increase production of pro-inflammatory cytokines and induce protective, long lasting cellular and humoral immunity (48, 71-73, 76, 131, 198).

Liposomes have also been shown to possess an inherent adjuvant effect by protecting vaccine components from degradation and facilitating antigen uptake by APCs (199-202). Incorporating innate immune stimulants, such as Monophosphoryl lipid A (MPL), poly(I:C) or CpG into liposomes has been shown to increase the immunogenicity of these adjuvants, thereby increasing vaccine induced immunity (117, 123, 203). Several liposome based vaccines are currently in clinical trials, however an improved understanding of their interaction with and recruitment of cell populations *in vivo* is required to fully understand their immunogenic properties (104).

Following vaccination, cells present at the injection site migrate to the local lymph node via the afferent lymphatic vessels. The signals received in the periphery are conveyed to lymphocytes in the lymph node, leading to the generation of an adaptive immune response specific for the injected antigen (204). Examination of the afferent lymph compartment during the innate phase of an immune response allows investigation of the peripheral biological pathways responsible for setting up an adaptive immune response. This can be achieved using an ovine pseudoafferent lymphatic cannulation model, which permits real time collection of cells and immune factors that leave the injection site after *in vivo* exposure to local stimuli (162). In the present study, we have utilised this unique experimental model to explore the *in vivo* action of the innate stimulator poly(I:C) when incorporated into a liposome formulation. We have quantified the real time kinetics of innate cellular recruitment, antigen transport and genetic signatures from the injection site into the local lymph node after vaccination with liposomal poly(I:C).

3.4   Materials and Methods

3.4.1   Immunisations

All injections consisted of 500µl sterile PBS mixtures of liposomes (12% soy bean lecithin:cholesterol (9:1) obtained from Lipoid GmBH, Ludwigshafen, Germany) containing 350µg of ovalbumin (OVA) and 25µg of A647-labelled OVA with or without 50µg of poly(I:C), kindly provided by Zoetis Research and Manufacturing (Parkville, Victoria, Australia). Liposomes and antigen with or without adjuvant were homogenised at 13,000 RPM for 10 minutes and extruded through a 0.2µm sterile filter. The liposome formulations were injected subcutaneously in the area drained by the prefemoral lymph node at 500µl per injection using a 25g needle. For antigen labelling, 5mg of OVA was resuspended at 1mg/ml in PBS and a 15M excess of Alexa-647 succinimidyl ester (Invitrogen, Carlsbad, CA, USA) resuspended in DMSO at 5mg/ml was added and incubated at room temperature for 1h. Unconjugated fluorophore was removed from OVA solution using an Amicon Ultracel 3K centrifugal filter (Millipore, Billerica, MA, USA) by centrifuging at 2000 x g for 30min and washed with PBS.

3.4.2   Pseudoafferent lymphatic cannulation surgery and flow cytometry

Ovine prefemoral pseudoafferent lymphatic cannulation was performed as previously described (196). The prefemoral lymph nodes of merino sheep were removed at one year of age and at least 2 months was allowed for reanastomosis of the afferent lymphatics with the larger efferent lymphatic vessel. A secondary surgery was performed to insert a 0.96mm x 0.58mm heparin coated polyvinyl chloride cannula into the pseudoafferent lymphatic vessel. The cannulae were exteriorised and placed in a sterile collection flask attached to the side of the sheep. Injections were given at least seven days post lymphatic surgery to allow for surgical recovery. Ten sheep with reliable flow of afferent lymph were used in this study and randomly assigned to the groups, liposome alone (n=5) and liposome + poly(I:C) (n=5). Handling of animals and experimental procedures were approved by the Monash University Animal Ethics Committee in accordance with the relevant licensing agreement. Afferent lymph was collected in sterile 50ml tubes containing 0.05IU of heparin (Pfizer, New York, NY, USA) and 20µl of 100 x cell culture penicillin-streptomycin (Invitrogen, Carlsbad, CA, USA) for a period of one hour. Afferent lymph was collected prior to injection (-2h) and 4h,

24h, 48h, 72h after injection. Immediately after collection, afferent lymph cells were prepared for flow cytometry as previously described (196). Samples were analysed on an LSR2 machine (Becton Dickinson, Franklin Lakes, NJ, USA) and sorted using an Influx cell sorter (Becton Dickinson). For flow cytometry analysis and cell sorting, DCs were gated based on MHC II expression, with DC subsets gated on high or low levels of SIRPα. Monocytes were gated based on high CD14 expression and low-intermediate MHC II expression. Neutrophils were distinguished from monocytes based on side scatter (ssc) and low MHC II expression. T cell populations were identified based on CD4, CD8 or γδ expression. B cells were gated based on CD45R and MHC II expression. Flow cytometry gating strategies can be found in Supplementary Figure 1. All flow cytometry experiments were performed on fresh afferent lymph cells, except for experiments detailing CD80/CD86 on A647-OVA+ DCs which were performed on thawed afferent lymph cells.

3.4.3   Vaccination strategy and blood collection

Adaptive immune responses were induced by randomly assigning and injecting six non-cannulated sheep with the respective formulation, followed by a boost injection of the same formulation four weeks later. Memory immune responses were measured by injecting the same six sheep with the same formulation three months after receiving the boost injection. Blood was collected prior to all injections, 7d and 10d after boost injection and 3d, 6d, 10d and 30d after tertiary injection.

3.4.4   Afferent lymph cell preparation for quantitative real time PCR

Following centrifugation and wash steps, total afferent lymph cells were resuspended at $1x10^7$/ml in Qiazol (Qiagen, Valencia, CA, USA). Following cell sorting, sorted afferent lymph cells were centrifuged immediately and resuspended in 350μl buffer RLT (Qiagen). Cellular RNA was extracted from total afferent lymph cells and sorted cells using an RNeasy Micro Kit (Qiagen) according to the manufacturer's instructions. RNA quantity was measured using a Nanodrop (Nanodrop Technologies, Wilmington, DE, USA). cDNA was synthesised from RNA using a Quantitect Reverse Transcription kit (Qiagen) according to manufacturer's instructions. Primers were designed using Primer 3 software on annotated ovine mRNA sequences (Supplementary Table 1). Real time PCR was performed on individual samples in triplicate using SYBR green master mix on an Eppendorf Realplex4 (Eppendorf, Hamburg, Germany). Gene expression was normalised to the housekeeping gene GAPDH.

3.4.5   ELISA for the identification of OVA-specific antibodies

An indirect ELISA was used to measure relative OVA-specific antibody levels in each serum sample. Briefly, 100µl of OVA (4µg/ml in PBS) was added to a flat bottom 96 well plate (Corning Costar, Tewksbury, MA, USA) and left to bind overnight at 4°C. The plate was washed with 0.05% tween in PBS, and blocked with 1% horse serum in PBS at 200µl/well for 1h at room temperature, washed and sera samples (diluted 1/500) added at 100µl/well for 1h. The wells were washed and 100µl of rabbit anti-sheep immunoglobulins/HRP antibody (ref P0163, DAKO, Braeside, VIC, AUS) (diluted 1/1000 in PBS) was added and allowed to incubate for 1h. Reactions were developed using Tetramethylbenzidine substrate (Invitrogen) at 100µl/well, stopped by the addition of 50µl/well of 2M H_2SO_4 and read at 450nm on a spectrophotometer (Molecular Devices, Sunnyvale, CA, USA).

3.4.6   Statistical analysis

Results are presented as mean ± standard error of the mean. For cellular data and real time PCR data, differences between groups and within a group were calculated with a two-way repeated measures ANOVA using a Sidak post-test to correct for multiple comparisons. For real time PCR data on sorted cells where gene expression was detected only within a single cell population, a one-way ANOVA was used to determine statistical significance over time. Significance was determined as the confidence interval being greater than 95% ($p < 0.05$).

3.5   Results

3.5.1   *Liposomal poly(I:C) enhanced the recruitment of neutrophils into afferent lymph*

The addition of poly(I:C) to the liposome formulation did not significantly alter the total volume or cell output in afferent lymph (Figure 1A), however it significantly increased the percentage of neutrophils in afferent lymph 4h after injection (Figure 1B). The percentage of monocytes in afferent lymph peaked 24h post injection in both groups, however this increase was statistically significant only when poly(I:C) was added to the formulation (Figure 1B). While the proportion of total dendritic cells (DCs) in afferent lymph remained relatively consistent over time in both groups, poly(I:C) increased the proportion of SIRPα^{high} DCs after injection, increasing from 56% prior to injection to 63% 24h after injection and 61% 48h after injection (Figure 1C). No change in the percentage of lymphocyte subpopulations identified in afferent lymph was observed over time in either vaccination group (Supplementary Figure 2).

3.5.2   *Liposomal poly(I:C) altered the kinetics of cellular antigen uptake in afferent lymph*

In order to investigate the cell types within afferent lymph that transport antigen to the lymph node, the vaccine formulations contained A647-labelled OVA. Injection with liposome alone induced a peak number of A647-OVA$^+$ DCs 4h after injection, whilst poly(I:C) delayed the peak of A647-OVA$^+$ DCs to 24h after injection (Figure 2A). No significant difference in the number of A647-OVA$^+$ DCs was seen after injection with poly(I:C) when compared to liposome alone. The average amount of antigen per cell was determined by calculating the mean fluorescence intensity (MFI) of A647-OVA$^+$ cells. Poly(I:C) significantly increased the amount of A647-OVA fluorescence within individual DCs at 4h and 24h (Figure 2A). This result was also observed in A647-OVA$^+$ monocytes 24h after injection with poly(I:C), despite no difference in the number of A647-OVA$^+$ monocytes at this time point when compared to liposome alone (Figure 2B). The number of A647-OVA$^+$ neutrophils was significantly higher 4h following poly(I:C) injection (Figure 2C), consistent with their increased recruitment at this time point (Figure 1B). Interestingly, a 3 fold increase in the level of A647-OVA fluorescence in neutrophils was seen 72h after injection with liposome alone when compared to poly(I:C). When investigating cellular antigen transport by the two DC subsets identified in afferent lymph, the SIRPα^{high} DCs were responsible for between five

and ten fold more antigen uptake in both injection groups, with peak antigen uptake observed 4h after injection (Figure 2D-E). Poly(I:C) uniquely increased the level of A647-OVA fluorescence in both SIRPα^{high} DCs and SIRPα^{low} DCs, 2.2 fold at 4h and 2.6 fold at 48h after injection, respectively, when compared to liposome alone (Figure 2D-E).
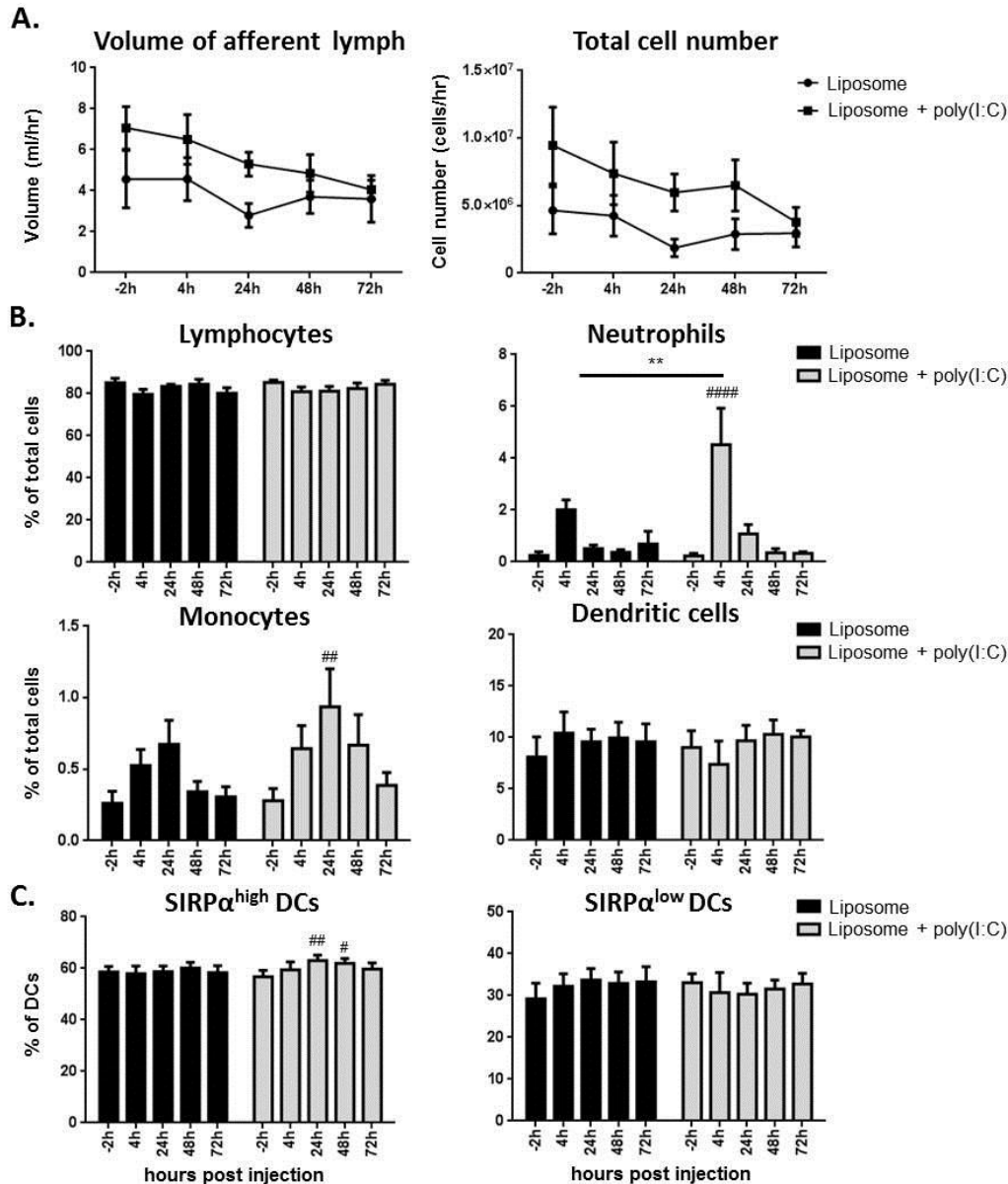
Figure 1. Temporal changes in afferent lymph volume and cellular composition after injection with liposome alone or liposome + poly(I:C). Changes over time in afferent lymph volume and total cell number (A), the percentage of lymphocytes, neutrophils, monocytes and dendritic cells in afferent lymph (B), the percentage of DCs that express high or low levels of SIRPα (C). Data expressed as mean ± SEM of five individually analysed animals at each time point in both treatment groups, * indicate significant differences between groups and [#] indicates significant differences from pre injection (-2h) within each group, **p<0.01, [#]p<0.05, [##]p<0.01, [###]p<0.001.
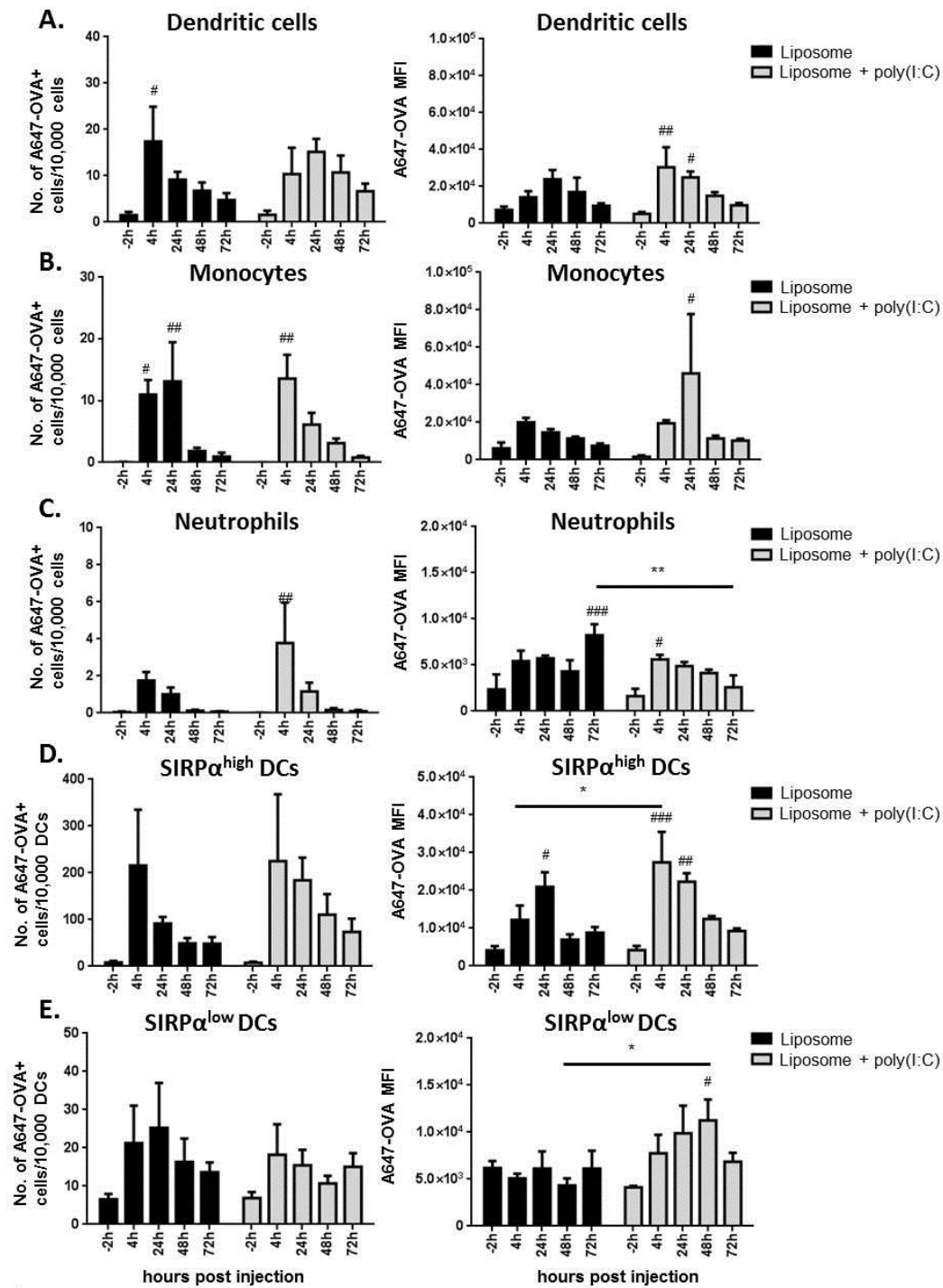
Figure 2. Temporal changes in the number and MFI of A647-OVA^{+} cells in afferent lymph after injection with liposome alone or liposome + poly(I:C). The number of A647-OVA[+] DCs (A), A647-OVA[+] monocytes (B), A647-OVA[+] neutrophils (C) per 10,000 cells in afferent lymph over time. Panels 2D and 2E show A647-OVA[+] SIRPα[high] DCs (D) and A647-OVA[+] SIRPα[low] DCs (E) numbers per 10,000 afferent lymph DCs. The second column in each panel shows the MFI of A647 in A647-OVA[+] cell types over time. Data expressed as mean ± SEM of five individually analysed animals at each time point in both treatment groups, * indicates significant differences between groups and [#] indicates significant differences from pre injection (-2h) within each group, *p<0.01, **p<0.01, [#]p<0.05, [##]p<0.01, [###]p<0.001.

3.5.3 Liposomal poly(I:C) increased the expression of co-stimulatory molecules on antigen carrying DCs

All afferent lymph DCs expressed both co-stimulatory molecules CD80 and CD86 prior to injection. However, injection with liposomal poly(I:C) induced a 2 fold increase in the MFI of CD80 on A647-OVA[+] DCs between 48h and 72h post injection (Figure 3A). Interestingly, the increase in CD80 was not associated with an increase in CD86 expression at these times (Figure 3B). The MFI of CD86 on A647-OVA[+] DCs peaked 4h after injection with both formulations and declined to baseline fluorescence levels by 72h (Figure 3B). No change in the expression of MHC II on antigen positive or negative DCs or monocytes was observed throughout the time course in this study.
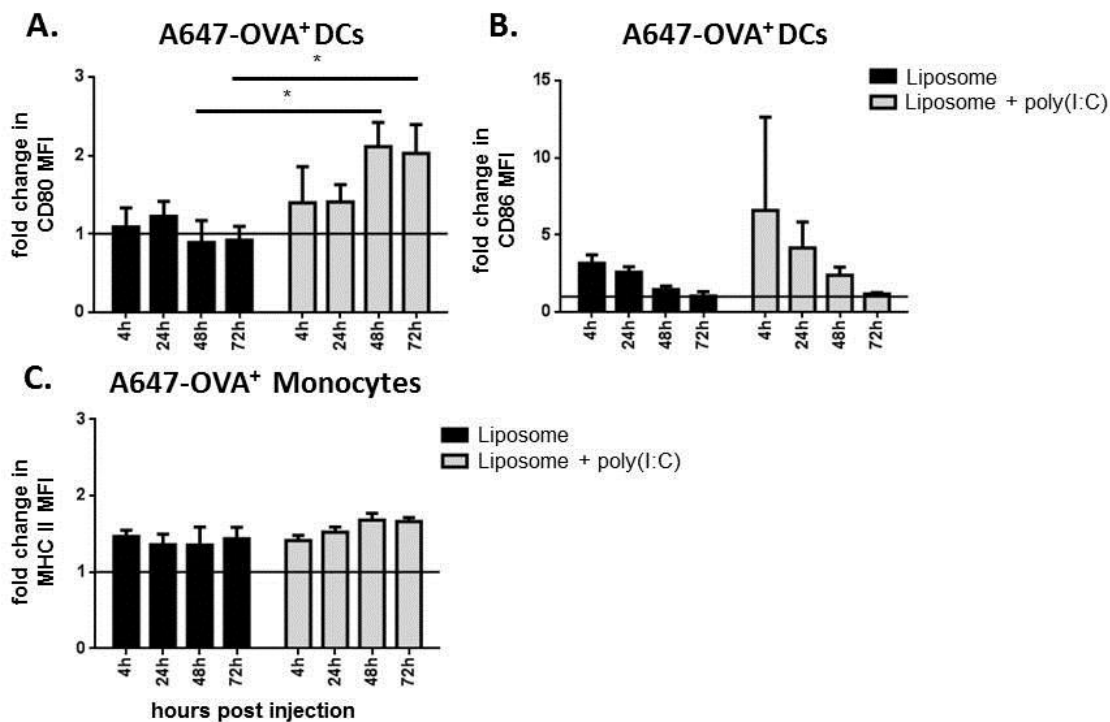
Figure 3. Temporal changes in the MFI of maturation markers on A647-OVA[+] monocytes and DCs in afferent lymph after injection with liposome alone or liposome + poly(I:C). Fold change over time in the MFI of CD80 on A647-OVA[+] DCs (A), CD86 on A647-OVA[+] DCs (B) and MHC II on A647-OVA[+] monocytes (C). Data expressed as mean ± SEM of five individually analysed animals at each time point in both treatment groups, * indicates significant differences between groups, *p<0.05.

3.5.4 Liposomal poly(I:C) enhanced the expression of anti-viral genes in afferent lymph cells

The expression of inflammatory and anti-viral genes Retinoic acid-inducible gene 1(RIG-I), Interferon-induced protein with tetratricopeptide repeats 3 (IFIT-3), TLR-7, C-X-C motif chemokine 10 (CXCL10), IL6, IL1β, C-C motif ligand 2 (CCL2) and IL17A was determined for all cells in afferent lymph. Injection of poly(I:C) induced significant increases in the expression of RIG-I, IL6 and CCL2 at 24h when compared to liposome alone (Figure 4). Peak expression of IFIT-3, CXCL10 and IL17A was also observed in the poly(I:C) group at this 24h time point (Figure 4). Both groups induced a similar trend in TLR-7 and IL1β expression, declining at 4h and returning to baseline levels by 24-72h after injection (Figure 4).

3.5.5 Relative expression of inflammatory and anti-viral genes in monocytes and DCs in afferent lymph

Peak expression of genes investigated in total afferent lymph cells occurred 24h after injection of poly(I:C), consistent with the recruitment of monocytes and DCs into afferent lymph. To determine the relative expression of these genes by these cell populations, SIRPα^{high} DCs, SIRPα^{low} DCs and monocytes from afferent lymph were sorted prior to injection (-2h), and 24h and 48h after injection of poly(I:C). The relative contribution of each cell type to gene expression was calculated by multiplying the normalised gene expression value per cell by the number of that cell type in afferent lymph at the time points analysed. The SIRPα^{high} DCs were the only cell population to express all seven genes, exclusively expressing RIG-I, TLR-3 and IL6 following injection of poly(I:C) (Figure 5). Significant increases from baseline were observed in RIG-I, CXCL10, TLR-3 and proteasome subunit alpha type-2 (PSMA2) expression in SIRPα^{high} DCs at 24h (Figure 5). The SIRPα^{high} DCs also expressed more CXCL10 at this time point when compared to SIRPα^{low} DCs and monocytes. The monocyte population contributed most significantly to IFIT-3 and CCL2 (MCP-1) expression at 24h when compared to SIRPα^{low} DCs and SIRPα^{high} DCs, respectively (Figure 5). PSMA2, a gene involved in proteolysis and presentation of antigen (205), was unique to the DC subsets, increasing significantly from baseline at 24h in the SIRPα^{high} DC population (Figure 5). Expression of the IL17A gene was not detected in any of the sorted cell populations.
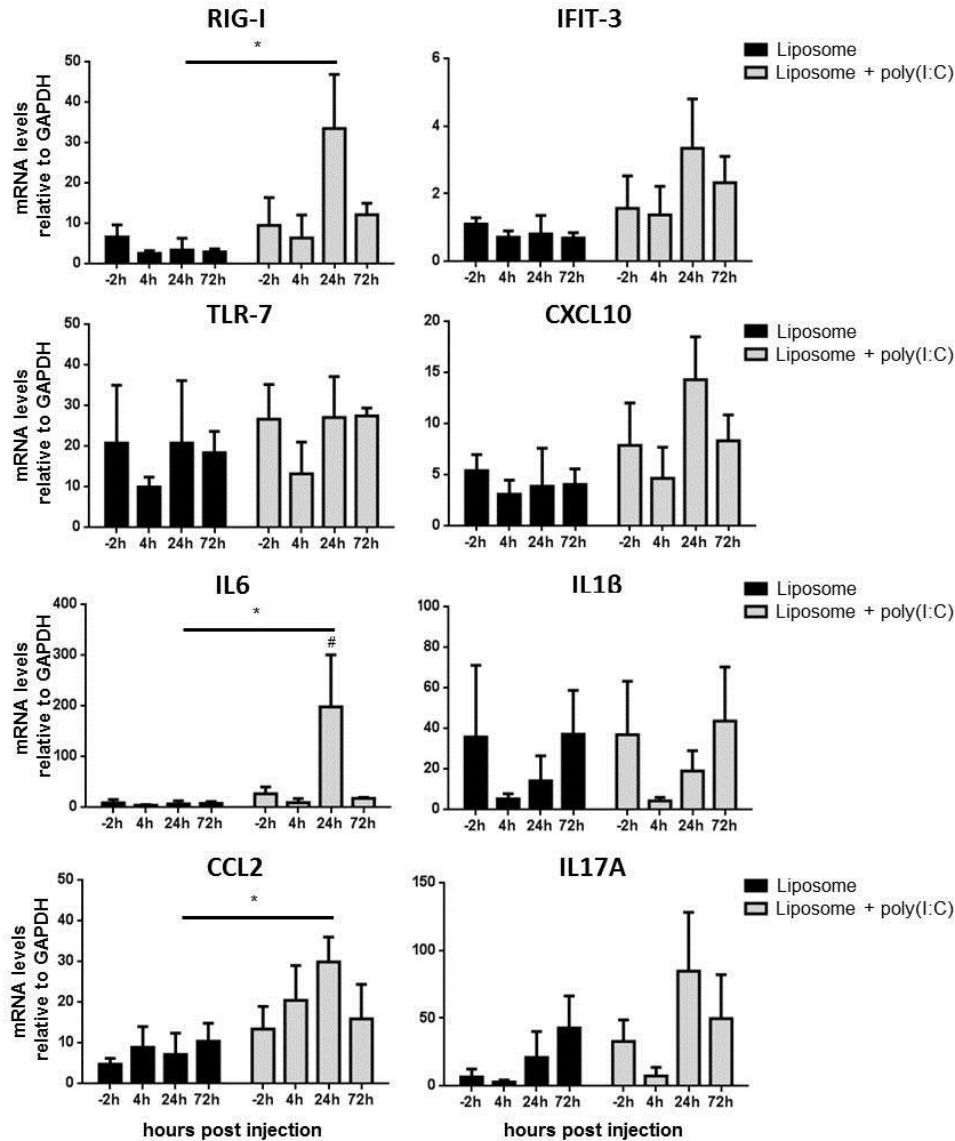
Figure 4. Changes in gene expression in total afferent lymph cells after injection with liposome alone or liposome + poly(I:C). RNA levels for RIG-I, IFIT-3, TLR-7, CXCL10, IL6, IL1β, CCL2 and IL17A are reported. Data expressed as mean ± SEM of three individually analysed animals at each time point in both treatment groups, * indicates significant differences between groups and [#] indicates significant differences from pre injection (-2h) within each group, *p<0.05, [#]p<0.05.
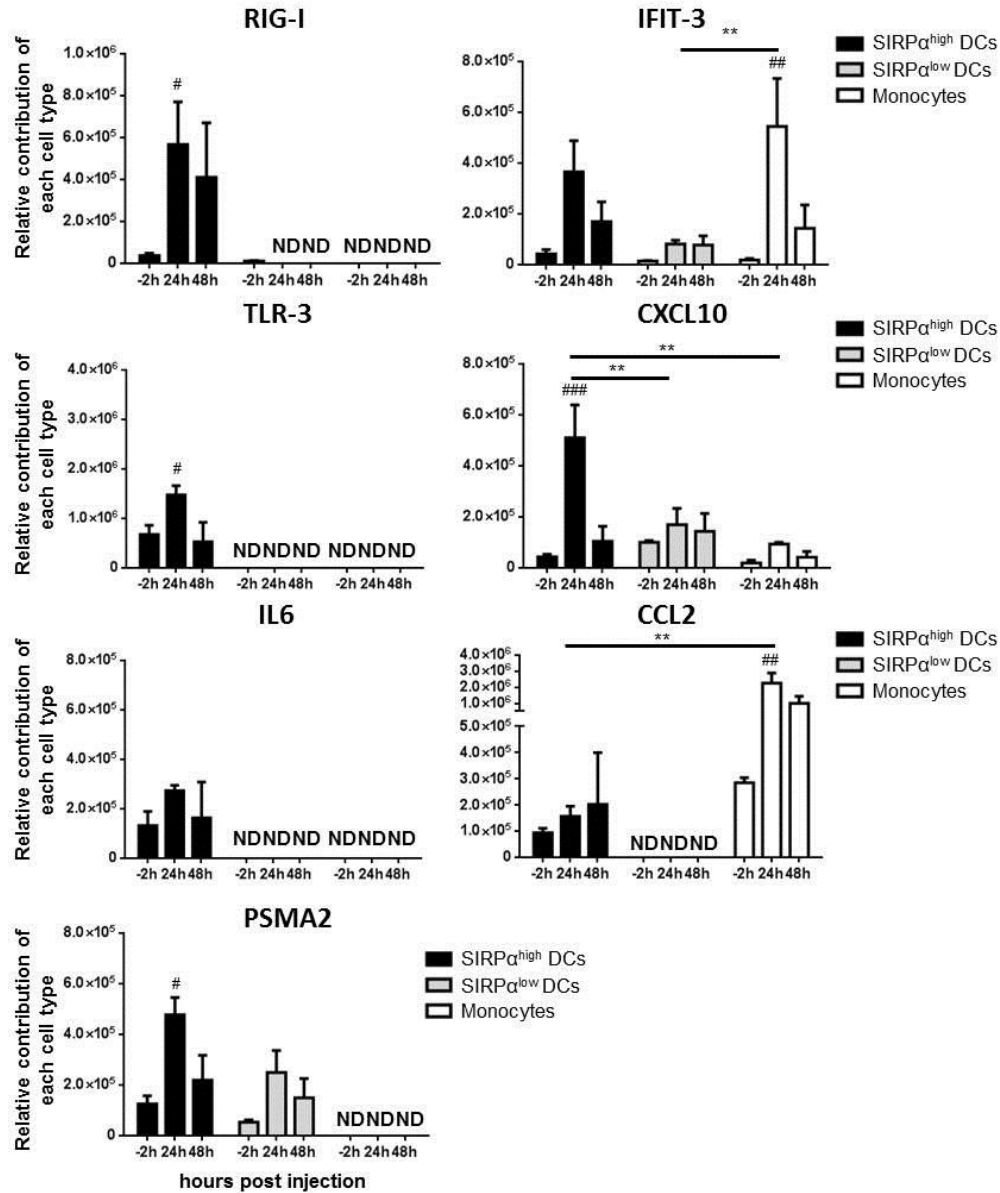
Figure 5. Identification of gene expression in selected sorted afferent lymph cells prior to injection, 24h and 48h following injection with liposome + poly(I:C). Expression is reported for the genes RIG-I, IFIT-3, TLR-3, CXCL10, IL6, CCL2 and PSMA2 in SIRPα^{high} DCs, SIRPα^{low} DCs and monocytes. ND indicates gene not detected in the cell type at that time point. Data expressed as mean ± SEM of three individually analysed animals at each time point in the liposome + poly(I:C) group, * indicates significant differences between cell types and # indicates significant differences from pre injection (-2h) within each cell type, **p<0.01, #p<0.05, ##p<0.01, ###p<0.001.

3.5.6 Liposomal poly(I:C) increased the production of systemic antigen-specific antibodies

OVA specific antibody concentration was measured in the sera of vaccinated animals after secondary and tertiary injections with both formulations. The addition of poly(I:C) to the liposome formulation induced significantly greater OVA-specific antibody levels in sera after secondary injection which remained elevated for the entire vaccination time course (Figure 6A). In the liposome alone group, significant increases in OVA-specific antibodies were only observed after tertiary vaccination (Figure 6A). Mean end-point OVA antibody titres were approximately 2 fold greater in the poly(I:C) group at 100 days when compared to liposome alone (Figure 6B).
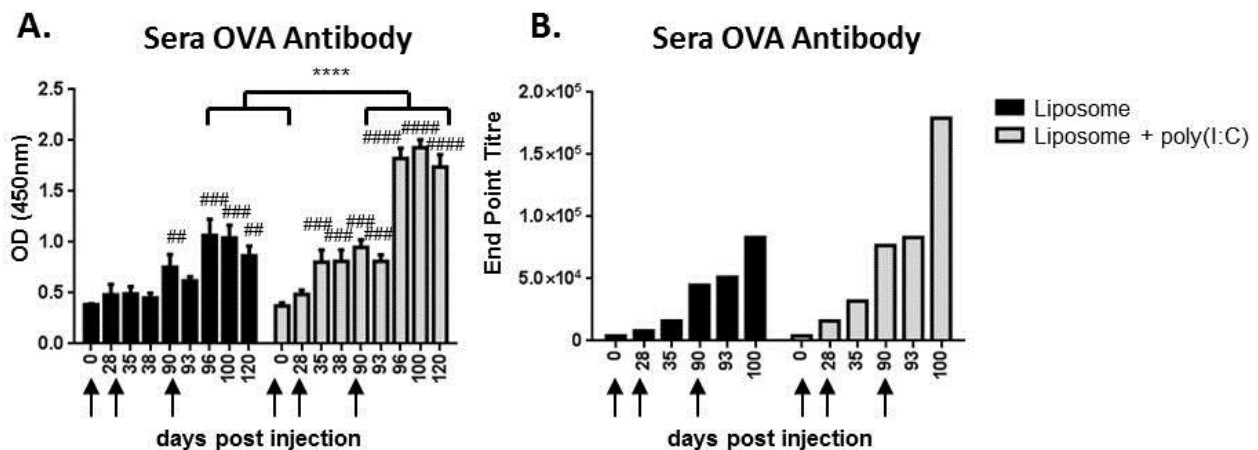
Figure 6. Temporal changes in OVA specific antibody concentration in the sera after boost injections with liposome alone or liposome + poly(I:C). OVA specific antibody concentration in sera is expressed as (A) OD (450nm) and (B) Mean end point titre. Arrows indicate injection days, where primary injection was given on day 0, secondary injection was given on day 28 and tertiary injection was given on day 90. Data expressed as mean ± SEM of five individually analysed animals at each time point in both treatment groups, * indicates significant differences between groups and [#] indicates differences from naïve (day 0) within each group, ****$p < 0.0001$, ##$p < 0.01$, ###$p < 0.001$, ####$p < 0.0001$

3.6   Discussion

The cellular and humoral immune responses induced by liposomal vaccine formulations can be improved by the addition of innate immune stimulants, including poly(I:C) (122). However, the *in vivo* mode of action of these formulations is unclear, and little is known regarding their effect at the site of vaccination which drives the subsequent immune response in the local draining lymph node. Using the ovine pseudoafferent lymphatic cannulation model, we were able to intercept the cells migrating from the skin into the local lymph node, allowing the quantification of cellular composition, phenotype and ability to carry antigen to the lymph node after vaccination with liposomal poly(I:C).

Immediately after vaccination with both liposomal formulations, there was a marked increase in the number of neutrophils in afferent lymph. The transient nature of this response is a characteristic feature of inflammation induced by subcutaneous injection (164). This was significantly increased with poly(I:C), in agreement with previous work, where several immune agonists have been shown to enhance the skin inflammatory response (162, 195). We also report significant increases in the inflammatory and anti-viral genes IL6, CCL2 and RIG-I 24h following injection of liposomal poly(I:C). Similarly, a study in humans found that injection of poly ICLC, a stabilised form of poly(I:C), induced transcriptional changes that mimic viral infection, including strong interferon responses and inflammasome signalling (95). This study also reported that naked poly ICLC induced mild to severe local and systemic side effects in the first week after injection (95). Throughout the course of the present study, no adverse reactions were observed at the site of injection (data not shown), suggesting that incorporating poly(I:C) into liposomal formulations may reduce the likelihood of local reactogenicity. Liposomes incorporating poly(I:C) and OVA antigen have been shown to induce strong CD8 T cell responses in mice whilst preventing the non-specific production of pro-inflammatory cytokines in the serum that occurred after injection of free poly(I:C) (120).

This study shows that, in addition to DCs, neutrophils and monocytes in afferent lymph are also able to transport antigen to the lymph node within 24h after injection. This has been observed previously, where afferent lymph monocytes contributed to antigen uptake following injection of several adjuvant formulations, including aluminium adjuvant,

Monophosphoryl lipid A (MPL) and CpG (161, 162, 196). In our study, monocytes were also the most significant contributors to the expression of the monocyte chemotactic gene CCL2 and the interferon-induced gene IFIT-3 at 24h. These cells also expressed the gene for the chemokine CXCL10 at this time point, suggesting they have acquired an activated, anti-viral phenotype as they migrate to lymph node after injection with liposomal poly(I:C). Similar results have also been observed in pigs, where genes involved in interferon signalling and chemotaxis were up-regulated in the draining lymph node 24h following injection of the adjuvant formulation Matrix-M (206). We show that monocytes from afferent lymph may represent a significant contributor to the enhanced antiviral genetic signatures observed in the draining lymph node following vaccination.

DCs were responsible for the majority of cellular antigen transport from 24-72h after vaccination with both formulations. The afferent lymph SIRPα^{high} DC subset was responsible for between 5 and 10 fold more antigen uptake than the SIRPα^{low} DC subset across the time course in both groups. This was also supported by increased expression of the antigen processing gene PSMA2 and TLR-3 over time in this DC subset. In ovine afferent lymph, the SIRPα^{high} DCs were shown to genetically and functionally represent the mouse CD11b$^+$ DCs, with enhanced antigen presentation to CD4 T cells. The SIRPα^{low} DCs were equivalent to the mouse CD8α$^+$ DCs and specialised in the cross-presentation of antigen to CD8 T cells (144, 156). In our study, the SIRPα^{high} DCs were the only cell population to express the receptor for poly(I:C) TLR3 and all immune genes investigated (excluding IL17A), suggesting they play a significant role in the immune response induced by poly(I:C). A previous study investigating TLR expression in ovine afferent lymph DCs showed increased expression of TLR3 in SIRPα^{high} DCs when compared to SIRPα^{low} DCs (207). However, in humans and mice, expression of TLR3 is typically associated with SIRPα^{low} DCs. In mice, TLR3 is expressed by CD8$^+$SIRPα$^-$ lymph node resident DCs and CD8$^-$CD103$^+$ migratory DCs (68). It will require additional markers and functional characterisation of afferent lymph SIRPα subsets in sheep to determine whether the increased expression of TLR3 in SIRPα^{high} DCs is a species specific difference or due to the exclusively migratory population studied in afferent lymph.

Both subsets of DCs ingested more antigen following injection of poly(I:C), however, in our study, the SIRPα^{low} DCs did not express the transcript for TLR-3. This suggests that the SIRPα^{low} DCs may respond to poly(I:C) through TLR-independent pathways, such as melanoma differentiation associated protein 5 (MDA5), which can be inducibly expressed in

most cell types (91). The SIRPα^{low} DCs exclusively expressed the interferon-stimulated genes IFIT-3, CXCL10 and PSMA2 (208), suggesting they are activated by type I interferon cytokines produced by cell populations at the site of injection, however confirmation of these hypotheses will require further investigation.

Injection of poly(I:C) induced antigen positive DCs to partially mature, as shown by discordant increases in expression of the co-stimulatory molecules CD80 and CD86. At no point in our study did antigen positive migratory DCs express elevated levels of both CD80 and CD86. This is at odds with an *in vitro* study that revealed liposomal poly(I:C) induced DCs to mature and increase their type I interferon production (123). In our study, no increase in MHC II expression on antigen positive monocytes was observed in this study. These are interesting findings, as we have previously reported both an increase in MHC II on antigen positive monocytes, and an increase in CD80/CD86 on antigen positive DCs 72h after injection of liposomal CpG (196). In the present study we show that, unlike liposomal CpG, liposomes alone and liposomal poly(I:C) are not sufficient to completely mature monocytes and DCs in afferent lymph. These results highlight that poly(I:C) and CpG target distinct pathways in afferent lymph to induce their adjuvant effects in the local lymph node.

The overall efficacy of a vaccine formulation can be quantified based on the level and persistence of circulating antigen specific antibodies following boost injection. We show significant increases and persistence in the concentration of OVA specific antibodies following boost injection with liposomal poly(I:C), but not with the liposome alone formulation. A study in mice also showed that vaccines containing liposomal antigen and adjuvant combinations were the most effective at inducing protective antibody responses when compared to liposome alone and adjuvant alone injections (209). This highlights that liposomal delivery systems can be improved by the addition of immunostimulatory components to elicit strong antigen specific humoral immunity.

The combined results of this study demonstrate that addition of poly(I:C) to liposomal vaccine formulations enhances the immediate inflammatory response at the site of injection, improves cellular associated antigen transport in afferent lymph, induces partial maturation of DCs and increases the production of antigen specific antibodies following vaccine challenge. We also show genetic signatures associated with interferon-mediated antiviral immune responses in afferent lymph DCs and monocytes after injection of liposomal poly(I:C). This study demonstrates the real time *in vivo* kinetics of the peripheral contribution to liposome

based delivery systems and provides an explanation for the immunogenic function of poly(I:C) when employed as an adjuvant within vaccines.

3.7   Supplemental figures

Supplementary Table 1. Primer sequences for genes investigated with real time PCR

Gene	Primer sequences (5'-3')
GAPDH	Forward: GTCCCCACCCCCAACGT
	Reverse: TCTCATCATACTTGGCAGGTTTCTC
IL-6	Forward: CCTCCAGGAACCCAGCTATG
	Reverse: GGAGACAGCGAGTGGACTGAA
IFIT-3	Forward: GTTGTCGAGGCTCTGGGAAA
	Reverse: TCCAGTGCCCTTAGCAACAG
TLR-7	Forward: TCTCCAAGGTGCTTT
	Reverse: CCACCAGACAAACCA
IL-1β	Forward: CGAACATGTCTTCCGTGATG
	Reverse: TCTCTGTCCTGGAGTTTGCAT
IL-17A	Forward: AGGAGCTACCATGGCGTCTA
	Reverse: CCTCACATGCTGTGGGAAGT
PSMA-2	Forward: TGGTGTATAGTGGCATGGGC
	Reverse: TGAGCTGTGGGAATGGGTTC
TLR-3	Forward: ACAATCAGCCACACGACCTT
	Reverse: AGATGTGGAAGCCAGGCAAA
RIG-I	Forward: GCCTCAGTTGGTGTTGGAGA
	Reverse: GACGTGTCGAGAGAAGCACA
CCL-2	Forward: GCTGTGATTTTCAAG
	Reverse: GGCGTCCTGGACCCATT
CXCL-10	Forward: GCTCATCACCCTGAGCTGTT
	Reverse: AGCTGTCAGTAGCAAGGCTG

Supplementary Figure 1. Flow cytometry gating strategies of cell populations and antigen positive cells in afferent lymph. (A) Preliminary gating for live cells using propidium iodide (PI), single cell identification and the size (FSC) and granularity (SSC) profile of live, single cells in afferent lymph. (B) DCs were gated based on SIRPα and MHC II expression, monocytes (M) and neutrophils (N) were firstly gated on SIRPα expression and further distinguished based on CD14 expression for monocytes and high SSC profile and no auto-fluorescence (empty FITC channel) for neutrophils. Lymphocytes (L) were defined based on low FSC/SSC profile and divided into T cells based on CD4, CD8 and γδ expression and divided into B cells based on CD45R and MHC II expression. (C) Antigen positivity was determined based on A647 fluorescence that is greater than pre vaccination levels. The mean fluorescence intensity (MFI) of CD80 and CD86 expression was investigated on A647 positive DCs and the MFI of MHC II investigated on A647 positive monocytes. Flow cytometry plots are of one representative animal.

Supplementary Figure 2. The percentage of lymphocyte subsets in afferent lymph over time after injection with liposome alone or liposome + poly(I:C). Data expressed as mean ± SEM of five individually analysed animals at each time point in both treatment groups.

Incorporation of CpG into a liposomal vaccine formulation increases the maturation of antigen loaded dendritic cells and monocytes to improve local and systemic immunity

Melanie R. Neeland*‡, Martin J. Elhay†, Jackie Nathanielsz†, Els N.T. Meeusen*‡, Michael J. de Veer*‡

*Biotechnology Research Laboratories, School of Biomedical Sciences, Monash University, VIC 3800, Australia

†Zoetis Research and Manufacturing Australia P/L, 45 Poplar Road, Parkville VIC 3052, Australia

‡Australian Research Council Centre of Excellence in Structural and Functional Microbial Genomics, Monash University, VIC 3800, Australia

Note: Supplemental and extended figures are supplied at the end of this chapter

Declaration for Chapter Four

In the case of Chapter Four, the nature and extent of my contribution to the work was the following:

Nature of contribution	Extent of contribution
I was responsible for the design of the majority of the experiments, I conducted the experimental work and analysed the data. Assistance was required for surgical procedures. I interpreted the results and wrote the manuscript with assistance from co-authors.	80%

The following co-authors contributed to the work.

Name	Nature of contribution	Extent of contribution for student co-authors only
Martin Elhay	Provided reagents, assisted with experimental design and manuscript editing	N/A
Jackie Nathanielsz	Provided reagents	N/A
Els Meeusen	Assisted with experimental design, interpretation of results and manuscript editing	N/A
Michael J de Veer	Assisted with experimental design, surgical procedures, interpretation of results and manuscript editing	N/A

The undersigned hereby certify that the above declaration correctly reflects the nature and extent of the candidate's and co-authors' contributions to this work.

Candidate's Signature			**Date 23.02.15**

Main Supervisor's Signature		**Date 23.02.15**

CHAPTER FOUR

Incorporation of CpG into a liposomal vaccine formulation increases the maturation of antigen loaded dendritic cells and monocytes to improve local and systemic immunity

4.1   Chapter Summary

The results presented within this chapter provide a comparison between the innate, adaptive and memory immune responses induced by a control liposome antigen formulation and a liposome antigen formulation incorporating the innate stimulator CpG. Chapter Three showed that poly(I:C) increased the recruitment of neutrophils 4h after injection and induced peak antigen uptake by DCs and monocytes 4h-24h after injection. Poly(I:C) induced discordant maturation of antigen positive DCs with CD86 increasing at 4h and CD80 increasing between 48h-72h after injection. The present chapter shows that CpG enhances the recruitment of neutrophils 4h after injection and induces peak antigen uptake by DCs 24h after injection. Antigen-positive monocytes demonstrate two peaks of antigen positivity following injection of CpG, first at 4h followed by a secondary peak between 48h-72h. These monocytes also up-regulate the expression of MHC II at 72h, a classical marker of their maturation into a DC phenotype. Antigen-positive DCs mature 72h after injection with CpG, as demonstrated by increased CD80 and CD86 at this time point. These responses at 72h are unique to CpG and are not observed following poly(I:C) or liposome alone injections. The present chapter also investigated the adaptive immune response in efferent lymph following CpG injection, revealing that CpG extends the process of lymph node cell shut down and increases the production of IFNγ by CD8 T cells. Whilst poly(I:C) increased antigen-specific humoral immunity following three injections, this chapter reveals that CpG is able to provide enhanced antigen-specific humoral immune responses after secondary injection.

4.2   Abstract

Liposomal vaccine formulations incorporating stimulants that target innate immune receptors have been shown to significantly increase vaccine immunity. Following vaccination, innate cell populations respond to immune stimuli, phagocytose and process antigen and migrate from the injection site, via the afferent lymphatic vessels, into the local lymph node. Here, the signals received in the periphery promote and sculpt the adaptive immune response. Effector lymphocytes then leave the lymph node via the efferent lymphatic vessel to perform their systemic function. We have directly cannulated the ovine lymphatic vessels to detail the *in vivo* innate and adaptive immune responses occurring in the local draining lymphatic network following vaccination with a liposome-based delivery system incorporating CpG. We show that CpG induces the rapid recruitment of neutrophils, enhances DC-associated antigen transport and influences the maturation of innate cells entering the afferent lymph. This translated into an extended period of lymph node shut down, the induction of IFNγ positive T cells and enhanced production of antigen specific antibodies. Taken together, the results of this study quantify the real time *in vivo* kinetics of the immune response in a large animal model after vaccination of a dose comparable to that administered to humans. It details enhancement of numerous immune mechanisms that provide an explanation for the immunogenic function of CpG when employed as an adjuvant within vaccines.

4.3   Introduction

The generation of a successful immune response to vaccination relies on appropriate activation of the innate immune system. Vaccine formulations incorporating stimulants that target innate immune receptors have been shown to significantly increase vaccine induced immunity (48). A major class of innate simulators under investigation to serve as adjuvants are the TLR ligands. These ligands bind to and stimulate TLRs, triggering a cascade of events that leads to the initiation of an immune response at the site of injection, ultimately resulting in the generation of an adaptive immune response in the local draining lymph node and the induction of immunological memory (8).

CpG is a synthetic oligonucleotide that signals predominantly through TLR 9 and mimics the immunostimulatory activity of bacterial DNA (210). When used as an adjuvant within vaccine formulations, CpG typically induces a strong type 1, proinflammatory immune response, generating long lasting cellular and humoral antigen specific immunity (87, 88, 210-213). The addition of CpG to the licenced human Anthrax vaccine induced antigen specific antibody titres in mice that were significantly higher and persisted for longer than those induced by the vaccine alone (79). Enhanced antibody titres generated by CpG have also been observed in large animal models (132, 214), non-human primates (80) and in human clinical trials (81-83). Complexing CpG into liposomes has been shown to further augment the stimulatory capacity of the adjuvant and increase cell mediated immunity (122, 125, 203, 215). In addition to acting as a delivery vehicle, liposomes protect the components from degradation and facilitate antigen uptake by APCs, leading to enhanced antigen recognition and vaccine specific immune responses (199-202). Several liposome based vaccines are currently in clinical trials, however the cellular targets of these formulations and the mechanisms of immune induction are yet to be defined (104).

The early immune response to vaccination is characterised by activation of cells present at the injection site and their subsequent migration to the local lymph node via the afferent lymphatics. The immunological signals received by innate cells at the periphery are conveyed to lymphocytes in the local lymph node, leading to the generation of an adaptive immune response where antigen specific lymphocytes emigrate via the efferent lymphatics to perform their tailored effector function (216). Examination of the afferent and efferent lymphatic

compartments during the innate and adaptive phases of an immune response allows investigation of the biological pathways at the injection site and within the draining lymph node responsible for vaccine immunity. We have directly cannulated these lymphatic vessels to explore the *in vivo* function of CpG when incorporated into a liposome vaccine formulation. We show that CpG significantly enhances multiple cellular responses at the site of injection that lead to increased antigen specific immunity in the efferent lymph and peripheral blood compartments.

4.4 Materials and Methods

4.4.1 Immunisations

All injections consisted of 500µl sterile PBS mixtures of liposomes (12% soy bean lecithin:cholesterol (9:1) obtained from Lipoid GmBH, Ludwigshafen, Germany) containing 400µg of ovalbumin (OVA) with or without the addition of 50µg of CpG, kindly provided by Zoetis (Parkville, VIC). The liposome preparations were injected subcutaneously in the area drained by the prefemoral lymph node at 500µl per injection using a 25 gauge needle. For antigen labelling, 5mg of OVA was resuspended at 1mg/ml in PBS and a 15M excess of A647 succinimidyl ester (Invitrogen) resuspended in DMSO at 5mg/ml was added and incubated at room temperature for 1h. Unconjugated fluorophore was removed from solution using an Amicon Ultracel 3K centrifugal filter (Millipore) by centrifuging at 2000 x g for 30min and washed with PBS five times.

4.4.2 Vaccination strategy and blood collection

One year old merino sheep were randomly assigned into two vaccination groups, liposome alone (n=5) and liposome with the addition of CpG (n=5). There were two cohorts of 10 animals, one for afferent lymphatic cannulation and the other for efferent lymphatic cannulation. Each animal received three injections of the respective formulation at both prefemoral drainage areas. Secondary injections were performed 4 weeks following primary injections, and tertiary injections were performed 3 months following secondary injections. Blood was collected prior to each injection, 7 and 10 days after secondary vaccination, and 3, 5, 7, 10 and 30 days after tertiary vaccination.

4.4.3 Pseudoafferent and efferent lymphatic cannulation surgery

Ovine prefemoral pseudoafferent and efferent lymphatic cannulations were performed as previously described (161, 197). For pseudoafferent lymphatic cannulation, the prefemoral lymph nodes of merino sheep were removed at one year of age and at least 2 months was allowed for reanastomosis of the afferent lymphatics with the larger efferent lymphatic vessel. A secondary surgery was performed to insert a 0.96mm x 0.58mm heparin coated polyvinyl chloride cannula into the pseudoafferent lymphatic vessel. For efferent lymphatic cannulation, a 0.96mm x 0.58mm heparin coated polyvinyl chloride cannula was inserted into the efferent

lymphatic vessel of the prefemoral lymph node. For both models, the cannulae were exteriorised and placed in a sterile collection flask attached to the side of the sheep. Injections were given at least seven days post lymphatic surgery to allow for surgical recovery. Handling of animals and experimental procedures were approved by the Monash University Animal Ethics Committee in accordance with the relevant licensing agreement.

4.4.4 Lymph collection and flow cytometry analysis

Afferent and efferent lymph was collected in sterile 50ml tubes containing 0.05IU of heparin (Pfizer) and 20µl of 100X cell culture penicillin-streptomycin (Invitrogen) for a period of one hour. Afferent lymph was collected prior to primary injection, and 4h, 24h, 48h and 72h post injection, generating the innate vaccination time course. Efferent lymph was collected prior to secondary injection, and 4h, 1d, 2d, 3d, 6d, 8d, 10d and 13d post injection generating the adaptive vaccination time course. Immediately after collection, afferent/efferent lymph cells and supernatant were separated by centrifugation at 400 x g at 4°C. The cell pellet was washed with 10ml of ice cold PBS + 2mM EDTA and resuspended in 1ml of 0.093mM ammonium chloride with 0.1M Tris (pH 7.2) to lyse red blood cells. After 3min incubation on ice, 9ml of ice cold FACS buffer (5% horse serum, 2mM EDTA in PBS) was added and the cells centrifuged, washed with FACS buffer and used for flow cytometry analysis. The surface marker antibodies used were anti-MHC II-pacific blue (clone 49.1, locally produced), anti-CD14-A700 (AbD Serotec), anti-CD172a (SIRPα) (clone DH59B, VMRD Inc. Pullman WA), anti-CD80 (AbD Serotec), anti-CD86 (AbD Serotec), anti-CD4-FITC (clone 44.38, AbD Serotec), anti-CD8-PE (clone 38.65, AbD Serotec), anti-γδ TCR-A647 and -FITC (clone 86D, locally produced), anti-CD45R (clone 20.96, locally produced), and anti-mouse IgG1 coupled to phycoerythrin (Caltag Laboratories). All samples for flow cytometry were prepared by resuspending 3×10^6 efferent lymph cells in 25µl of Fc-block (2% BSA, 2mM EDTA, 0.05% azide, 5% sheep serum in PBS) and then adding 25µl of surface marker antibody mixes. For intracellular cytokine staining, efferent lymph cells were resuspended in 150µl of 1% PFA for 20min on ice, centrifuged at 400 x g and washed twice in 500µl saponin buffer (1% horse serum, 0.05% azide, 0.1% saponin in PBS). The intracellular antibody mixes were then added (anti-IFNγ-A647 and anti-IL-4-FITC, AbD Serotec). All samples for flow cytometry were performed on an LSR2 machine (Becton Dickinson) and analysed using the FlowJo software. For all flow cytometry gating strategies, see Supplemental Figures 1 and 2*.

*for further gating strategies, see chapter two, figures 4 and 6

4.4.5   ELISA for the identification of OVA-specific antibodies

An indirect ELISA was used to measure relative OVA-specific antibody levels in each efferent lymph and serum sample. Briefly, 100μl of OVA (4μg/ml in PBS) was added to a flat bottom 96 well plate (immunosorb, NUNC) and left to bind overnight at 4°C. The plate was washed with 0.05% PBST, and blocked with 1% horse serum in PBS at 200μl/well for 1h at room temperature, and sera samples (diluted 1/500) and efferent lymph samples (diluted 1/2000) added at 100μl/well for 1h. The wells were washed before 100μl of rabbit anti-sheep immunoglobulins/HRP antibody (DAKO, ref P0163) (diluted 1/1000 in PBS) was added and allowed to incubate for 1h. Reactions were developed using TMB substrate (Invitrogen) at 100μl/well, stopped by the addition of 50μl/well of 2M H_2SO_4 and read at 450nm on a spectrophotometer (Molecular Devices, Spectramax Plus).

4.4.6   Statistical analysis

Results are presented as mean ± standard error of the mean, with n=5 in each treatment group. Differences between groups and within each group were calculated with a 2 way repeated measures (RM) ANOVA using a Sidak post test to correct for multiple comparisons. Significance was determined as the confidence interval being greater than 95% ($p < 0.05$). The statistical software used was GraphPad Prism, version 6.01.

4.5   Results

4.5.1   Addition of CpG to liposomal antigen formulations alters the kinetics of innate cellular recruitment into afferent lymph

Whilst no statistically significant change in afferent lymph volume and total cell number was observed in either group after primary vaccination (Figure 1A), the addition of CpG to liposomal OVA formulations elicited a dramatic and transient increase in the recruitment of neutrophils in afferent lymph, increasing 11 fold 4h after injection and returning to baseline by 24h (Figure 1B). Although not significant, CpG induced a unique trend of monocyte recruitment, with a primary peak at 4h, decline to baseline at 24h, followed by a secondary peak at 48-72h (Figure 1B). This trend is distinct from that observed when other TLR ligands have been used as adjuvants in this model (162). Whilst total DC percentages were relatively consistent over the time course in both groups, CpG increased the percentage of the SIRPα^{high} DC subset at 48h and 72h after injection, increasing to 65% of DCs at 72h (Figure 1C). Lymphocyte populations in afferent lymph were also investigated, where CD4 T cells, CD8 T cells, γδ T cells and B cells were all identified, however these did not change significantly over time in either group*.

4.5.2   Liposomal CpG increases the total number of antigen carrying cells in afferent lymph but not the capacity of individual cells to ingest antigen

In order to investigate the cell types within afferent lymph that transport antigen to the lymph node, the liposome injections contained A647-labelled OVA. CpG induced the greatest number of A647-OVA$^+$ neutrophils at 4h (Figure 2C) and A647-OVA$^+$ DC at 24h (Figure 2A) when compared to liposome alone. Both injections induced A647-OVA uptake by monocytes, with CpG inducing a two wave trend of A647-OVA$^+$ monocytes, first at 4h, followed by a secondary peak between 48-72h (Figure 2B), a similar trend to that observed in the total CpG monocytes in Figure 1B. When investigating the mean fluorescence intensity (MFI) of A647-OVA$^+$ cells, it was observed that whilst CpG increased the number of DCs and neutrophils carrying antigen, this was not associated with an increase in the amount of A647-OVA fluorescence within individual cells above the liposome alone control (Figure 2).

*see section 4.7 for extended figure

Figure 1. Vaccination induces temporal changes in the volume and cellular composition of afferent lymph. Changes over time in total volume of afferent lymph and total cell number in afferent lymph (A), the percentage of lymphocytes, neutrophils, monocytes and DCs (B), and the percentage of DC subsets, SIRPα[high] DCs and SIRPα[low] DCs (C). Data expressed as mean ± SEM of five individually analysed animals at each time point in both treatment groups, * indicate differences between groups and # indicate differences from baseline (-2h) within each group, *p<0.05, #p<0.05, ##p<0.01, ###p<0.001.

Figure 2. Vaccination induces temporal changes in the number of antigen positive cell populations and the level of antigen uptake. The number of A647-OVA$^+$ DCs (A), A647-OVA$^+$ monocytes (B) and A647-OVA$^+$ neutrophils (C) per 10, 000 cells in afferent lymph over time, and mean fluorescence intensity (MFI) of these A647-OVA$^+$ cells over time. Data expressed as mean $\pm$ SEM of five individually analysed animals at each time point in both treatment groups, * indicate differences between groups and $^\#$ indicate differences from baseline (-2h) within each group, *p<0.05, **p<0.01, $^\#$p<0.05, $^{\#\#}$p<0.01, $^{\#\#\#}$p<0.001, $^{\#\#\#\#}$P<0.0001.

4.5.3 *SIRPα^high DCs traffic more antigen into afferent lymph than SIRPα^low DCs*

While SIRPα^high DCs are only 2 fold more abundant in afferent lymph (Figure 1C), there were between 5 and 10 fold more A647-OVA$^+$ SIRPα^high DCs when compared to A647-OVA$^+$ SIRPα^low DCs in both groups (Figure 3B). The number of A647-OVA$^+$ SIRPα^high DCs was highest 4h post injection of the liposome alone formulation, however the amount of fluorescence within each SIRPα^high DC peaked 24h after injection (Figure 3A). Conversely, the addition of CpG to the liposome formulation caused the number of A647-OVA$^+$ SIRPα^high DCs to peak at 24h and the level of A647-OVA fluorescence to peak between 4 and 24h after injection (Figure 3A). CpG induced a 2 fold increase in the A647-OVA fluorescence of SIRPα^high DCs at 4h when compared to liposome alone (Figure 3A). CpG did not increase the number of A647-OVA$^+$ SIRPα^low DCs above the liposome alone injection, however CpG increased the amount of A647-OVA fluorescence within individual SIRPα^low DCs at 24h (Figure 3B).
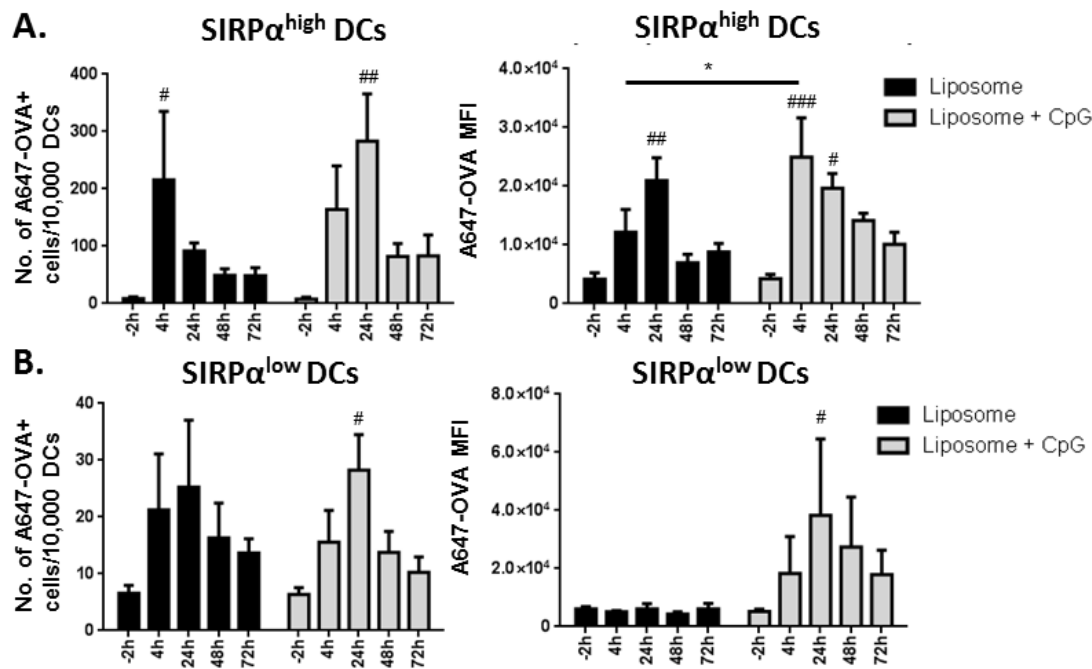
Figure 3. Vaccination induces temporal changes in the number of antigen positive DC subsets and the level of antigen uptake. The number of A647-OVA$^+$ SIRPα^high DCs (A), A647-OVA$^+$ SIRPα^low DCs (B) per 10, 000 DCs in afferent lymph over time, and the change in mean fluorescence intensity (MFI) of these A647-OVA$^+$ DCs over time. Data expressed as mean ± SEM of five individually analysed animals at each time point in both treatment groups, * indicate differences between groups and # indicate differences from baseline (-2h) within each group, *$p < 0.05$, #$p < 0.05$, ##$p < 0.01$, ###$p < 0.001$.

4.5.4 Liposomal CpG induces the maturation of antigen carrying monocytes and DCs in afferent lymph 72h post vaccination

Injection with CpG induced a significant increase in the mean fluorescence intensity (MFI) of MHC II on A647-OVA$^+$ monocytes, with a mean fold change of 2.0 at 72h (Figure 4A). The MFI of MHC II did not increase on any other A647-OVA$^+$ cell population in afferent lymph (data not shown). All afferent lymph DCs expressed both costimulatory molecules CD80 and CD86 prior to injection. Significant increases in the MFI of CD80/CD86 on A647-OVA$^+$ DCs were observed after injection with liposomal CpG, with a mean fold change of 2.32 and 6.33, respectively, at 72h (Figure 4B, C). This maturation effect was unique to A647-OVA$^+$ monocytes and DCs, and was not observed in any A647-OVA$^-$ cell population in either group (data not shown). Afferent lymph B cells were also shown to express CD80, however expression did not change significantly over time or between groups.
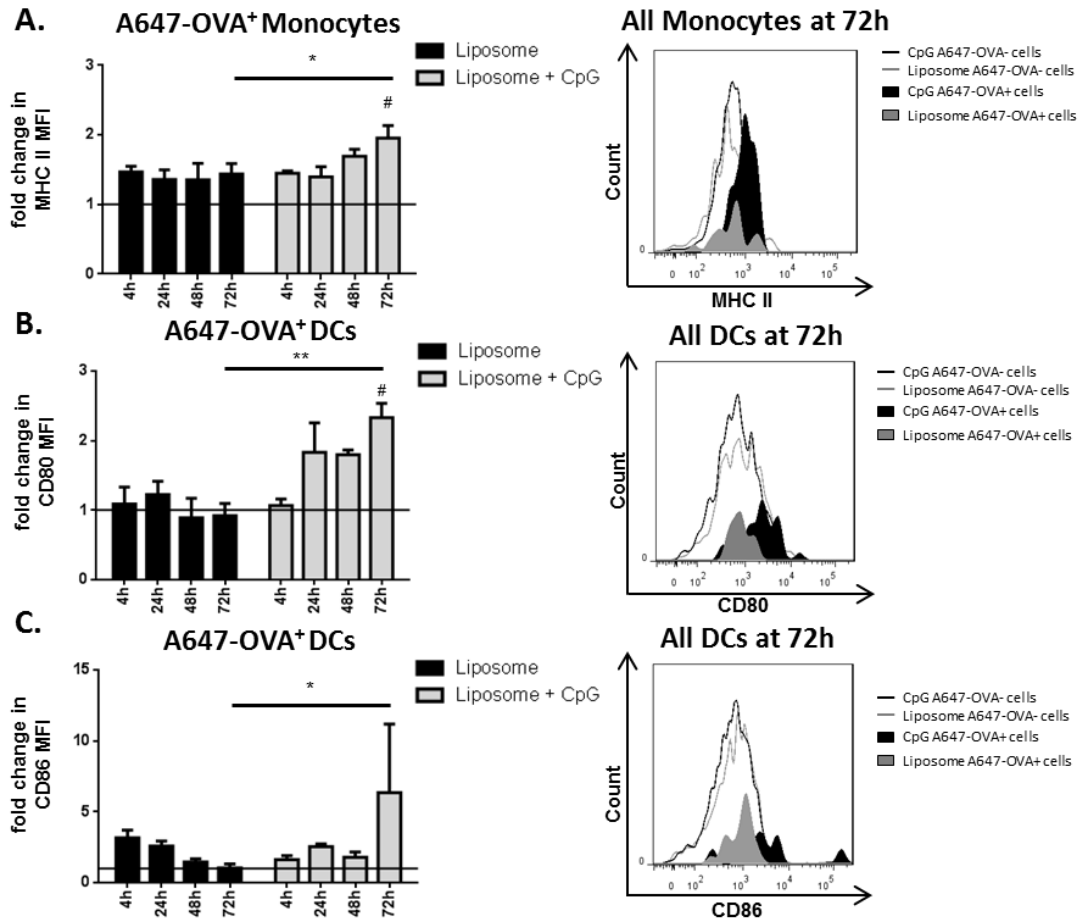
Figure 4. Vaccination induces temporal changes in the MHC II expression on antigen positive monocytes and CD80/CD86 expression on antigen positive DCs. Fold change over time in the mean fluorescence intensity (MFI) of MHC II on A647-OVA$^+$ monocytes (A), CD80 on A647-OVA$^+$ DCs (B), CD86 on A647-OVA$^+$ DCs (C), and the respective flow cytometry plots of the MFI of A647-OVA$^+$ cells compared with A647-OVA$^-$ cells. All flow cytometry plots are of one representative animal from each treatment group. Data expressed as mean ± SEM of five individually analysed animals at each time point in both treatment groups, * indicate differences between groups and $^#$ indicate differences from 4h within each group, *p<0.05, **p<0.01, $^#$p<0.05.

4.5.5 The adaptive response in efferent lymph: CpG extends lymph node cell shut down and increases lymphocyte traffic

Secondary vaccination with the liposomal formulations induced temporal changes in the total volume and number of cells within efferent lymph flowing from the local lymph node. Both injections caused a marked reduction in cell output, but not volume, 4h after injection, reducing from approximately 5×10^7 cells per hour prior to injection to 1×10^7 cells per hour 4h after injection (Figure 5A). This phenomenon is a process known as lymph node cell shut down (174). CpG extended the duration of lymph node cell shut down by a further 24h, with cell numbers remaining at approximately 1×10^7 cells per hour. This was followed by a dramatic and unique increase in the number of cells and lymph volume leaving the lymph node 2d post injection (Figure 5A). All lymphocyte populations were equally reduced during the period of lymph node cell shut down induced by both injections (Figure 5B). The increase in cell number 2d after injection with CpG was due to an increase in the number of conventional α-β CD4 and CD8 T cells (Figure 5B). Interestingly, CpG also increased the number of CD8 T cells expressing the γδ TCR at 2d post injection (Figure 5B).

4.5.6 Vaccination with liposomal CpG increases IFNγ production by CD8 T cells in efferent lymph

Prior to secondary injection of both liposomal formulations, there were a greater percentage of IFNγ$^+$ lymphocytes circulating in efferent lymph when compared to IL-4$^+$ lymphocytes, 0.5% and 0.09%, respectively (Figure 6A). Following injection, the percentage of IFNγ$^+$ CD4 and CD8 T cells remained higher than IL-4$^+$ cells, while equal percentages of γδ T cells were observed with both cytokines (Figure 6B-D). Injection of CpG induced a significant 3 fold increase in the number of IFNγ$^+$ lymphocytes 3d after injection (Figure 6A). This effect was due to an increase in the percentage of both IFNγ$^+$ CD8 T cells, increasing from 1.6% prior to injection to 3.6% 3d after injection, and IFNγ$^+$ CD4 T cells, increasing from 0.5% prior to injection to 1.3% 3d after injection (Figure 6B-C). Additionally, there were significantly more IFNγ$^+$ CD8 T cells at both 2 and 3d after injection with CpG when compared to liposome alone (Figure 6B). CpG did not significantly increase the percentage of γδ T cells producing IFNγ or IL-4.

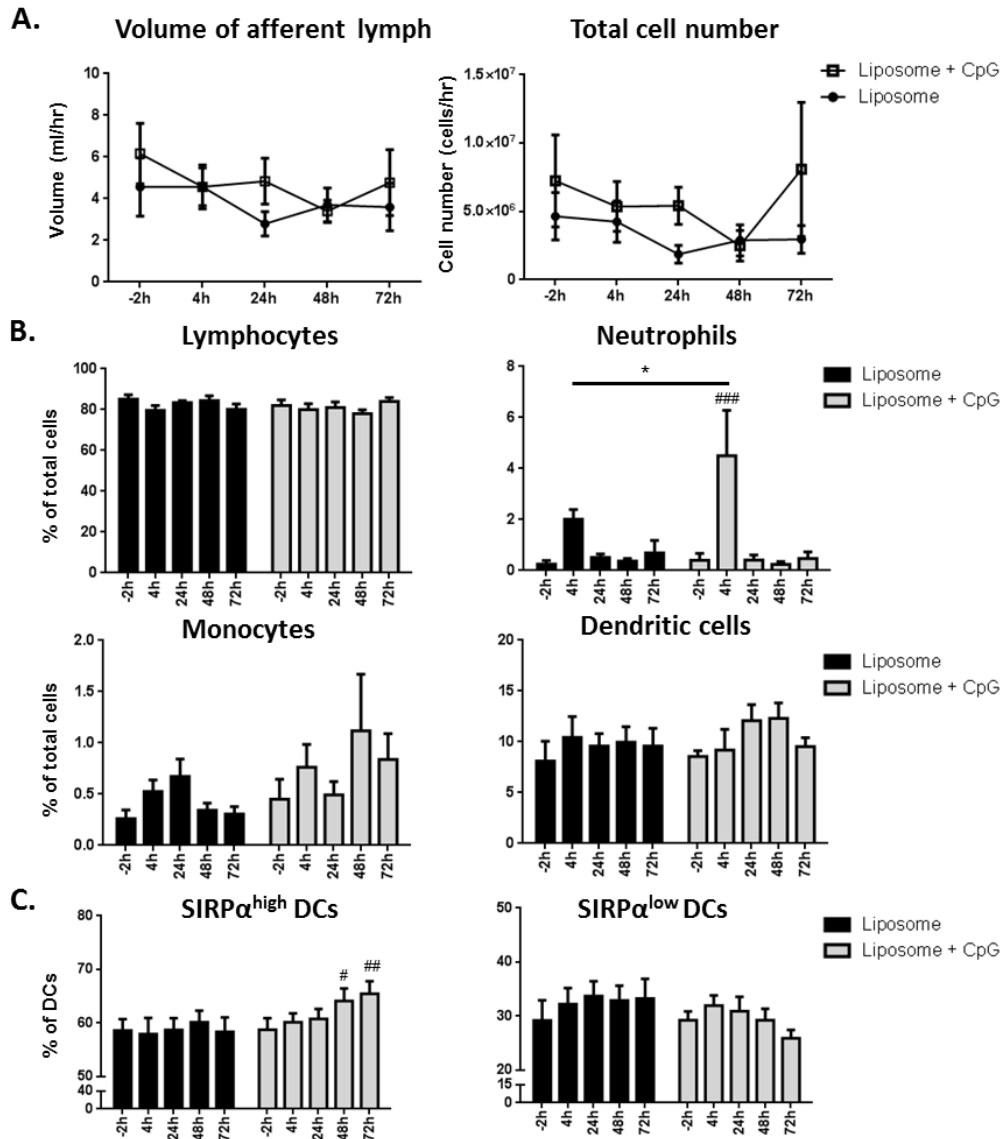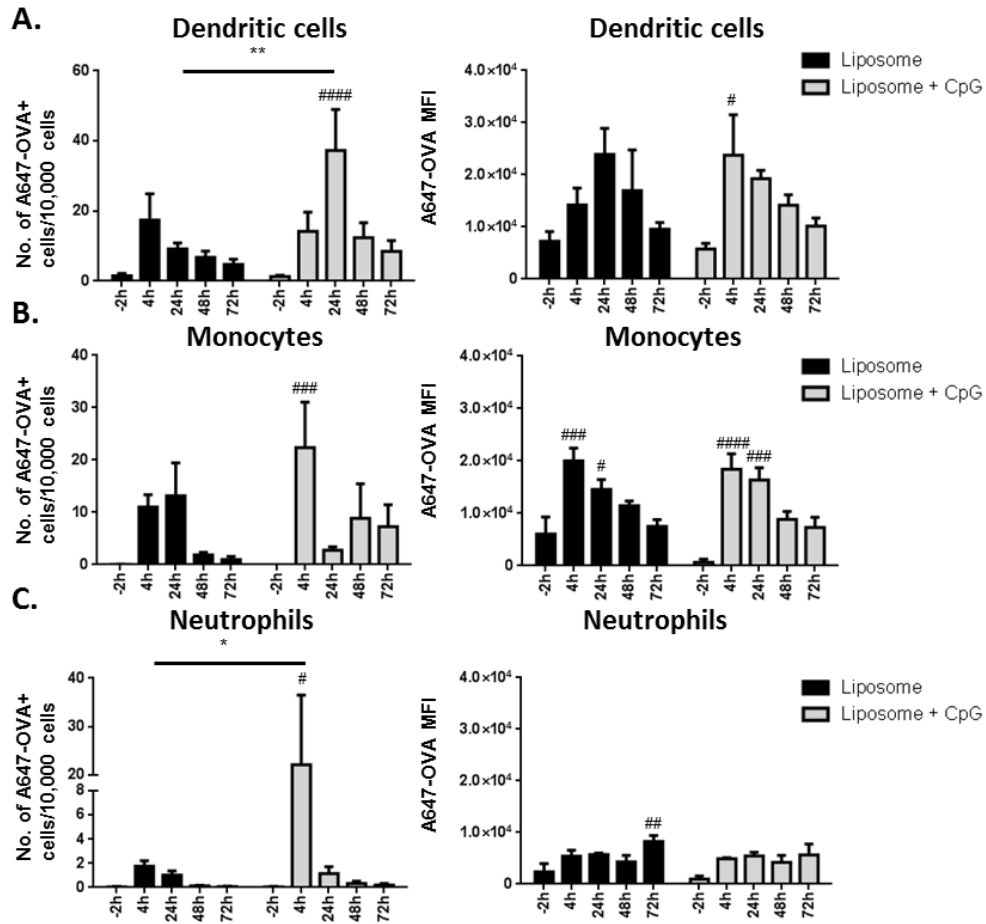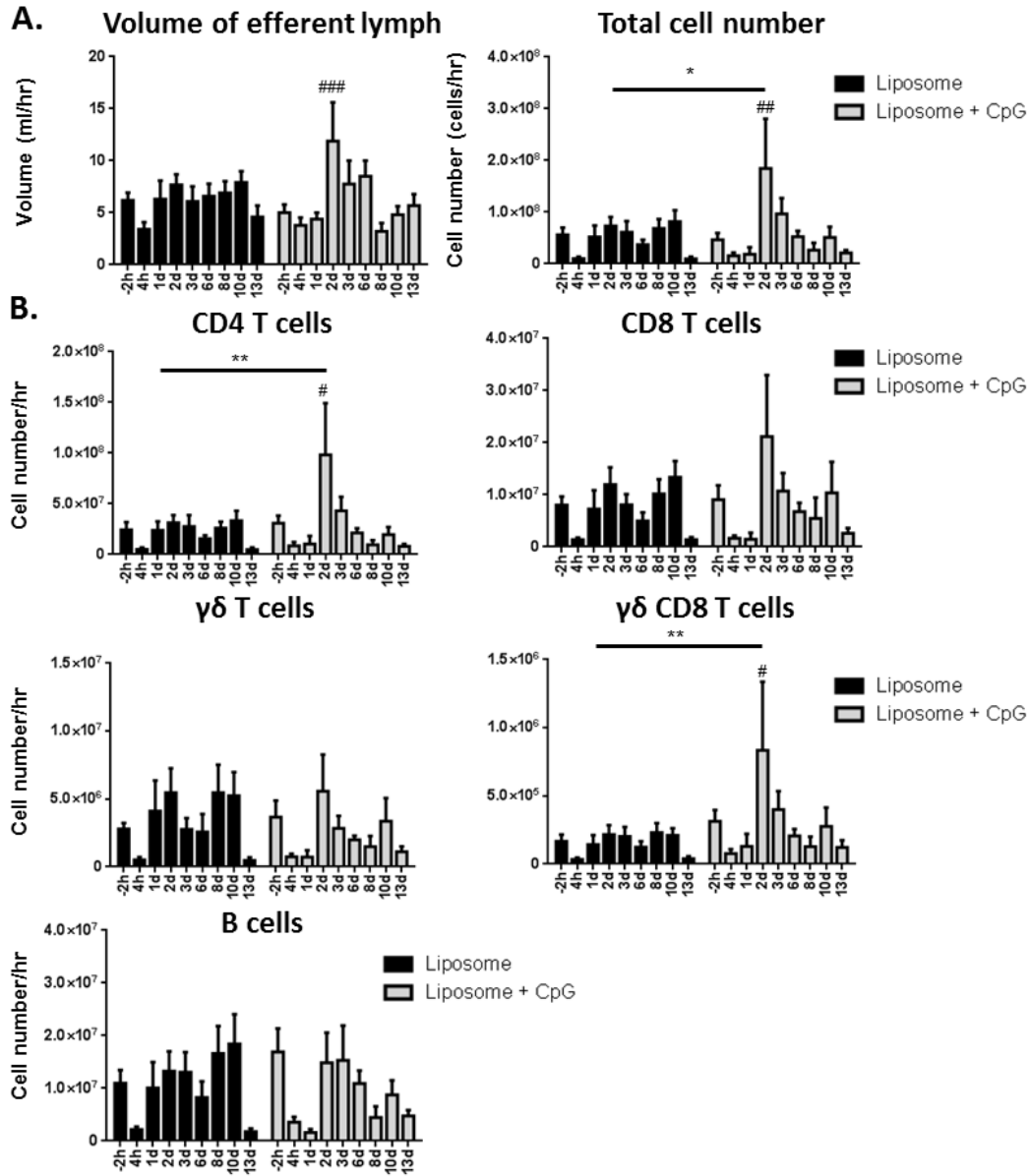**Figure 5.** Vaccination induces temporal changes in the volume and cellular composition of efferent lymph. Changes in total volume of efferent lymph and total cell number in efferent lymph over time (A). Changes in the cell number per hour of CD4 T cells, CD8 T cells, γδ T cells, γδ CD8 T cells and B cells (B) in efferent lymph over time. Data expressed as mean ± SEM of five individually analysed animals at each time point in both treatment groups, * indicate differences between groups and # indicate differences from baseline (-2h) within each group, *p<0.05, **p<0.01, #p<0.05, ##p<0.01, ###p<0.001.
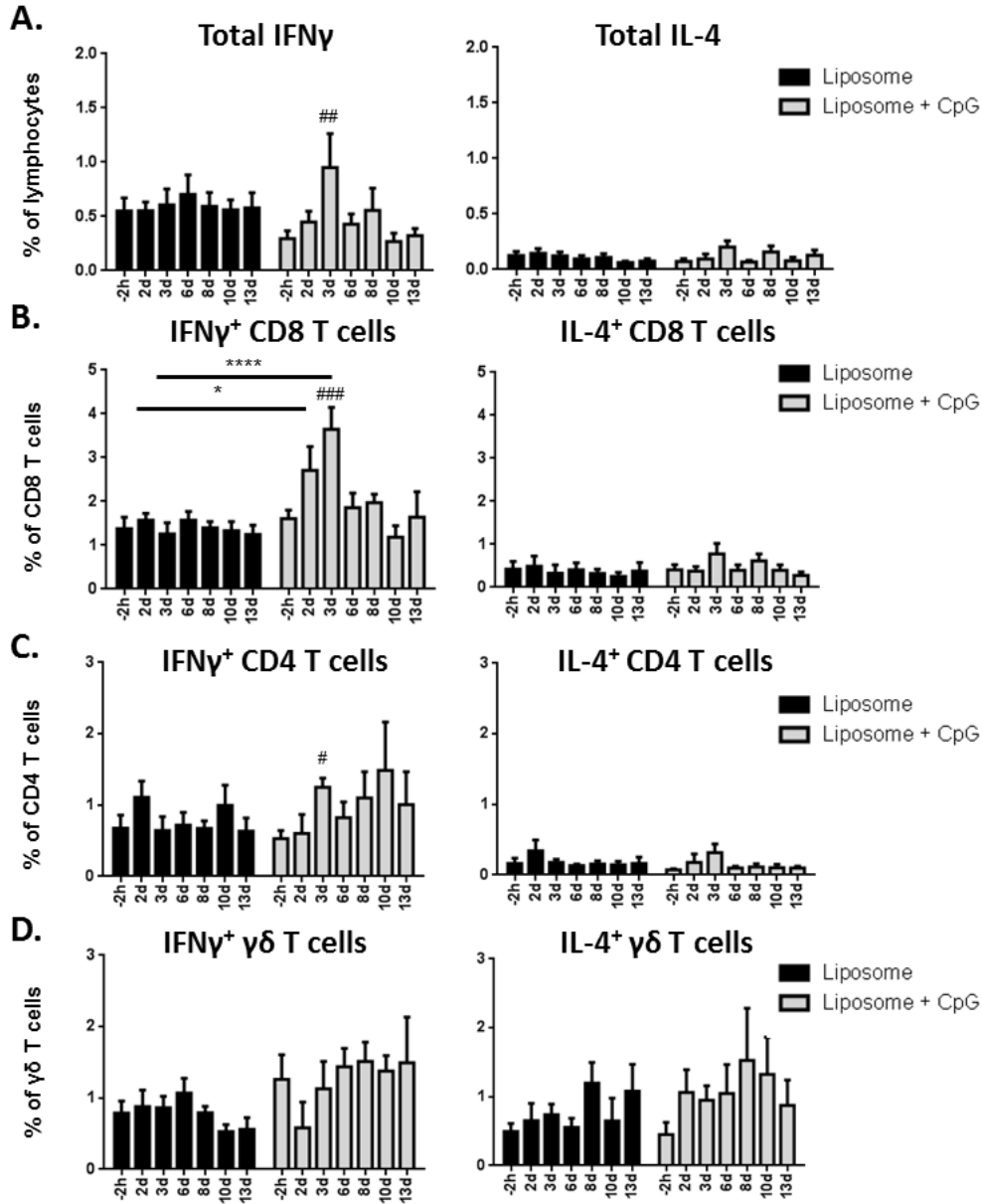
Figure 6. Vaccination induces temporal changes in IFNγ and IL-4 production by lymphocyte populations in efferent lymph. IFNγ and IL-4 positive total lymphocytes (A), CD8 T cells (B), CD4 T cells (C), and γδ T cells (D) in efferent lymph over time. Data expressed as mean ± SEM of five individually analysed animals at each time point in both treatment groups, * indicate differences between groups and # indicate differences from baseline (-2h) within each group, *p<0.05, ****p<0.0001, #p<0.05, ##p<0.01, ###p<0.001.

4.5.7 Liposomal CpG increases antigen specific antibodies in efferent lymph and sera following vaccination

OVA specific antibody levels were measured in the efferent lymph and sera of vaccinated sheep. In the efferent lymph, secondary vaccination with CpG induced greater OVA specific antibody between 3 and 13d after vaccination when compared to liposome alone (Figure 7A). In fact, mean end point antibody titres from efferent lymph were approximately 35 fold greater at day 5 in the CpG group (Figure 7A). This effect was also observed in the sera, where secondary vaccination with CpG induced greater OVA specific antibody 7 and 10d post vaccination when compared to liposome alone (Figure 7B). Tertiary vaccination with both liposomal formulations further increased OVA specific antibody levels in the sera (Figure 7C). CpG induced greater antigen specific antibody levels than liposome alone from day 6 that continued to remain elevated for 30d after vaccination (Figure 7C). Additionally, antigen specific antibodies were vastly more concentrated in the efferent lymph than the sera, highlighting efferent lymphatic cannulation as an ideal model to assess both cellular and humoral immunity induced by vaccination.
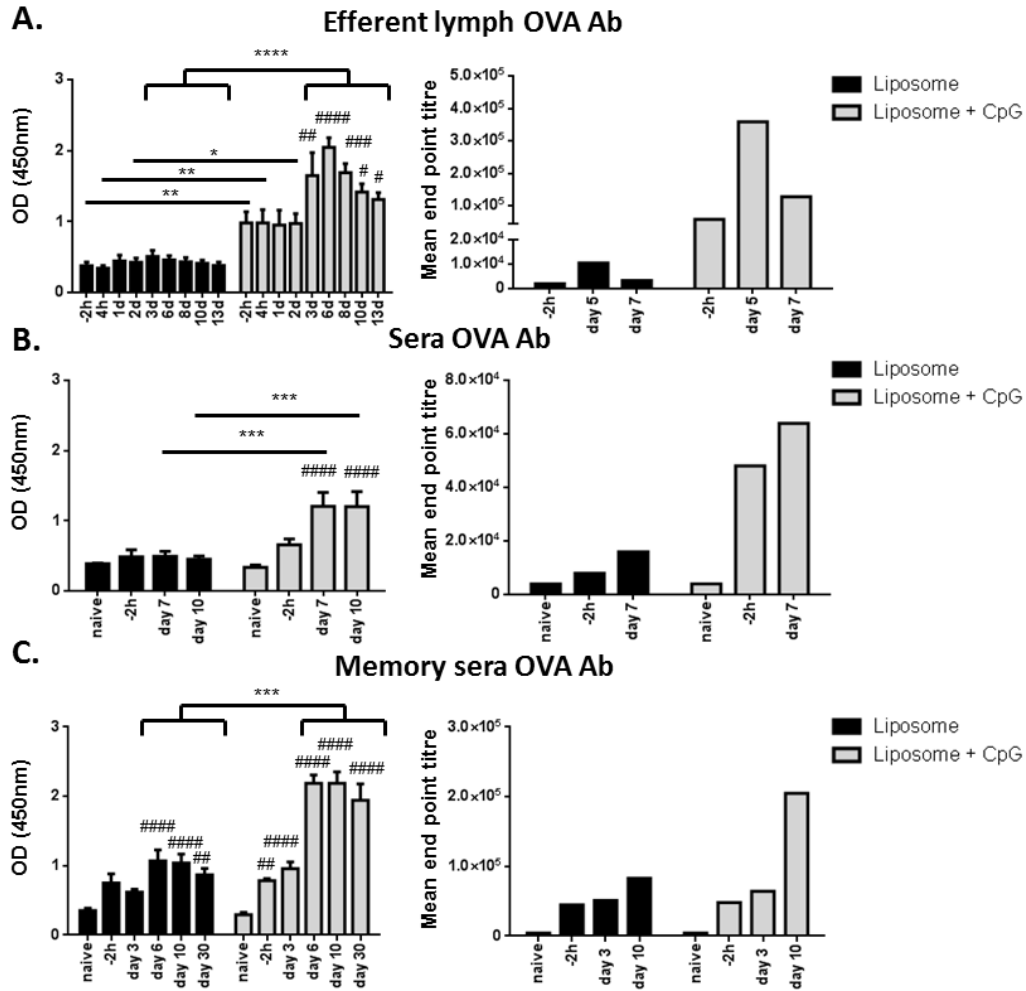
Figure 7. Vaccination increases antigen specific antibody concentration in efferent lymph and sera. OVA specific antibody concentration in efferent lymph after secondary injection expressed as OD (450nm) and mean end point titre at baseline (-2h) and at different times after injection (A). OVA specific antibody concentration in sera after secondary (B) or tertiary (C) injection expressed as OD (450nm) and mean end point titre prior to primary injection (naïve), prior to secondary or tertiary injection (-2h), and at different days after injection. Data expressed as mean $\pm$ SEM of five individually analysed animals at each time point in both treatment groups, * indicate differences between groups and # indicate differences from baseline (-2h) within each group, ***p<0.001, ****p<0.0001, #p<0.05, ##p<0.01, ###p<0.001, ####P<0.0001.

4.6   Discussion

The immunogenicity of liposomal vaccine formulations can be improved by the addition of immunostimulatory components (104, 217). Several recent studies have demonstrated that incorporating innate immune agonists into liposomes improves both cell mediated and humoral antigen specific immunity in mice (122, 125). However, little is known about the effect of liposomal adjuvant formulations on migratory cell populations obtained *in vivo* from non-manipulated tissues. By directly cannulating ovine lymphatic vessels, we were able to intercept and characterise the cells migrating from the skin and lymph nodes into the draining lymphatic network.

The majority of inflammatory stimuli, including sterile cell damage, microorganisms and vaccine adjuvants, induce an early inflammatory environment at the site of injection, characterised by an influx of neutrophils from the blood (164). Typically, the more potent the stimuli the longer this inflammatory environment persists, and the stronger the ensuing immune response. This is desirable when clearing a persistent infection, however a mild inflammatory response with a strong immune outcome is preferable for human vaccination where excess inflammation can lead to enhanced reactogenicity (95). Our studies have shown that injection with most vaccine adjuvants and even sterile saline results in the rapid recruitment of neutrophils and monocytes within afferent lymph following injection (161, 162, 195). Consistent with this, injection of sterile liposomes alone or containing CpG induced neutrophils and monocytes to rapidly enter the afferent lymph within 4h. Interestingly, the addition of CpG, a bacterial PAMP, increased the total number of neutrophils leaving the injection site but did not significantly prolong the duration of a non-specific neutrophil associated inflammatory response at the site of injection.

Consistent with previous studies utilising this model (161, 162), the number and percentage of total DCs in afferent lymph is remarkably unaffected by vaccine adjuvants, including liposomes and CpG. This is in contrast to some murine studies, where dendritic cells accumulate within the lymph node following injection with CpG (218). This phenomenon may be the result of DC recruitment from the blood into the lymph node, or increased damage at the site of injection from relatively higher vaccine doses that may cause aberrant migration. However, when we calculated the relative contribution of antigen transport by

each afferent lymph cell type, DCs were the major cell type responsible and this was significantly enhanced by CpG 24h after injection.

Several innate immune agonists have been shown to activate DC maturation *in vitro,* characterised by upregulation of MHC II and the co-stimulatory molecules CD80 and CD86 (219-222). There are limited studies that show migratory DCs, which display a highly mature phenotype, can further mature in response to inflammatory stimuli (140). In the present study, CpG induced an increase in expression of CD80 and CD86 on antigen positive migratory DCs 72h after vaccination. No increase in MHC II expression on afferent lymph DCs was observed throughout the time course. CpG has also been shown to induce the maturation of naive human blood monocytes into functionally mature DCs over 2-4 days *in vitro*, demonstrated by an increase in MHC II expression (223, 224). From our data, it appears that this is occurring *in vivo* within the peripheral tissues prior to emigration to the lymph node, but only with monocytes that have taken up the antigen, presumably in concert with CpG within the liposomes. Of the vaccine adjuvants we have tested within ovine lymphatics (161, 162, 195), CpG uniquely triggers antigen carrying monocytes and DCs to increase their T cell activating machinery at the injection site before migrating to the local lymph node. Taken together with increased DC antigen uptake over the vaccination time course, these results may provide an explanation for the increased antigen specific adaptive immunity induced by CpG (122, 125, 209).

Although CpG increased the number of afferent lymph neutrophils and monocytes carrying antigen, this was generally not associated with an increase in the amount of fluorescence within each cell above the liposome alone control. This suggests that CpG does not increase the phagocytic ability of these cell types, but rather induces greater recruitment of these cells to the injection site where antigen is present. Interestingly, monocytes and DCs contained comparable levels of antigen fluorescence, approximately 2 fold greater than the mean fluorescence of neutrophils across the time course. A significant increase in the amount of antigen fluorescence within each cell was observed in both the SIRPα^{high} and SIRPα^{low} DC subsets after injection with CpG. A recent comparative genomics study revealed that the ovine afferent lymph SIRPα^{high} DCs are genetically and functionally equivalent to the mouse CD11b$^+$ DCs and human BDCA1$^+$ DC, whist the SIRPα^{low} DCs represent the mouse CD8α$^+$ DCs and human BDCA3$^+$ DCs (144). Consistent with other studies (144, 147, 154, 195), the SIRPα^{high} DC subset transported the majority of DC-associated antigen after injection with both formulations. The fact that these cells have been shown to be more efficient at CD4 T

cell activation via classical MHC II presentation (156) and the observation that CpG increased the ability of these cells to take up antigen, suggest that this may lead to increased CD4 T cell stimulation in the local lymph node.

Recent studies have shown that a subset of the afferent lymph SIRPα^{low} DCs are efficient at activating CD8 T cells via the cross presentation pathway (147). Similarly, studies in mice have also demonstrated that skin derived DC populations are able to cross present viral antigens to CD8 T cells in the lymph node (225). In our study, despite existing at low numbers in afferent lymph, antigen positive SIRPα^{low} DCs demonstrated an improved ability to ingest antigen after injection with CpG when compared to liposome alone. Whether this subset is responsible for the significant increase in the number of CD8 T cells expressing IFNγ exiting the lymph node will require further investigation. CpG-induced increases in IFNγ production by CD8 T cells have been observed previously (226, 227), and incorporating CpG into liposomes was shown to enhance antigen specific cell mediated immune responses (228).

Unlike the conventional α-β TCR CD4 and CD8 expressing T cells, the percentages of γδ T cells expressing IFNγ or IL-4 were similar and did not change significantly over the vaccination time course suggesting that CpG does not skew these cells to induce a specific immune phenotype following vaccination. Interestingly, the γδ T cell population were responsible for almost all of the IL-4 positive cells present over the time course. The production of both IFNγ and IL-4 by γδ T cells has been observed previously, where γδ T cells exhibit both pro inflammatory and regulatory functions, depending on the type or severity of the infection (229, 230).

Our study shows that secondary injection with both formulations induced a rapid reduction in the number of cells leaving the lymph node immediately after vaccination. This phenomenon, known as lymph node cell shut down, has been observed in several studies utilising the ovine efferent lymphatic cannulation model (174, 186, 231). In our study, this process was extended by an additional 24h after vaccination with CpG and was observed in all lymphocyte populations. A similar effect has been shown previously, where the addition of the adjuvant ISCOMATRIX™ to the Flu antigen induced an extended lymph node cell shut down period (186). It was hypothesised that this cell shut down occurred to increase the time for antigen carrying APCs and antigen specific lymphocytes to interact in the lymph node, promoting the generation of an adaptive immune response (174). The acute increase in the

number of IFNγ producing CD4 and CD8 T cells leaving the lymph node immediately following CpG induced cell shut down and the significant increase in the concentration of antigen specific antibodies observed in our study support this hypothesis.

Injection of CpG induced a significant increase in antigen specific antibody in both the efferent lymph and peripheral blood of vaccinated animals, suggesting that the liposomal CpG vaccine formulation has both local and systemic effects on adaptive immunity. In fact, tertiary injection of CpG increased antigen specific antibodies that remained elevated in the circulation for 30 days after vaccination. This has been shown previously where liposome vaccine formulations containing CpG were up to 30 times more effective than un-encapsulated CpG at inducing antigen specific antibodies to influenza and hepatitis B antigens (209). The elevation of antigen specific antibody induced by CpG occurred after secondary vaccination, however tertiary vaccination was required for the liposome alone injections to demonstrate any significant increase in antigen specific antibody. This reinforces previous observations that liposomal formulations without the addition of immune stimulatory components often show limited immunogenicity and require multiple boost injections to elicit strong immunity (104).

This is the first study to characterise the action of liposomal vaccine formulations incorporating CpG in the local draining lymphatic network of vaccinated animals. We have shown that the addition of CpG to these formulations significantly enhances antigen uptake by afferent lymph cell populations and induces their maturation prior to their migration to the local lymph node. This ultimately leads to an extended lymph node cell shut down period, promoting the generation of an adaptive immune response, characterised by increased CD8 T cell IFNγ production and the persistence of local and systemic antigen specific antibodies. Taken together, the results of this study establish an *in vivo* explanation for the increased immune response induced by CpG and enhance our understanding of the immunogenic function of liposomal vaccine formulations.

4.7   Supplemental and extended figures
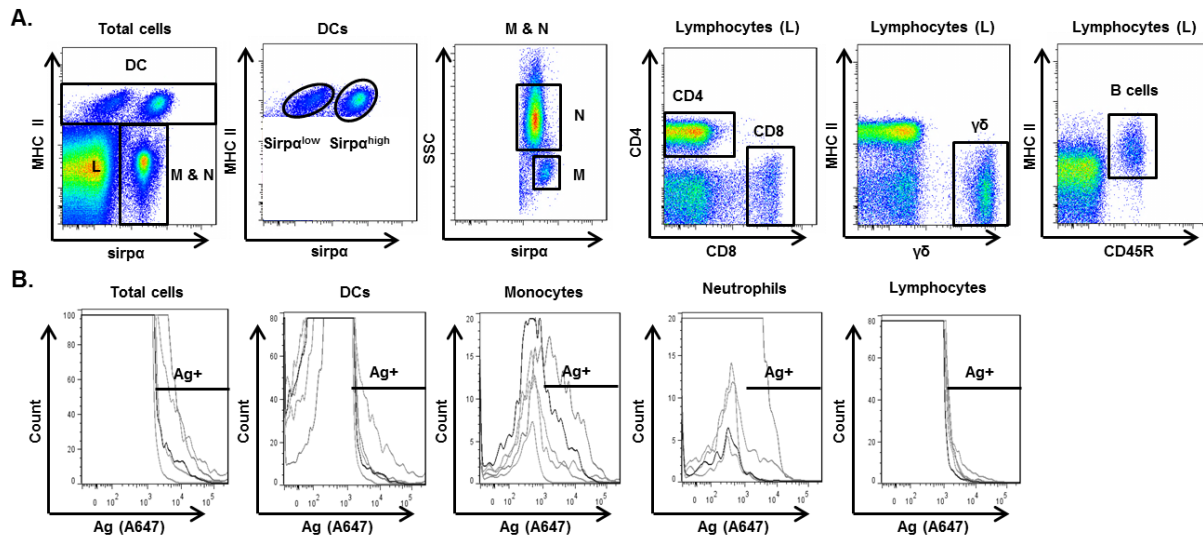
Supplementary Figure 1. Flow cytometry gating strategies of cell populations and antigen positive cells in afferent lymph. (A) DCs are gated based on SIRPα and MHC II expression, monocytes and neutrophils are firstly gated on SIRPα expression and further defined based on SSC profile, lymphocytes are divided into T cells based on CD4, CD8 and γδ expression and divided into B cells based on CD45R and MHC II expression. (B) Antigen positivity is determined based on A647-OVA+ fluorescence that is greater than pre vaccination levels. Flow cytometry plots are of one representative animal.
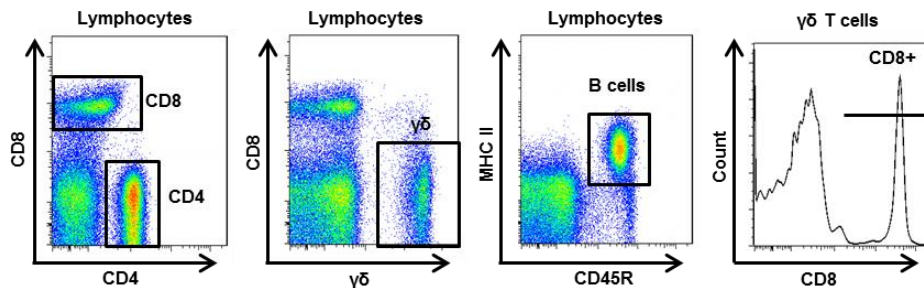
Supplementary Figure 2. Flow cytometry gating strategies of cell populations in efferent lymph. Lymphocytes are divided into T cells based on CD4, CD8 and γδ expression and divided into B cells based on CD45R and MHC II expression. γδ CD8+ T cells are further gated firstly on expression of γδ and then expression of CD8. Flow cytometry plots are of one representative animal.
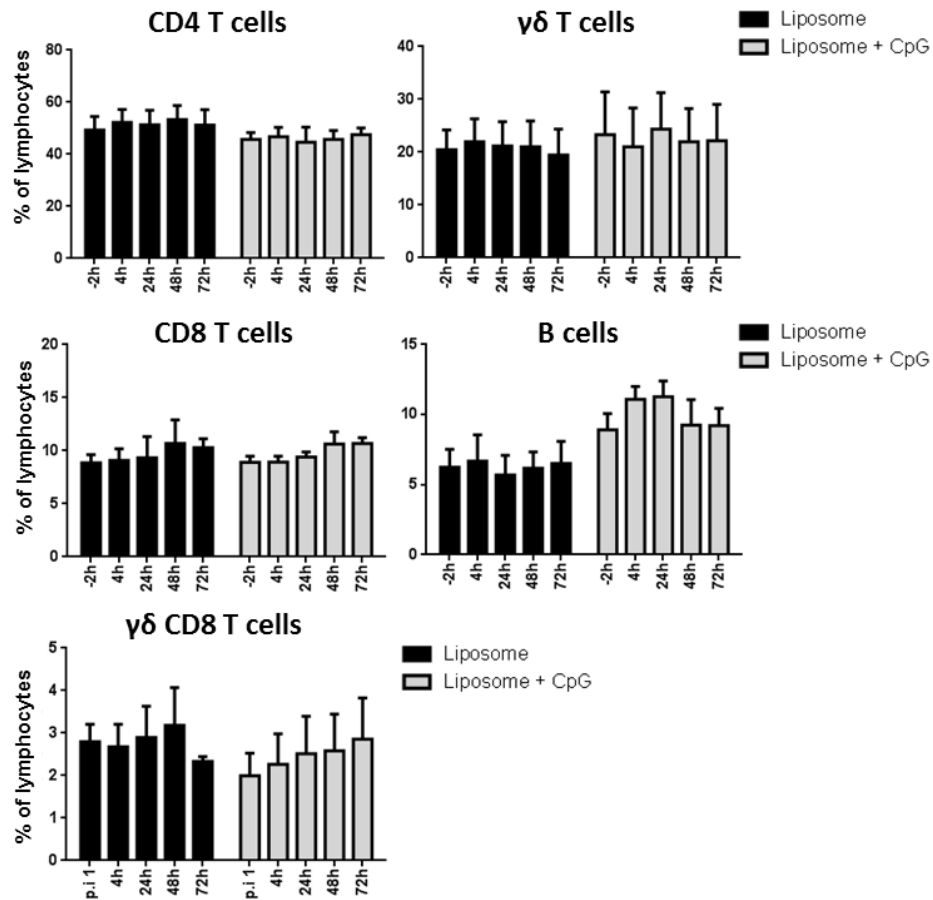
Extended Figure 1. The percentage of lymphocyte subsets in afferent lymph over time after injection with liposome alone or liposome + CpG. Data expressed as mean ± SEM of five individually analysed animals at each time point in both treatment groups.

Transcriptional profile in afferent lymph cells following vaccination with liposomes incorporating CpG

Melanie R. Neeland*, Martin J. Elhay†, David R. Powell[+,++], Fernando J. Rossello[+,++], Els N.T. Meeusen*[#], Michael J. de Veer*

*Biotechnology Research Laboratories, Department of Physiology and [#]Department of Microbiology, Monash University, VIC 3800, Australia

† Zoetis Research and Manufacturing Australia P/L, 45 Poplar Road, Parkville VIC 3052, Australia

[+] Victorian Bioinformatics Consortium, Monash University, VIC 3800, Australia

[++] Life Sciences Computation Centre, Victorian Life Sciences Computation Initiative, Carlton VIC 3053, Australia

Note: Supplemental figures are supplied at the end of this chapter

Declaration for Chapter Five
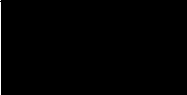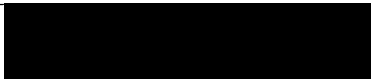
In the case of Chapter Five, the nature and extent of my contribution to the work was the following:

Nature of contribution	Extent of contribution
I was responsible for the design of the majority of the experiments. Bioinformatic analysis of RNA sequencing data was performed by co-authors on the manuscript. I performed further gene expression analysis of RNA sequencing data. I conducted the experiments and analysis for the real time PCR data. I interpreted the results and wrote the manuscript with assistance from co-authors.	70%

The following co-authors contributed to the work.

Name	Nature of contribution	Extent of contribution for student co-authors only
Martin Elhay	Provided reagents, assisted with experimental design and manuscript editing	N/A
David Powell	Bioinformatic analysis of RNA sequencing data	N/A
Fernando Rossello	Bioinformatic analysis of RNA sequencing data	N/A
Els Meeusen	Assisted with experimental design, interpretation of results and manuscript editing	N/A
Michael de Veer	Assisted with experimental design, surgical procedures, interpretation of results and manuscript editing	N/A

The undersigned hereby certify that the above declaration correctly reflects the nature and extent of the candidate's and co-authors' contributions to this work.

Candidate's Signature	████████	**Date 23.02.15**

Main Supervisor's Signature	████████	**Date 23.02.15**

CHAPTER FIVE

Transcriptional profile in afferent lymph cells following vaccination with liposomes incorporating CpG

5.1   Chapter Summary

The results presented within this chapter characterise the global transcriptional profile of afferent lymph cells following injection with liposomal CpG. Chapter Four revealed that CpG uniquely induced the maturation of antigen-positive DCs and monocytes in afferent lymph 72h after injection. However, the immunological pathways targeted by CpG at the injection site and the molecular mechanisms controlling these effects were unclear. The present chapter utilises functional analysis of next generation RNA-sequencing data to reveal the overexpression of interferon, anti-viral and cytotoxic gene pathways in afferent lymph cells 72h following vaccination with liposomal CpG. Selected gene expression analysis of sorted afferent lymph cell populations using real time PCR shows that antiviral gene signatures are most prominent in lymphocytes and that all cell types distinctly respond to liposomal CpG, some even in the absence of detectable TLR9 expression.

5.2   Abstract

Vaccine formulations incorporating innate immune stimulants are highly immunogenic, however the biological signals that originate in the peripheral tissues at the site of injection and are transmitted to the local lymph node to induce immunity remain unclear. By directly cannulating the ovine afferent lymphatic vessels, we have previously shown that it takes 72 hours for mature antigen-loaded dendritic cells and monocytes to appear within afferent lymph following injection of a liposomal formulation containing the TLR ligand CpG. In this present study, we characterise the global transcriptional signatures at this time point in ovine afferent lymph cells as they migrate from the injection site into the lymphatics following vaccination with a liposome antigen formulation incorporating CpG. We show that at 72h post vaccination, liposomes alone induce no changes in gene expression and inflammatory profiles within afferent lymph; however the incorporation of CpG drives interferon, antiviral and cytotoxic gene programs. This study also measures the expression of key genes within individual cell types in afferent lymph. Antiviral gene signatures are most prominent in lymphocytes, which may play a significant and unexpected role in sustaining the immune response to vaccination at the site of injection. These findings provide a comprehensive analysis of the *in vivo* immunological pathways that connect the injection site with the local draining lymph node following vaccination.

5.3   Introduction

Vaccine formulations incorporating adjuvants that target innate immune pathways significantly enhance antigen specific immunity; however the specific mechanisms of action of different adjuvants are not completely understood. Vaccine-induced immune responses generated at the site of injection are conveyed to the draining lymph node via cells and molecules trafficking through the afferent lymphatics. Examination of the afferent lymph compartment during the primary immune response can therefore reveal the biological pathways responsible for setting up an adaptive immune response in the local lymph node (204). We have previously reported the use of an ovine lymphatic cannulation model to characterise the *in vivo* cellular immune response that connects the periphery with the local draining lymph node in response to a number of adjuvants and vaccine formulations (161, 162, 195).

Liposomal vaccine formulations incorporating innate immune agonists have been shown to augment the stimulatory capacity of the adjuvant and increase cell mediated immunity (122, 123, 125, 203, 215). Liposomes facilitate the delivery of antigen to APCs and help prevent the potentially harmful systemic side effects induced by soluble immunomodulators (199-201, 232). Several liposome based vaccines are currently in clinical trials; however the cellular targets of these formulations and the molecular mechanisms controlling these effects are only beginning to be elucidated (104).

We have previously shown that an oil-based deposition adjuvant incorporating liposomes and poly(I:C) induced an early broad inflammatory gene expression profile that resolved into an antiviral transcriptional profile in afferent lymph cells 72h after injection (194). Whether these changes in gene expression at 72h, despite no changes in cellular profiles, were based on the depot effects of the oil or are a characteristic of liposomal-TLR agonist formulations remains unclear. Previous studies incorporating CpG into a liposomal formulation show marked changes in cellular profiles in afferent lymph 72h post injection (196). These include the maturation of antigen-loaded migratory dendritic cells and monocytes in afferent lymph. In the present study, we investigate the global and cell type specific transcriptional signatures of cells in afferent lymph 72h after injection of liposomal CpG *in vivo.* This study provides evidence that it is the TLR-adjuvant that drives the changes in gene expression that connect

the peripheral injection site with the local lymph node for the generation of an adaptive immune response following vaccination.

5.4   Materials and Methods

5.4.1   Immunisations

All injections consisted of 500µl sterile PBS mixtures of liposomes (12% soy bean lecithin:cholesterol (9:1) obtained from Lipoid GmBH, Ludwigshafen, Germany) containing 400µg of ovalbumin (OVA) with or without the addition of 50µg of CpG (P class CpG 23877 5' JU*C-G*T*C*G*A*C*G*A*T*C*G*G*C*G*G*C*C*G*C*C*G*T   3' (Patent # US 2013/0084306 Al). J precedes an iodo-modified nucleotide and * and - indicate a stabilised or standard phosphodiester bond, respectively. The liposome formulations and CpG were kindly provided by Pfizer Animal Health, now Zoetis Research and Manufacturing (Parkville, VIC, AUS). The liposome preparations were injected subcutaneously in the area drained by the prefemoral lymph node at 500µl per injection using a 25 gauge needle.

5.4.2   Pseudoafferent lymphatic cannulation

Ovine prefemoral pseudoafferent lymphatic cannulation was performed as previously described (161). The prefemoral lymph nodes of merino sheep were removed at one year of age. After reanastomosis of the afferent lymphatics with the larger efferent lymphatic, a secondary surgery was performed where a 0.96mm x 0.58mm heparin coated polyvinyl chloride cannula was inserted into the pseudoafferent lymphatic vessel of the sheep. The cannulae was exteriorised and placed in a sterile collection flask attached to the side of the sheep. Eight sheep with reliable flow of afferent lymph were used in this study and randomly assigned to the groups, liposome (n=4) and liposome + CpG (n=4). Handling of animals and experimental procedures were approved by the Monash University Animal Ethics Committee in accordance with the relevant licensing agreement.

5.4.3   Lymph collection, FACS and RNA extraction

Afferent lymph was collected in sterile 50ml tubes containing 0.05IU of heparin (Pfizer) and 20µl 100 x cell culture penicillin-streptomycin (Invitrogen) for a period of one hour. Afferent lymph was collected for one hour prior to injection (-2h) and for one hour 72h after injection (72h). Immediately after collection, afferent lymph cells and supernatant were separated by centrifugation at 400 x g at 4°C. The cell pellet was washed with 10ml of ice cold PBS + 2mM EDTA and resuspended in 1ml of red cell lysis buffer (0.093mM

ammonium chloride, 0.1M Tris (pH 7.2). Cells were incubated on ice for 3 minutes and resuspended in 9ml of ice cold wash buffer twice (5% horse serum, 2mM EDTA in PBS). Following these preparation steps, afferent lymph cells were used for RNA analysis and fluorescence activated cell sorting (FACS). For RNA analysis, cells were resuspended at $1x10^7$/ml in Qiazol (Qiagen) and stored at 80°C until required. For analysis and FACS, samples were prepared by resuspending 3×10^6 afferent lymph cells in 25μl of Fc-block (2% BSA, 2mM EDTA, 0.05% azide, 5% sheep serum in PBS) and then adding 25μl of antibody mixes. The antibodies used were anti-MHC II-pacific blue (clone 49.1, locally produced), anti-CD14-A700 (AbD Serotec), anti-CD172a (SIRPα) (clone DH59B, VMRD Inc. Pullman WA), anti-CD4-FITC (clone 44.38, AbD Serotec), anti-CD8-PE (clone 38.65, AbD Serotec), anti-γδ TCR-FITC (clone 86D, locally produced), anti-CD45R (clone 20.96, locally produced), and anti-mouse IgG1 coupled to phycoerythrin (Caltag Laboratories). Lymphocytes (purity: 92%), monocytes (purity: 97%), SIRPα^{high} DCs (purity: 90%) and SIRPα^{low} DCs (purity: 94%) from four animals were sorted using an Influx cell sorter (Becton Dickinson) using the gating strategies identified in Figure 1A. Cellular RNA was extracted from total afferent lymph cells and sorted afferent lymph cells using an RNeasy Micro Kit (Qiagen) according to the manufacturer's instructions. RNA quantity was measured using a Nanodrop (Nanodrop Technologies) and RNA quality as assessed using an Agilent Bioanalyzer (Agilent Technologies).

5.4.4   RNA sequencing

Total afferent lymph cell RNA from three animals in both vaccine groups at pre (-2h) and 72h were sent for mRNA library preparation and next generation sequencing at the Medical Genomics Facility at the Monash Institute of Medical Research (Clayton, Australia). Libraries were generated with 100ng of total RNA using the Truseq Stranded Total RNA kit (Illumina). Clusters were generated using on-board clustering on the Illumina Hiseq1500. 1 x 100bp single read Rapid Mode sequencing was performed on the Illumina Hiseq1500 according to manufacturer's instructions. The targeted minimum number of reads per sample was 20 million reads (Supplementary Table 1).

5.4.5   Analysis of RNA sequencing data

Sample sequencing reads were aligned to the complete sheep genome [ENSEMBLE version, release 74 (Oar v3.1.74), 2013] using Star v20201 (default parameters (233)). Alignment performance was assessed using RNA-SeqQC(234) (Supplementary Table 1). Duplication

rates were calculated using Picard (http://picard.sourceforge.net). Exonic read-counts were quantified using htseq-count (235). A summary of transcript-associated reads can be found in Supplementary Table 2. Differential expression analysis was performed using edgeR (236) with library normalization using the TMM method (237) and the dispersion estimated using a trended model across the expression level. Each animal was treated as a separate replicate. Genes having fewer than 50 total reads across all replicates were excluded from the analysis. P-values were adjusted for multiple testing to control the false discovery rate (FDR), then a threshold of 0.05 was applied to select the significantly differentially expressed genes. An arbitrary cut-off of ±1.5 fold change in expression was then applied to identify changes in gene expression that are more likely to be biologically significant.

5.4.6   Functional annotation

The Metacore knowledge database and software suite (Thomson Reuters) was used to identify biological processes and networks that were over-represented by genes differentially expressed in the data set. The biological processes and networks are ranked based on the likelihood that the assembly of genes within a given category occurred by random chance, which is displayed as a p-value. For visualisation of the interactions between the interferon and antiviral pathways, expression data were overlayed on a custom map created in Pathway Map Creator (Thomson Reuters).

5.4.7   Real time PCR

Real time PCR was performed on the RNA sequencing samples to validate the RNA sequencing results and identify gene expression within sorted individual cell types. For both sets of samples, cDNA was synthesised from RNA using a Quantitect Reverse Transcription kit (Qiagen) according to manufacturer's instructions. Primers were designed to span an intro region where possible using Primer 3 software on annotated ovine mRNA sequences (Supplementary Table 3). Real time PCR was performed on individual samples in triplicate using SYBR green master mix on an Eppendorf Realplex4 (Eppendorf). A standard curve using defined dilutions of pooled cDNA was run with each primer pair to obtain the PCR efficiency and relative copy number. These were then normalised to the housekeeping gene GAPDH which showed the least variation relative to input cell number and treatment. Differences between and within cell populations were calculated with a two-way ANOVA using a Sidak post-test. When gene expression was detected only within a single cell population, a Student's t-test was performed to calculate statistical significance from pre

injection. Significance was determined as the confidence interval being greater than 95% (p<0.05). The statistical software used was GraphPad Prism, version 6.01.

5.5   Results

5.5.1   Composition of afferent lymph 72h following vaccination with liposome alone or liposomes incorporating CpG

Afferent lymph is primarily composed of lymphocytes, dendritic cells and monocytes (Figure 1B). Two subsets of dendritic cells were identified, distinguished based on high or low expression of the cell surface marker SIRPα (CD172a) (Figure 1B).   CD4 T cells, CD8 T cells, γδ T cells and B cells were identified within the lymphocyte population. Approximately 10% of the lymphocyte population was not identified using these markers (Figure 1B). No changes in the percentage of total lymphocytes or dendritic cells was observed after vaccination, however liposomal CpG induced a significant increase in the percentage of monocytes in afferent lymph at 72h when compared to liposome alone (Figure 1C). The SIRPα^{high} DCs increased in response to liposomal CpG when compared to pre injection, however this was not significant between groups (Figure 1D). No significant changes in the percentage of lymphocyte subsets was observed following injection with both formulations (Figure 1E).
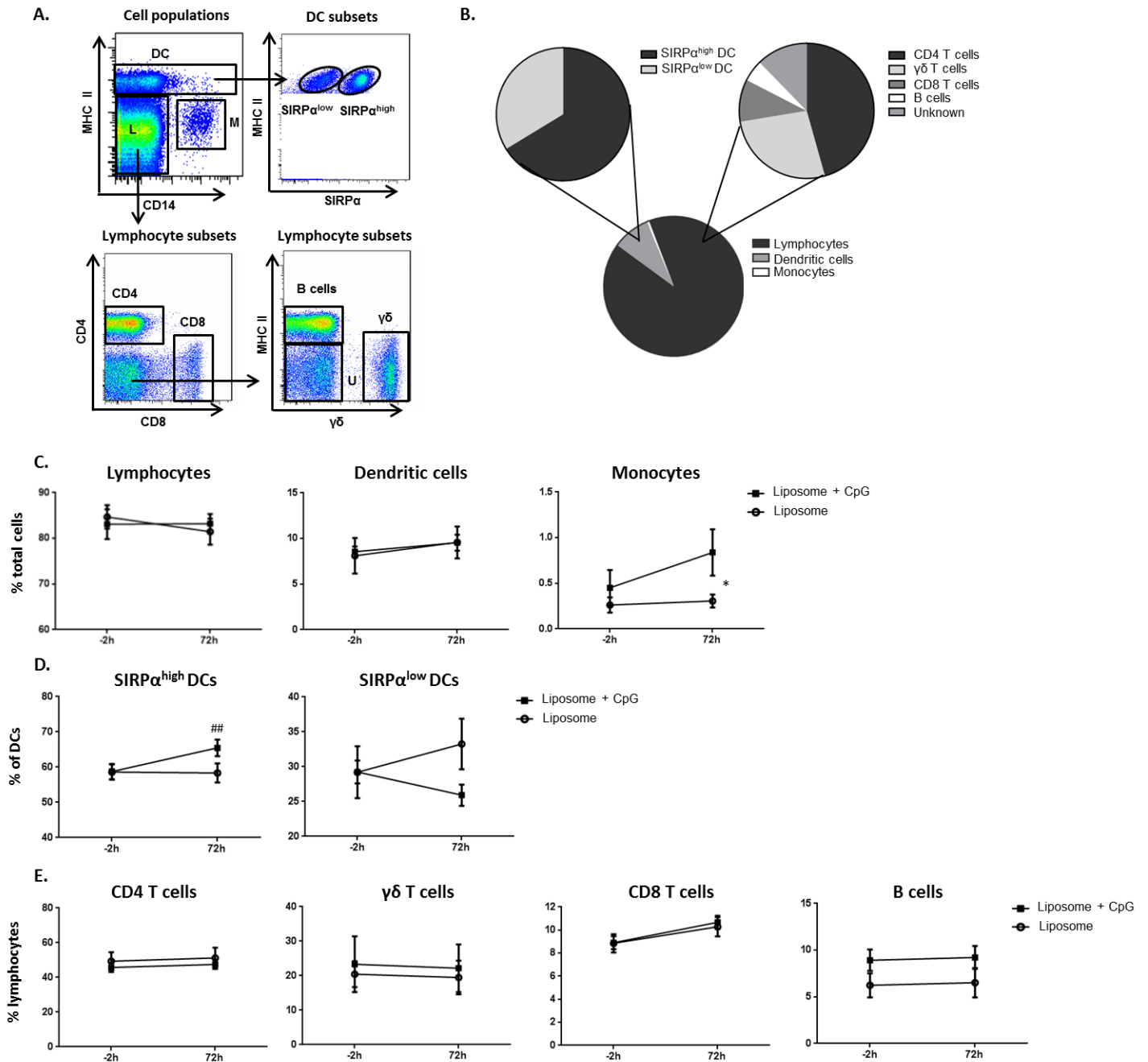
Figure 1. Cellular composition of afferent lymph prior to and 72h following vaccination with liposome alone and liposome + CpG. (A) Gating strategies used to identify cell populations for analysis and cell sorting. (B) Resting cellular composition of afferent lymph expressed as the mean percentages from 10 individually analysed animals. Composition of major cell populations (C), DC subsets (D) and lymphocyte subsets (E) in afferent lymph prior to and 72h following vaccination with liposomes alone and liposome + CpG. Data expressed as mean ± SEM of five individually analysed animals at each time point in both groups, * indicates significant difference between liposome alone and liposome + CpG and [#] indicates significant difference within liposome + CpG at 72h from pre injection, *p<0.05, [##]p<0.01.

5.5.2   Global gene expression profile of afferent lymph cells following vaccination

Differential gene expression in afferent lymph cells within treatment groups (pre vs 72h for both formulations) and between treatment groups (72h liposome alone vs. 72h liposome + CpG) was calculated from RNA sequencing data based on the following parameters: $p < 0.05$, $FDR < 0.01$, $\pm$ 1.5 fold change and at least 50 reads across all replicates, where fulfilment of all four parameters was re9quired to reach significance. Real time PCR was performed to validate the differential gene expression analysis, as described previously (238), demonstrating a highly significant correlation between the fold changes reported by RNA sequencing and real time PCR (Figure 2, Spearman's correlation r=0.9273 p=0.0003). Vaccination with OVA in liposomes alone induced the differential expression of one gene 72h after injection. This gene was identified as a novel protein coding gene (Table 1). Vaccination with the OVA liposome + CpG formulation induced the differential expression of 125 genes in afferent lymph cells 72h after injection, 80 of which related to the immune system, 19 related to other physiological systems, 9 with unknown function and 17 that were novel protein coding genes (Table 1). The differential gene expression analysis between the groups at 72h revealed 78 genes were differentially expressed in the CpG group compared to the liposome alone group at this time point, 53 of which related to the immune system, 12 related to other physiological systems, 1 with unknown function and 12 were novel protein coding genes (Table 1).

Enrichment analysis using Metacore software revealed overexpression of the following networks after injection with liposomal CpG: interferon signalling (p=4.919e-18), innate immune response to RNA viral infection (p=1.104e-16), apoptosis (p=6.283e-4), inflammation (p=7.019e-3) and chemotaxis (p=1.314e-2). Individual genes were allocated to functional groups based on data in the literature and Metacore analysis. The mean fold change value and functional analysis of every differentially expressed gene relating to the immune system within the liposome + CpG group is reported in Figure 3. A list of all 125 genes differentially expressed within the liposome + CpG group and the individual responses from each animal can be found in Supplementary Table 4.
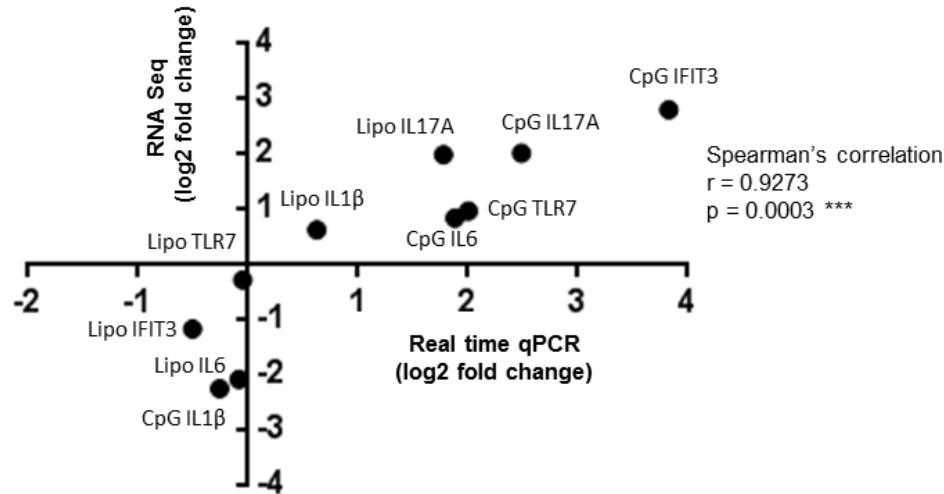
Figure 2. Correlation of fold change values reported with RNA sequencing and real time PCR. A subset of genes that were shown to be differentially expressed or unchanged in the RNA sequencing data set were also investigated with real time PCR on the same samples (IL1β, IL6, IFIT3, TLR7, IL17A). Results are presented as log2 fold change from pre-injection at the 72h time point of three animals in the liposome and liposome + CpG groups. A Spearman's correlation test revealed a significant correlation (r = 0.9273, p = 0.0003) between results obtained with RNA sequencing and real time PCR.

Table 1. Total number of genes differentially expressed in RNA sequencing data

	Liposome alone (compared to baseline)	**Liposome + CpG (compared to baseline)**	**Liposome + CpG (compared to liposome alone)**
Total number of DE genes	1	125	78
Number of genes related to immune system	0	80	53
Number of genes related to other systems	0	19	12
Number of genes with unknown function	0	9	1
Number of genes unknown	1	17	12

*DE = differentially expressed, where p<0.05, FDR<0.01 and ± 1.5 fold mean fold change was required to reach significance.

5.5.3 Vaccination with liposomal CpG induces a genetic profile in afferent lymph highly enriched for anti-viral and interferon-mediated immunity

Genes within the interferon response pathway that were the most highly up-regulated following injection with liposomal CpG include IFIT3, IFIT2, ISG17, IFIT1, ISG20, IFI44, MX1, BATF2, IFI6 and PKR (Figure 3A) (208). CpG induced significant up-regulation of many antiviral genes. The most highly expressed include RIG-I, OAS1, RSAD2, BST-2A, OAS2, HERC5 and LGP2 (Figure 3B). Interactions between the interferon-response genes and the antiviral genes are shown in Figure 4, which leads to the initiation of the innate antiviral inflammatory immune response.

5.5.4 Injection with liposomal CpG up-regulated genes involved in cell migration/maturation and intracellular DNA-sensing

Genes involved in cellular processes such as migration, maturation and antigen presentation were significantly enhanced in afferent lymph cells following injection of liposomal CpG (Figure 3C). These include CLEC4F, CMPK2, CXCL9 (MIG), CXCL10 (IP-10), CXCL11 (I-TAC), SAMD9 and SIGLEC1. Interestingly, CLEC4F demonstrated the greatest increase in expression (7.16 fold). Only Fibronectin-1 (FN-1) was down-regulated (Figure 3C). Intracellular DNA-sensing was also a significant feature of the liposomal CpG injection, characterised by up-regulation of genes including FOXS1, MB21D1, TRIM26, TRIM56 and ZBP1 (Figure 3F). Of these genes, ZBP1, a gene involved in cytosolic viral DNA sensing (239), was the most highly expressed (Figure 3F).

5.5.5 Apoptotic signatures in afferent lymph following vaccination with liposomal CpG

A significant feature revealed during enrichment analysis was the up-regulation of genes involved in the apoptotic network. The individual genes involved in the apoptotic response and their mean fold change expression values are listed in Figure 3D. These genes include DAXX, FASL, GZMA (Granzyme-A), PRF1 (Perforin), TNFSF10, TREX1, UBA7 and XAF1. Interestingly, CD5L, shown to be an inhibitor of apoptosis (240), is 3.7 fold down-regulated from pre-injection in the CpG group (Figure 3A).
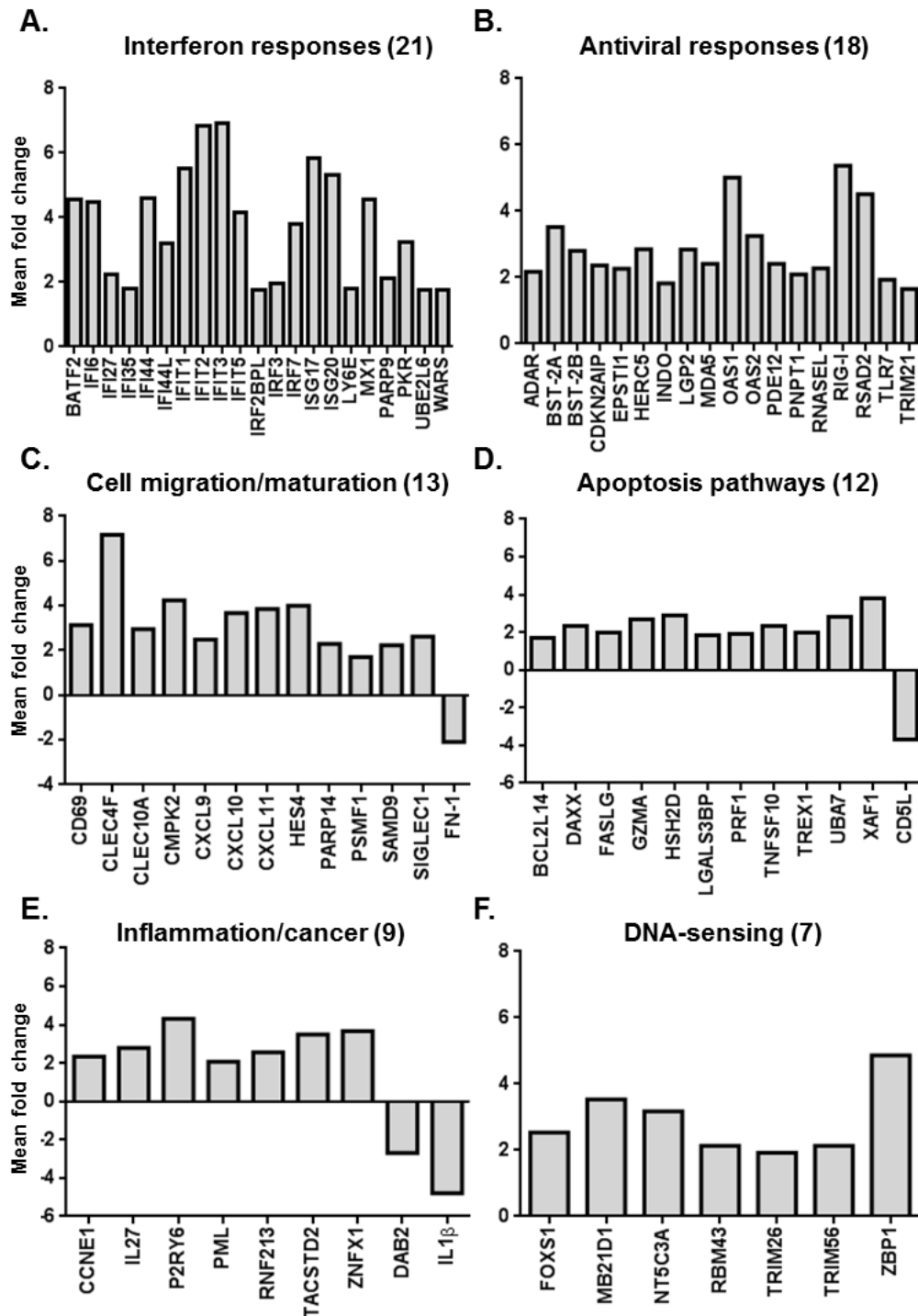
Figure 3. CpG induces the differential expression of a broad range of immune genes within afferent lymph cells. Genes were allocated to functional groups based on literature and Metacore analysis. Results are presented for three animals in the liposome + CpG group as mean fold change from pre-injection at the 72h time point.

5.5.6 Liposomal CpG induces a unique inflammatory gene profile in afferent lymph

IL27 and IL1β were the only inflammatory cytokines differentially expressed 72h following injection of liposomal CpG (Figure 3E). Interestingly, IL1β was down-regulated following liposomal CpG injection (Figure 3E). The G Protein-coupled receptor, P2RY6 which is involved in the pro-inflammatory immune response (241), was 4.3 fold up-regulated following injection of liposomal CpG (Figure 3E).
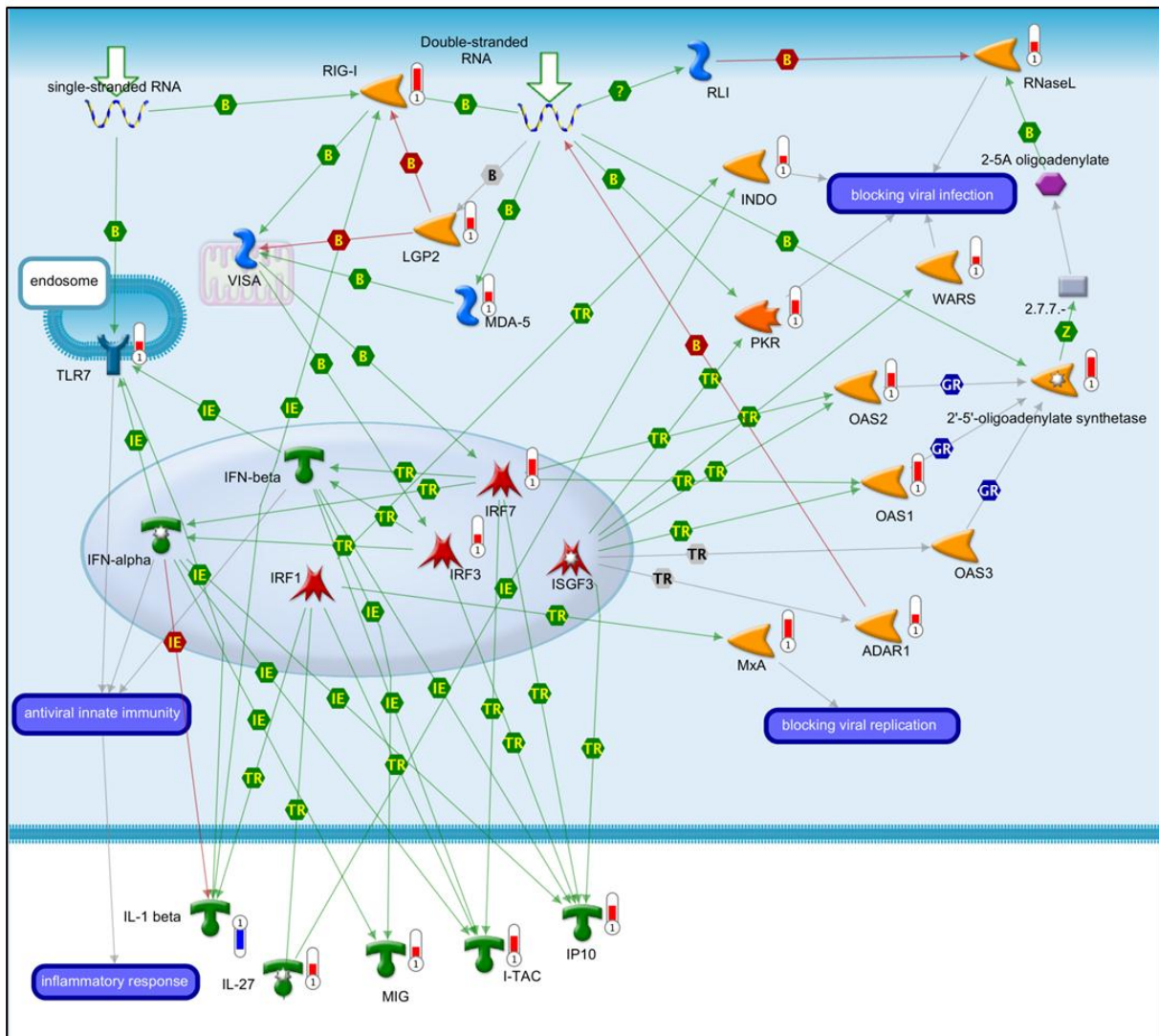
Figure 4. CpG induces the persistence of interferon, antiviral and chemotactic genes in afferent lymph. The Metacore Pathway Map Creator (Thomson Reuters) was used to highlight the induction of these pathways 72h following injection of liposome + CpG. Expression values are represented by thermometers, where up-regulated values are red and down-regulated values are blue. If no thermometer is shown, no significant change in expression was observed. Green lines indicate positive interaction; red lines indicate negative interaction; grey lines indicate unspecified interaction. B: binding; TR: transcriptional regulation; IE: influence on expression; Z: catalyses; GR: group relation.

5.5.7 *Gene expression in sorted cell populations following injection with liposomal CpG*

To determine which afferent lymph cell populations expressed a subset of the differentially expressed genes identified from RNA sequencing, RNA was extracted from SIRPα^{high} DCs, SIRPα^{low} DCs, monocytes and lymphocytes sorted from afferent lymph prior to injection (-2h) and 72h after injection of liposomal CpG. These cells were analysed for expression of IFIT3, RIG-I, TLR-9, PSMA2, CLEC4F, IL6, CXCL10 and IL17A genes by real time PCR and normalised to the housekeeping gene GAPDH (Figure 5). The lymphocyte population demonstrated the greatest increase in expression of genes IFIT3, RIG-I and TLR-9 at 72h (Figure 5). RIG-I was not detected in monocytes prior to injection, however was induced in this population 72h after injection with liposomal CpG (Figure 5). Interestingly, TLR-9 was not detected in monocytes at either time point or in lymphocytes prior to injection however was significantly induced in lymphocytes 72h following liposomal CpG injection (Figure 5). PSMA2, a gene involved in antigen processing and presentation (205), is uniquely expressed by all DCs and significantly increased in the SIRPα^{low} DC subset at 72h (Figure 5). Interestingly, IL6 expression is restricted to the SIRPα^{high} DC subset (Figure 5). CLEC4F was induced at 72h in all cell populations excluding the SIRPα^{low} DCs, with the greatest significance observed in the monocyte population (Figure 5). CXCL10 was expressed by all cell populations at both time points, however a significant increase in expression was observed in monocytes at 72h (Figure 5). IL17A was expressed only in the lymphocyte population 72h after injection of liposomal CpG (Figure 5).
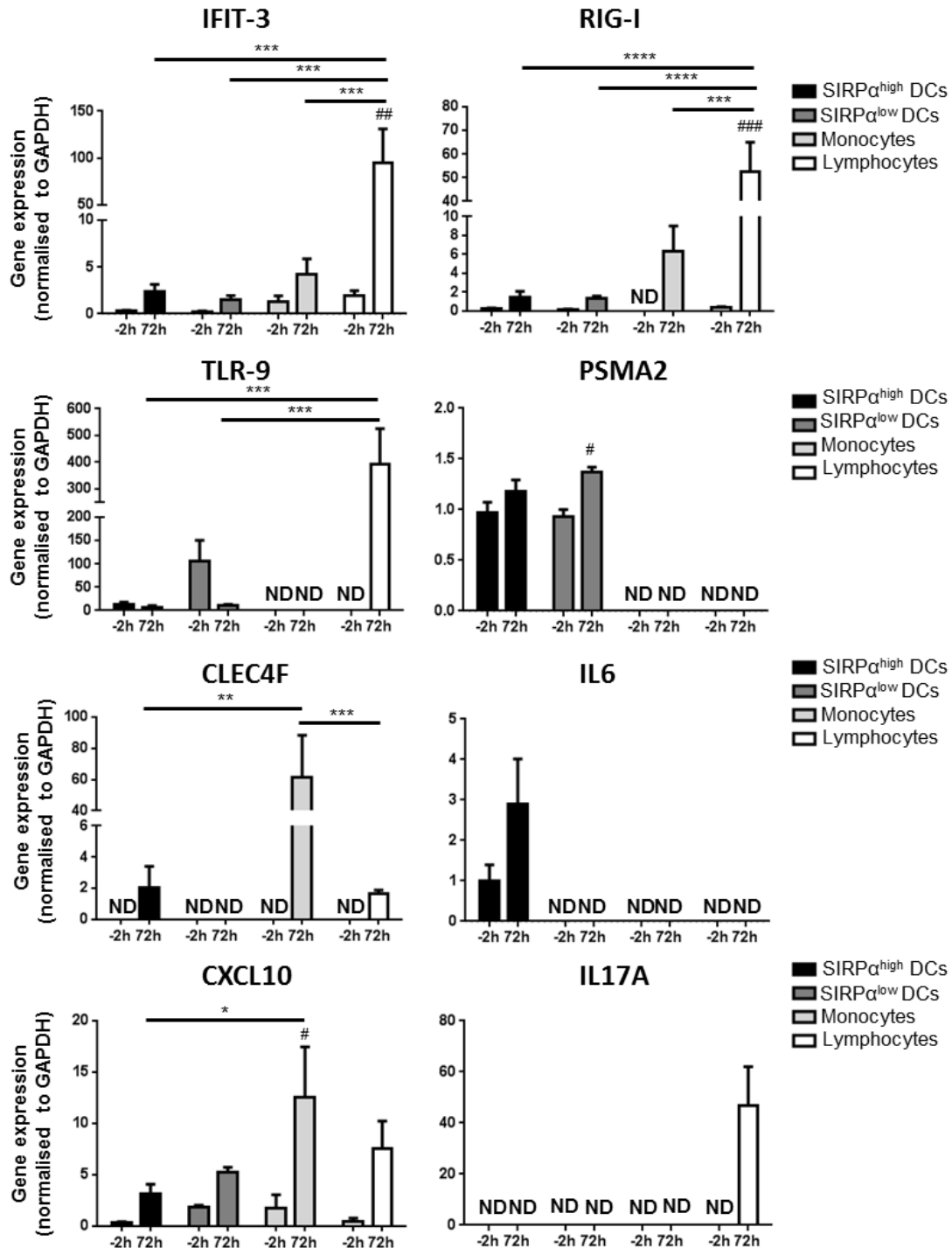
Figure 5. Gene expression in sorted afferent lymph cell populations prior to injection and 72h following injection with liposome + CpG. Gene expression was calculated by normalising experimental gene expression with the housekeeping gene GAPDH. ND indicates gene not detected in the cell type at that time point. Data expressed as mean ± SEM of four individually analysed animals at each time point in the liposome + CpG group, * indicates differences between cell types and # indicates significant differences from pre injection (-2h) within each cell type, *p<0.05, **p<0.01, ***p<0.001, ****p<0.0001, #p<0.05, ##p<0.01, ###p<0.001.

5.6   Discussion

Vaccine-induced immune responses generated at the site of injection are conveyed to the draining lymph node via cells and molecules trafficking through afferent lymph. While elegant murine models can detect the cell types that originate within the periphery, it is very difficult to quantify the kinetics and overall numbers of cell types that migrate. By directly cannulating the ovine afferent lymphatic vessels, we have previously shown that vaccination with liposomal CpG induces the maturation of migratory dendritic cells and monocytes in afferent lymph, however this only occurs 72h after injection (196). We have also shown that an oil-based liposomal-poly(I:C) formulation induces transcription of a broad range of inflammatory genes early after injection, that resolved within 48h. The only gene signatures that remained up-regulated within cells contained in the lymphatic compartment beyond 48h were primarily anti-viral, yet it was unclear whether this was due to the poly(I:C) adjuvant, liposomes or the depot effects of the oil (194). As liposomal CpG is a more potent adjuvant in sheep than liposomal poly(I:C) (data not shown), we were interested to determine if CpG also induced changes in gene expression within afferent lymph cells 72h post injection, once the percentage of all inflammatory cells, excluding monocytes, had subsided to control levels. In the present study, we have quantified the global transcriptional signatures in non-manipulated afferent lymph cells as they migrate from the site of injection into the lymphatics 72h after injection of liposomal CpG. This study provides a comprehensive analysis of the immune response induced in the periphery that connects the injection site with the local lymph node for the generation of an adaptive immune response following vaccination.

CpG has been shown to induce strong Th1 interferon cytokine responses, however the molecular mechanisms controlling these effects are not completely understood (226, 227). We show that injection with liposomal CpG induces a global transcriptional profile in afferent lymph that is reflective of the *in vivo* innate immune response to viral and bacterial infection. The up-regulation of multiple interferon effectors is required to induce a functional Th1 immune response capable of combating viral or bacterial infection (242, 243). Sustained expression of interferon-induced genes over several days results in resistance to viral infection and DNA damage, without harm to host cells (244, 245). The interferon-mediated antiviral transcriptional immune response observed in our study supports evidence that CpG may be an effective adjuvant for protection against viral infection (246-248). The presence of

this response at 72 hours may also be important in shaping the polarisation of adaptive T cells, which is typically observed 3-5 days following vaccination.

Transcriptional responses induced by human vaccination have also been investigated. Subcutaneous injection of polyICLC, a stabilised analogue of poly(I:C), induced the up-regulation of genes involved in interferon and inflammasome signalling in the circulation of all subjects (95). The potent yellow fever vaccine, YF17D, was also shown to induce the up-regulation of several interferon stimulated genes, including the OAS and MX families (192). Similarly, 24 hours after injection of the adjuvant formulation, Matrix-M, genes including CXCL11, ISG15, MX1, OAS1 and RSAD2 were up-regulated in the draining lymph node of pigs (206). Our present study reveals that these genetic signatures observed in the circulation and in draining lymph nodes following vaccination are transported to the local lymph node by cells within afferent lymph.

Interestingly, despite no change in the percentage of lymphocytes in afferent lymph over time, this population demonstrated the greatest up-regulation of interferon and antiviral genetic signatures observed after injection of liposomal CpG, including IFIT-3, RIG-I and TLR-9 genes. TLR-9 expression was undetectable in lymphocytes prior to injection and was heavily induced following vaccination. Naïve human B cells constitutively express low to undetectable levels of TLR-9 and have been shown to up-regulate TLR-9 expression following BCR activation (249). It is therefore possible that the up-regulation of TLR-9 observed in our lymphocyte population is primarily within afferent lymph B cells that are activated following vaccination. Populations of B cells draining within afferent lymph are distinct form those present within lymph nodes and blood, and express higher levels of antigen presentation molecules (170). It will require more detailed experiments to confirm which lymphocytes within afferent lymph up-regulate TLR-9.

The up-regulation of genes involved in the cytotoxic T cell response (Granzyme-A, Perforin and Fas ligand) and the chemotaxis of T cells (CXCL9, CXCL10 and CXCL11) was also observed following injection, further supporting the hypothesis that lymphocytes play an important role in the early immune response to vaccination. Indeed, innate lymphoid cells (ILCs) have been shown to play significant roles in tissue immunity and the innate response to pathogens, including Th1 ILCs (cytotoxic NK cells) and Th17 ILCs (Rorγt+ ILCs)(33). It is likely that the cytotoxic signatures observed in our study originate from NK cells. These cells are well known for their cytolytic activity (250), have been shown to express

intracellular TLR-9 and are activated by CpG (251, 252). Additionally, activated IFNγ-producing NK cells have previously been identified in afferent lymph (253). The presence of Th17 ILCs in afferent lymph remains to be elucidated, however Th17-related signatures have been observed in afferent lymph 48h-72h following injection of poly(I:C) (194). It is unlikely these signatures are due to the activation of classical T cells as part of the antigen-specific adaptive immune response, as the model used in this study requires surgical removal of the local lymph node prior to cannulation of the afferent lymphatic vessel (204), thereby removing the contribution of lymph node feedback. Together, these results provide further evidence indicating lymphocytes are key mediators of information transfer from the periphery to the lymph node during the innate response to vaccination.

Transcriptional pathways involved in the innate response to intracellular DNA were also up-regulated following injection of liposomal CpG. These include TLR7, RIGI, MDA5, LGP2, IRF3, IRF7, TRIM56 and ZBP1 (254). The peak activation of TLR-signalling genes in response to CpG and poly(I:C) has been shown to occur between 24 and 48h after injection, returning to baseline expression by 72h (194, 255). In this study, we report expression of these genes out to at least 72h following injection of liposomal CpG. This is consistent with our previous reports, where liposomal CpG induced late activation of monocytes and DCs when compared to liposomes alone and liposomal poly(I:C) (195, 196). In the present study, we also show a significant increase in CMPK2, a gene involved in the activation and differentiation of monocytes and macrophages (256, 257). SIGLEC1, a lectin expressed on monocytes following TLR-9 stimulation (258), was also up-regulated in our study. The functional role of SIGLEC1 is not entirely clear, however it has been shown to bind to CD43 on activated T cells (258). Additionally, up-regulation of HES4, a biomarker of maturing DCs (259), was observed 72h after injection of liposomal CpG. These results begin to unveil the transcriptional pathways induced by CpG that result in the late activation and maturation of monocytes and DCs in afferent lymph (196).

This study also reveals a significant increase in PSMF1, a gene that encodes the protein for the proteasome inhibitor PI31 subunit that is involved in MHC class I cross-presentation (260). PSMA2, a related gene that is also involved in cross-presentation (205), was shown to be expressed in both SIRPα^{high} DCs and SIRPα^{low} DCs, however a significant increase after vaccination was only observed in the SIRPα^{low} DCs subset. This is an interesting finding as the SIRPα^{low} DC subset is generally believed to be uniquely responsible for cross-presentation (147). However, future research is required to determine the functional capacity

of these cells following *in vivo* activation by CpG, Interestingly, CLEC4F and CLEC10A, pattern recognition receptors from the C-type lectin family, were also up-regulated following injection of liposomal CpG. The biological functions of these receptors are not completely understood, however CLEC4F has been identified on infiltrating monocytes in the liver and CLEC10A is expressed on circulating monocytes and dendritic cells (261, 262). We also show CLEC4F to be the most highly expressed gene following injection of CpG and to be induced in SIRPα^{high} DCs, monocytes and lymphocytes in afferent lymph, implying this gene may play an important role in the immune response to vaccination.

Whilst the primary goal of an adjuvant formulation is to enhance immunity, it is also important for these responses to be negatively regulated to prevent inappropriate inflammation and tissue damage (70). This is likely to be critical with CpG as it does not induce self-tolerance, where multiple injections of CpG continue to enhance tissue inflammation and systemic cytokine responses in mice (263, 264). In the present study, the most heavily down-regulated gene 72h after injection of liposomal CpG was IL1β. This gene is most commonly associated with activation of the inflammasome, and this process must be tightly controlled (265). Our results indicate that liposome associated CpG either induces a mechanism that reduces transcription from the IL1β gene in afferent lymph cells or blocks the recruitment of IL1β-expressing cells into the afferent lymph. It also implies that liposomal CpG preferentially induces a mechanism that down regulates the inflammasome whilst still providing the pro-inflammatory signals required to promote immunity (120).

The complex immune response to vaccination requires the synergistic interaction of multiple biological pathways, highlighting the need for a systems biology approach to vaccine development. Vaccine formulations incorporating innate immune stimulants are highly immunogenic, however the biological pathways they target at the site of injection to induce immunity in the local lymph node are unclear. Functional analysis revealed up-regulation of genes involved in anti-viral innate immunity, interferon signalling and granzyme-A mediated apoptosis. We also investigated the cell populations in afferent lymph responsible for these transcriptional signatures, determining that different cell types distinctly respond to liposomal CpG, some even in the absence of detectable TLR9 expression. Together with our previous report characterising the local and systemic immune response induced by liposomal CpG (196), these findings reveal novel *in vivo* immunological pathways that connect the periphery with the local draining lymph node and how these are shaped by innate immune agonists following vaccination.

5.7   Supplemental figures

Supplementary Table 1. Summary of the alignments statistics. Duplication percentages were calculated by counting the number of duplicated reads divided by the total number of mapped reads.

Sample	Total reads (no.)	Quality Filtered Reads (no.)	Uniquely Mapped Reads (%)	Multi-mapped reads (%)	Duplication (%)	Unmapped Reads (%)
S1-VAC1-PRE	21,551,188	21,414,788	86.4	9.1	61.2	4.5
S1-VAC1-POST	30,186,326	30,030,404	87.8	9.5	53.5	2.7
S2-VAC1-PRE	19,448,978	19,316,764	87.3	9.3	50.0	3.4
S2-VAC1-POST	22,668,524	22,540,197	88.0	9.1	49.4	2.9
S3-VAC1-PRE	24,545,525	24,407,594	88.2	8.9	51.4	2.9
S3-VAC1-POST	23,375,545	23,244,160	87.6	9.6	53.3	2.8
S4-VAC2-PRE	29,321,491	29,157,172	88.1	9.1	52.4	2.8
S4-VAC2-POST	32,513,972	32,341,552	88.4	8.9	57.4	2.7
S5-VAC2-PRE	24,367,522	24,227,580	87.0	10.0	55.3	3.0
S5-VAC2-POST	22,098,164	21,963,712	86.3	10.7	57.9	3.0
S6-VAC2-PRE	24,905,083	24,767,269	87.6	9.6	52.7	2.8
S6-VAC2-POST	23,999,217	23,859,377	87.8	8.1	53.2	3.0

Supplementary Table 2. Summary of transcript-associated reads. Rates are per mapped read. Intragenic rate refers to the fraction of reads that map to genes (introns or exons). Exonic rate is the fraction of reads that map to exons. Intronic rate is the fraction of reads mapping to introns. Intergenic rate is the fraction mapping to genomic regions between genes. Expression profile efficiency is the ratio of exon reads to total mapped reads. Transcripts/genes detected is the number of transcripts/genes with at least 5 sequencing reads.

Sample	Intragenic Rate	Exonic Rate	Intronic Rate	Intergenic Rate	Expression Profiling Efficiency (frac.)	Transcripts Detected (no.)	Genes Detected (no.)
S1-VAC1-PRE	0.709	0.420	0.289	0.290	0.420	14,261	10,878
S1-VAC1-POST	0.712	0.418	0.294	0.287	0.418	14,982	11,088
S2-VAC1-PRE	0.715	0.437	0.277	0.285	0.437	14,541	10,826
S2-VAC1-POST	0.713	0.410	0.303	0.287	0.410	14,587	10,855
S3-VAC1-PRE	0.711	0.426	0.285	0.288	0.426	14,900	11,051
S3-VAC1-POST	0.711	0.448	0.263	0.288	0.426	14,862	11,023
S4-VAC2-PRE	0.709	0.419	0.290	0.290	0.419	14,970	11,095
S4-VAC2-POST	0.711	0.436	0.275	0.288	0.436	14,981	11,102
S5-VAC2-PRE	0.708	0.445	0.263	0.291	0.445	14,859	11,018
S5-VAC2-POST	0.719	0.464	0.255	0.280	0.464	14,686	10,924
S6-VAC2-PRE	0.710	0.443	0.268	0.289	0.443	15,022	11,143
S6-VAC2-POST	0.706	0.451	0.255	0.294	0.451	15,058	11,152

Supplementary Table 3. Primer sequences for genes investigated with real time PCR

Gene	Primer sequences (5'-3')
GAPDH	Forward: GTCCCCACCCCCAACGT
	Reverse: TCTCATCATACTTGGCAGGTTTCTC
IL-6	Forward: CCTCCAGGAACCCAGCTATG
	Reverse: GGAGACAGCGAGTGGACTGAA
IFIT-3	Forward: GTTGTCGAGGCTCTGGGAAA
	Reverse: TCCAGTGCCCTTAGCAACAG
TLR-7	Forward: TCTCCAAGGTGCTTT
	Reverse: CCACCAGACAAACCA
IL-1β	Forward: CGAACATGTCTTCCGTGATG
	Reverse: TCTCTGTCCTGGAGTTTGCAT
IL-17A	Forward: AGGAGCTACCATGGCGTCTA
	Reverse: CCTCACATGCTGTGGGAAGT
PSMA-2	Forward: TGGTGTATAGTGGCATGGGC
	Reverse: TGAGCTGTGGGAATGGGTTC
TLR-9	Forward: CCCTGGAGAAGCTGG
	Reverse: GACAGGTCCACGAAG
RIG-I	Forward: GCCTCAGTTGGTGTTGGAGA
	Reverse: GACGTGTCGAGAGAAGCACA
CLEC4F	Forward: ATTCAACCGTGCGTTTTGGG
	Reverse: TCATTCCACTTCCGCTGCAT
CXCL10	Forward: GCTCATCACCCTGAGCTGTT
	Reverse: AGCTGTCAGTAGCAAGGCTG

Supplementary Table 4. Individual animal responses (counts per million) of all genes differentially expressed from pre-injection in the CpG group.

GENE NAME	ENSEMBL ID	CpG sheep 1 pre (-2h)	CpG sheep 1 72h	CpG sheep 2 pre (-2h)	CpG sheep 2 72h	CpG sheep 3 pre (-2h)	CpG sheep 3 72h
P2RY6	ENSOARG00000006714	2.79	21.03	2.27	26.07	2.59	11.43
NOVEL	ENSOARG00000007039	35.45	138.12	41.9	105.82	38.17	114.85
ISG17	ENSOARG00000007233	31.23	1028.33	100.17	1082.18	78.48	334.65
IFIT5	ENSOARG00000014815	14.42	246.9	28	190.67	28.98	74.75
BST-2A	ENSOARG00000025182	22.31	266.69	42.09	237.04	44.68	113.67
IFIT2	ENSOARG00000015169	22.07	1008.95	78.99	1280.17	75.53	280.68
ZBP1	ENSOARG00000017418	35.05	711.83	62.63	375.67	39.86	159.21
NOVEL	ENSOARG00000019272	11.07	271.63	28.36	194.91	22.56	65.86
IFI6	ENSOARG00000003341	34.18	762.33	97.99	552.49	60.73	233.78
OAS1	ENSOARG00000002881	30.51	907.87	71.9	334.5	50.3	210.37
DDX58	ENSOARG00000014731	13.54	495.51	34.63	168.64	24.97	104.23
IFIT1	ENSOARG00000015177	34.5	1245.2	109.62	860.82	75	272.79
IFIT3	ENSOARG00000014800	15.93	997.75	67.08	655.81	38.97	172.36
SIGLEC1	ENSOARG00000002007	6.21	23.57	6.36	24.82	5.17	18.14
CMPK2	ENSOARG00000014636	65.01	931.37	92.62	572.89	73.04	198.31
MB21D1	ENSOARG00000006104	5.98	68.1	9.09	52.05	9.54	19.14
ISG20	ENSOARG00000010964	3.66	152	16.54	145.46	12.66	39.92
IFI44	ENSOARG00000013440	46.69	1029.43	109.35	699.2	80.62	227.79
BST-2B	ENSOARG00000016787	5.74	46.04	10.91	34.25	8.47	22.68
XAF1	ENSOARG00000000888	26.29	399.65	55.54	311.98	47.71	112.76
HES4	ENSOARG00000007304	0.72	9.69	1.27	10.29	2.14	8.35
FOXS1	ENSOARG00000001757	13.3	89.81	20.18	52.53	18.82	43.54
IFI27	ENSOARG00000014413	1137.61	4526.44	1168.3	4115.25	1504.26	2634.51
RSAD2	ENSOARG00000014648	46.21	497.09	42.09	369.8	29.61	83.37
OAS2	ENSOARG00000009097	159.58	1967.33	351.23	1280.46	261.92	672.3
NOVEL	ENSOARG00000005557	27.65	279.67	41.81	184.81	41.47	76.11
CXCL9	ENSOARG00000016543	58.48	243.05	88.17	387.6	113.17	265.89
ZNFX1	ENSOARG00000012500	374.93	4664.49	651.37	3442.99	492.8	1001.7
PKR	ENSOARG00000009740	43.34	411.4	51.45	284.47	63.85	104.6
SPATS2L	ENSOARG00000015954	2.79	16.49	4.18	19.53	6.87	18.42
SNORD12	ENSOARG00000022705	6.37	29.55	9.73	36.36	9.45	20.14
LGP2	ENSOARG00000018383	65.57	543.82	109.8	441.57	111.29	207.65
IFI44L	ENSOARG00000013421	70.83	854.48	122.8	424.73	113.61	246.21
MX1	ENSOARG00000010283	94.09	2455.9	290.78	1438.23	144.74	454.49
GZMA	ENSOARG00000007970	3.59	21.16	6.73	28.76	6.6	15.69
SNORD12	ENSOARG00000024331	6.85	34.98	11.54	42.62	11.24	21.86
NOVEL	ENSOARG00000001815	38	293.42	65.81	155.75	63.49	136.53
IRF7	ENSOARG00000006626	41.19	473.73	89.62	665.91	71.97	137.35
NOVEL	ENSOARG00000015072	30.99	304.34	38.54	186.44	35.67	59.96
FAM26F	ENSOARG00000018074	7.49	24.88	9.91	46.47	12.31	25.58
IP-10	ENSOARG00000016611	21.59	373.47	57.63	447.63	83.11	141.97
HERC5	ENSOARG00000000530	37.44	295.96	42.99	138.82	41.29	74.57
TRANK1	ENSOARG00000016617	206.35	1891.12	237.88	778.95	212.15	431.63
NT5C3A	ENSOARG00000006503	24.38	190.75	34.72	190.96	28.45	42.18

GENE NAME	ENSEMBL ID	CpG sheep 1 pre (-2h)	CpG sheep 1 72h	CpG sheep 2 pre (-2h)	CpG sheep 2 72h	CpG sheep 3 pre (-2h)	CpG sheep 3 72h
CLEC4F	ENSOARG00000011222	0.24	42.19	6.73	62.63	1.07	23.04
NOVEL	ENSOARG00000000904	26.61	266.82	39.18	156.71	27.29	47.81
RNF213	ENSOARG00000000942	790.41	5874.71	1019.32	1952.53	938.96	2151.89
NOVEL	ENSOARG00000019033	23.34	109.26	28.18	62.72	30.94	51.8
CXCL11	ENSOARG00000016668	0.88	14.71	1.64	9.81	1.96	4.17
NOVEL	ENSOARG00000008211	4.06	33.88	4.09	12.31	3.75	9.89
ATXN3	ENSOARG00000012754	25.18	107.13	24	81	26.31	39.37
CD69	ENSOARG00000021063	109.87	820.95	199.97	1209.27	179.07	280.95
UBA7	ENSOARG00000011997	84.93	685.1	113.44	387.22	108.71	174.63
MDA5	ENSOARG00000006142	93.85	504.58	100.9	322.66	112.99	183.79
EPSTI1	ENSOARG00000007427	68.2	367.77	90.72	197.02	79.37	157.39
NOVEL	ENSOARG00000001138	134.24	892.27	155.25	355.85	146.07	291.02
HSH2D	ENSOARG00000000506	29.32	238.44	24.72	81.1	31.57	48.81
NOVEL	ENSOARG00000000896	59.12	770.1	119.98	517.18	55.74	115.75
CXorf21	ENSOARG00000018770	13.78	65.62	15.36	46.18	22.12	28.39
TRIM56	ENSOARG00000015270	30.83	120.94	32.54	81.39	26.49	45.81
TMEM106A	ENSOARG00000005269	14.5	53.94	16.73	35.02	17.12	27.67
SERTAD1	ENSOARG00000011360	19.12	73.18	31.63	115.35	31.3	45.9
CMTR2	ENSOARG00000011167	9.08	40.54	12.36	20.2	12.57	26.22
DAXX	ENSOARG00000009519	148.66	854.89	242.51	658.03	199.22	321.5
RTP4	ENSOARG00000020495	57.92	474.48	86.62	292.84	77.14	103.87
NOVEL	ENSOARG00000021075	43.02	160.38	63.72	118.33	54.4	88.36
LAYN	ENSOARG00000014248	7.57	34.98	6.73	17.03	5.35	13.06
C21orf91	ENSOARG00000015776	39.84	161.96	47.81	168.26	45.3	57.51
RBM43	ENSOARG00000009199	76.48	240.85	65.45	232.14	66.53	101.6
FAM111B	ENSOARG00000011604	8.45	30.72	5.64	28.19	14.18	20.32
UBE2L6	ENSOARG00000009969	50.27	152.82	62.9	121.41	64.3	95.43
CDKN2AIP	ENSOARG00000007148	83.02	400.61	130.07	434.45	98.81	157.85
NOVEL	ENSOARG00000004500	72.42	253.15	53.72	257.63	57.16	82.64
IL1B	ENSOARG00000020866	23.98	13.47	112.35	26.07	361.08	7.26
NOVEL	ENSOARG00000002441	18.88	93.59	18.09	54.64	15.43	24.13
IRF3	ENSOARG00000013335	43.18	171.17	65.99	125.16	47.53	83.19
ZNFX1-AS1_2	ENSOARG00000022293	39.44	91.94	44.36	122.85	42.27	67.22
BCL2L14	ENSOARG00000020888	44.22	72.36	49.27	89.28	40.22	102.69
SNORD12	ENSOARG00000023569	1.91	11.06	3	10.2	2.32	5.81
PARP9	ENSOARG00000020150	77.92	360.55	89.08	222.23	96.76	137.62
ADAR	ENSOARG00000002952	179.5	881	221.15	511.12	199.85	316.78
PDE12	ENSOARG00000013642	63.1	302.56	69.26	242.72	58.95	79.2
RNASEL	ENSOARG00000018978	3.43	25.63	8.18	19.63	8.03	14.24
PML	ENSOARG00000004233	98.23	466.44	138.89	278.51	115.57	198.4
CLEC10A	ENSOARG00000009867	2.47	12.78	1.45	13.66	3.21	4.63
TNFSF10	ENSOARG00000020741	105.01	508.91	96.62	269.37	99.52	146.87
APOBEC3Z1	ENSOARG00000016213	10.76	217.14	60.99	339.79	46.28	77.38
INDO	ENSOARG00000002251	290.32	775.46	386.04	988.87	456.24	737.62
COX7A1	ENSOARG00000005289	11.31	30.23	13.27	46.27	13.56	19.78
WARS	ENSOARG00000002035	646.36	1778.98	712.45	1575.6	743.83	1102.75
FASLG	ENSOARG00000014582	7.01	23.43	8.91	23.86	8.56	13.88

GENE NAME	ENSEMBL ID	CpG sheep 1 pre (-2h)	CpG sheep 1 72h	CpG sheep 2 pre (-2h)	CpG sheep 2 72h	CpG sheep 3 pre (-2h)	CpG sheep 3 72h
IFI35	ENSOARG00000004413	79.11	255.35	108.17	237.04	115.13	168.91
TRIM26	ENSOARG00000015605	122.13	472.7	184.25	385.1	156.06	244.84
AKAP7	ENSOARG00000013910	3.27	25.97	4.09	12.31	3.57	5.62
SAMD9	ENSOARG00000018615	337.72	1923.35	385.59	821.57	395.06	564.8
PARP14	ENSOARG00000020160	207.54	1189.67	224.24	531.04	237.66	322.86
TLR7	ENSOARG00000011288	15.54	56.83	14	37.33	18.99	22.32
BATF2	ENSOARG00000011372	0.08	2.82	0.18	2.41	0.45	0.73
IRF2BPL	ENSOARG00000002269	21.43	66.59	34.72	62.72	27.29	43.18
TACSTD2	ENSOARG00000008349	0.08	2.54	0.82	4.04	0.71	2.54
ATAD1	ENSOARG00000014098	74.81	274.79	91.99	251.86	93.55	112.49
PNPT1	ENSOARG00000002164	89.55	350.24	97.53	271.19	87.13	112.22
FN1	ENSOARG00000019329	147.23	68.03	149.98	86.01	304.9	35.83
NOVEL	ENSOARG00000009583	22.87	97.23	33.18	117.94	30.68	31.3
TREX1	ENSOARG00000000153	9.8	39.1	17	53.01	19.62	22.59
NOVEL	ENSOARG00000006790	47.88	181.2	42.45	70.52	46.19	75.29
CCNE1	ENSOARG00000004067	5.42	23.78	7.82	36.36	9.19	9.53
NOVEL	ENSOARG00000008702	20.63	76.34	28.45	48.97	28.8	38.65
IL27	ENSOARG00000003180	1.91	7.22	2.36	17.41	2.94	4.45
PRF1	ENSOARG00000006139	52.98	231.43	85.35	216.94	118.96	142.88
TRIM38	ENSOARG00000001519	71.15	205.39	91.99	186.25	89.62	121.38
STOML1	ENSOARG00000004309	4.54	16.01	3.82	9.62	4.19	8.35
CDADC1	ENSOARG00000008439	25.81	94.62	29.27	59.55	30.94	37.47
CD5L	ENSOARG00000006980	3.35	0.27	1	0.29	1.69	0.27
LY6E	ENSOARG00000001470	61.74	264.69	98.26	149.88	98.63	149.41
LGALS3BP	ENSOARG00000003257	48.52	227.04	75.08	126.51	79.37	102.69
TRIM21	ENSOARG00000000944	42.86	116.54	42.27	73.88	46.46	63.96
NOVEL	ENSOARG00000002737	1.99	11.82	1.36	7.6	1.43	2.18
C19orf66	ENSOARG00000014804	48.28	156.47	68.45	211.07	54.76	65.5
DAB2	ENSOARG00000009431	4.62	1.17	3.45	1.54	11.41	1.63
U6	ENSOARG00000021887	0.08	1.79	0.36	1.73	0.09	0.64
FBXO33	ENSOARG00000008856	63.82	163.96	63.72	199.04	67.51	75.75
PSMF1	ENSOARG00000018814	70.35	227.31	95.53	161.72	93.19	129.82
XRN2	ENSOARG00000004443	176.95	608.61	175.07	463.7	177.64	212.82
ATL3	ENSOARG00000002871	91.3	270.33	106.9	281.97	117.89	137.44

Mathematical modelling of DC trafficking and T cell activation in the local lymph node

Melanie R. Neeland [a], Qianqian Wu [b], Els N.T. Meeusen [ac], Kate Smith-Miles [bd]
Michael J. de Veer [a*], Mark B. Flegg [bd*]

[a] Department of Physiology, [b] School of Mathematical Sciences and
[c] Department of Microbiology at Monash University, VIC 3800, Australia
[d] Monash Academy for Cross & Interdisciplinary Mathematical Applications,
Monash University, VIC 3800, Australia
*Contributed equally

The current status of this manuscript is 'in preparation'

CHAPTER SIX

Mathematical modelling of DC trafficking and T cell activation in the local lymph node

6.1   Chapter Summary

The results of this thesis have characterised the cellular response in the lymphatic system to liposomes incorporating poly(I:C) or CpG. Chapters Three and Four have shown that the addition of poly(I:C) or CpG to the liposome formulation enhance cell-associated antigen uptake and induce distinct patterns of DC and monocyte maturation in afferent lymph. The results also show that the adjuvanted formulations enhance local and systemic antigen-specific adaptive immunity. However, even under the strongest immunogenic stimuli of CpG, the number of antigen-positive DCs migrating to the lymph node was less than 0.5% of all cells within afferent lymph. Given such a small number of antigen-positive DCs, and the fact that cognate T cells exist at a very low frequency of approximately 1 in 1 million, we were interested to investigate if the number of antigen-positive DCs were sufficient to induce the observed adaptive response. As this is difficult to experimentally determine in sheep, we developed a mathematical model of DC trafficking and T cell activation to determine the probability that a cognate interaction occurs in the lymph node and the time taken for this response to occur. This also allowed us to investigate the extent to which the adjuvanted formulations influence T cell activation. The mathematical model was developed using DC-T cell interaction data from the literature and our own experimental data obtained from the lymphatic cannulation studies. The development of a mathematical model using real time *in vivo* measurements of DC-associated antigen trafficking after vaccination has implications for vaccine design and provides important information to help answer fundamental questions in immunology.

6.2   Introduction

A major goal in vaccine development is the induction of effective antigen-specific T cell immunity. This is particularly important for diseases without effective vaccines, including HIV, malaria and hepatitis C, which require strong T cell responses to induce protective immunity. DCs are essential for the activation of naïve T cells and are regularly targeted in novel vaccines (266). In order to induce naïve T cells to proliferate and differentiate, DCs must deliver two signals. The first signal is antigen presented on MHC class I or class II molecules. The second signal is derived from cell associated co-stimulatory molecules and soluble cytokines which act as T cell activation factors. Most vaccine formulations incorporate vaccine antigen/s with an adjuvant that typically activates innate immune pathways present in almost all subsets of DCs. The co-delivery of antigen and innate immune adjuvant enhances T cell priming via a number of mechanisms, including increased antigen uptake by immature DCs, enhanced maturation of DCs and/or enhanced recruitment of immune cell populations to the site of vaccination (8, 266). It is unclear, however, if the best approach in vaccine development is to target more numbers of immature DCs that are capable of engulfing antigen or to target fewer numbers of mature DCs that are efficient at providing immunostimulatory signals to cognate T cells in the lymph node.

The generation of T cell immunity therefore requires the acquisition of antigen by DCs and the subsequent breakdown and presentation of this antigen on MHC molecules present on the surface of the DC. The DCs loaded with MHC-antigen complexes then migrate to the lymph node where they interact with rare antigen specific naïve T cells that express T cell receptors (TCRs) capable of binding to and recognising the MHC-peptide complex on the DC (267). For this process to occur, antigen positive DCs (Ag+ DCs) must locate the cognate T cell in the lymph node, present at a frequency of approximately 1 in 10^6 (268). The estimated TCR repertoire consists of at least $2x10^7$ receptors, each with different antigen specificity (269). The DCs must therefore scan a large number of T cells for a cognate interaction to occur and an effective immune response to be established. The mechanisms by which this occurs and the kinetics of DC and T cell interactions in the lymph node are only beginning to be understood.

Two-photon imaging experiments have significantly contributed to the understanding of DC-T cell interactions. A study by Miller and colleagues in 2004 revealed that DCs survive in the lymph node for approximately 60h and suggested that DCs do not leave the lymph node (268). This study also investigated the movement and velocity of DCs and T cells, demonstrating that DCs move significantly slower (2-3μm/min) than T cells (>10μm/min) in the lymph node (268). Several studies have demonstrated that DC and T cell interactions occur by chance, as T cells move in random directions until they encounter an obstacle in their path (268, 270, 271). To enable visualisation of these rare events, two-photon imaging studies often employ adoptive transfer or genetic approaches that result in higher numbers of Ag+ DCs and frequencies of antigen-specific T cells that are well beyond the physiological range (269). T cells also migrate further and remain in the lymph node longer than can be analysed with two photon imaging, which is limited to a 30-60 minute observation window (269). To assess these parameters *in vivo*, the afferent and efferent lymphatic vessels can be cannulated in large animal models. Ag+ DCs migrate from the injection site into the lymph node via the afferent lymphatic vessels. Following cognate interaction, activated T cells leave the lymph node via the efferent lymphatic vessels which eventually drain back into the circulation (204). Data obtained using the lymphatic cannulation models can therefore enhance the understanding of the relationship between lymph node input and output, and the strength of the adaptive immune response generated.

A recent study by Thomas and colleagues in 2012 used the ovine efferent lymphatic cannulation model to show that the transit time of T cells through a lymph node is heterogeneous, suggesting that they move randomly within the lymph node from the point of entry to the point of exit (272). A probability distribution indicated that the mean T cell transit times through a lymph node range from 24 to 44 hours. These transit times were similar to that observed previously in mice, where lymph node migration times were estimated to be between 24 and 30 hours (273). Consistent with the two-photon imaging studies (268), DCs have not been observed in ovine efferent lymph in homeostatic conditions, providing further evidence that DCs are recycled in the lymph node (196). These studies indicate that the parameters of DC and T cell interaction in the lymph node are remarkably similar between species.

Our previous work has utilised the ovine lymphatic cannulation models to quantify antigen uptake and cellular trafficking to and from the lymph node in real time following vaccination of a liposomal formulation containing the innate immune agonist CpG (196). We showed that

this formulation induced an antigen-specific immune response that was significantly greater than the liposome alone formulation and liposomes incorporating poly(I:C). While our data show that numerous cell types enter the site of injection and traffic to the lymph node via the afferent lymphatics, only DCs can activate naïve T cells. Following vaccination with liposomal CpG, the number of Ag+ DCs that migrated to the lymph node was less than 0.5% of all cells within the afferent lymph. Despite such a small number of Ag+ DCs migrating to the lymph node, and the extremely low cognate T cell frequency of approximately 1 in 10^6, an effective adaptive immune response was generated. This suggested that a cognate interaction occurred, however with this needle-in-a-haystack problem, it was unclear how the antigen loaded DC and cognate T cells located each other in the lymph node.

A number of studies have used computational or mathematical modelling of lymph node cell dynamics to confirm results obtained from experimental data or explore hypotheses that would be difficult or impossible to explore experimentally (269). These models are often based on known data of cell interactions and are then manipulated to predict immunological outcomes to real or hypothetical immune stimuli. In this chapter, we aimed to develop a mathematical model of DC trafficking and T cell activation in the local lymph node using DC-T cell interaction data from two-photon experimental studies in the literature and our own experimental data obtained from lymphatic cannulation studies. Using this mathematical model, we show that the addition of CpG or poly(I:C) to the liposomal vaccine formulation enhances the probability that the total TCR repertoire will be scanned after vaccination. We also estimate the minimum number of Ag+ DCs that must migrate from the site of injection for the TCR repertoire to be scanned and the time taken for this process to occur. The development of a mathematical model using real time *in vivo* measurements of DC-associated antigen trafficking after vaccination has implications for vaccine design and the ability to induce an optimal number of Ag+ DCs at the site of injection for increased vaccine efficacy and safety.

6.3   Developing the mathematical model

Using parameters from the literature and our own experimental data (Table 1), we have developed a two compartment model of T cell circulation. Our model includes a 'lymph node' compartment and a 'system' compartment (Figure 1). The 'lymph node' compartment includes DC numbers that have entered via the afferent lymph from the site of vaccination as well as cognate T cells trafficking to and from the 'system' via the circulation and lymphatic network. Our model describes the cellular trafficking to and from a single lymph node, in this case it represents the prefemoral lymph node from which the experimental values were obtained (204).

Table 1. Parameters from the literature and experimental data that are used in the model.

From the literature		Our experimental data				
DC survival time (κ)	60h (268)	No. of CD4 T cells recirculating	2.76×10^7 per hr			
T cell recirculation time	24h (272)	No. of CD4 T cells in LN	1.9×10^7			
Cognate CD4 T cells	1 in 10^6 (269)	Mean weight of LN	1.9g			
CD4 TCR repertoire	2×10^7 (269)	Volume of LN (V)	1.9×10^{12} µm^3			
T cell velocity (v)	660µm per hr (274)	**No. of Ag+ DC per hr in AL**	**4h**	**24h**	**48h**	**72h**
T cell turning rate (λ)	30 turns per hr (274)	Liposome	6969	2118	2096	1349
DC radius (r_d)	20-25µm (268)	Liposome + CpG	5595	15700	2574	6109
T cell radius (r_t)	3µm (275)	Liposome + poly(I:C)	5070	8691	6947	3045

*AL = afferent lymph

Ag+ DCs enter the lymph node from the site of vaccination but do not leave the lymph node. This characteristic was included in the model as our experimental data revealed that DCs are not observed in efferent lymph under homeostatic conditions or at any time point after vaccination (196). DCs survive for approximately 60 hours after lymph node entry (268), and this value from the literature is used as the DC survival time in our model. Unlike DCs, T cells continually recirculate between the lymph node and the system. Each T cell takes approximately 24 hours to transit through the lymph node, as observed in a study

investigating T cell recirculation to and from a single lymph node in the ovine model (272). The frequency of cognate T cells in the lymph node exists at 1 in 10^6 and the total TCR repertoire is approximately 2 x 10^7 (269). Therefore, we use 20 different 'types' of cognate T cells to represent the cognate T cell repertoire in our model. Our experimental data shows that the mean number of T cells entering and exiting the lymph node under homeostatic conditions is 2.76×10^7 T cells per hour. Given that each T cell takes approximately 24 hours to circulate through the lymph node (272), this implies there are 6.62×10^8 T cells cycling through an individual lymph node every 24 hours. Therefore, given that 1 in 10^6 T cells in the lymph node are antigen specific, a total of 662 T cells that are able to interact with the Ag+ DC (or approximately 33 of each type of cognate T cell) traverse the lymph node every 24 hours. We have chosen this value to reflect the TCR repertoire as it is the most reliable data on T cell trafficking within a lymph node. The total repertoire is likely to be larger; however without knowing precisely how many CD4 T cells are present in the whole animal, it is difficult to estimate the total repertoire. This is reflective of observed CD4 T cell migration and at this stage the model does not include CD8 T cell migration. Therefore, all future reference to T cell activation in this model is in relation to Ag+ DC-CD4 T cell interactions.

A compartment model such as ours assumes that intra-compartment distributions of interacting cell populations are well-mixed. That is, DCs and T cells are uniformly positioned randomly within the lymph node at any given moment in time. It has been shown that T cell motion in the lymph node is random in nature (276-278). T cells have been shown to be highly motile, crawling with a mean, unbiased, velocity of 11μm per minute (or $v = 660$μm per hour) and turn at a rate of 0.5 turns per minute (or $\lambda = 30$ turns per hour) (274). The volume of DC and T cell interaction is 1.9 x 10^{12}μm³, which has been determined from our own experimental data revealing that the mean mass of an ovine prefemoral lymph node is 1.9g. Whilst on the micrometre scale T cells appear to have velocity-jump motion, it is important to note that the expected jump distance v/λ is much smaller than the typical distances cognate T cells are required to cover in search of Ag+ DCs in the lymph node. For this reason, it is appropriate to model the motion of T cells using Brownian motion parameterised by a diffusion constant of $D = v^2/(3\lambda)$ (276).

An antigen-specific DC will scan a cognate T cell when the T cell is within range of its dendrites. We assume that this process is very efficient since DCs are effective at dismissing non-cognate T cells. In our model, we therefore assume that if the cell centres of a particular

DC and T cell pair are within a distance of $R = r_d + r_t$, the T cell is presented with antigen and this T cell type is considered to be 'found'. DCs are significantly larger than T cells, with a radius of 20-25μm (r_d), compared to a radius of 3 μm (r_t,), respectively (268, 275). We therefore set $R \approx 25$ μm. The rate Λ at which diffusing T cells (with diffusion constant D) find spherical targets of radius R (the distance accessible to DC dendrites) within a well-mixed domain of volume V is well documented in mathematics literature (279) and has been shown to be exponentially distributed with a rate constant given by;

$$\Lambda = 4\pi RD/V. \qquad\qquad [1]$$

Importantly, this rate describes the rate at which one particular DC will contact one particular T cell. Therefore, according to the Law of Mass Action, the rate at which a particular cognate T cell 'type' is scanned is given by $\Lambda N_d N_t$ where N_d and N_t are the number of Ag+ DCs and type-specific T cells co-existing in the lymph node at a given time.
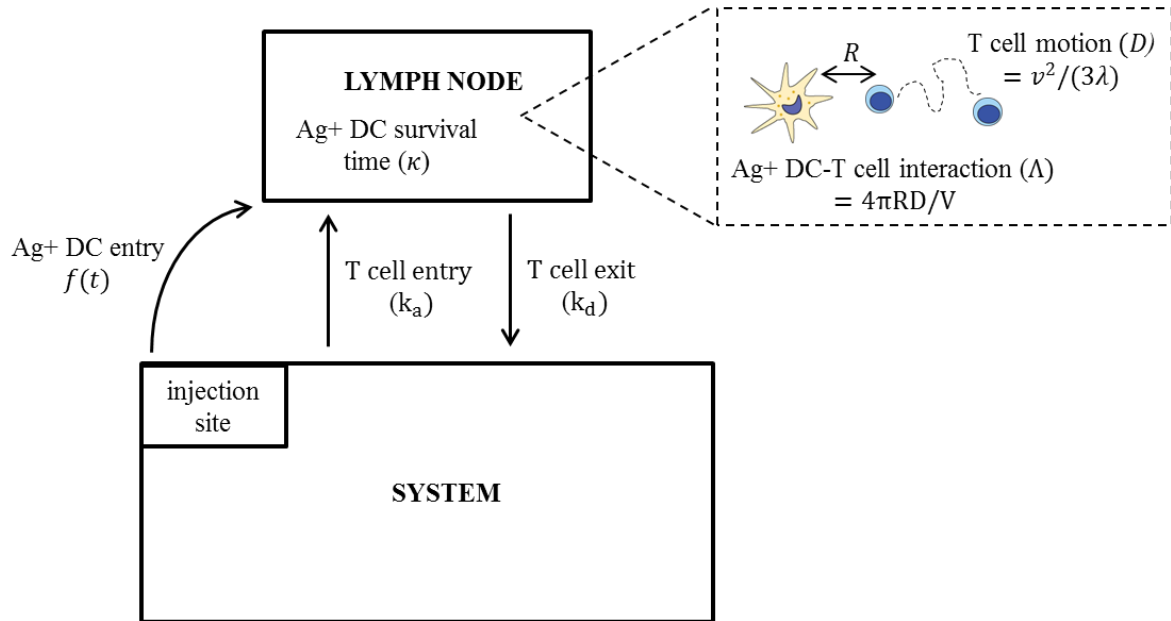
Figure 1. Two compartment model of T cell circulation and interaction with Ag+ DCs in the lymph node. T cells continually recirculate between the lymph node and the system. T cells enter the lymph node from the system at a rate of k_a and leave the lymph node to return to the system at a rate of k_d. Ag+ DCs enter the lymph node from the injection site at a rate of $f(t)$ and survive in the lymph node for time κ. Within the lymph node, interactions between Ag+ DCs and T cells occur when the cells are within radius R. The rate of interaction is determined by distance R, the diffusive motion of T cells (D) and the volume of the lymph node (V).

Since equation [1] is an exponential rate constant, we can construct a Markov model for the state of a particular type of cognate T cell in the lymph node. Considering that there may be N T cells of a particular type, we can define the state of this type of T cell to be 'found' or 'not found' by an Ag+ DC. The Markov model proposes that there can be 0-N number of that type of cognate T cell in the lymph node at a given time. This number is represented by the index i. The rate at which i increases from i to $i + 1$ is given by arrival rate per cell k_a of T cells into the lymph node. The rate at which i decreases from i to $i - 1$ is given by the departure rate per cell k_d of T cells from the lymph node into the system. Under homeostatic conditions, cognate T cells are present only in the 'not found' state and cannot transition to a 'found' state until Ag+ DCs are introduced into the system.

Under homeostatic conditions and in the absence of Ag+ dendritic cells, a probability distribution for i has an analytic mathematical form;

$$P_i = \left(\frac{k_d}{k_d+k_a}\right)^N \left(\frac{k_a}{k_d}\right)^i \binom{N}{i},$$
[2]

where P_i is the probability of i (having i number of type specific T cells simultaneously in the lymph node) and $\binom{N}{i}$ is the Binomial coefficient describing the number of combinations of i distinct T cells that can be chosen from the possible N T cells in the whole system. This distribution of probabilities is chosen as the initial condition.

Once Ag+ DCs are introduced into the system, the rate at which the 'found' state can be achieved is given by the number of Ag+ DCs, the rate of DC-T cell interaction and the number of cognate T cells in the lymph node, or $\Lambda N_d i$. A diagram of the Markovian state space of this model, together with the rates by which the states change is given in Figure 2.

NOT FOUND
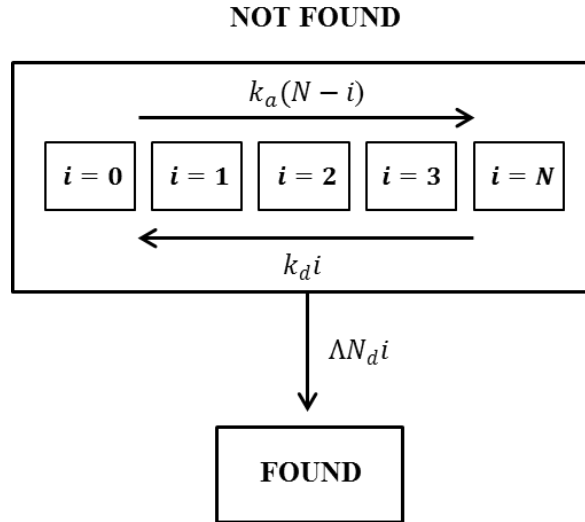
Figure 2. The Markov model that describes the state of cognate T cells in the lymph node at a given time. The number of cognate T cells in the lymph node can range from 0-N (where N is the total number of cognate T cells in the system). This number is denoted by the index i, and is governed by the arrival (k_a) and departure rates (k_d) of all circulating T cells. Cognate T cells can exist at one of two states, 'not found' or 'found' by an Ag+ DC. The rate at which a cognate T cell transitions to the 'found' state from the 'not found' state is dependent on the rate of DC-T cell interaction (Λ), the number of Ag+ DCs in the lymph node (N_d) and the number of cognate T cells present in the lymph node at that time (i).

Finally, we need to determine N_d (the number of Ag+ DCs in the lymph node). This quantity is dynamic because Ag+ DCs enter the lymph node at variable rates $f(t)$ at different times t after vaccination and DCs die at a rate of $\kappa = 1/60$ per hour (that is, $1/60^{th}$ of the DC population in the lymph node dies every hour). The population N_d can be computed by solving the ordinary differential equation

$$\frac{dN_d}{dt} = f(t) - \kappa N_d .$$ [3]

Using the afferent lymphatic cannulation model, we have obtained data for $f(t)$ at times $t = 4, 24, 48, 72$ hours after vaccination with liposomes alone, liposomal CpG and liposomal poly(I:C) (Figure 3).
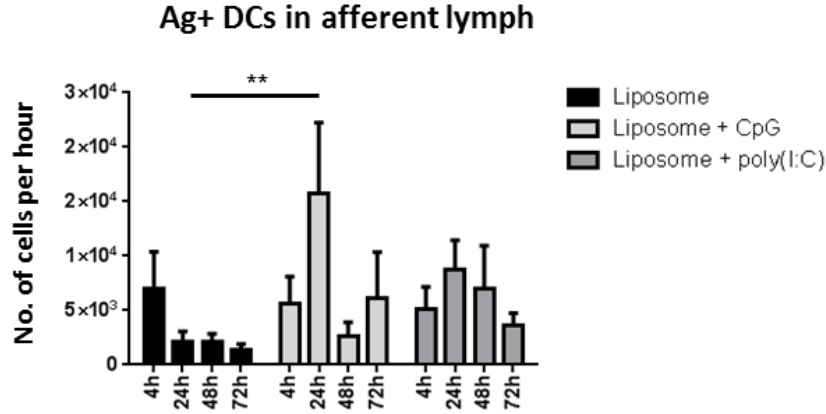
Figure 3. Quantification of Ag+ DC migration from the site of injection into the lymph node via afferent lymph following vaccination with three liposomal formulations. Data expressed as mean ± SEM of five individually analysed animals at each time point in all treatment groups, **$p<0.01$.

As we only investigated the kinetics of Ag+ DC migration at 4 time points after vaccination, rather than a more comprehensive kinetic analysis, we are forced to assume a form for $f(t)$ against which we will fit the data. A natural form for this distribution is the Gamma distribution $f(t) \sim \overline{N_d}\, \Gamma\,(2,\theta)$ with a shape parameter of 2. We chose this distribution for two reasons. Firstly, this distribution of times typically arises from the waiting time of two queued events. These two events include DC migration into the lymph node, where an initial event must occur (DCs finding and ingesting the antigen at the injection site) before the final event (DC entry into the lymph node). Secondly, it allows for a description of vaccine-specific inflow of DCs using just two, important, parameters; the total number of Ag+ DCs migrating to the lymph node $\overline{N_d}$, and the average time taken (spread of times) after vaccination for DCs to reach the lymph node (2θ). The lsqcurvefit (least squares curve fit) function in Matlab was used with 10^6 maximum function evaluations and maximum iterations to find the parameters $\overline{N_d}$ and θ for each of the vaccine formulations. Importantly, the numerical fits of the derived $f(t)$ functions for each formulation describe relative total DC influx and duration well (Figure 4). It is important to note that whilst equation [3] can be solved explicitly for N_d as a function of time, we found it just as convenient to solve this equation numerically using a forward Euler solution methodology since it was already required of us to solve the Markov model numerically using small numerical time steps.
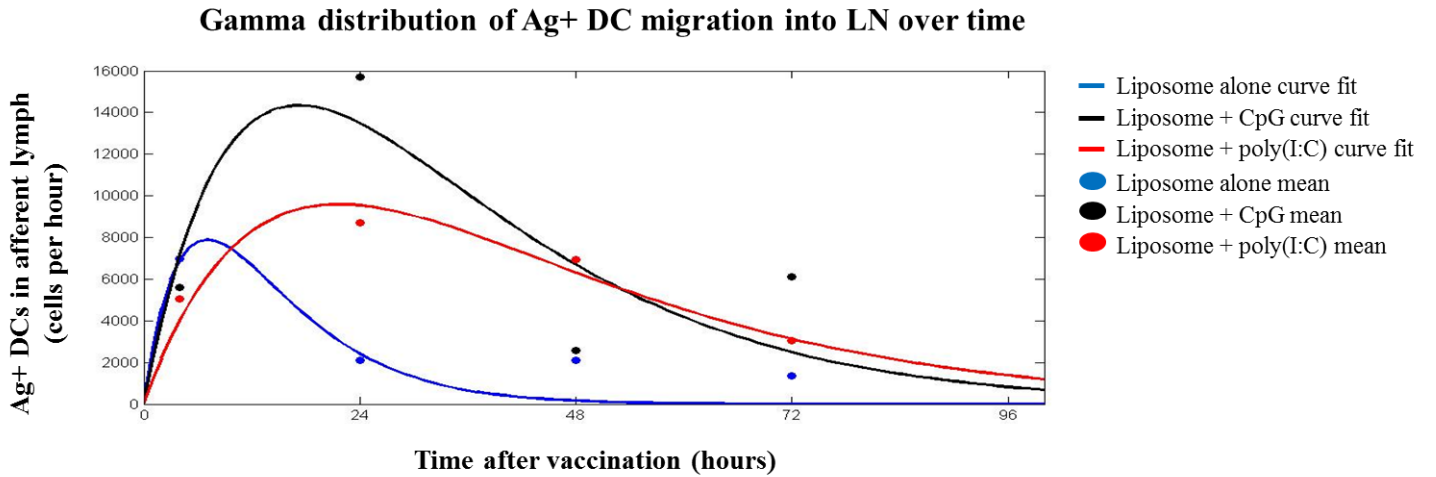
Figure 4. Distribution of Ag+ DC entry into the lymph node using data obtained from afferent lymphatic cannulation. A curve (sold line) was fit to mean Ag+ DC numbers (closed circles) for liposome alone (blue), liposome + CpG (black) and liposome + poly(I:C) (red) at 4h, 24h, 48h and 72h post vaccination. The gamma distribution for each vaccine formulation was used to define the total number of Ag+ DCs migrating to the lymph node over the complete vaccination time course and the average time taken for these DCs to reach the lymph node.

The completely defined Markov model (Figure 2) provides a calculation of the probability that, at a given time in the future, a cognate T cell has been scanned by an Ag+ DC. Whilst the process of antigen presentation involves a series of complex biological events, the scanning mechanism once contact has been made is highly robust and relatively rapid (on the scale of minutes) (268). Therefore a single interaction between a DC and a cognate T cell is considered to correspond with successful presentation of antigen. If an interaction event has occurred, the T cell in question is described as 'found' or 'scanned'.

The efficacy of a vaccine formulation can be evaluated based on the ability of Ag+ DCs to scan the entire repertoire of n naïve T cell types. If we denote the (numerically calculated) probability of being 'found' for any one naïve T cell type as $p_f(t)$ we can determine the probability, ϕ_j, that j T cell types of the T cell repertoire have been scanned as a function of time (assuming that each T cell type contains the same number of T cells N) using the binomial distribution

$$\phi_j(t) = \binom{n}{j} p_f(t)^j (1 - p_f(t))^{n-j}.$$ [4]

143

The measure of vaccine efficacy that may now be clearly defined from this model is the average proportion of the TCR repertoire that has been scanned $\left(\lim_{t\to\infty} \sum_{j=0}^{n} \frac{j}{n} \phi_j(t)\right)$. In this model, if the proportion of the TCR repertoire scanned reaches 95%, the entire TCR repertoire is considered scanned. The proportion of the repertoire scanned may never reach 100%. This is due to stochasticity and the subsequent probability that Ag+ DCs and cognate T cells moving randomly in the lymph node will miss each other by pure chance.

6.4 Results of the model

6.4.1. Liposomal vaccine formulations induce distinct kinetic profiles of Ag+ DC LN entry

The least squares curve fit function in Matlab was used to find the average total number of Ag+ DCs in the lymph node and the average time taken for these Ag+ DCs to enter the lymph node for the liposome alone, liposomal CpG and liposomal poly(I:C) vaccine formulations. The results demonstrate that the liposomal vaccine formulations induce distinct kinetic profiles of Ag+ DC lymph node entry (Table 3). The liposome alone formulation induced the least number of Ag+ DCs (1.5093×10^5) however these DCs took an average of only 7 hours to enter the lymph node after vaccination. Liposomal poly(I:C) induced less Ag+ DCs (5.6496×10^5) than liposomal CpG (6.7115×10^5), however the Ag+ DCs from the poly(I:C) group entered the lymph node more slowly than the CpG group (21.67h and 17.21h, respectively).

Table 3. Total number and time taken for Ag+ DC LN entry for each formulation

	Total Ag+ DC in LN $(\overline{N_d})$	Time (θ)
Liposome	1.5093×10^5	7.03h
Liposome + CpG	6.7115×10^5	17.21h
Liposome + poly(I:C)	5.6496×10^5	21.67h

6.4.2. Liposomal CpG induces the fastest TCR repertoire scanning

Using the distribution of Ag+ DCs entering the lymph node (Figure 5A) and the mathematical modelling of DC-T cell interaction, we predict that vaccination with liposomal CpG should induce faster TCR repertoire scanning than vaccination with liposomal poly(I:C) or liposomes alone. This is shown in Figure 5, where vaccination with the liposomal CpG formulation induced the greatest number of Ag+ DCs that are alive in the LN (Figure 5A) and scans all 660 cognate T cells (in our system) faster than liposomal poly(I:C) and

liposomes alone (Figure 5B). This can also be shown graphically using the percentage of the TCR repertoire scanned, where liposomal CpG scans the repertoire faster (31h) than liposomal poly(I:C) (38h) and liposomes alone (51h) (Figure 5C). Despite liposomal poly(I:C) inducing an intermediate number of Ag+ DCs and the greatest duration of Ag+ DC lymph node entry (Table 3, Figure 5A), our model predicts that liposomal CpG scans the repertoire 7h faster than this formulation (Figure 5C). Interestingly, all vaccine formulations, including liposome alone, induce enough Ag+ DCs to scan our representation of the cognate TCR repertoire within four days after vaccination (Figure 5B-C).
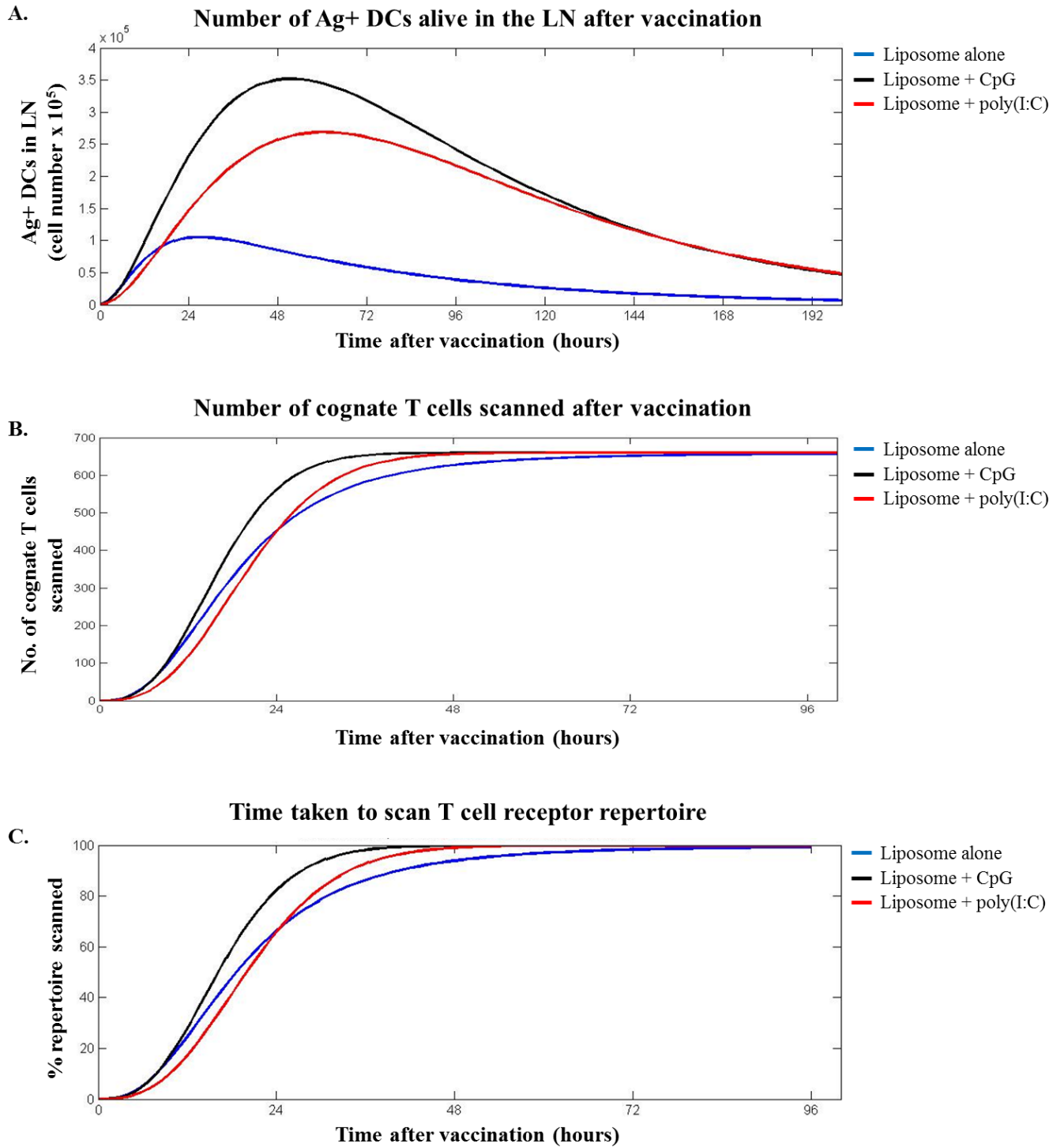
A.

B.

C.

Figure 5. The average time for Ag+ DCs to scan the TCR repertoire after vaccination. (A) the number and distribution of Ag+ DCs that are alive in the LN over time, (B) the number of cognate T cells scanned over time and (C) the percentage of the TCR repertoire scanned over time (in hours) following vaccination with each liposomal vaccine formulation.

6.4.3   What is the minimum number of Ag+ DCs required to scan the TCR repertoire?

Our model predicts that all three liposomal vaccine formulations induce the migration of a sufficient number of Ag+ DCs from the peripheral injection site to scan the TCR repertoire within four days. Even the liposome control formulation, which induces considerably less Ag+ DCs than the adjuvanted formulations (Table 3, Figure 5A), is able to scan the TCR repertoire. This suggests that the liposomal CpG and poly(I:C) formulations are inducing high Ag+ DC numbers that may be saturating the system. We therefore wanted to investigate the extent of this saturation and estimate the minimum number of Ag+ migratory DCs that are required to scan the TCR repertoire. To do this, we used our mathematical model to run a simulation that reduces Ag+ DC numbers arriving in the lymph node and examines the effect on the percentage of the repertoire scanned, given the finite lifetime of DCs. This simulation estimated that 95% of the repertoire can be scanned if an average of only 1.3×10^5 Ag+ DCs enter the lymph node (Figure 6). The liposomal CpG and poly(I:C) formulations induce approximately 5.2 fold and 4.3 fold more Ag+ DCs than required to scan the repertoire, respectively.

Interestingly, as Ag+ DC numbers are theoretically reduced, liposomal poly(I:C) becomes the most efficient formulation, where only 1.25×10^5 Ag+ DCs are required to scan the repertoire, when compared to liposomal CpG (1.27×10^5 Ag+ DCs) and liposome alone (1.33×10^5 Ag+ DCs) (Figure 6). In this simulation, as we are controlling for Ag+ DC number, the only experimental difference between the formulations is the time taken for DCs to enter the lymph node. Indeed, liposomal poly(I:C) induced the largest time distribution for Ag+ DC lymph node entry (Table 3, Figure 5A). This suggests that, if all of our liposomal vaccine formulations induced the average minimum of 1.3×10^5 Ag+ DCs, the vaccine which induces the Ag+ DCs to enter the lymph node over the largest amount of time will scan more of the repertoire than the vaccines that induce lymph node entry over a shorter amount of time. Therefore, at reduced Ag+ DC numbers, it is the duration of Ag+ DC lymph node entry that becomes a critical factor for deep TCR repertoire scanning. However, this does not take into account how long it takes to scan the repertoire. We next aimed to determine the effect of theoretically reducing Ag+ DC numbers on the time taken to scan the TCR repertoire.

The minimum number of Ag+ DCs required to scan the repertoire
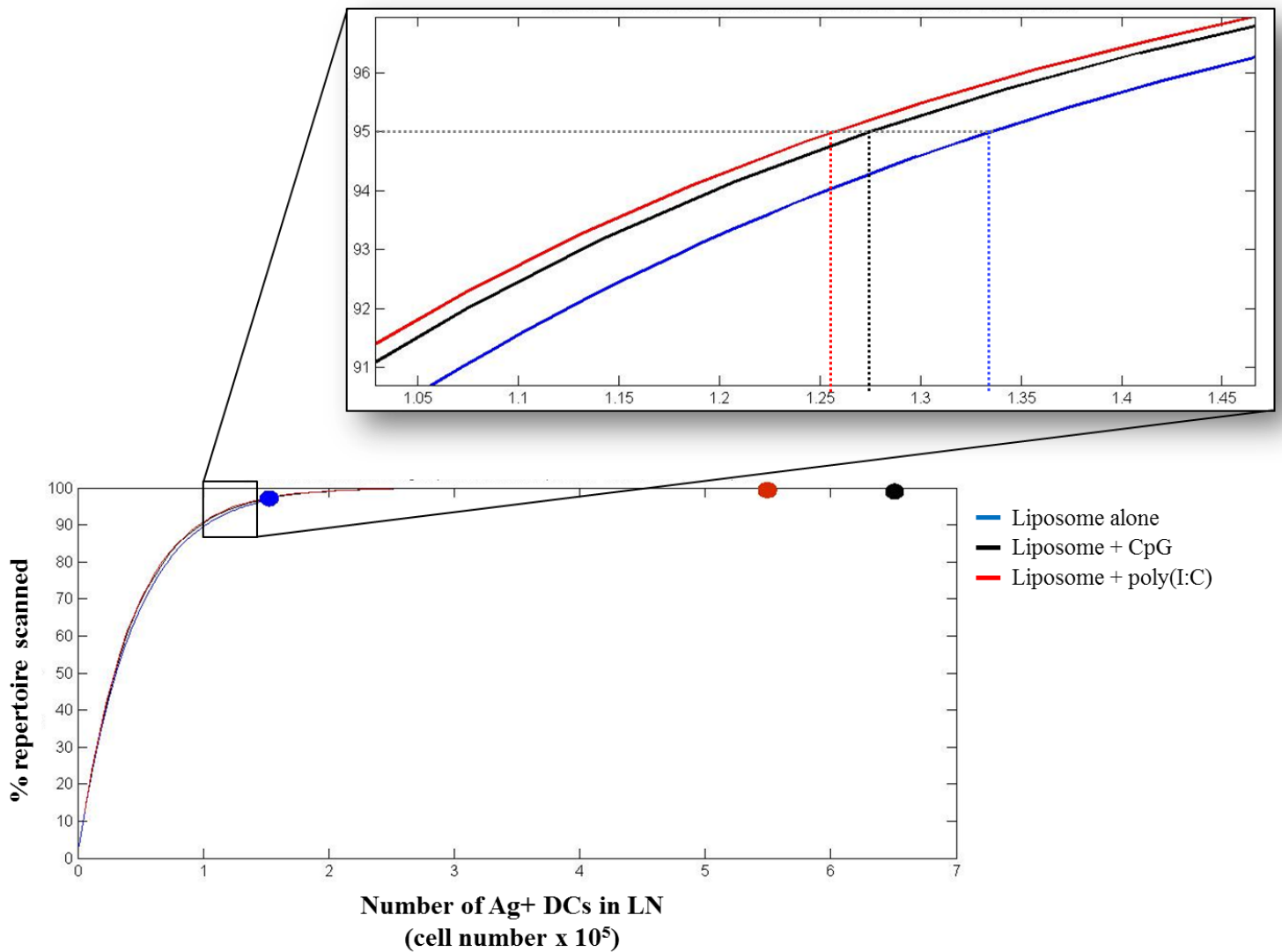
Figure 6. Our model was used to perform a simulation where Ag+ DC numbers entering the lymph node were reduced and the resulting effect on the percentage of the TCR repertoire scanned was determined. The inserted graph is a magnification that shows the minimum number of migratory Ag+ DCs required for the TCR repertoire to be scanned for each liposomal vaccine formulation (dotted lines). Coloured circles represent the actual numbers of Ag+ DC numbers observed experimentally for liposome alone (blue), liposomal poly(I:C) (red) and liposomal CpG (black).

6.4.4. If Ag+ DC numbers are reduced, how long does it take for the repertoire to be scanned?

The second simulation provided in Figure 7 predicts how long it takes for the TCR repertoire to be scanned when Ag+ DC numbers entering the lymph node are reduced and provides a comparison between liposome alone, liposomal poly(I:C) and liposomal CpG. If we use the minimum number of Ag+ DCs required to scan 95% of the repertoire for each vaccine formulation (as revealed in Figure 6), it will take approximately 61, 86 and 97 hours to scan the repertoire for liposome alone, liposomal CpG and liposomal poly(I:C) formulations, respectively (Figure 7).
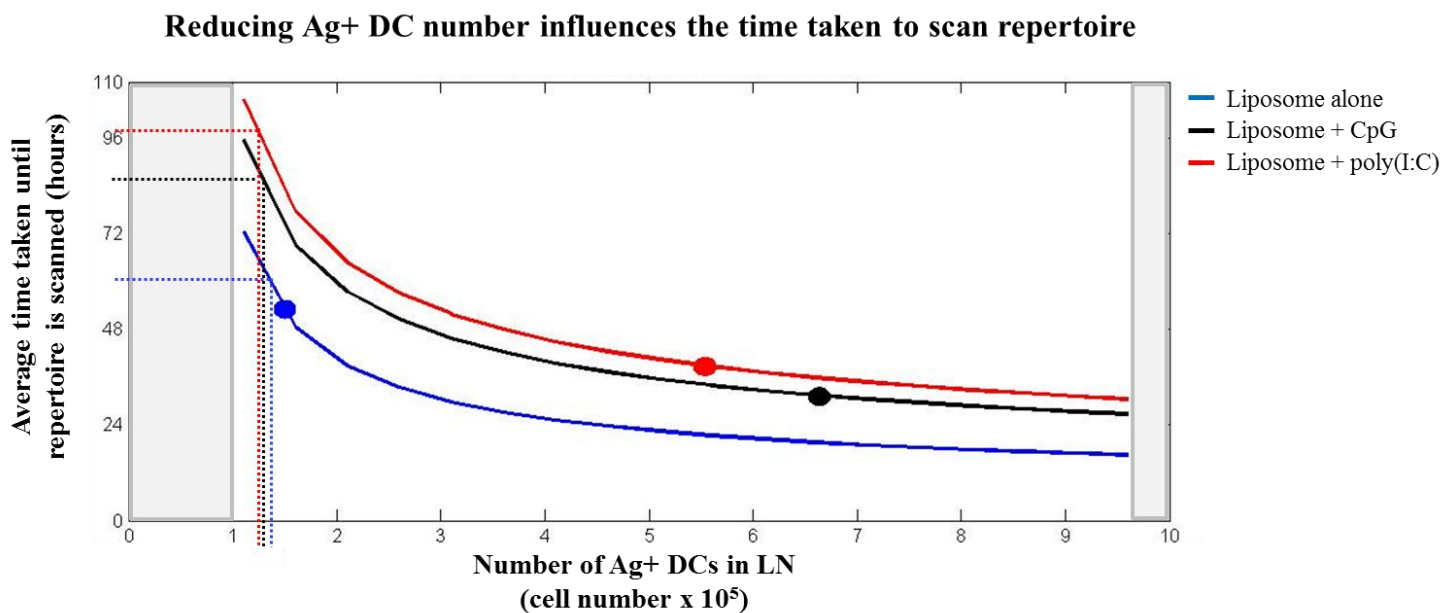
Figure 7. Our model was used to perform a simulation that reduces the number of Ag+ DCs entering the lymph node and provides the corresponding time taken for 95% of the TCR repertoire to be scanned at these numbers. Dotted lines indicate, if Ag+ DC numbers are reduced to the minimum number required for each vaccine formulation (as revealed in Figure 6), the time taken for the entire repertoire to be scanned. Coloured circles represent the actual numbers of Ag+ DC numbers observed experimentally for liposome alone (blue), liposomal poly(I:C) (red) and liposomal CpG (black). Shaded area (1) indicates that the repertoire will not be scanned within 10 days if the Ag+ DC number is reduced below this number. Shaded area (2) indicates that if Ag+ DC number is increased above this number no improvement in the time taken to scan the repertoire will be observed.

We have previously shown that, at theoretically reduced Ag+ DC numbers, the Ag+ DCs that enter the lymph node over a larger amount of time will scan more of the repertoire than Ag+ DCs that enter the lymph node over a shorter amount of time. Interestingly, this second simulation reveals that, whilst liposomal poly(I:C) will scan more of the repertoire than the other formulations at lower Ag+ DC numbers (Figure 6), liposomal poly(I:C) will take the longest amount of time to scan the TCR repertoire when compared to liposome alone and liposomal CpG (Figure 7). That is, a longer duration of Ag+ DC entry enhances the probability that the entire TCR repertoire will be scanned, however this process will take longer to occur. Conversely, a shorter duration of Ag+ DC entry leads decreases the probability that the TCR repertoire will be scanned, however if successful, this process will occur faster.

The simulation in Figure 7 also reveals that, for any vaccine formulation, the entire TCR repertoire will not be scanned within 10 days (the maximal time limit of this simulation) if the Ag+ DC number is reduced to less than $1x10^5$. Conversely, no improvement in the time taken to scan the T cell repertoire will be seen if Ag+ DC numbers are increased beyond $9.6x10^5$ (Figure 7).

6.5   Discussion

The ability to target DCs at the site of injection for the induction of antigen-specific T cell immunity represents a major strategy in vaccine development. We have previously shown that the addition of poly(I:C) or CpG to liposomal vaccine formulations alters the kinetics and increases the number and maturation of Ag+ DCs in afferent lymph. The sum of these effects lead to enhanced antigen-specific adaptive immunity (196, 280), however the relative contribution of each individual response on T cell activation remained unclear. We therefore developed a mathematical model to determine the relative effect of vaccine-induced changes in the kinetics of Ag+ DC influx on TCR repertoire scanning in the local draining lymph node. This mathematical model was used to estimate the minimum number of Ag+ DCs required in the lymph node to scan our estimate of the TCR repertoire, and the extent to which reducing Ag+ DC number influences the time taken for an antigen-specific response to occur.

Our model revealed that all vaccine formulations induced more Ag+ DCs than required to scan the TCR repertoire. At these induced Ag+ DC numbers, we estimate the repertoire is scanned in under two days for the adjuvanted formulations, with CpG inducing this response 7h faster than poly(I:C). Despite the success of all three formulations in scanning the repertoire, we see vast differences in the resulting adaptive immunity, indicating that antigen uptake is not a limiting factor in this vaccine scenario. This was most evident when comparing CpG and liposome alone, where CpG increased the number of IFNγ+ CD8 T cells in efferent lymph and enhanced systemic antigen-specific antibody concentration after secondary vaccination. Liposome alone, however, did not increase adaptive immunity in efferent lymph and only produced antigen-specific antibodies after tertiary injection. This suggested that although liposomes alone induced the migration of enough Ag+ DCs to scan all cognate T cells in the lymph node, these DCs were not efficiently activating the T cells to produce a potent adaptive immune response. The addition of CpG increased the expression of co-stimulatory molecules CD80 and CD86 on Ag+ DCs in afferent lymph. Up-regulation of CD80/CD86 has been shown to enhance T cell activation (281) and provides an explanation for the enhanced adaptive immunity observed with CpG when compared to liposome alone, despite both vaccines scanning the TCR repertoire within approximately 2 days.

This initial result from our model has important implications for vaccine design, suggesting that enhancing Ag+ DC activation and maturation at the site of injection, rather than enhancing antigen uptake, is more likely to be a critical factor for inducing an effective adaptive immune response. The results suggest that even if a vaccine induces enough Ag+ DCs at the site of injection to scan all cognate T cells, a strong antigen-specific immune response is unlikely to be induced unless these Ag+ DCs are able to effectively activate the cognate T cell. This highlights the necessity of incorporating adjuvants within vaccines that are able to potentiate immune responses at the site of injection for enhanced immunity in the local lymph node.

Whilst the primary goal of an adjuvant formulation is to enhance immunity, it is also important to balance these responses to prevent inappropriate inflammation and reduce the risk of harmful side effects. Given that poly(I:C) and CpG induce an excess of Ag+ DCs, we wanted to determine the minimum number of Ag+ DCs actually required in the lymph node to scan our estimate of the TCR repertoire. This simulation using our model revealed that poly(I:C) and CpG are inducing between 4 and 5 fold more Ag+ DCs than needed to scan the repertoire and that an average of only 1.3×10^5 Ag+ DCs are required in the lymph node. These are important predictions that need to be confirmed experimentally. To do this, a fixed number of Ag+ DCs can be directly inserted into the afferent lymphatic vessel and the resulting antigen-specific T cell immunity in efferent lymph determined. These are technically difficult experiments that require surgical optimisations currently underway in our laboratory. Nevertheless, these preliminary findings may suggest that the commercial vaccine formulations investigated in our study are utilising high antigen doses that induce more Ag+ DCs than required to further enhance immunity and may increase the risk of side effects. These results also suggest that increasing the amount of antigen within each Ag+ DC, and consequently increasing their ability to present antigen (282), may lead to enhanced cognate T cell activation, rather than increasing the number of Ag+ DCs that contain a low amount of antigen.

Similar modelling approaches have been used to enhance our understanding of the relationship between antigen dose and the immune response generated in the local lymph node. One study developed a virtual human model that qualitatively and quantitatively captures cell migration, activation and priming between the lung and the draining lymph node in TB infection (283). The simulations reveal that strong activation of DCs leading to

maximal antigen presentation could represent a novel strategy for the development of new treatments against TB (283). A follow up study by the same group sought to determine whether increasing antigen dose can enhance T cell priming in the local lymph node, with the hypothesis that increasing bacterial numbers in the lung would lead to more antigen in the lymph node, which should ultimately enhance T cell priming (284). Interestingly, the data revealed that within a 10 to 50 fold range, antigen dose had little effect on antigen-specific T cell priming in the lymph node. For vaccine design, it is therefore important to consider the dose-dependent relationship between antigen and T cell priming, as the priming of T cells appears to be readily saturated by antigen.

If antigen dosage is reduced, as explored in our model by theoretically reducing the number of Ag+ DCs, the time taken for Ag+ DCs to enter the lymph node becomes a critical factor for both the proportion of the TCR repertoire scanned and the time taken for this process to occur. Given a fixed minimum number of Ag+ DCs, our model predicted that if the Ag+ DCs enter the lymph node over a longer period of time (poly(I:C)), the greater the proportion of the TCR repertoire scanned, however this process will take longer to occur. This process takes longer to occur as there are less Ag+ DCs present in the lymph node at a given instant. However, these Ag+ DCs are present in the lymph node over a longer period of time, thereby enhancing the proportion of the TCR repertoire scanned. This can also be explained given the 24h T cell circulation rate, where a longer duration of Ag+ DCs that are alive in the lymph node enhances the probability that interactions between an Ag+ DC and all recirculating cognate T cells will occur. On the other hand, if Ag+ DCs enter the lymph node over a shorter period of time (liposome alone), the probability that interactions between Ag+ DCs and recirculating cognate T cell will occur is reduced.

Overall, these findings suggest that if the antigen dose within a vaccine is reduced to the minimal amount, Ag+ DCs from the site of injection must migrate to the lymph node over a longer period of time in order to guarantee all cognate T cells are scanned. The caveat, however, is that this process will take longer to occur. It seems, therefore, that reducing antigen dosage leads to a trade-off between the proportion of the repertoire scanned and the time taken for an antigen-specific response to occur. For example, liposomal poly(I:C) scans more of the repertoire when Ag+ DC numbers are reduced to the minimal amount, however this process takes 36h longer to occur than liposome alone. CpG, however, appears to satisfy both criteria, enhancing the proportion of the repertoire scanned when compared to liposome

alone whilst scanning the repertoire 11 hours faster than poly(I:C). Our model therefore reveals that it is necessary to consider the kinetic profile of DC migration from the site of injection into the lymph node when reducing antigen dosage within vaccines.

The current preliminary model includes several assumptions and limitations that should be discussed. Firstly, we assume the migration of Ag+ DCs into the lymph node is in the form of a gamma distribution. Whilst the properties of this distribution describe the experimental data, we were forced to fit this distribution using only four time points post vaccination. As this curve is used to determine the total number of Ag+ DCs in the lymph node, it would have been ideal to perform a series of lymph collections to reveal the number of Ag+ DCs for the entire 72h period after vaccination rather than four selected time points. Whilst the time points analysed were chosen as they best represent the changes observed in DC migration following vaccination, specific experiments should be performed in the future to develop a more comprehensive model of DC migration. Secondly, the current model has been developed for classical MHC-II CD4 T cell activation using the entire lymph node. The complexity of the lymph node, including structural and functional zones, was not included in this model nor was the process of cross presentation to CD8 T cells. A goal for the future is to design a 3D model of the lymph node that includes T cell zones that can model interactions between Ag+ DCs and CD4/CD8 T cells. However, further research to determine the specific details of these processes within the ovine lymph node is required before this can be achieved. This model intentionally focuses on the contribution of antigen positive DCs migrating from the injection site on T cell activation in the lymph node. It is also clear, however, that lymph node resident DCs are able to take up antigen (285). A future goal of this model is to incorporate the contribution of lymph node resident DCs on antigen presentation to T cells. In order to do this, the number of antigen positive DCs present in the lymph node at corresponding time points after vaccination could be quantified and incorporated into the working model.

We have used TCR repertoire scanning as a measure of vaccine efficacy in our model under the assumption that the TCR repertoire consists of at least 2×10^7 receptors and that cognate T cells exist at a frequency of 1 in 10^6. Whilst this is a valid estimate from the literature (286, 287), an experimentally measurable output of vaccine-induced TCR clones needs to be developed. This is technically feasible through deep sequencing of the TCR in efferent lymph post vaccination; however these would then need to be confirmed experimentally with antigenic peptides, which is extremely laborious in sheep. Whilst the number of OVA-

specific T cells induced after stimulation is often determined in transgenic mice (288, 289), this is not easily obtained in sheep. The best available measure of antigen-specificity in our model is to assess T cell proliferation or cytokine production following antigen stimulation (290). This allows determination of the number of antigen-specific CD4 and CD8 T cells generated in efferent lymph following primary vaccination however offers little information of TCR diversity. A combination of deep sequencing of TCR diversity and the 3D lymph node model may allow us to investigate the effect of processes such as lymph node shut down on the number of antigen-specific T cells generated following primary vaccination. Finally, as mentioned previously, the results of this model need to be confirmed experimentally before it can be used to predict the efficacy of vaccine formulations.

In this chapter, we developed a preliminary mathematical model of DC trafficking and T cell activation in the local lymph node using known parameters from the literature and experimental data obtained from the lymphatic cannulation model. To our knowledge, this is the first study to mathematically model T cell activation following vaccination using real *in vivo* measures of DC migration from the site of injection and single lymph node T cell recirculation rates. Whilst only a small percentage of DCs migrating in afferent lymph carry antigen, we have revealed that the Ag+ DC numbers induced by all formulations are sufficient to scan our representation of the cognate T cell repertoire. Theoretically reducing antigen dosage using the parameters of our model revealed that the time taken for DCs to enter the lymph node is a critical factor for TCR repertoire scanning at low Ag+ DC numbers. The model predicts a trade-off between the proportion of the repertoire scanned and the time taken for this to occur, where a larger distribution of DC migration to the lymph node increases the proportion of the repertoire scanned however this process takes longer to occur, and vice versa. Overall, whilst this model requires experimental confirmation, the preliminary results provide important information for novel vaccine development, including the optimal number of antigen positive DCs required in afferent lymph, the effects of reducing antigen dosage and the contribution of migratory DC kinetics on vaccine efficacy.

CHAPTER SEVEN

General Discussion

General discussion

Despite the remarkable success of vaccination, there are a range of human and veterinary diseases that are in need of new or improved vaccines. The rational design of vaccines for these diseases relies on increased understanding of the immunological mechanisms that contribute to vaccine immunity, the development of novel vaccine delivery systems and the characterisation of immune stimulants that are able to enhance vaccine efficacy without side effects. Current subunit vaccines are able to drive durable and protective antibody mediated immune responses. However, the development of therapeutic vaccines against cancer and chronic infections may require the induction of effective cytotoxic T cell responses that are able to kill infected or malignant cells (291). Vaccine formulations incorporating stimulants that target innate immune receptors have been shown to significantly increase cell-mediated vaccine immunity. When incorporated into liposome-based delivery systems, the TLR ligands CpG and poly(I:C) are able to induce protective cellular and humoral immune responses in mice (120, 125). However, the cellular targets of these liposomal adjuvant formulations and the *in vivo* mechanisms of immune induction in other animals remain to be elucidated.

By directly cannulating the ovine lymphatic vessels, the results of this thesis revealed that the addition of poly(I:C) or CpG to liposomal vaccine formulations enhanced the immediate inflammatory response at the site of injection, improved antigen uptake by innate cell populations and induced genetic signatures associated with innate anti-viral immune responses in afferent lymph. Liposomal poly(I:C) and CpG also increased the production of antigen-specific antibodies in the circulation following vaccine challenge. This work demonstrates that liposomal vaccine formulations require the addition of innate adjuvants to enhance their immunogenicity. Several studies have compared the responses to free adjuvant and free antigen with those induced by particulate delivery. A recent study showed that nanoparticle-encapsulated OVA with CpG was more effective at inducing antigen-specific CTLs, even if 10 times more free OVA and 5 times more free CpG were used (292). Similar results were observed with liposomal poly(I:C), where stronger antigen-specific CD8 T cell responses were observed when compared to free poly(I:C) (120, 293). Together, these findings suggest that combinations of liposomes and innate adjuvants demonstrate higher efficacy than when either is administered alone. The mechanisms behind this

enhanced immunogenicity are not completely clear, however it is believed that incorporating adjuvants into liposomes protects them from degradation and facilitates the delivery of antigen and adjuvant into the one APC (104). It has also been shown that liposomes travel to the draining lymph node, prolonging antigen retention and increasing antigen uptake by lymph node resident DCs (285).

Liposomal adjuvant formulations can therefore reduce antigen and adjuvant dosage without sacrificing immunogenicity. Nucleic acid based TLR ligands, including poly(I:C) and CpG, have been linked to over-stimulation of the immune system, leading to adverse events (294). This toxicity has been the major hurdle preventing their clinical application. Recent results from clinical studies show that poly ICLC, a stabilised analogue of poly(I:C), induces local site reactions and mild flu-like symptoms in healthy individuals (95). CpG was shown to be generally safe and well tolerated in healthy individuals, however autoimmune responses and hematologic events were observed in patients with severe infectious disease or cancer (295). Encapsulating innate stimulators is likely to limit their systemic availability and reduce any off-target effects. Incorporating poly(I:C) into a liposome prevented the systemic release of pro-inflammatory cytokines that occurred following injection of free poly(I:C) (120, 293). Combined with the safety profile of liposomes when used as an antigen delivery vehicle (104), these results suggest that liposomal adjuvant formulations are safe and effective candidates for inclusion in novel vaccines. Indeed, liposomes combined with the hepatitis B surface antigen and the TLR 4 ligand MPL, an adjuvant recently approved for human use, induced strong and persistent cell mediated immunity in humans. Additionally, no serious adverse events were reported (118). Whilst these results are promising, the safety and efficacy of liposomal CpG and poly(I:C) need to be evaluated in a clinical setting.

In this thesis, the enhanced immunogenic properties of liposomal CpG and poly(I:C) were not associated with an increase in pro-inflammatory cytokines within the lymphatic system. Soluble IL1β, TNFα and IL6 were not detected in afferent lymph at any time point after vaccination with the liposomal adjuvant formulations. The inability to detect these cytokines may be due to the sensitivity of the ovine cytokine ELISA reagents, where the most sensitive reading is in the ng/ml concentration range. Alternatively, formulation with liposomes may prevent or reduce the release of these cytokines into the lymphatic network following injection. The results also show that whilst poly(I:C) and CpG enhanced the immediate inflammatory response at the site of injection, as demonstrated by a rapid increase

in the number of neutrophils in afferent lymph, neither adjuvant prolonged the duration of this inflammatory response to 24h after injection. This has important implications for vaccine safety, where extended non-specific inflammatory responses have been linked to increased vaccine reactogenicity and site reactions (95). The combined results of this thesis provide important evidence for the safety and efficacy of liposomal CpG and poly(I:C), utilising an outbred animal model following a dose and volume comparable to that administered to humans.

Vaccines against a number of animal diseases are required not only to improve the health of companion animals and increase production of livestock, but also to prevent the animal-to-human transmission of infectious diseases (2). The liposomal adjuvant formulations investigated in these studies were supplied by Pfizer Animal Health (now Zoetis Research and Manufacturing). In addition to the current studies and previous reports from our laboratory (162, 194, 195), other groups have investigated the immunostimulatory effects of TLR ligands in livestock when used as adjuvants within vaccine formulations. Intrapulmonary administration of CpG was shown to stimulate systemic innate responses in sheep, including elevation of the anti-viral effector molecule $2'5'$-A synthetase. The dose required to induce these effects could be reduced by 80% if CpG was formulated with the oil-in-water delivery system Emulsigen (296). Another study showed that subcutaneous immunisation with CpG and a vaccine containing *M. bovis* culture filtrate (CFP) combined with BCG induced greater protection against bovine tuberculosis than CFP-BCG or BCG alone (297). In contrast, a recent study investigating the effect of CpG on protective immunity against alcelaphine herpesvirus-1 (A1HV-1) malignant catarrhal fever, a fatal lymphoproliferative disease of cattle, showed that intramuscular injection of CpG with Emulsigen and attenuated A1HV-1 or attenuated A1HV-1 alone did not improve immunity (298). These studies highlight that adjuvant formulations need to be evaluated in the target species. It is unlikely that one formulation will tick all the boxes, and as such further studies are required to define optimal formulations, dosage and routes of administration, which may have to be tailored to each antigen.

The present findings also show that liposomal CpG and poly(I:C) target distinct pathways at the site of injection to induce their immunological effects. Liposomal CpG uniquely increased dendritic cell associated antigen transport and induced the maturation of monocytes and dendritic cells 72h after injection. These immunostimulatory properties were not observed with liposomal poly(I:C) or liposomes alone. Together with the enhanced antigen-

specific humoral immunity observed with this formulation, these findings suggest that CpG is a more effective adjuvant in this model when compared to poly(I:C). A major goal in vaccine development is the ability to target DCs at the site of injection for the induction of antigen specific T cell immunity (266). Several studies in mice have investigated the ability of adjuvant formulations to induce DC activation in lymph nodes draining the site of injection. One study showed a rapid increase in the number of DCs in the draining lymph node within 24h of a single injection of nanoparticles containing the TLR 7/8 agonist R848 (292). A second study showed that nanoparticle-encapsulated CpG with OVA antigen more potently activated and induced the maturation of cross-presenting DCs in the draining lymph node 20h after injection when compared to free CpG. The number of DCs in the lymph node that were double positive for both the adjuvant and the antigen also increased after injection with this formulation (291). Combined with the results documented in this thesis, this suggests that the enhanced Th1 cellular immune responses observed with these adjuvant formulations may be due to the activation of DCs at the peripheral injection site, leading to enhanced T cell activation in the local lymph node. These studies also suggest that DCs may be activated within the lymph node to enhance T cell priming.

This thesis also shows that injection with liposomal CpG enhanced IFNγ production by CD8 T cells in the efferent lymph of the draining lymph node. A recent pre-clinical study reported that a hepatitis B peptide vaccine adjuvanted with CpG significantly enhanced IFNγ production and cytotoxic responses in PBMCs from patients with chronic hepatitis B infection (299). Another study reported that CpG was capable of inducing proliferative PBMC responses to hepatitis B vaccine antigen in HIV-infected adults (300). Similarly, subjects who received $1/10^{th}$ the dose of a commercial influenza vaccine combined with CpG had 4-7 fold higher IFNγ producing PBMCs after antigen challenge when compared to low dose vaccine alone recipients (97). Most work investigating vaccine efficacy in humans relies on measurements taken from peripheral blood, however, interactions between antigens and the immune system largely take place in peripheral tissues and lymph nodes (301). Understanding the responses that occur in these tissues, in combination with results obtained from human peripheral blood, may assist in the design of novel vaccines that induce effective local immunity for the induction of a protective antigen-specific immune response.

The mathematical model developed in this thesis further confirms that the pathways targeted by adjuvants at the site of injection influence immunological outcomes. The model predicts that all liposomal formulations induce a sufficient number of antigen-positive DCs to scan

our estimate of the cognate TCR repertoire. However, as stated previously, the adjuvanted formulations induced greater immunity than the control formulation. This suggests that it is the activation status, rather than the number, of migratory DCs carrying antigen that contribute to enhanced immunity. No increase in expression of the co-stimulatory molecules CD80/CD86 was observed on antigen-positive DCs following injection of liposome alone, suggesting that even if a vaccine induces enough antigen-positive DCs at the site of injection to scan the repertoire, an antigen-specific response may not be induced unless these DCs are able to efficiently activate cognate T cells. Instead, the absence of co-stimulation may lead to T cell anergy (302). The model suggests that maximising the maturation of antigen-carrying DCs at the site of injection, rather the increasing the number of immature DCs carrying antigen, is a worthy approach in novel vaccine development. Indeed, lymph node resident DCs are also able to become activated and take up antigen, thereby representing an alternative approach to target dendritic cells draining the site of vaccination.

Delivery systems and adjuvants are therefore necessary components of vaccines that are able to potentiate immune responses to antigens that are not highly immunogenic, reduce antigen dosage, drive the immune system toward a preferred type of response and enhance immunity in immune-compromised individuals. There are a number of adjuvant systems currently in development that are specifically aimed at boosting Th1 immune responses (301, 303, 304), and the results documented here suggest CpG is an excellent inducer of Th1 immunity in sheep. The precise mechanisms that explain the enhanced immunogenicity induced by adjuvants remain unclear. For example, the modes of action of aluminium-based adjuvants, which have been incorporated in human vaccines for well over 80 years, are still not completely understood (305). Our mathematical model suggests that enhancing co-stimulation is a critical factor for vaccine efficacy and current commercial adjuvanted vaccines are likely to induce more antigen-positive DCs than are required for an effective adaptive immune response. Further expanding our knowledge of the mechanisms of adjuvant immunomodulation is crucial for the development of new adjuvants with specific properties. This informed, mechanistic-based design of adjuvant systems is likely to accelerate the development of novel and effective vaccines.

A systems biology approach to vaccinology has the potential to elucidate the mechanisms involved in the generation of an immune response and identify the biomarkers responsible for vaccine protection. The tools of systems biology include high-throughput technologies such as RNA sequencing, that are used in combination with immunological assays, such as flow

cytometry and antibody profiling, to generate a system-wide unbiased analysis of the immune response to vaccination (190). Systems approaches have been used to identify genetic biomarkers that contribute to the differences in immunity observed in humans following vaccination. A recent study reported that genes involved in inflammation and antigen presentation are important in characterising high and low antibody responses to rubella vaccination (306). Another study used predictive modelling to determine that the gene expression signatures of individuals in the first week after influenza vaccination can predict the antibody responses observed in these individuals 30 days after vaccination (193). Studies such as these can lead to a greater understanding of the mechanisms of protective immunity which will help guide the development of novel vaccines that are able to combat global diseases.

The systems biology approach of this thesis revealed significant differences in the cellular and transcriptional immune profiles from the site of injection following vaccination with nucleic acid based innate immune stimulators incorporated into liposomal vaccine formulations. These findings have provided the foundation for future studies utilising lymphatic cannulation and mathematical modelling to investigate the pathways that are predictive of a successful vaccine outcome. These studies have the potential to elucidate the mechanisms responsible for the variability in immunity observed between high and low vaccine responders and identify potential correlates of protection within vaccines.

In conclusion, the work presented in this thesis provides a comprehensive analysis of the real time *in vivo* immune response induced by the nucleic acid adjuvants poly(I:C) and CpG when incorporated into a liposome-based delivery system. The results demonstrate that liposomal vaccine formulations require the addition of adjuvants to enhance their immunogenicity and that poly(I:C) and CpG induce distinct and overlapping responses in the lymphatic system which characterise their immunological effects. Whilst the safety and efficacy of liposomal adjuvant formulations needs to be evaluated in a clinical setting, their ability to enhance T cell immunity whilst reducing antigen dosage suggest they are ideal candidates for inclusion in vaccines against diseases that require effective cell mediated immune responses. Collectively, this body of research enhances our understanding of the complex immune response to vaccination that is required for the development of effective vaccines against globally important diseases.

References

1.   Almond, J. W. 2007. Vaccine renaissance. *Nat Rev Microbiol* 5: 478-481.

2.   Meeusen, E. N., J. Walker, A. Peters, P. P. Pastoret, and G. Jungersen. 2007. Current status of veterinary vaccines. *Clin Microbiol Rev* 20: 489-510, table of contents.

3.   Keith, J. A., L. Agostini Bigger, P. A. Arthur, E. Maes, and R. Daems. 2013. Delivering the promise of the Decade of Vaccines: opportunities and challenges in the development of high quality new vaccines. *Vaccine* 31 Suppl 2: B184-193.

4.   Gutierrez, A. H., D. M. Spero, C. Gay, M. Zimic, and A. S. De Groot. 2012. New vaccines needed for pathogens infecting animals and humans: One Health. *Human vaccines & immunotherapeutics* 8: 971-978.

5.   McManus, D. P. 2005. Prospects for development of a transmission blocking vaccine against Schistosoma japonicum. *Parasite Immunol* 27: 297-308.

6.   Pulendran, B., and R. Ahmed. 2011. Immunological mechanisms of vaccination. *Nat Immunol* 12: 509-517.

7.   Riedel, S. 2005. Edward Jenner and the history of smallpox and vaccination. *Proc (Bayl Univ Med Cent)* 18: 21-25.

8.   de Veer, M., and E. Meeusen. 2011. New developments in vaccine research--unveiling the secret of vaccine adjuvants. *Discov Med* 12: 195-204.

9.   Germain, R. N. 2010. Vaccines and the future of human immunology. *Immunity* 33: 441-450.

10.   Plotkin, S. A. 2009. Vaccines: the fourth century. *Clin Vaccine Immunol* 16: 1709-1719.

11.   Hilleman, M. R. 1998. Six decades of vaccine development--a personal history. *Nat Med* 4: 507-514.

12.   Dempsey, P. W., S. A. Vaidya, and G. Cheng. 2003. The art of war: Innate and adaptive immune responses. *Cell Mol Life Sci* 60: 2604-2621.

13.   Janeway, C. A., Jr., and R. Medzhitov. 2002. Innate immune recognition. *Annu Rev Immunol* 20: 197-216.

14.   Kauffman, H. F. 2006. Innate immune responses to environmental allergens. *Clinical reviews in allergy & immunology* 30: 129-140.

15. Yoneyama, M., M. Kikuchi, T. Natsukawa, N. Shinobu, T. Imaizumi, M. Miyagishi, K. Taira, S. Akira, and T. Fujita. 2004. The RNA helicase RIG-I has an essential function in double-stranded RNA-induced innate antiviral responses. *Nat Immunol* 5: 730-737.

16. Inohara, Chamaillard, C. McDonald, and G. Nunez. 2005. NOD-LRR proteins: role in host-microbial interactions and inflammatory disease. *Annu Rev Biochem* 74: 355-383.

17. Heegaard, P. M., L. Dedieu, N. Johnson, M. F. Le Potier, M. Mockey, F. Mutinelli, T. Vahlenkamp, M. Vascellari, and N. S. Sorensen. 2011. Adjuvants and delivery systems in veterinary vaccinology: current state and future developments. *Arch Virol* 156: 183-202.

18. Buettner, M., and U. Bode. 2012. Lymph node dissection - understanding the immunological function of lymph nodes. *Clin Exp Immunol* 169: 205-212.

19. Geginat, J., M. Paroni, F. Facciotti, P. Gruarin, I. Kastirr, F. Caprioli, M. Pagani, and S. Abrignani. 2013. The CD4-centered universe of human T cell subsets. *Semin Immunol* 25: 252-262.

20. Luckheeram, R. V., R. Zhou, A. D. Verma, and B. Xia. 2012. CD4(+)T cells: differentiation and functions. *Clinical & developmental immunology* 2012: 925135.

21. Kim, H. P., J. Imbert, and W. J. Leonard. 2006. Both integrated and differential regulation of components of the IL-2/IL-2 receptor system. *Cytokine & growth factor reviews* 17: 349-366.

22. Sharma, R., R. Kapila, M. R. Haq, V. Salingati, M. Kapasiya, and S. Kapila. 2013. Age-associated aberrations in mouse cellular and humoral immune responses. *Aging clinical and experimental research*.

23. Macedo, G. C., A. Bozzi, H. R. Weinreich, A. Bafica, H. C. Teixeira, and S. C. Oliveira. 2011. Human T cell and antibody-mediated responses to the Mycobacterium tuberculosis recombinant 85A, 85B, and ESAT-6 antigens. *Clinical & developmental immunology* 2011: 351573.

24. Del Prete, G. 1992. Human Th1 and Th2 lymphocytes: their role in the pathophysiology of atopy. *Allergy* 47: 450-455.

25. Couper, K. N., D. G. Blount, and E. M. Riley. 2008. IL-10: The master regulator of immunity to infection. *Journal of Immunology* 180: 5771-5777.

26. Mestas, J., and C. C. Hughes. 2004. Of mice and not men: differences between mouse and human immunology. *J Immunol* 172: 2731-2738.

27.   Tsai, H. C., and R. Wu. 2013. Cholera toxin directly enhances IL-17A production from human CD4+ T cells. *J Immunol* 191: 4095-4102.

28.   Krueger, J. G., S. Fretzin, M. Suarez-Farinas, P. A. Haslett, K. M. Phipps, G. S. Cameron, J. McColm, A. Katcherian, I. Cueto, T. White, S. Banerjee, and R. W. Hoffman. 2012. IL-17A is essential for cell activation and inflammatory gene circuits in subjects with psoriasis. *J Allergy Clin Immun* 130: 145-+.

29.   Li, M. O., Y. S. Y. Wan, and R. A. Flavell. 2007. T cell-produced transforming growth factor-beta 1 controls T cell tolerance and regulates Th1- and Th17-cell differentiation. *Immunity* 26: 579-591.

30.   Lakshmi Narendra, B., K. Eshvendar Reddy, S. Shantikumar, and S. Ramakrishna. 2013. Immune system: a double-edged sword in cancer. *Inflammation research : official journal of the European Histamine Research Society ... [et al.]*.

31.   Spits, H., D. Artis, M. Colonna, A. Diefenbach, J. P. Di Santo, G. Eberl, S. Koyasu, R. M. Locksley, A. N. McKenzie, R. E. Mebius, F. Powrie, and E. Vivier. 2013. Innate lymphoid cells--a proposal for uniform nomenclature. *Nat Rev Immunol* 13: 145-149.

32.   Ussher, J. E., P. Klenerman, and C. B. Willberg. 2014. Mucosal-associated invariant T-cells: new players in anti-bacterial immunity. *Frontiers in immunology* 5: 450.

33.   Spits, H., and T. Cupedo. 2012. Innate lymphoid cells: emerging insights in development, lineage relationships, and function. *Annu Rev Immunol* 30: 647-675.

34.   Van Kaer, L., V. V. Parekh, and L. Wu. 2011. Invariant natural killer T cells: bridging innate and adaptive immunity. *Cell and tissue research* 343: 43-55.

35.   Arrenberg, P., R. Halder, and V. Kumar. 2009. Cross-Regulation Between Distinct Natural Killer T Cell Subsets Influences Immune Response to Self and Foreign Antigens. *Journal of cellular physiology* 218: 246-250.

36.   Shibata, K. 2012. Close link between development and function of gamma-delta T cells. *Microbiology and immunology* 56: 217-227.

37.   Paul, S., A. K. Singh, Shilpi, and G. Lal. 2013. Phenotypic and Functional Plasticity of Gamma-Delta (gammadelta) T Cells in Inflammation and Tolerance. *International reviews of immunology*.

38.   Hsieh, B., M. D. Schrenzel, T. Mulvania, H. D. Lepper, L. DiMolfettoLandon, and D. A. Ferrick. 1996. In vivo cytokine production in murine listeriosis - Evidence for immunoregulation by gamma delta(+)3T cells. *Journal of Immunology* 156: 232-237.

39.   Hiromatsu, K., Y. Yoshikai, G. Matsuzaki, S. Ohga, K. Muramori, K. Matsumoto, J. A. Bluestone, and K. Nomoto. 1992. A Protective Role of Gamma-Delta T-Cells in

Primary Infection with Listeria-Monocytogenes in Mice. *Journal of Experimental Medicine* 175: 49-56.

40.   Sumaria, N., B. Roediger, L. G. Ng, J. Qin, R. Pinto, L. L. Cavanagh, E. Shklovskaya, B. Fazekas de St Groth, J. A. Triccas, and W. Weninger. 2011. Cutaneous immunosurveillance by self-renewing dermal gamma delta T cells. *Journal of Experimental Medicine* 208: 505-518.

41.   Shibata, K., H. Yamada, H. Hara, K. Kishihara, and Y. Yoshikai. 2007. Resident Vdelta1+ gammadelta T cells control early infiltration of neutrophils after Escherichia coli infection via IL-17 production. *J Immunol* 178: 4466-4472.

42.   Dejima, T., K. Shibata, H. Yamada, H. Hara, Y. Iwakura, S. Naito, and Y. Yoshikai. 2011. Protective role of naturally occurring interleukin-17A-producing gammadelta T cells in the lung at the early stage of systemic candidiasis in mice. *Infect Immun* 79: 4503-4510.

43.   Kaech, S. M., E. J. Wherry, and R. Ahmed. 2002. Effector and memory T-cell differentiation: implications for vaccine development. *Nat Rev Immunol* 2: 251-262.

44.   Miller, J. D., R. G. van der Most, R. S. Akondy, J. T. Glidewell, S. Albott, D. Masopust, K. Murali-Krishna, P. L. Mahar, S. Edupuganti, S. Lalor, S. Germon, C. Del Rio, M. J. Mulligan, S. I. Staprans, J. D. Altman, M. B. Feinberg, and R. Ahmed. 2008. Human effector and memory CD8+ T cell responses to smallpox and yellow fever vaccines. *Immunity* 28: 710-722.

45.   Akira, S., M. Yamamoto, and K. Takeda. 2003. Role of adapters in Toll-like receptor signalling. *Biochem Soc Trans* 31: 637-642.

46.   Buonaguro, L., and B. Pulendran. 2011. Immunogenomics and systems biology of vaccines. *Immunol Rev* 239: 197-208.

47.   Brunner, R., E. Jensen-Jarolim, and I. Pali-Scholl. 2010. The ABC of clinical and experimental adjuvants--a brief overview. *Immunol Lett* 128: 29-35.

48.   Coffman, R. L., A. Sher, and R. A. Seder. 2010. Vaccine adjuvants: putting innate immunity to work. *Immunity* 33: 492-503.

49.   Boyle, J., D. Eastman, C. Millar, S. Camuglia, J. Cox, M. Pearse, J. Good, and D. Drane. 2007. The utility of ISCOMATRIX adjuvant for dose reduction of antigen for vaccines requiring antibody responses. *Vaccine* 25: 2541-2544.

50.   Schwarz, T. F., T. Horacek, M. Knuf, H. G. Damman, F. Roman, M. Drame, P. Gillard, and W. Jilg. 2009. Single dose vaccination with AS03-adjuvanted H5N1

vaccines in a randomized trial induces strong and broad immune responsiveness to booster vaccination in adults. *Vaccine* 27: 6284-6290.

51.   Glenny, A. T. 1930. Insoluble Precipitates in Diphtheria and Tetanus Immunization. *Br Med J* 2: 244-245.

52.   Grun, J. L., and P. H. Maurer. 1989. Different T helper cell subsets elicited in mice utilizing two different adjuvant vehicles: the role of endogenous interleukin 1 in proliferative responses. *Cell Immunol* 121: 134-145.

53.   Kool, M., T. Soullie, M. van Nimwegen, M. A. Willart, F. Muskens, S. Jung, H. C. Hoogsteden, H. Hammad, and B. N. Lambrecht. 2008. Alum adjuvant boosts adaptive immunity by inducing uric acid and activating inflammatory dendritic cells. *J Exp Med* 205: 869-882.

54.   Eisenbarth, S. C., O. R. Colegio, W. O'Connor, F. S. Sutterwala, and R. A. Flavell. 2008. Crucial role for the Nalp3 inflammasome in the immunostimulatory properties of aluminium adjuvants. *Nature* 453: 1122-1126.

55.   Marrack, P., A. S. McKee, and M. W. Munks. 2009. Towards an understanding of the adjuvant action of aluminium. *Nat Rev Immunol* 9: 287-293.

56.   Duthie, M. S., H. P. Windish, C. B. Fox, and S. G. Reed. 2011. Use of defined TLR ligands as adjuvants within human vaccines. *Immunol Rev* 239: 178-196.

57.   Harper, D. M., E. L. Franco, C. M. Wheeler, A. B. Moscicki, B. Romanowski, C. M. Roteli-Martins, D. Jenkins, A. Schuind, S. A. Costa Clemens, and G. Dubin. 2006. Sustained efficacy up to 4.5 years of a bivalent L1 virus-like particle vaccine against human papillomavirus types 16 and 18: follow-up from a randomised control trial. *Lancet* 367: 1247-1255.

58.   Khan, K. N., M. Kitajima, K. Hiraki, A. Fujishita, I. Sekine, T. Ishimaru, and H. Masuzaki. 2009. Toll-Like Receptors in Innate Immunity: Role of Bacterial Endotoxin and Toll-Like Receptor 4 in Endometrium and Endometriosis. *Gynecol Obstet Inves* 68: 40-52.

59.   Evans, J. T., C. W. Cluff, D. A. Johnson, M. J. Lacy, D. H. Persing, and J. R. Baldridge. 2003. Enhancement of antigen-specific immunity via the TLR4 ligands MPL adjuvant and Ribi.529. *Expert Rev Vaccines* 2: 219-229.

60.   Didierlaurent, A. M., S. Morel, L. Lockman, S. L. Giannini, M. Bisteau, H. Carlsen, A. Kielland, O. Vosters, N. Vanderheyde, F. Schiavetti, D. Larocque, M. Van Mechelen, and N. Garcon. 2009. AS04, an aluminum salt- and TLR4 agonist-based

adjuvant system, induces a transient localized innate immune response leading to enhanced adaptive immunity. *J Immunol* 183: 6186-6197.

61. Casella, C. R., and T. C. Mitchell. 2008. Putting endotoxin to work for us: monophosphoryl lipid A as a safe and effective vaccine adjuvant. *Cell Mol Life Sci* 65: 3231-3240.

62. Botos, I., L. Liu, Y. Wang, D. M. Segal, and D. R. Davies. 2009. The toll-like receptor 3:dsRNA signaling complex. *Biochim Biophys Acta* 1789: 667-674.

63. Alexopoulou, L., A. C. Holt, R. Medzhitov, and R. A. Flavell. 2001. Recognition of double-stranded RNA and activation of NF-kappaB by Toll-like receptor 3. *Nature* 413: 732-738.

64. Hemmi, H., O. Takeuchi, T. Kawai, T. Kaisho, S. Sato, H. Sanjo, M. Matsumoto, K. Hoshino, H. Wagner, K. Takeda, and S. Akira. 2000. A Toll-like receptor recognizes bacterial DNA. *Nature* 408: 740-745.

65. Leonard, J. N., R. Ghirlando, J. Askins, J. K. Bell, D. H. Margulies, D. R. Davies, and D. M. Segal. 2008. The TLR3 signaling complex forms by cooperative receptor dimerization. *Proc Natl Acad Sci U S A* 105: 258-263.

66. Liu, L., I. Botos, Y. Wang, J. N. Leonard, J. Shiloach, D. M. Segal, and D. R. Davies. 2008. Structural basis of toll-like receptor 3 signaling with double-stranded RNA. *Science* 320: 379-381.

67. Takeshita, F., C. A. Leifer, I. Gursel, K. J. Ishii, S. Takeshita, M. Gursel, and D. M. Klinman. 2001. Cutting edge: Role of Toll-like receptor 9 in CpG DNA-induced activation of human cells. *J Immunol* 167: 3555-3558.

68. Jelinek, I., J. N. Leonard, G. E. Price, K. N. Brown, A. Meyer-Manlapat, P. K. Goldsmith, Y. Wang, D. Venzon, S. L. Epstein, and D. M. Segal. 2011. TLR3-specific double-stranded RNA oligonucleotide adjuvants induce dendritic cell cross-presentation, CTL responses, and antiviral protection. *J Immunol* 186: 2422-2429.

69. Tighe, H., K. Takabayashi, D. Schwartz, G. Van Nest, S. Tuck, J. J. Eiden, A. Kagey-Sobotka, P. S. Creticos, L. M. Lichtenstein, H. L. Spiegelberg, and E. Raz. 2000. Conjugation of immunostimulatory DNA to the short ragweed allergen amb a 1 enhances its immunogenicity and reduces its allergenicity. *J Allergy Clin Immunol* 106: 124-134.

70. Richards, K. H., and A. Macdonald. 2011. Putting the brakes on the anti-viral response: negative regulators of type I interferon (IFN) production. *Microbes Infect* 13: 291-302.

71. Longhi, M. P., C. Trumpfheller, J. Idoyaga, M. Caskey, I. Matos, C. Kluger, A. M. Salazar, M. Colonna, and R. M. Steinman. 2009. Dendritic cells require a systemic type I interferon response to mature and induce CD4+ Th1 immunity with poly IC as adjuvant. *J Exp Med* 206: 1589-1602.

72. Trumpfheller, C., M. Caskey, G. Nchinda, M. P. Longhi, O. Mizenina, Y. Huang, S. J. Schlesinger, M. Colonna, and R. M. Steinman. 2008. The microbial mimic poly IC induces durable and protective CD4+ T cell immunity together with a dendritic cell targeted vaccine. *Proc Natl Acad Sci U S A* 105: 2574-2579.

73. Salem, M. L., S. A. El-Naggar, A. Kadima, W. E. Gillanders, and D. J. Cole. 2006. The adjuvant effects of the toll-like receptor 3 ligand polyinosinic-cytidylic acid poly (I:C) on antigen-specific CD8+ T cell responses are partially dependent on NK cells with the induction of a beneficial cytokine milieu. *Vaccine* 24: 5119-5132.

74. Cao, Y., Z. Lu, P. Li, P. Sun, Y. Fu, X. Bai, H. Bao, Y. Chen, D. Li, and Z. Liu. 2012. Improved neutralising antibody response against foot-and-mouth-disease virus in mice inoculated with a multi-epitope peptide vaccine using polyinosinic and poly-cytidylic acid as an adjuvant. *J Virol Methods* 185: 124-128.

75. Stahl-Hennig, C., M. Eisenblatter, E. Jasny, T. Rzehak, K. Tenner-Racz, C. Trumpfheller, A. M. Salazar, K. Uberla, K. Nieto, J. Kleinschmidt, R. Schulte, L. Gissmann, M. Muller, A. Sacher, P. Racz, R. M. Steinman, M. Uguccioni, and R. Ignatius. 2009. Synthetic double-stranded RNAs are adjuvants for the induction of T helper 1 and humoral immune responses to human papillomavirus in rhesus macaques. *PLoS Pathog* 5: e1000373.

76. Park, H., L. Adamson, T. Ha, K. Mullen, S. I. Hagen, A. Nogueron, A. W. Sylwester, M. K. Axthelm, A. Legasse, M. Piatak, Jr., J. D. Lifson, J. M. McElrath, L. J. Picker, and R. A. Seder. 2013. Polyinosinic-polycytidylic acid is the most effective TLR adjuvant for SIV Gag protein-induced T cell responses in nonhuman primates. *J Immunol* 190: 4103-4115.

77. Klinman, D. M., G. Yamshchikov, and Y. Ishigatsubo. 1997. Contribution of CpG motifs to the immunogenicity of DNA vaccines. *J Immunol* 158: 3635-3639.

78. Krieg, A. M., A. K. Yi, J. Schorr, and H. L. Davis. 1998. The role of CpG dinucleotides in DNA vaccines. *Trends Microbiol* 6: 23-27.

79. Tross, D., and D. M. Klinman. 2008. Effect of CpG oligonucleotides on vaccine-induced B cell memory. *Journal of Immunology* 181: 5785-5790.

80. Klinman, D. A., H. Xie, S. F. Little, D. Currie, and B. E. Ivins. 2004. CpG oligonucleotides improve the protective immune response induced by the anthrax vaccination of rhesus macaques. *Vaccine* 22: 2881-2886.

81. Cooper, C. L., H. L. Davis, J. B. Angel, M. L. Morris, S. M. Elfer, I. Seguin, A. M. Krieg, and D. W. Cameron. 2005. CPG 7909 adjuvant improves hepatitis B virus vaccine seroprotection in anti retroviral-treated HIV-infected adults. *Aids* 19: 1473-1479.

82. Cooper, C. L., H. L. Davis, M. L. Morris, S. M. Efler, M. Al Adhami, A. M. Krieg, D. W. Cameron, and J. Heathcote. 2004. CPG 7909, an immunostimulatory TLR9 agonist oligodeoxynucleotide, as adjuvant to Engerix-B (R) HBV vaccine in healthy adults: A double-blind phase I/II study. *J Clin Immunol* 24: 693-701.

83. Halperin, S. A., G. Van Nest, B. Smith, S. Abtahi, H. Whiley, and J. J. Eiden. 2003. A phase I study of the safety and immunogenicity of recombinant hepatitis B surface antigen co-administered with an immunostimulatory phosphorothioate oligonucleotide adjuvant. *Vaccine* 21: 2461-2467.

84. Klinman, D. M., A. K. Yi, S. L. Beaucage, J. Conover, and A. M. Krieg. 1996. CpG motifs present in bacteria DNA rapidly induce lymphocytes to secrete interleukin 6, interleukin 12, and interferon gamma. *Proc Natl Acad Sci U S A* 93: 2879-2883.

85. Sun, S., X. Zhang, D. F. Tough, and J. Sprent. 1998. Type I interferon-mediated stimulation of T cells by CpG DNA. *J Exp Med* 188: 2335-2342.

86. Roman, M., E. Martin-Orozco, J. S. Goodman, M. D. Nguyen, Y. Sato, A. Ronaghy, R. S. Kornbluth, D. D. Richman, D. A. Carson, and E. Raz. 1997. Immunostimulatory DNA sequences function as T helper-1-promoting adjuvants. *Nat Med* 3: 849-854.

87. Jung, J., A. K. Yi, X. Zhang, J. Choe, L. Li, and Y. S. Choi. 2002. Distinct response of human B cell subpopulations in recognition of an innate immune signal, CpG DNA. *J Immunol* 169: 2368-2373.

88. Overstreet, M. G., H. Freyberger, I. A. Cockburn, Y. C. Chen, S. W. Tse, and F. Zavala. 2010. CpG-enhanced CD8(+) T-cell responses to peptide immunization are severely inhibited by B cells. *European Journal of Immunology* 40: 124-133.

89. Takeuchi, O., and S. Akira. 2008. MDA5/RIG-I and virus recognition. *Curr Opin Immunol* 20: 17-22.

90. Takahasi, K., M. Yoneyama, T. Nishihori, R. Hirai, H. Kumeta, R. Narita, M. Gale, Jr., F. Inagaki, and T. Fujita. 2008. Nonself RNA-sensing mechanism of RIG-I helicase and activation of antiviral immune responses. *Molecular cell* 29: 428-440.

91.   Kumar, H., S. Koyama, K. J. Ishii, T. Kawai, and S. Akira. 2008. Cutting edge: cooperation of IPS-1- and TRIF-dependent pathways in poly IC-enhanced antibody production and cytotoxic T cell responses. *J Immunol* 180: 683-687.

92.   Lahoud, M. H., F. Ahmet, J. G. Zhang, S. Meuter, A. N. Policheni, S. Kitsoulis, C. N. Lee, M. O'Keeffe, L. C. Sullivan, A. G. Brooks, R. Berry, J. Rossjohn, J. D. Mintern, J. Vega-Ramos, J. A. Villadangos, N. A. Nicola, M. C. Nussenzweig, K. J. Stacey, K. Shortman, W. R. Heath, and I. Caminschi. 2012. DEC-205 is a cell surface receptor for CpG oligonucleotides. *Proc Natl Acad Sci U S A* 109: 16270-16275.

93.   Okada, H., P. Kalinski, R. Ueda, A. Hoji, G. Kohanbash, T. E. Donegan, A. H. Mintz, J. A. Engh, D. L. Bartlett, C. K. Brown, H. Zeh, M. P. Holtzman, T. A. Reinhart, T. L. Whiteside, L. H. Butterfield, R. L. Hamilton, D. M. Potter, I. F. Pollack, A. M. Salazar, and F. S. Lieberman. 2011. Induction of CD8+ T-cell responses against novel glioma-associated antigen peptides and clinical activity by vaccinations with {alpha}-type 1 polarized dendritic cells and polyinosinic-polycytidylic acid stabilized by lysine and carboxymethylcellulose in patients with recurrent malignant glioma. *J Clin Oncol* 29: 330-336.

94.   Rosenfeld, M. R., M. C. Chamberlain, S. A. Grossman, D. M. Peereboom, G. J. Lesser, T. T. Batchelor, S. Desideri, A. M. Salazar, and X. Ye. 2010. A multi-institution phase II study of poly-ICLC and radiotherapy with concurrent and adjuvant temozolomide in adults with newly diagnosed glioblastoma. *Neuro-oncology* 12: 1071-1077.

95.   Caskey, M., F. Lefebvre, A. Filali-Mouhim, M. J. Cameron, J. P. Goulet, E. K. Haddad, G. Breton, C. Trumpfheller, S. Pollak, I. Shimeliovich, A. Duque-Alarcon, L. Pan, A. Nelkenbaum, A. M. Salazar, S. J. Schlesinger, R. M. Steinman, and R. P. Sekaly. 2011. Synthetic double-stranded RNA induces innate immune responses similar to a live viral vaccine in humans. *Journal of Experimental Medicine* 208: 2357-2366.

96.   Sogaard, O. S., N. Lohse, Z. B. Harboe, R. Offersen, A. R. Bukh, H. L. Davis, H. C. Schonheyder, and L. Ostergaard. 2010. Improving the immunogenicity of pneumococcal conjugate vaccine in HIV-infected adults with a toll-like receptor 9 agonist adjuvant: a randomized, controlled trial. *Clinical infectious diseases : an official publication of the Infectious Diseases Society of America* 51: 42-50.

97.   Cooper, C. L., H. L. Davis, M. L. Morris, S. M. Efler, A. M. Krieg, Y. Li, C. Laframboise, M. J. Al Adhami, Y. Khaliq, I. Seguin, and D. W. Cameron. 2004.

Safety and immunogenicity of CPG 7909 injection as an adjuvant to Fluarix influenza vaccine. *Vaccine* 22: 3136-3143.

98.   Sagara, I., R. D. Ellis, A. Dicko, M. B. Niambele, B. Kamate, O. Guindo, M. S. Sissoko, M. P. Fay, M. A. Guindo, O. Kante, R. Saye, K. Miura, C. Long, G. E. Mullen, M. Pierce, L. B. Martin, K. Rausch, A. Dolo, D. A. Diallo, L. H. Miller, and O. K. Doumbo. 2009. A randomized and controlled Phase 1 study of the safety and immunogenicity of the AMA1-C1/Alhydrogel + CPG 7909 vaccine for Plasmodium falciparum malaria in semi-immune Malian adults. *Vaccine* 27: 7292-7298.

99.   Cunningham, C., S. Campion, J. Teeling, L. Felton, and V. H. Perry. 2007. The sickness behaviour and CNS inflammatory mediator profile induced by systemic challenge of mice with synthetic double-stranded RNA (poly I:C). *Brain, behavior, and immunity* 21: 490-502.

100. Zhao, L., A. Seth, N. Wibowo, C. X. Zhao, N. Mitter, C. Yu, and A. P. Middelberg. 2014. Nanoparticle vaccines. *Vaccine* 32: 327-337.

101. Treuel, L., X. Jiang, and G. U. Nienhaus. 2013. New views on cellular uptake and trafficking of manufactured nanoparticles. *Journal of the Royal Society, Interface / the Royal Society* 10: 20120939.

102. Roldao, A., M. C. Mellado, L. R. Castilho, M. J. Carrondo, and P. M. Alves. 2010. Virus-like particles in vaccine development. *Expert Rev Vaccines* 9: 1149-1176.

103. Kushnir, N., S. J. Streatfield, and V. Yusibov. 2012. Virus-like particles as a highly efficient vaccine platform: Diversity of targets and production systems and advances in clinical development. *Vaccine* 31: 58-83.

104. Nordly, P., H. B. Madsen, H. M. Nielsen, and C. Foged. 2009. Status and future prospects of lipid-based particulate delivery systems as vaccine adjuvants and their combination with immunostimulators. *Expert Opin Drug Del* 6: 657-672.

105. Watson, D. S., A. N. Endsley, and L. Huang. 2012. Design considerations for liposomal vaccines: influence of formulation parameters on antibody and cell-mediated immune responses to liposome associated antigens. *Vaccine* 30: 2256-2272.

106. Henriksen-Lacey, M., D. Christensen, V. W. Bramwell, T. Lindenstrom, E. M. Agger, P. Andersen, and Y. Perrie. 2010. Liposomal cationic charge and antigen adsorption are important properties for the efficient deposition of antigen at the injection site and ability of the vaccine to induce a CMI response. *J Control Release* 145: 102-108.

107. Nakanishi, T., J. Kunisawa, A. Hayashi, Y. Tsutsumi, K. Kubo, S. Nakagawa, H. Fujiwara, T. Hamaoka, and T. Mayumi. 1997. Positively charged liposome functions

as an efficient immunoadjuvant in inducing immune responses to soluble proteins. *Biochem Bioph Res Co* 240: 793-797.

108. Herzog, C., K. Hartmann, V. Kunzi, O. Kursteiner, R. Mischler, H. Lazar, and R. Gluck. 2009. Eleven years of Inflexal V-a virosomal adjuvanted influenza vaccine. *Vaccine* 27: 4381-4387.

109. Bovier, P. A. 2008. Epaxal: a virosomal vaccine to prevent hepatitis A infection. *Expert Rev Vaccines* 7: 1141-1150.

110. Joseph, A., N. Itskovitz-Cooper, S. Samira, O. Flasterstein, H. Eliyahu, D. Simberg, I. Goldwaser, Y. Barenholz, and E. Kedar. 2006. A new intranasal influenza vaccine based on a novel polycationic lipid--ceramide carbamoyl-spermine (CCS) I. Immunogenicity and efficacy studies in mice. *Vaccine* 24: 3990-4006.

111. Even-Or, O., A. Joseph, N. Itskovitz-Cooper, S. Samira, E. Rochlin, H. Eliyahu, I. Goldwaser, S. Balasingam, A. J. Mann, R. Lambkin-Williams, E. Kedar, and Y. Barenholz. 2011. A new intranasal influenza vaccine based on a novel polycationic lipid-ceramide carbamoyl-spermine (CCS). II. Studies in mice and ferrets and mechanism of adjuvanticity. *Vaccine* 29: 2474-2486.

112. Brunel, F., A. Darbouret, and J. Ronco. 1999. Cationic lipid DC-Chol induces an improved and balanced immunity able to overcome the unresponsiveness to the hepatitis B vaccine. *Vaccine* 17: 2192-2203.

113. Korsholm, K. S., E. M. Agger, C. Foged, D. Christensen, J. Dietrich, C. S. Andersen, C. Geisler, and P. Andersen. 2007. The adjuvant mechanism of cationic dimethyldioctadecylammonium liposomes. *Immunology* 121: 216-226.

114. Agger, E. M., I. Rosenkrands, J. Hansen, K. Brahimi, B. S. Vandahl, C. Aagaard, K. Werninghaus, C. Kirschning, R. Lang, D. Christensen, M. Theisen, F. Follmann, and P. Andersen. 2008. Cationic liposomes formulated with synthetic mycobacterial cordfactor (CAF01): a versatile adjuvant for vaccines with different immunological requirements. *PLoS One* 3: e3116.

115. Duerr, A., J. N. Wasserheit, and L. Corey. 2006. HIV vaccines: new frontiers in vaccine development. *Clinical infectious diseases : an official publication of the Infectious Diseases Society of America* 43: 500-511.

116. Pialoux, G., H. Hocini, S. Perusat, B. Silberman, D. Salmon-Ceron, L. Slama, V. Journot, E. Mathieu, C. Gaillard, K. Petitprez, O. Launay, G. Chene, and A. V. S. Group. 2008. Phase I study of a candidate vaccine based on recombinant HIV-1

gp160 (MN/LAI) administered by the mucosal route to HIV-seronegative volunteers: the ANRS VAC14 study. *Vaccine* 26: 2657-2666.

117. Brandt, L., M. Elhay, I. Rosenkrands, E. B. Lindblad, and P. Andersen. 2000. ESAT-6 subunit vaccination against Mycobacterium tuberculosis. *Infection and Immunity* 68: 791-795.

118. Vandepapeliere, P., Y. Horsmans, P. Moris, M. Van Mechelen, M. Janssens, M. Koutsoukos, P. Van Belle, F. Clement, E. Hanon, M. Wettendorff, N. Garcon, and G. Leroux-Roels. 2008. Vaccine adjuvant systems containing monophosphoryl lipid A and QS21 induce strong and persistent humoral and T cell responses against hepatitis B surface antigen in healthy adult volunteers. *Vaccine* 26: 1375-1386.

119. Stewart, V. A., S. M. McGrath, D. S. Walsh, S. Davis, A. S. Hess, L. A. Ware, K. E. Kester, J. F. Cummings, J. R. Burge, G. Voss, M. Delchambre, N. Garcon, D. B. Tang, J. D. Cohen, and D. G. Heppner, Jr. 2006. Pre-clinical evaluation of new adjuvant formulations to improve the immunogenicity of the malaria vaccine RTS,S/AS02A. *Vaccine* 24: 6483-6492.

120. Nordly, P., F. Rose, D. Christensen, H. M. Nielsen, P. Andersen, E. M. Agger, and C. Foged. 2011. Immunity by formulation design: Induction of high CD8(+) T-cell responses by poly(I:C) incorporated into the CAF01 adjuvant via a double emulsion method. *J Control Release* 150: 307-317.

121. Senchi, K., S. Matsunaga, H. Hasegawa, H. Kimura, and A. Ryo. 2013. Development of oligomannose-coated liposome-based nasal vaccine against human parainfluenza virus type 3. *Frontiers in microbiology* 4: 346.

122. Zaks, K., M. Jordan, A. Guth, K. Sellins, R. Kedl, A. Izzo, C. Bosio, and S. Dow. 2006. Efficient immunization and cross-priming by vaccine adjuvants containing TLR3 or TLR9 agonists complexed to cationic liposomes. *J Immunol* 176: 7335-7345.

123. Wang, C., Y. Zhuang, Y. J. Zhang, Z. C. Luo, N. N. Gao, P. Li, H. Pan, L. T. Cai, and Y. F. Ma. 2012. Toll-like receptor 3 agonist complexed with cationic liposome augments vaccine-elicited antitumor immunity by enhancing TLR3-IRF3 signaling and type I interferons in dendritic cells. *Vaccine* 30: 4790-4799.

124. Fujimura, T., S. Nakagawa, T. Ohtani, Y. Ito, and S. Aiba. 2006. Inhibitory effect of the polyinosinic-polycytidylic acid/cationic liposome on the progression of murine B16F10 melanoma. *Eur J Immunol* 36: 3371-3380.

125. Jaafari, M. R., A. Badiee, A. Khamesipour, A. Samiei, D. Soroush, M. T. Kheiri, F. Barkhordari, W. R. McMaster, and F. Mahboudi. 2007. The role of CpG ODN in

enhancement of immune response and protection in BALB/c mice immunized with recombinant major surface glycoprotein of Leishmania (rgp63) encapsulated in cationic liposome. *Vaccine* 25: 6107-6117.

126. Barnier-Quer, C., A. Elsharkawy, S. Romeijn, A. Kros, and W. Jiskoot. 2013. Adjuvant effect of cationic liposomes for subunit influenza vaccine: influence of antigen loading method, cholesterol and immune modulators. *Pharmaceutics* 5: 392-410.

127. Joseph, A., I. Louria-Hayon, A. Plis-Finarov, E. Zeira, Z. Zakay-Rones, E. Raz, T. Hayashi, K. Takabayashi, Y. Barenholz, and E. Kedar. 2002. Liposomal immunostimulatory DNA sequence (ISS-ODN): an efficient parenteral and mucosal adjuvant for influenza and hepatitis B vaccines. *Vaccine* 20: 3342-3354.

128. Klinman, D. M., D. Currie, I. Gursel, and D. Verthelyi. 2004. Use of CpG oligodeoxynucleotides as immune adjuvants. *Immunological Reviews* 199: 201-216.

129. Scheerlinck, J. P., K. J. Snibson, V. M. Bowles, and P. Sutton. 2008. Biomedical applications of sheep models: from asthma to vaccines. *Trends Biotechnol* 26: 259-266.

130. Hein, W. R., and P. J. Griebel. 2003. A road less travelled: large animal models in immunological research. *Nat Rev Immunol* 3: 79-84.

131. Cao, Y., Z. Lu, Y. Li, P. Sun, D. Li, P. Li, X. Bai, Y. Fu, H. Bao, C. Zhou, B. Xie, Y. Chen, and Z. Liu. 2013. Poly(I:C) combined with multi-epitope protein vaccine completely protects against virulent foot-and-mouth disease virus challenge in pigs. *Antiviral Res* 97: 145-153.

132. Mapletoft, J. W., M. Oumouna, H. G. Townsend, S. Gomis, L. A. Babiuk, and S. V. Littel-van Den Hurk. 2006. Formulation with CpG oligodeoxynucleotides increases cellular immunity and protection induced by vaccination of calves with formalin-inactivated bovine respiratory syncytial virus. *Virology* 353: 316-323.

133. Linghua, Z., G. Yong, T. Xingshan, and Z. Fengzhen. 2006. Co-administration of porcine-specific CpG oligodeoxynucleotide enhances the immune responses to pseudorabies attenuated virus vaccine in newborn piglets in vivo. *Developmental and comparative immunology* 30: 589-596.

134. Hein, W. R., T. Barber, S. A. Cole, L. Morrison, and A. Pernthaner. 2004. Long-term collection and characterization of afferent lymph from the ovine small intestine. *J Immunol Methods* 293: 153-168.

135. Schwartz-Cornil, I., M. Epardaud, and M. Bonneau. 2006. Cervical duct cannulation in sheep for collection of afferent lymph dendritic cells from head tissues. *Nature Protocols* 1: 874-879.

136. Schwartz-Cornil, I., M. Epardaud, J. P. Albert, C. Bourgeois, F. Gerard, I. Raoult, and M. Bonneau. 2005. Probing leukocyte traffic in lymph from oro-nasal mucosae by cervical catheterization in a sheep model. *J Immunol Methods* 305: 152-161.

137. Bujdoso, R., J. Hopkins, B. M. Dutia, P. Young, and I. McConnell. 1989. Characterization of sheep afferent lymph dendritic cells and their role in antigen carriage. *J Exp Med* 170: 1285-1301.

138. Beh, K. J., and A. K. Lascelles. 1985. The effect of adjuvants and prior immunization on the rate and mode of uptake of antigen into afferent popliteal lymph from sheep. *Immunology* 54: 487-495.

139. Hope, J. C., C. J. Howard, H. Prentice, and B. Charleston. 2006. Isolation and purification of afferent lymph dendritic cells that drain the skin of cattle. *Nat Protoc* 1: 982-987.

140. Bertho, N., F. Marquet, F. Pascale, C. Kang, M. Bonneau, and I. Schwartz-Cornil. 2011. Steady state pig dendritic cells migrating in skin draining pseudo-afferent lymph are semi-mature. *Vet Immunol Immunopathol* 144: 430-436.

141. Thielke, K. H., R. Pabst, and H. J. Rothkotter. 1999. Quantification of proliferating lymphocyte subsets appearing in the intestinal lymph and the blood. *Clin Exp Immunol* 117: 277-284.

142. Pugh, C. W., G. G. MacPherson, and H. W. Steer. 1983. Characterization of nonlymphoid cells derived from rat peripheral lymph. *J Exp Med* 157: 1758-1779.

143. Matsuno, K., S. Kudo, T. Ezaki, and K. Miyakawa. 1995. Isolation of dendritic cells in the rat liver lymph. *Transplantation* 60: 765-768.

144. Contreras, V., C. Urien, R. Guiton, Y. Alexandre, T. P. Vu Manh, T. Andrieu, K. Crozat, L. Jouneau, N. Bertho, M. Epardaud, J. Hope, A. Savina, S. Amigorena, M. Bonneau, M. Dalod, and I. Schwartz-Cornil. 2010. Existence of CD8alpha-like dendritic cells with a conserved functional specialization and a common molecular signature in distant mammalian species. *J Immunol* 185: 3313-3325.

145. Epardaud, M., M. Bonneau, F. Payot, C. Cordier, J. Megret, C. Howard, and I. Schwartz-Cornil. 2004. Enrichment for a CD26hi SIRP- subset in lymph dendritic cells from the upper aero-digestive tract. *J Leukoc Biol* 76: 553-561.

146.	Howard, C. J., P. Sopp, J. Brownlie, L. S. Kwong, K. R. Parsons, and G. Taylor. 1997. Identification of two distinct populations of dendritic cells in afferent lymph that vary in their ability to stimulate T cells. *J Immunol* 159: 5372-5382.

147.	Hope, J. C., E. Guzman, C. Cubillos-Zapata, S. A. Stephens, S. C. Gilbert, H. Prentice, P. Sopp, C. J. Howard, and B. Charleston. 2012. Migratory sub-populations of afferent lymphatic dendritic cells differ in their interactions with Mycobacterium bovis Bacille Calmette Guerin. *Vaccine* 30: 2357-2367.

148.	Gliddon, D. R., J. C. Hope, G. P. Brooke, and C. J. Howard. 2004. DEC-205 expression on migrating dendritic cells in afferent lymph. *Immunology* 111: 262-272.

149.	Marquet, F., M. Bonneau, F. Pascale, C. Urien, C. Kang, I. Schwartz-Cornil, and N. Bertho. 2011. Characterization of dendritic cells subpopulations in skin and afferent lymph in the swine model. *PLoS One* 6: e16320.

150.	Bimczok, D., E. N. Sowa, H. Faber-Zuschratter, R. Pabst, and H. J. Rothkotter. 2005. Site-specific expression of CD11b and SIRPalpha (CD172a) on dendritic cells: implications for their migration patterns in the gut immune system. *Eur J Immunol* 35: 1418-1427.

151.	Yrlid, U., V. Cerovic, S. Milling, C. D. Jenkins, L. S. Klavinskis, and G. G. MacPherson. 2006. A distinct subset of intestinal dendritic cells responds selectively to oral TLR7/8 stimulation. *Eur J Immunol* 36: 2639-2648.

152.	Liu, L., M. Zhang, C. Jenkins, and G. G. MacPherson. 1998. Dendritic cell heterogeneity in vivo: two functionally different dendritic cell populations in rat intestinal lymph can be distinguished by CD4 expression. *J Immunol* 161: 1146-1155.

153.	Hope, J. C., P. Sopp, R. A. Collins, and C. J. Howard. 2001. Differences in the induction of CD8(+) T cell responses by subpopulations of dendritic cells from afferent lymph are related to IL-1 alpha secretion. *J Leukocyte Biol* 69: 271-279.

154.	Stephens, S. A., J. Brownlie, B. Charleston, and C. J. Howard. 2003. Differences in cytokine synthesis by the sub-populations of dendritic cells from afferent lymph. *Immunology* 110: 48-57.

155.	Milling, S., U. Yrlid, V. Cerovic, and G. MacPherson. 2010. Subsets of migrating intestinal dendritic cells. *Immunological Reviews* 234: 259-267.

156.	Milling, S. W. F., C. D. Jenkins, U. Yrlid, V. Cerovic, H. Edmond, V. McDonald, M. Nassar, and G. MacPherson. 2009. Steady-state migrating intestinal dendritic cells induce potent inflammatory responses in naive CD4(+) T cells. *Mucosal Immunol* 2: 156-165.

157.   Crozat, K., R. Guiton, V. Contreras, V. Feuillet, C. A. Dutertre, E. Ventre, T. P. V. Manh, T. Baranek, A. K. Storset, J. Marvel, P. Boudinot, A. Hosmalin, I. Schwartz-Cornil, and M. Dalod. 2010. The XC chemokine receptor 1 is a conserved selective marker of mammalian cells homologous to mouse CD8 alpha(+) dendritic cells. *Journal of Experimental Medicine* 207: 1283-1292.

158.   Carter, R. W., C. Thompson, D. M. Reid, S. Y. Wong, and D. F. Tough. 2006. Preferential induction of CD4+ T cell responses through in vivo targeting of antigen to dendritic cell-associated C-type lectin-1. *J Immunol* 177: 2276-2284.

159.   Segura, E., and J. A. Villadangos. 2009. Antigen presentation by dendritic cells in vivo. *Curr Opin Immunol* 21: 105-110.

160.   Crozat, K., R. Guiton, M. Guilliams, S. Henri, T. Baranek, I. Schwartz-Cornil, B. Malissen, and M. Dalod. 2010. Comparative genomics as a tool to reveal functional equivalences between human and mouse dendritic cell subsets. *Immunol Rev* 234: 177-198.

161.   de Veer, M., J. Kemp, J. Chatelier, M. J. Elhay, and E. N. Meeusen. 2010. The kinetics of soluble and particulate antigen trafficking in the afferent lymph, and its modulation by aluminum-based adjuvant. *Vaccine* 28: 6597-6602.

162.   de Veer, M., J. Kemp, J. Chatelier, M. J. Elhay, and E. N. Meeusen. 2012. Modulation of soluble and particulate antigen transport in afferent lymph by monophosphoryl lipid A. *Immunol Cell Biol* 90: 404-410.

163.   Bonneau, M., M. Epardaud, F. Payot, V. Niborski, M. I. Thoulouze, F. Bernex, B. Charley, S. Riffault, L. A. Guilloteau, and I. Schwartz-Cornil. 2006. Migratory monocytes and granulocytes are major lymphatic carriers of Salmonella from tissue to draining lymph node. *J Leukoc Biol* 79: 268-276.

164.   Egan, P. J., W. Kimpton, H. F. Seow, V. M. Bowles, M. R. Brandon, and A. D. Nash. 1996. Inflammation-induced changes in the phenotype and cytokine profile of cells migrating through skin and afferent lymph. *Immunology* 89: 539-546.

165.   Mackay, C. R., W. L. Marston, and L. Dudler. 1990. Naive and Memory T-Cells Show Distinct Pathways of Lymphocyte Recirculation. *Journal of Experimental Medicine* 171: 801-817.

166.   Haig, D. M., G. Hutchinson, J. Thomson, D. Yirrell, and H. W. Reid. 1996. Cytolytic activity and associated serine protease expression by skin and afferent lymph CD8+ T cells during orf virus reinfection. *J Gen Virol* 77 (Pt 5): 953-961.

167. Rothkotter, H. J., T. Huber, N. N. Barman, and R. Pabst. 1993. Lymphoid-Cells in Afferent and Efferent Intestinal Lymph - Lymphocyte Subpopulations and Cell-Migration. *Clin Exp Immunol* 92: 317-322.

168. Van Rhijn, I., V. P. Rutten, B. Charleston, M. Smits, W. van Eden, and A. P. Koets. 2007. Massive, sustained gammadelta T cell migration from the bovine skin in vivo. *J Leukoc Biol* 81: 968-973.

169. Vrieling, M., W. Santema, I. Van Rhijn, V. Rutten, and A. Koets. 2012. gammadelta T cell homing to skin and migration to skin-draining lymph nodes is CCR7 independent. *J Immunol* 188: 578-584.

170. Geherin, S. A., S. R. Fintushel, M. H. Lee, R. P. Wilson, R. T. Patel, C. Alt, A. J. Young, J. B. Hay, and G. F. Debes. 2012. The Skin, a Novel Niche for Recirculating B Cells. *Journal of Immunology* 188: 6027-6035.

171. Haig, D. M., J. Hopkins, and H. R. Miller. 1999. Local immune responses in afferent and efferent lymph. *Immunology* 96: 155-163.

172. Halliday, A. M., W. I. Morrison, and W. D. Smith. 2009. Kinetics of the local cellular response in the gastric lymph of immune and susceptible sheep to infection with Teladorsagia circumcincta. *Parasite Immunol* 31: 402-411.

173. Halliday, A. M., C. M. Routledge, S. K. Smith, J. B. Matthews, and W. D. Smith. 2007. Parasite loss and inhibited development of Teladorsagia circumcincta in relation to the kinetics of the local IgA response in sheep. *Parasite Immunol* 29: 425-434.

174. Wee, J. L., D. L. Greenwood, X. Han, and J. P. Scheerlinck. 2011. Inflammatory cytokines IL-6 and TNF-alpha regulate lymphocyte trafficking through the local lymph node. *Vet Immunol Immunopathol* 144: 95-103.

175. Cahill, R. N., H. Frost, and Z. Trnka. 1976. The effects of antigen on the migration of recirculating lymphocytes through single lymph nodes. *J Exp Med* 143: 870-888.

176. Windon, R. G., P. J. Chaplin, L. Beezum, A. Coulter, R. Cahill, W. Kimpton, D. Drane, M. Pearse, A. Sjolander, J. M. Tennent, and J. Y. Scheerlinck. 2000. Induction of lymphocyte recruitment in the absence of a detectable immune response. *Vaccine* 19: 572-578.

177. Seabrook, T. J., P. J. Borron, L. Dudler, J. B. Hay, and A. J. Young. 2005. A novel mechanism of immune regulation: interferon-gamma regulates retention of CD4 T cells during delayed type hypersensitivity. *Immunology* 116: 184-192.

178. Gamvrellis, A., K. Walsh, L. Tatarczuch, P. Smooker, M. Plebanski, and J. P. Scheerlinck. 2013. Phenotypic analysis of ovine antigen presenting cells loaded with nanoparticles migrating from the site of vaccination. *Methods* 60: 257-263.

179. Vasilakos, J. P., R. M. Smith, S. J. Gibson, J. M. Lindh, L. K. Pederson, M. J. Reiter, M. H. Smith, and M. A. Tomai. 2000. Adjuvant activities of immune response modifier R-848: comparison with CpG ODN. *Cell Immunol* 204: 64-74.

180. Yrlid, U., S. W. Milling, J. L. Miller, S. Cartland, C. D. Jenkins, and G. G. MacPherson. 2006. Regulation of intestinal dendritic cell migration and activation by plasmacytoid dendritic cells, TNF-alpha and type 1 IFNs after feeding a TLR7/8 ligand. *J Immunol* 176: 5205-5212.

181. Moingeon, P., C. de Taisne, and J. Almond. 2002. Delivery technologies for human vaccines. *Br Med Bull* 62: 29-44.

182. Cubillos-Zapata, C., E. Guzman, A. Turner, S. C. Gilbert, H. Prentice, J. C. Hope, and B. Charleston. 2011. Differential effects of viral vectors on migratory afferent lymph dendritic cells in vitro predict enhanced immunogenicity in vivo. *J Virol* 85: 9385-9394.

183. Nichani, A. K., J. D. M. Campbell, E. J. Glass, S. P. Graham, S. C. Craigmile, C. G. D. Brown, and R. L. Spooner. 2003. Characterization of efferent lymph cells and their function following immunization of cattle with an allogenic Theileria annulata infected cell line. *Vet Immunol Immunop* 93: 39-49.

184. Vrieling, M., W. Santema, M. Vordermeier, V. Rutten, and A. Koets. 2013. Hsp70 vaccination-induced primary immune responses in efferent lymph of the draining lymph node. *Vaccine* 31: 4720-4727.

185. Uwiera, R. R., V. Gerdts, R. A. Pontarollo, L. A. Babiuk, D. M. Middleton, and P. J. Griebel. 2001. Plasmid DNA induces increased lymphocyte trafficking: a specific role for CpG motifs. *Cell Immunol* 214: 155-164.

186. Windon, R. G., P. J. Chaplin, P. McWaters, M. Tavarnesi, M. Tzatzaris, W. G. Kimpton, R. N. Cahill, L. Beezum, A. Coulter, D. Drane, A. Sjolander, M. Pearse, J. P. Scheerlinck, and J. M. Tennent. 2001. Local immune responses to influenza antigen are synergistically enhanced by the adjuvant ISCOMATRIX. *Vaccine* 20: 490-497.

187. Rothel, J. S., L. A. Corner, M. W. Lightowlers, H. F. Seow, P. McWaters, G. Entrican, and P. R. Wood. 1998. Antibody and cytokine responses in efferent lymph following vaccination with different adjuvants. *Vet Immunol Immunop* 63: 167-183.

188. Emery, D. L., J. S. Rothel, and P. R. Wood. 1990. Influence of Antigens and Adjuvants on the Production of Gamma-Interferon and Antibody by Ovine Lymphocytes. *Immunology and Cell Biology* 68: 127-136.

189. Mooney, M., S. McWeeney, G. Canderan, and R. P. Sekaly. 2013. A systems framework for vaccine design. *Curr Opin Immunol* 25: 551-555.

190. Li, S., H. I. Nakaya, D. A. Kazmin, J. Z. Oh, and B. Pulendran. 2013. Systems biological approaches to measure and understand vaccine immunity in humans. *Semin Immunol* 25: 209-218.

191. Querec, T. D., R. S. Akondy, E. K. Lee, W. Cao, H. I. Nakaya, D. Teuwen, A. Pirani, K. Gernert, J. Deng, B. Marzolf, K. Kennedy, H. Wu, S. Bennouna, H. Oluoch, J. Miller, R. Z. Vencio, M. Mulligan, A. Aderem, R. Ahmed, and B. Pulendran. 2009. Systems biology approach predicts immunogenicity of the yellow fever vaccine in humans. *Nat Immunol* 10: 116-125.

192. Gaucher, D., R. Therrien, N. Kettaf, B. R. Angermann, G. Boucher, A. Filali-Mouhim, J. M. Moser, R. S. Mehta, D. R. Drake, 3rd, E. Castro, R. Akondy, A. Rinfret, B. Yassine-Diab, E. A. Said, Y. Chouikh, M. J. Cameron, R. Clum, D. Kelvin, R. Somogyi, L. D. Greller, R. S. Balderas, P. Wilkinson, G. Pantaleo, J. Tartaglia, E. K. Haddad, and R. P. Sekaly. 2008. Yellow fever vaccine induces integrated multilineage and polyfunctional immune responses. *J Exp Med* 205: 3119-3131.

193. Nakaya, H. I., J. Wrammert, E. K. Lee, L. Racioppi, S. Marie-Kunze, W. N. Haining, A. R. Means, S. P. Kasturi, N. Khan, G. M. Li, M. McCausland, V. Kanchan, K. E. Kokko, S. Li, R. Elbein, A. K. Mehta, A. Aderem, K. Subbarao, R. Ahmed, and B. Pulendran. 2011. Systems biology of vaccination for seasonal influenza in humans. *Nat Immunol* 12: 786-795.

194. Burke, M. L., M. D. Veer, J. Pleasance, M. Neeland, M. Elhay, P. Harrison, and E. Meeusen. 2013. Innate immune pathways in afferent lymph following vaccination with poly(I:C)-containing liposomes. *Innate immunity*.

195. de Veer, M., M. Neeland, M. Burke, J. Pleasance, J. Nathanielsz, M. Elhay, and E. Meeusen. 2013. Cell recruitment and antigen trafficking in afferent lymph after injection of antigen and poly(I:C) containing liposomes, in aqueous or oil-based formulations. *Vaccine* 31: 1012-1018.

196. Neeland, M. R., M. J. Elhay, J. Nathanielsz, E. N. Meeusen, and M. J. de Veer. 2014. Incorporation of CpG into a Liposomal Vaccine Formulation Increases the Maturation

of Antigen-Loaded Dendritic Cells and Monocytes To Improve Local and Systemic Immunity. *J Immunol* 192: 3666-3675.

197.   Hall, J. G. 1967. A method for collecting lymph from the prefemoral lymph node of unanaesthetised sheep. *Quarterly journal of experimental physiology and cognate medical sciences* 52: 200-205.

198.   Ishii, K. J., and S. Akira. 2007. Toll or toll-free adjuvant path toward the optimal vaccine development. *J Clin Immunol* 27: 363-371.

199.   Lonez, C., M. Vandenbranden, and J. M. Ruysschaert. 2008. Cationic liposomal lipids: From gene carriers to cell signaling. *Prog Lipid Res* 47: 340-347.

200.   Ma, Y. F., Y. Zhuang, X. F. Xie, C. Wang, F. Wang, D. M. Zhou, J. Q. Zeng, and L. T. Cai. 2011. The role of surface charge density in cationic liposome-promoted dendritic cell maturation and vaccine-induced immune responses. *Nanoscale* 3: 2307-2314.

201.   Zhang, Y. M., M. Rusckowski, N. Liu, C. Liu, and D. J. Hnatowich. 2001. Cationic liposomes enhance cellular/nuclear localization of 99mTc-antisense oligonucleotides in target tumor cells. *Cancer Biother Radiopharm* 16: 411-419.

202.   De Oliveira, M. C., V. Boutet, E. Fattal, D. Boquet, J. M. Grognet, P. Couvreur, and J. R. Deverre. 2000. Improvement of in vivo stability of phosphodiester oligonucleotide using anionic liposomes in mice. *Life Sci* 67: 1625-1637.

203.   Shargh, V. H., M. R. Jaafari, A. Khamesipour, I. Jaafari, S. A. Jalali, A. Abbasi, and A. Badiee. 2012. Liposomal SLA co-incorporated with PO CpG ODNs or PS CpG ODNs induce the same protection against the murine model of leishmaniasis. *Vaccine* 30: 3957-3964.

204.   Neeland, M. R., E. N. Meeusen, and M. J. de Veer. 2014. Afferent lymphatic cannulation as a model system to study innate immune responses to infection and vaccination. *Vet Immunol Immunopathol* 158: 86-97.

205.   Knuehl, C., A. Seelig, B. Brecht, P. Henklein, and P. M. Kloetzel. 1996. Functional analysis of eukaryotic 20S proteasome nuclear localization signal. *Experimental cell research* 225: 67-74.

206.   Fossum, C., B. Hjertner, V. Ahlberg, W. Charerntantanakul, K. McIntosh, L. Fuxler, N. Balagunaseelan, P. Wallgren, and K. Lovgren Bengtsson. 2013. Early inflammatory response to the saponin adjuvant Matrix-M in the pig. *Vet Immunol Immunopathol*.

207. Nalubamba, K. S., A. G. Gossner, R. G. Dalziel, and J. Hopkins. 2007. Differential expression of pattern recognition receptors in sheep tissues and leukocyte subsets. *Vet Immunol Immunopathol* 118: 252-262.

208. de Veer, M. J., M. Holko, M. Frevel, E. Walker, S. Der, J. M. Paranjape, R. H. Silverman, and B. R. Williams. 2001. Functional classification of interferon-stimulated genes identified using microarrays. *J Leukoc Biol* 69: 912-920.

209. Joseph, A., I. Louria-Hayon, A. Plis-Finarov, E. Zeira, Z. Zakay-Rones, E. Raz, T. Hayashi, K. Takabayashi, Y. Barenholz, and E. Kedar. 2002. Liposomal immunostimulatory DNA sequence (ISS-ODN): an efficient parenteral and mucosal adjuvant for influenza and hepatitis B vaccines. *Vaccine* 20: 3342-3354.

210. Bode, C., G. Zhao, F. Steinhagen, T. Kinjo, and D. M. Klinman. 2011. CpG DNA as a vaccine adjuvant. *Expert Rev Vaccines* 10: 499-511.

211. Davis, H. L., R. Weeranta, T. J. Waldschmidt, L. Tygrett, J. Schorr, and A. M. Krieg. 1998. CpG DNA is a potent enhancer of specific immunity in mice immunized with recombinant hepatitis B surface antigen. *Journal of Immunology* 160: 870-876.

212. Lipford, G. B., M. Bauer, C. Blank, R. Reiter, H. Wagner, and K. Heeg. 1997. CpG-containing synthetic oligonucleotides promote B and cytotoxic T cell responses to protein antigen: a new class of vaccine adjuvants. *European Journal of Immunology* 27: 2340-2344.

213. Chu, R. S., O. S. Targoni, A. M. Krieg, P. V. Lehmann, and C. V. Harding. 1997. CpG oligodeoxynucleotides act as adjuvants that switch on T helper 1 (Th1) immunity. *Journal of Experimental Medicine* 186: 1623-1631.

214. Zhang, L. H., X. S. Tian, and F. Z. Zhou. 2008. In vivo oral administration effects of various oligodeoxynucleotides containing synthetic immunostimulatory motifs in the immune response to pseudorabies attenuated virus vaccine in newborn piglets. *Vaccine* 26: 224-233.

215. Gursel, I., M. Gursel, K. J. Ishii, and D. M. Klinman. 2001. Sterically stabilized cationic liposomes improve the uptake and immunostimulatory activity of CpG oligonucleotides. *Journal of Immunology* 167: 3324-3328.

216. Neeland, M. R., E. N. Meeusen, and M. J. de Veer. 2013. Afferent lymphatic cannulation as a model system to study innate immune responses to infection and vaccination. *Vet Immunol Immunopathol*.

217. Jiang, Z. H., and R. R. Koganty. 2003. Synthetic vaccines: the role of adjuvants in immune targeting. *Curr Med Chem* 10: 1423-1439.

218. Yang, G. X., Z. X. Lian, K. Kikuchi, Y. J. Liu, A. A. Ansari, S. Ikehara, and M. E. Gershwin. 2005. CD4- plasmacytoid dendritic cells (pDCs) migrate in lymph nodes by CpG inoculation and represent a potent functional subset of pDCs. *J Immunol* 174: 3197-3203.

219. Sparwasser, T., E. S. Koch, R. M. Vabulas, K. Heeg, G. B. Lipford, J. W. Ellwart, and H. Wagner. 1998. Bacterial DNA and immunostimulatory CpG oligonucleotides trigger maturation and activation of murine dendritic cells. *Eur J Immunol* 28: 2045-2054.

220. Carrasco, C. P., R. C. Rigden, I. E. Vincent, C. Balmelli, M. Ceppi, O. Bauhofer, V. Tache, B. Hjertner, F. McNeilly, H. G. van Gennip, K. C. McCullough, and A. Summerfield. 2004. Interaction of classical swine fever virus with dendritic cells. *J Gen Virol* 85: 1633-1641.

221. Behboudi, S., D. Chao, P. Klenerman, and J. Austyn. 2000. The effects of DNA containing CpG motif on dendritic cells. *Immunology* 99: 361-366.

222. Hackstein, H., A. Knoche, A. Nockher, J. Poeling, T. Kubin, M. Jurk, J. Vollmer, and G. Bein. 2011. The TLR7/8 ligand resiquimod targets monocyte-derived dendritic cell differentiation via TLR8 and augments functional dendritic cell generation. *Cell Immunol* 271: 401-412.

223. Gursel, M., D. Verthelyi, and D. M. Klinman. 2002. CpG oligodeoxynucleotides induce human monocytes to mature into functional dendritic cells. *Eur J Immunol* 32: 2617-2622.

224. Ziegler-Heitbrock, L., P. Ancuta, S. Crowe, M. Dalod, V. Grau, D. N. Hart, P. J. Leenen, Y. J. Liu, G. MacPherson, G. J. Randolph, J. Scherberich, J. Schmitz, K. Shortman, S. Sozzani, H. Strobl, M. Zembala, J. M. Austyn, and M. B. Lutz. 2010. Nomenclature of monocytes and dendritic cells in blood. *Blood* 116: e74-80.

225. Bedoui, S., P. G. Whitney, J. Waithman, L. Eidsmo, L. Wakim, I. Caminschi, R. S. Allan, M. Wojtasiak, K. Shortman, F. R. Carbone, A. G. Brooks, and W. R. Heath. 2009. Cross-presentation of viral and self antigens by skin-derived CD103+ dendritic cells. *Nat Immunol* 10: 488-495.

226. Cobb, D., S. Guo, and R. B. Smeltz. 2013. CpG and interleukin-15 synergize to enhance IFN-gamma production by activated CD8+ T cells. *BioMed research international* 2013: 924023.

227. Zhao, K., H. Wang, and C. Y. Wu. 2011. The immune responses of HLA-A*0201 restricted SARS-CoV S peptide-specific CD8(+) T cells are augmented in varying degrees by CpG ODN, PolyI:C and R848. *Vaccine* 29: 6670-6678.

228. Andrews, C. D., M. S. Huh, K. Patton, D. Higgins, G. Van Nest, G. Ott, and K. D. Lee. 2012. Encapsulating immunostimulatory CpG oligonucleotides in listeriolysin O-liposomes promotes a Th1-type response and CTL activity. *Mol Pharm* 9: 1118-1125.

229. Ferrick, D. A., M. D. Schrenzel, T. Mulvania, B. Hsieh, W. G. Ferlin, and H. Lepper. 1995. Differential Production of Interferon-Gamma and Interleukin-4 in Response to Th1-Stimulating and Th2-Stimulating Pathogens by Gamma-Delta T-Cells in-Vivo. *Nature* 373: 255-257.

230. Pinheiro, M. B., L. R. Antonelli, R. Sathler-Avelar, D. M. Vitelli-Avelar, S. Spindola-de-Miranda, T. M. P. D. Guimaraes, A. Teixeira-Carvalho, O. A. Martins, and V. P. C. P. Toledo. 2012. CD4-CD8-alpha beta and gamma delta T Cells Display Inflammatory and Regulatory Potentials during Human Tuberculosis. *Plos One* 7.

231. Young, A. J., T. J. Seabrook, W. L. Marston, L. Dudler, and J. B. Hay. 2000. A role for lymphatic endothelium in the sequestration of recirculating gamma delta T cells in TNF-alpha-stimulated lymph nodes. *Eur J Immunol* 30: 327-334.

232. Kamath, A. T., B. Mastelic, D. Christensen, A. F. Rochat, E. M. Agger, D. D. Pinschewer, P. Andersen, P. H. Lambert, and C. A. Siegrist. 2012. Synchronization of Dendritic Cell Activation and Antigen Exposure Is Required for the Induction of Th1/Th17 Responses. *Journal of Immunology* 188: 4828-4837.

233. Dobin, A., C. A. Davis, F. Schlesinger, J. Drenkow, C. Zaleski, S. Jha, P. Batut, M. Chaisson, and T. R. Gingeras. 2013. STAR: ultrafast universal RNA-seq aligner. *Bioinformatics* 29: 15-21.

234. DeLuca, D. S., J. Z. Levin, A. Sivachenko, T. Fennell, M. D. Nazaire, C. Williams, M. Reich, W. Winckler, and G. Getz. 2012. RNA-SeQC: RNA-seq metrics for quality control and process optimization. *Bioinformatics* 28: 1530-1532.

235. Anders S, P. P., Huber W. 2014. HTSeq — A Python framework to work with high-throughput sequencing data, . 1-5.

236. McCarthy, D. J., Y. Chen, and G. K. Smyth. 2012. Differential expression analysis of multifactor RNA-Seq experiments with respect to biological variation. *Nucleic acids research* 40: 4288-4297.

237. Robinson, M. D., and A. Oshlack. 2010. A scaling normalization method for differential expression analysis of RNA-seq data. *Genome biology* 11: R25.

238. Griffith, M., O. L. Griffith, J. Mwenifumbo, R. Goya, A. S. Morrissy, R. D. Morin, R. Corbett, M. J. Tang, Y. C. Hou, T. J. Pugh, G. Robertson, S. Chittaranjan, A. Ally, J. K. Asano, S. Y. Chan, H. I. Li, H. McDonald, K. Teague, Y. Zhao, T. Zeng, A. Delaney, M. Hirst, G. B. Morin, S. J. Jones, I. T. Tai, and M. A. Marra. 2010. Alternative expression analysis by RNA sequencing. *Nature methods* 7: 843-847.

239. Yanai, H., D. Savitsky, T. Tamura, and T. Taniguchi. 2009. Regulation of the cytosolic DNA-sensing system in innate immunity: a current view. *Curr Opin Immunol* 21: 17-22.

240. Kim, W. K., H. R. Hwang, H. Kim do, P. Y. Lee, Y. J. In, H. Y. Ryu, S. G. Park, K. H. Bae, and S. C. Lee. 2008. Glycoproteomic analysis of plasma from patients with atopic dermatitis: CD5L and ApoE as potential biomarkers. *Experimental & molecular medicine* 40: 677-685.

241. Lattin, J. E., K. Schroder, A. I. Su, J. R. Walker, J. Zhang, T. Wiltshire, K. Saijo, C. K. Glass, D. A. Hume, S. Kellie, and M. J. Sweet. 2008. Expression analysis of G Protein-Coupled Receptors in mouse macrophages. *Immunome research* 4: 5.

242. Schoggins, J. W., S. J. Wilson, M. Panis, M. Y. Murphy, C. T. Jones, P. Bieniasz, and C. M. Rice. 2011. A diverse range of gene products are effectors of the type I interferon antiviral response. *Nature* 472: 481-U545.

243. Zhou, A., J. M. Paranjape, S. D. Der, B. R. Williams, and R. H. Silverman. 1999. Interferon action in triply deficient mice reveals the existence of alternative antiviral pathways. *Virology* 258: 435-440.

244. Schoggins, J. W., and C. M. Rice. 2011. Interferon-stimulated genes and their antiviral effector functions. *Curr Opin Virol* 1: 519-525.

245. Cheon, H., E. G. Holvey-Bates, J. W. Schoggins, S. Forster, P. Hertzog, N. Imanaka, C. M. Rice, M. W. Jackson, D. J. Junk, and G. R. Stark. 2013. IFN beta-dependent increases in STAT1, STAT2, and IRF9 mediate resistance to viruses and DNA damage. *Embo J* 32: 2751-2763.

246. Steinhagen, F., C. Meyer, D. Tross, M. Gursel, T. Maeda, S. Klaschik, and D. M. Klinman. 2012. Activation of type I interferon-dependent genes characterizes the "core response" induced by CpG DNA. *J Leukoc Biol* 92: 775-785.

247. Tross, D., L. Petrenko, S. Klaschik, Q. Zhu, and D. M. Klinman. 2009. Global changes in gene expression and synergistic interactions induced by TLR9 and TLR3. *Molecular immunology* 46: 2557-2564.

248. Nichani, A. K., R. S. Kaushik, A. Mena, Y. Popowych, D. Dent, H. G. Townsend, G. Mutwiri, R. Hecker, L. A. Babiuk, and P. J. Griebel. 2004. CpG oligodeoxynucleotide induction of antiviral effector molecules in sheep. *Cell Immunol* 227: 24-37.

249. Bernasconi, N. L., N. Onai, and A. Lanzavecchia. 2003. A role for Toll-like receptors in acquired immunity: up-regulation of TLR9 by BCR triggering in naive B cells and constitutive expression in memory B cells. *Blood* 101: 4500-4504.

250. Vivier, E., D. H. Raulet, A. Moretta, M. A. Caligiuri, L. Zitvogel, L. L. Lanier, W. M. Yokoyama, and S. Ugolini. 2011. Innate or adaptive immunity? The example of natural killer cells. *Science* 331: 44-49.

251. Souza-Fonseca-Guimaraes, F., M. Parlato, R. B. de Oliveira, D. Golenbock, K. Fitzgerald, I. N. Shalova, S. K. Biswas, J. M. Cavaillon, and M. Adib-Conquy. 2013. Interferon-gamma and granulocyte/monocyte colony-stimulating factor production by natural killer cells involves different signaling pathways and the adaptor stimulator of interferon genes (STING). *J Biol Chem* 288: 10715-10721.

252. Booth, J. S., A. K. Nichani, P. Benjamin, A. Dar, A. M. Krieg, L. A. Babiuk, and G. K. Mutwiri. 2007. Innate immune responses induced by classes of CpG oligodeoxynucleotides in ovine lymph node and blood mononuclear cells. *Vet Immunol Immunopathol* 115: 24-34.

253. Lund, H., P. Boysen, J. C. Hope, S. K. Sjurseth, and A. K. Storset. 2013. Natural Killer Cells in Afferent Lymph Express an Activated Phenotype and Readily Produce IFN-gamma. *Frontiers in immunology* 4: 395.

254. Barber, G. N. 2011. Cytoplasmic DNA innate immune pathways. *Immunol Rev* 243: 99-108.

255. Klaschik, S., D. Tross, and D. M. Klinman. 2009. Inductive and suppressive networks regulate TLR9-dependent gene expression in vivo. *J Leukoc Biol* 85: 788-795.

256. Xu, Y., M. Johansson, and A. Karlsson. 2008. Human UMP-CMP kinase 2, a novel nucleoside monophosphate kinase localized in mitochondria. *J Biol Chem* 283: 1563-1571.

257. Xiao, H., L. Shan, H. Zhu, and F. Xue. 2012. Detection of significant pathways in osteoporosis based on graph clustering. *Molecular medicine reports* 6: 1325-1332.

258. York. 2007. A macrophage marker, Siglec-1, is increased on circulating monocytes in patients with systemic sclerosis and induced by type I Interferons and Toll-like receptor agonists (vol 56, pg 1010, 2007). *Arthritis and Rheumatism* 56: 1675-1675.

259.	Jin, P., T. H. Han, J. Q. Ren, S. Saunders, E. Wang, F. M. Marincola, and D. F. Stroncek. 2010. Molecular signatures of maturing dendritic cells: implications for testing the quality of dendritic cell therapies. *J Transl Med* 8.

260.	Kloetzel, P. M. 2004. The proteasome and MHC class I antigen processing. *Biochim Biophys Acta* 1695: 225-233.

261.	Yang, C. Y., J. B. Chen, T. F. Tsai, Y. C. Tsai, C. Y. Tsai, P. H. Liang, T. L. Hsu, C. Y. Wu, M. G. Netea, C. H. Wong, and S. L. Hsieh. 2013. CLEC4F Is an Inducible C-Type Lectin in F4/80-Positive Cells and Is Involved in Alpha-Galactosylceramide Presentation in Liver. *Plos One* 8.

262.	Mortezai, N., H. N. Behnken, A. K. Kurze, P. Ludewig, F. Buck, B. Meyer, and C. Wagener. 2013. Tumor-associated Neu5Ac-Tn and Neu5Gc-Tn antigens bind to C-type lectin CLEC10A (CD301, MGL). *Glycobiology* 23: 844-852.

263.	Weaver, L. K., and E. M. Behrens. 2014. A158: CpG-Induced Macrophage Activation Syndrome Develops Through an Organism Level Resistance to Toll-like Receptor 9 Tolerance. *Arthritis & rheumatology* 66 Suppl 11: S204.

264.	Behrens, E. M., S. W. Canna, K. Slade, S. Rao, P. A. Kreiger, M. Paessler, T. Kambayashi, and G. A. Koretzky. 2011. Repeated TLR9 stimulation results in macrophage activation syndrome-like disease in mice. *The Journal of clinical investigation* 121: 2264-2277.

265.	Gross, O., C. J. Thomas, G. Guarda, and J. Tschopp. 2011. The inflammasome: an integrated view. *Immunol Rev* 243: 136-151.

266.	Cohn, L., and L. Delamarre. 2014. Dendritic cell-targeted vaccines. *Frontiers in immunology* 5: 255.

267.	Chen, L., and D. B. Flies. 2013. Molecular mechanisms of T cell co-stimulation and co-inhibition. *Nat Rev Immunol* 13: 227-242.

268.	Miller, M. J., A. S. Hejazi, S. H. Wei, M. D. Cahalan, and I. Parker. 2004. T cell repertoire scanning is promoted by dynamic dendritic cell behavior and random T cell motility in the lymph node. *P Natl Acad Sci USA* 101: 998-1003.

269.	Mirsky, H. P., M. J. Miller, J. J. Linderman, and D. E. Kirschner. 2011. Systems biology approaches for understanding cellular mechanisms of immunity in lymph nodes during infection. *Journal of theoretical biology* 287: 160-170.

270.	Bousso, P., and E. Robey. 2003. Dynamics of CD8+ T cell priming by dendritic cells in intact lymph nodes. *Nat Immunol* 4: 579-585.

271. Mempel, T. R., S. E. Henrickson, and U. H. Von Andrian. 2004. T-cell priming by dendritic cells in lymph nodes occurs in three distinct phases. *Nature* 427: 154-159.

272. Thomas, N., L. Matejovicova, W. Srikusalanukul, J. Shawe-Taylor, and B. Chain. 2012. Directional Migration of Recirculating Lymphocytes through Lymph Nodes via Random Walks. *Plos One* 7.

273. Sprent, J., and A. Basten. 1973. Circulating T and B lymphocytes of the mouse. II. Lifespan. *Cell Immunol* 7: 40-59.

274. Miller, M. J., S. H. Wei, M. D. Cahalan, and I. Parker. 2003. Autonomous T cell trafficking examined in vivo with intravital two-photon microscopy. *Proc Natl Acad Sci U S A* 100: 2604-2609.

275. Gretz, J. E., A. O. Anderson, and S. Shaw. 1997. Cords, channels, corridors and conduits: critical architectural elements facilitating cell interactions in the lymph node cortex. *Immunol Rev* 156: 11-24.

276. Preston, S. P., S. L. Waters, O. E. Jensen, P. R. Heaton, and D. I. Pritchard. 2006. T-cell motility in the early stages of the immune response modeled as a random walk amongst targets. *Physical review. E, Statistical, nonlinear, and soft matter physics* 74: 011910.

277. Zheng, H., B. Jin, S. E. Henrickson, A. S. Perelson, U. H. von Andrian, and A. K. Chakraborty. 2008. How antigen quantity and quality determine T-cell decisions in lymphoid tissue. *Mol Cell Biol* 28: 4040-4051.

278. Beauchemin, C., N. M. Dixit, and A. S. Perelson. 2007. Characterizing T cell movement within lymph nodes in the absence of antigen. *J Immunol* 178: 5505-5512.

279. Chandrasekhar, S. 1943. Stochastic problems in physics and astronomy. *Rev Mod Phys* 15: 0001-0089.

280. Neeland, M. R., M. J. Elhay, E. N. Meeusen, and M. J. de Veer. 2014. Vaccination with liposomal poly(I:C) induces discordant maturation of migratory dendritic cell subsets and anti-viral gene signatures in afferent lymph cells. *Vaccine*.

281. Banchereau, J., F. Briere, C. Caux, J. Davoust, S. Lebecque, Y. J. Liu, B. Pulendran, and K. Palucka. 2000. Immunobiology of dendritic cells. *Annu Rev Immunol* 18: 767-811.

282. Linderman, J. J., T. Riggs, M. Pande, M. Miller, S. Marino, and D. E. Kirschner. 2010. Characterizing the dynamics of CD4+ T cell priming within a lymph node. *J Immunol* 184: 2873-2885.

283. Marino, S., S. Pawar, C. L. Fuller, T. A. Reinhart, J. L. Flynn, and D. E. Kirschner. 2004. Dendritic cell trafficking and antigen presentation in the human immune response to Mycobacterium tuberculosis. *Journal of Immunology* 173: 494-506.

284. Myers, A. J., S. Marino, D. E. Kirschner, and J. L. Flynn. 2013. Inoculation Dose of Mycobacterium tuberculosis Does Not Influence Priming of T Cell Responses in Lymph Nodes. *Journal of Immunology* 190: 4707-4716.

285. Zhuang, Y., Y. Ma, C. Wang, L. Hai, C. Yan, Y. Zhang, F. Liu, and L. Cai. 2012. PEGylated cationic liposomes robustly augment vaccine-induced immune responses: Role of lymphatic trafficking and biodistribution. *J Control Release* 159: 135-142.

286. Arstila, T. P., A. Casrouge, V. Baron, J. Even, J. Kanellopoulos, and P. Kourilsky. 1999. A direct estimate of the human alphabeta T cell receptor diversity. *Science* 286: 958-961.

287. Naylor, K., G. Li, A. N. Vallejo, W. W. Lee, K. Koetz, E. Bryl, J. Witkowski, J. Fulbright, C. M. Weyand, and J. J. Goronzy. 2005. The influence of age on T cell generation and TCR diversity. *J Immunol* 174: 7446-7452.

288. Clarke, S. R., M. Barnden, C. Kurts, F. R. Carbone, J. F. Miller, and W. R. Heath. 2000. Characterization of the ovalbumin-specific TCR transgenic line OT-I: MHC elements for positive and negative selection. *Immunol Cell Biol* 78: 110-117.

289. Chapman, T. J., M. R. Castrucci, R. C. Padrick, L. M. Bradley, and D. J. Topham. 2005. Antigen-specific and non-specific CD4+ T cell recruitment and proliferation during influenza infection. *Virology* 340: 296-306.

290. Bujdoso, R., P. Young, G. D. Harkiss, and I. McConnell. 1989. Antigen presentation in the sheep: generation of antigen-specific T-cell lines. *Immunology* 66: 559-564.

291. de Titta, A., M. Ballester, Z. Julier, C. Nembrini, L. Jeanbart, A. J. van der Vlies, M. A. Swartz, and J. A. Hubbell. 2013. Nanoparticle conjugation of CpG enhances adjuvancy for cellular immunity and memory recall at low dose. *Proc Natl Acad Sci U S A* 110: 19902-19907.

292. Ilyinskii, P. O., C. J. Roy, C. P. O'Neil, E. A. Browning, L. A. Pittet, D. H. Altreuter, F. Alexis, E. Tonti, J. Shi, P. A. Basto, M. Iannacone, A. F. Radovic-Moreno, R. S. Langer, O. C. Farokhzad, U. H. von Andrian, L. P. Johnston, and T. K. Kishimoto. 2014. Adjuvant-carrying synthetic vaccine particles augment the immune response to encapsulated antigen and exhibit strong local immune activation without inducing systemic cytokine release. *Vaccine* 32: 2882-2895.

293.   Hafner, A. M., B. Corthesy, and H. P. Merkle. 2013. Particulate formulations for the delivery of poly(I:C) as vaccine adjuvant. *Advanced drug delivery reviews* 65: 1386-1399.

294.   Takeuchi, O., and S. Akira. 2010. Pattern recognition receptors and inflammation. *Cell* 140: 805-820.

295.   Scheiermann, J., and D. M. Klinman. 2014. Clinical evaluation of CpG oligonucleotides as adjuvants for vaccines targeting infectious diseases and cancer. *Vaccine*.

296.   Nichani, A. K., M. A. Dar, A. M. Krieg, K. K. Mirakhur, R. S. Kaushik, P. J. Griebel, A. Manuja, H. G. Townsend, L. A. Babiuk, and G. K. Mutwiri. 2007. Systemic innate immune responses following intrapulmonary delivery of CpG oligodeoxynucleotides in sheep. *Vet Immunol Immunopathol* 115: 357-368.

297.   Wedlock, D. N., M. Denis, M. A. Skinner, J. Koach, G. W. de Lisle, H. M. Vordermeier, R. G. Hewinson, S. van Drunen Littel-van den Hurk, L. A. Babiuk, R. Hecker, and B. M. Buddle. 2005. Vaccination of cattle with a CpG oligodeoxynucleotide-formulated mycobacterial protein vaccine and Mycobacterium bovis BCG induces levels of protection against bovine tuberculosis superior to those induced by vaccination with BCG alone. *Infect Immun* 73: 3540-3546.

298.   Parameswaran, N., G. C. Russell, K. Bartley, D. M. Grant, D. Deane, H. Todd, M. P. Dagleish, and D. M. Haig. 2014. The effect of the TLR9 ligand CpG-oligodeoxynucleotide on the protective immune response to alcelaphine herpesvirus-1-mediated malignant catarrhal fever in cattle. *Vet Res* 45: 59.

299.   Wang, S., Q. Han, G. Zhang, N. Zhang, Z. Li, J. Chen, Y. Lv, N. Li, F. Xing, N. Tian, Q. Zhu, and Z. Liu. 2011. CpG oligodeoxynucleotide-adjuvanted fusion peptide derived from HBcAg epitope and HIV-Tat may elicit favorable immune response in PBMCs from patients with chronic HBV infection in the immunotolerant phase. *International immunopharmacology* 11: 406-411.

300.   Angel, J. B., C. L. Cooper, J. Clinch, C. D. Young, A. Chenier, K. G. Parato, M. Lautru, H. Davis, and D. W. Cameron. 2008. CpG increases vaccine antigen-specific cell-mediated immunity when administered with hepatitis B vaccine in HIV infection. *Journal of immune based therapies and vaccines* 6: 4.

301.   Koff, W. C., D. R. Burton, P. R. Johnson, B. D. Walker, C. R. King, G. J. Nabel, R. Ahmed, M. K. Bhan, and S. A. Plotkin. 2013. Accelerating next-generation vaccine development for global disease prevention. *Science* 340: 1232910.

302. Schwartz, R. H. 2003. T cell anergy. *Annu Rev Immunol* 21: 305-334.

303. Cooper, C. L., J. B. Angel, I. Seguin, H. L. Davis, and D. W. Cameron. 2008. CPG 7909 adjuvant plus hepatitis B virus vaccination in HIV-infected adults achieves long-term seroprotection for up to 5 years. *Clinical infectious diseases : an official publication of the Infectious Diseases Society of America* 46: 1310-1314.

304. Waddington, C. S., W. T. Walker, C. Oeser, A. Reiner, T. John, S. Wilkins, M. Casey, P. E. Eccleston, R. J. Allen, I. Okike, S. Ladhani, E. Sheasby, K. Hoschler, N. Andrews, P. Waight, A. C. Collinson, P. T. Heath, A. Finn, S. N. Faust, M. D. Snape, E. Miller, and A. J. Pollard. 2010. Safety and immunogenicity of AS03B adjuvanted split virion versus non-adjuvanted whole virion H1N1 influenza vaccine in UK children aged 6 months-12 years: open label, randomised, parallel group, multicentre study. *Bmj* 340: c2649.

305. Oleszycka, E., and E. C. Lavelle. 2014. Immunomodulatory properties of the vaccine adjuvant alum. *Curr Opin Immunol* 28: 1-5.

306. Haralambieva, I. H., A. L. Oberg, I. G. Ovsyannikova, R. B. Kennedy, D. E. Grill, S. Middha, B. M. Bot, V. W. Wang, D. I. Smith, R. M. Jacobson, and G. A. Poland. 2013. Genome-wide characterization of transcriptional patterns in high and low antibody responders to rubella vaccination. *PLoS One* 8: e62149.